UNIVERSITY OF MIAMI

DEEP REEF BIOEROSION AND DEPOSITION: SEDIMENTOLOGY OF
MESOPHOTIC CORAL REEFS IN THE U.S. VIRGIN ISLANDS

By

David Kurt Weinstein

A DISSERTATION

Submitted to the Faculty
of the University of Miami
in partial fulfillment of the requirements for
the degree of Doctor of Philosophy

Coral Gables, Florida

December 2014

UNIVERSITY OF MIAMI

A dissertation submitted in partial fulfillment of
the requirements for the degree of
Doctor of Philosophy

DEEP REEF BIOEROSION AND DEPOSITION: SEDIMENTOLOGY OF
MESOPHOTIC CORAL REEFS IN THE U.S. VIRGIN ISLANDS

David Kurt Weinstein

Approved:

_____
James S. Klaus, Ph.D.
Associate Professor of
Geological Sciences

_____
R. Pamela Reid, Ph.D.
Professor of Marine Geology
and Geophysics

_____
Donald F. McNeill, Ph.D.
Scientist of Marine Geology
and Geophysics

_____
Peter K. Swart, Ph.D.
Lewis G. Weeks
Professor of Marine Geology
and Geophysics

_____
William E. Kiene, Ph.D.
Associate Science Coordinator
Southeast Atlantic, Gulf of Mexico and
Caribbean Region NOAA Office of
National Marine Sanctuaries

_____
Tyler B. Smith, Ph.D.
Research Associate Professor
Center for Marine and
Environmental Studies
University of the Virgin Islands

_____
M. Brian Blake, Ph.D.
Dean of the Graduate School

WEINSTEIN, DAVID KURT   (Ph.D., Marine Geology and Geophysics)

<u>Deep Reef Bioerosion and Deposition:</u>   (December 2014)
<u>Sedimentology of Mesophotic Coral</u>
<u>Reefs in the U.S. Virgin Islands</u>

Abstract of a dissertation at the University of Miami.

Dissertation supervised by Professor James S. Klaus.
No. of pages in text. (308)

The structural complexity and geomorphic diversity of coral reefs are vital foundational characteristics responsible for the many ecological and economic benefits these ecosystems provide. Shallow-water coral reef geomorphology and structural sustainability is mostly determined by varying reef sedimentary components including: (1) sediment production (matrix) and deposition, (2) framework production and secondary carbonate accretion; (3) bioerosion; and (4) cementation. However, little is known regarding the variability and influence of these sedimentary processes in mesophotic coral ecosystems (MCEs), deep reef communities 30-150 m below sea-level. Despite recent increases in biological and ecological MCE studies, many crucial sedimentological research questions remain unaddressed. These unaddressed questions impede a greater understanding of mesophotic reef structural sustainability and potentially related habitat heterogeneity, carbonate reef shelf development and variability in mesophotic depths, and the general origins of modern coral reef biodiversity.

Critical gaps in knowledge of mesophotic coral reef geomorphology and structural sustainability were addressed in this dissertation by conducting one of the first extensive sedimentological analyses of a mesophotic coral reef ecosystem. Beyond a general exploration of MCEs, the overall research goal was to identify basic sedimentary processes integral to the development, modification, and sustainability of mesophotic

coral reef structure. The goal was also to determine the variability of the identified processes at different mesophotic reef habitats and investigate how these processes and potential variability impact shelf-wide habitat heterogeneity and long-term accretion. To address these goals, sedimentary analyses and ecological surveys were conducted at mesophotic coral reef habitats with distinct structurally characteristics, and neighboring shallow-water reef counterparts in the northern U.S. Virgin Islands (USVI). Analyses at all reefs were designed to address four specific aims: (1) categorization and comparison of various mesophotic reef sediment and cement attributes; (2) determination of exposed consolidated substrate reef bioerosion rates, and the distribution and variability of bioeroding groups; (3) quantification and determination of primary coral mesophotic reef framework builder linear growth and calcification rate variability, and comparison to live mesophotic framework bioerosion and secondary accretion rates; and (4) application of study results for carbonate budget analysis and assessment of geomorphic carbonate production status.

Sediment and cement analysis (first aim) indicated that distinct MCE habitats produce subfacies. The interpreted hydrodynamic and biological interactions controlling mesophotic USVI subfacies have implications towards paleoenvironmental interpretations of ancient mesophotic reef deposits with similar sediment and cement characteristics. Significant differences in exposed consolidated substrate bioerosional processes were discovered between the analyzed habitats. These differences were found to primarily result from variation in parrotfish biomass and related controls on substrate exposure time and location in macroboring succession. Results also broadly confirm pervious hypothesizes that bioerosion decreases with depth along a carbonate shelf and

have implications leaning toward rejection of traditional reef accretion theories. Analysis of coral growth identified statistically significant differences in mesophotic coral reef calcification rates, implying another potential long-term mechanism for enhancing mesophotic reef structural heterogeneity. However, on a larger scale, linear extension rates were found to fit within previously proposed models of decreasing coral growth rate with increasing depth.

Mesophotic coral reef sedimentary analyses were compared in a newly developed carbonate budget model to analyze structural sustainability and consider implications of these analyses on mesophotic reef habitat heterogeneity and Holocene carbonate shelf accretion. All USVI mesophotic habitats examined were identified with net positive carbonate production despite significant variability in geomorphic production states. Additionally, comparisons with earlier benthic surveys suggest higher net USVI mesophotic reef carbonate production in the recent past, potentially implying these deeper reefs are not fully immune to modern global stressors impacting shallow-water reefs. Results indicated that mesophotic reef accretion was not the main driver of shelf-scale topographic relief. However, mesophotic carbonate production variability substantially contributes to habitat-scale structural relief and complexity and relatedly to overall ecosystem diversity. Specific mesophotic reef sedimentology research methods and the need for similar studies at other mesophotic reef habitats were suggested. Comprehensive sedimentology analysis of mesophotic coral reefs in the USVI provide new insight into reef structural sustainability, geomorphic status, and potential impacts from global stressors, and should be considered when developing specific reef sustainability models and management strategies.

ACKNOWLEDGEMENTS

This dissertation is the culmination of more than six years of research and would never have been completed without significant contributions from many people both in and out of Miami. I apologize if I have left anyone out.

First, I am extremely grateful for the opportunity that was offered to me by my PhD adviser Jim Klaus, who took me on as one of his first graduate students. More than providing me with a solid understanding of sedimentology, Jim's guidance and advice taught me how to balance all the various aspects involved with being a successful scientist. Through his patience, guidance, and support, Jim has enabled me to achieve more than I ever thought possible, and I am confident we will have meaningful collaborations for the rest of our careers.

Augmenting the dedicated efforts of my adviser, my other committee members each contributed irreplaceable support, guidance, and advice. Tyler Smith (as well as his wife, colleagues, and students) tirelessly worked with me in the field, offering everything from his skills, time, and even his home, to make me feel welcome in St. Thomas. He also made sure that every field component of my research was completed fully and safely. Bill Kiene provided invaluable knowledge of bioerosion that few people in this word possess, and greatly contributed to the development of this research. Pam Reid graciously invited me, with open arms, into her lab, and supplied me with essential field opportunities and professional contacts. She constantly advocated for me, and provided moral support, guidance, and friendship that ensured all aspects of this dissertation could be completed. Beyond this, she taught me how to successfully write grant proposals and

improve my writing skills (though as this shows, I still must work on brevity). Don McNeil and Peter Swart both graciously offered their time, personal and laboratory resources, and suggestions to me, while gently coping with the many questions I asked them. Other scientists who directly contributed to this research, and for who I am grateful, include: Pat Blackwelder, Elizabeth Babock, Chris Langdon, Kevin Helmle (and Dustin Marshall), Harold Hudson, Elizabeth Kadison, Sharmila Giri, Xaymara Serrano, Jermiah Blondeau, Megan Gonzalez and too many more too list.

As for other mentors, I am continually appreciative of my undergraduate adviser, Alan Kaufman, who has continued to provide support and mentorship throughout this process. I also cannot thank Robert Ginsburg enough for introducing me to coral reef geology, teaching me how to think about the fundamental questions, and constantly inspiring me to learn more. I would also like to thank one of my oldest friends, Andrew Shansby, for inspiring me to become a geologist, my brother Jeremy Weinstein for introducing me to the underwater world and for interesting me in travel, and to Ross Cunning, who helped me ultimately figure out my dissertation topic one night at the Wetlab (another essential location for my graduate career). I must also specifically thank my father, Alan Weinstein, who not only edited all my graduate school proposals, grants, abstracts, and applications, but also this entire dissertation.

Next, I would like to thank my officemate Arash Sharifi, for technical support and advice on many fronts. Additional thanks go out to other past officemates (Art, Al, Chelsea, and Viviana) for providing support, friendship, and interesting conversation. I am highly appreciative of our UM Diving Safety Officer, Rick Gomez, who took a chance on me and taught me scientific and technical diving skills, worked directly with

iv

me in the field, and ensured that every dive component of this research was completed safely and successfully. Significant dive support was also provided by Steve Posterman, Kevin Iglesas, Matt Kammann, and multiple current and former students and staff from the University of the Virgin Islands.

I truly am appreciative of Alyson Kuba, who worked with me as an undergraduate for multiple years, essentially keeping me organized, productive, and just helping me to ensure the overloaded tasks I took on got completed. Meghan Jones and Christopher Kaiser allowed me to mentor them for their undergraduate research and contributed substantially to the final dissertation. Additionally, I would like to thank all (too many to list) other student research assistants from the "UM Mesophotic Geology Laboratory," providing substantial assistance with data collection and analysis enabled me to greatly increase the scope of this research from the original proposed objectives.

The RSMAS community overall has made my experience in graduate school truly unforgettable and something I will always cherish. I am a Hurricane! Specifically, I have to thank the main core of my graduate school friends including Andy Kough, Falko Judt, Adam and Jenny Greer, Will Komaromi, Marcela Ulate-Medrano, Andrew Margolin, Adam Harrison, Ross Cunning, and Sarah Larson. From Fantasy Fests, camping trips, travel and vacations, taco nights, liquid brunches, art walks, religious debates, pool parties, and much more, you guys have given me amazing memories that will last a lifetime. Thank you all for your love and support. I will miss you all very much but know we will all stay in touch and have many more adventures together. I would also like to thank Nina Atkin, Alex Rosenblatt, Steve Hertz, Laura Goldstein, and countless others for all the support you have given me over the years.

Lastly, but most of all, I would like to thank my amazing family. Throughout the course of my graduate school career, as well as my entire life, my parents, Alan and Beverly, have supported and encouraged me completely, guided me though important life decisions, and have supported me in every way they could. Amazing family vacations to national parks inspired in me a love of nature and foreshadowed my future interest in geology. I am also so appreciative and thankful to my siblings, Debra and Jeremy, and my sister-in-law, Lisa. Teaching me to follow my passions, my amazing siblings have all been tremendous sources of support and inspiration, while keeping this geologist "grounded" in the real world. I look forward to sharing many more adventures and happy occasions with you for the rest of our lives.

More information at: http://www.rsmas.miami.edu/users/dweinstein/

TABLE OF CONTENTS

Page

LIST OF FIGURES

LIST OF TABLES

CHAPTER 1. GENERAL INTRODUCTION AND HABITAT DESCRIPTION

The establishment of relief in an otherwise flat marine environment and the ability of skeletal framework to withstand ambient water movement constitute the basic geological definition of a reef. The resultant structural complexity, spatial zonation, and geomorphic diversity created by reefs provide vital ecosystem services crucial for sustained environmental health, global sustenance, coastal protection, and economic prosperity. Known as one of the most productive and biologically diverse ecosystems on the planet (Connell, 1978; Birkeland, 1997), coral reefs are estimated to harbor a quarter to a third of all marine species (Plaisance et al., 2011). The goods and services coral reefs provide produce over $375 billion to the global economy (Pandolfi et al., 2005). Additionally, coral reefs are extremely important ecosystems for the nourishment of human beings around the world. Slightly less than 50% of the total annual commercial catch in the South Pacific region comes from coral reefs (Dalzell et al., 1996). The study of coral reefs is also indispensable in the petroleum industry as a result of the significant number of major hydrocarbon reservoirs discovered in ancient reefal deposits. Carbonate reservoirs, some of which are ancient reef deposits, represent half of the known recoverable hydrocarbons globally (Roehl and Choquette, 1986; Sarg, 1988).

The initial solid physical foundation of a coral reef is dependent on the calcification rates of framework building organisms (Stearn and Scoffin, 1977; Scoffin et al., 1980; Harney and Fletcher, 2003; Mallela and Perry, 2007; Perry et al., 2008). Long-term reef geomorphology and the accretion of carbonate deposits are shaped by a balance between three primary components of reef sedimentology: (1) sediment production (matrix) and deposition, (2) *in situ* framework assembly, and (3) cementation (Stearn and

Scoffin, 1977; Riding, 2002; Hubbard, 2009; Hubbard, 2009). Bioerosion, another critical component of reef sedimentology, is also thought to be a major controller of the architectural integrity of a reef (Hubbard, 2009). Successful coral reef ecosystem management, mitigation, and resource contingency planning require comprehension of all fundamental coral reef processes in all coral reef habitats, past and present.

Coral reef geomorphology is known to display characteristic species zonation along the depth profiles on which reefs develop. Therefore, water depth often functions as the primary reef ecological and geological gradient. Results from many studies have increased the overall understanding of reef sedimentary processes in shallow-water reefs (for a comprehensive review see Hutchings, 1986). Far less data is available regarding deeper reef sedimentology. In the past, most direct sedimentary analyses at mesophotic depths were conducted at relatively few sites at the tail end of transects perpendicular to the shore, with greater concentration applied to shallower geomorphologies such as back-reefs, lagoons, reef crests, and shallow fore-reefs (Moore and Shedd, 1977; Kobluk and Kozelj, 1985; Boss and Liddell, 1987; Chazottes et al., 1995; Perry, 1999). Therefore, many basic sedimentary processes within deeper reefs, known as mesophotic coral ecosystems (MCEs), are less understood than those within shallow-water reefs (Menza et al., 2007).

Deep reef mesophotic coral ecosystem communities, most commonly defined as residing 30-150 m below sea-level, have recently captured the attention of the scientific community (Puglise et al., 2009) as a result of the global decline in the health of shallow-water reefs (Gardner et al., 2003; Hughes et al., 2003) and the theory of deep reef refugia (Glynn, 1996; Riegl and Piller, 2003; Lesser et al., 2009; Bongaerts et al., 2010; Chollett

and Mumby, 2013). Despite a continual increase in the number of published studies pertaining to MCEs (Fig. 1.1), the majority of which address physiology and ecology, many of the crucial research and resource management needs outlined in *The Mesophotic Coral Ecosystems Research Strategy* (Puglise et al., 2009) remain unaddressed. Among these needs is an understanding of the basic sedimentary processes that construct, maintain, and modify mesophotic reef framework and how these processes affect mesophotic reef sustainability and structural integrity. Very few modern studies have examined mesophotic reefs from a geological perspective (Goreau and Goreau, 1973; James and Ginsburg, 1979; Morsilli et al., 2012; Abbey et al., 2013). Developing sound environmental management strategies will require an understanding of principal mesophotic sedimentary processes.

Dissertation objectives

The overarching goal of this dissertation is to determine the significance and variability of the key sedimentary processes involved in the development, maintenance, and destruction of mesophotic reefs developed on a low-angle shelf, and at the same time contribute to the exploration of MCEs. By doing so, new insight will be provided regarding the depositional environment of mesophotic reefs. The goals were addressed by determining the variability of primary sedimentary processes, such as sediment production and cementation, coral framework and rubble bioerosion, and coral growth, between mesophotic habitats with different structural characteristics, and with their shallow-water counterparts. The *central null hypothesis* was that the aforementioned sedimentary processes within mesophotic reefs do not vary significantly between

neighboring habitats with different geomorphologies or with shallow-water reefs found within the same region.

To test the central hypothesis, mesophotic and shallow-water reefs south of St. Thomas, U. S. Virgin Islands (USVI) were studied to pursue four *specific aims*:

1. Categorize mesophotic reef sediments and cement, and determine the existence and potential implications of related fine-scale sedimentary facies (Chapter 2).

2. Determine bioerosion rates and relative abundances of bioeroding groups in exposed consolidated substrates, as well as the variability of bioerosion in different mesophotic reef habitats (Chapter 3).

3. Quantify and determine variability in growth rates (linear extension and calcification) of the primary platy coral framework builder in USVI mesophotic reef habitats, and the effect of living framework bioerosion and secondary accretion (Chapter 4).

4. Calculate complete mesophotic reef habitat carbonate budgets to assess the geomorphological carbonate production status, and evaluate mesophotic reef accretion potential and contributions to carbonate shelf development (Chapter 5).

Previous research

Coral reef deposition and morphology

Despite confusion regarding a precise geological definition of reefs (Heckel, 1974), for the purposes of this dissertation, reefs will be defined as three-dimensional

structures produced by the deposition of calcareous sessile organisms establishing topographic relief above surrounding sediment. Coral are the primary builders of modern reefs and are able to create vast carbonate deposits, but it is not known if reef building is a required function of coral communities or a common by-product of high productivity (Kleypas et al., 2001). Regardless of the facilitating community, reef buildups are comprised of many different organisms with specific depositional functions.

Framework builders (most commonly coral, microorganisms (producing stromatolites), crustose coralline algae (CCA), mollusks, etc.) are classified as coalescing into large communities that produce calcifying structures which act as core wave-resistant reef foundation building blocks. The combination of one or multiple framework builder communities (and additional bioerosional activities) often induces complex structures with numerous cavities (Garrett et al., 1971). *Secondary encrusters* (most commonly CCA, bryozoans, foraminifers, gastropods, serpulids, etc.) help bind reef framework and potentially contribute large amounts of carbonate to the overall structure (Rasser and Riegl, 2002; Gherardi and Bosence, 2005). Direct s*ediment contributors* (most commonly crinoids, benthic foraminifers and sessile epibenthic organisms like *Halimeda*) help to form reef mounds that assist with reef growth. They also provide "mortar" that fill framework voids and help solidify the reef deposit (James et al., 1976; Tucker and Wright, 1990). Many of the mentioned organisms can be classified into multiple groups depending on the abundance of all species at a given location and additional processes (such as bioerosion). Along with water energy levels, these three main depositional groups and other organisms categorized as *bafflers*, *binders*, and *precipitators* help determine the type of reef deposit (Tucker and Wright, 1990).

From a structural and compositional perspective, Riding (2002) defined three main reef types: (1) Cement-supported reefs; (2) Matrix-supported reefs (cluster reefs, agglutinated microbial reefs, segment reefs); and (3) Skeleton-supported reefs (frame reefs). The main biological component of modern coral reefs consists of a thin benthos veneer draped upon a biologically-produced non-living foundation. The non-living structural components of a coral reef consist of its framework, rubble, cement, and sediment (allochthonous and autochthonous).

Caribbean coral reef rubble and sediments, created largely through bioerosional processes, are analogous to tropical forest leaf litter. Reef "rubble litter" accounts for 70% of the carbonate originally produced by calcifying organisms that gets incorporated into the geomorphic structure (Stearn and Scoffin, 1977; Hubbard et al., 1990). Studies have suggested that reef deposit interiors are often primarily composed of cemented coral rubble, not *in situ* coral framework (Hubbard et al., 1990; Blanchon et al., 1997). However, an informal qualitative review of peer-reviewed coral reef geology research suggests that coral rubble analysis is much less common than that of coral reef framework. Additionally, taphonomic uncertainties such as exposure time and unknown sample age, initial framework bioerosion, rubble transport, and collection randomness can impede the interpretation of data obtained from coral rubble. These facts emphasize a fundamental "coral rubble problem" that must be addressed (Weinstein et al., 2014). Despite limitations, coral rubble analysis may still improve the interpretation of substrate availability, bioerosion intensity, and residence time, and therefore warrants inclusion in this dissertation. For example, Holmes et al. (2000) found that analysis of live massive coral types correlated with analysis of branching coral rubble from the same locations

when quantifying "bioerosion levels." These results were interpreted to imply that productivity, residence time, and depositional environment type have a greater impact on bioerosion then differences in skeletal structure and taxonomic affinity (Holmes et al., 2000). Regardless, the combination of all non-living structural components of a reef, including coral rubble, produces the complex geomorphologies partially responsible for the establishment of diverse coral ecosystems.

Modern large-scale reef geomorphology classifications and theories of reef development are largely extensions of the original fringing, barrier, and atoll reef classification first suggested by Darwin (1842). The classifications relate more to the generalized topographic features of reefs. Because modern reefs are primarily thin biological surfaces on ancient reef structures, they are not generally believed to be responsible for the larger scale topographic features and spatial distribution of Holocene reefs (Stoddart, 1969). These distinctions primarily result from sea-level changes, biological productivity, and antecedent topography (Tucker and Wright, 1990; Locker et al., 2010).

The internal structure and morphology of any reef essentially results from the interaction of four main sedimentary reef processes: (1) construction; (2) destruction; (3) cementation; and (4) sedimentation (Riding, 2002). Riding (2002) suggested that reef structure ultimately determines the sedimentary composition the habitat deposit, thus he considered it to be "the fundamental attribute of a reef." Similarly, when analyzing results from multiple studies, Graham and Nash (2013) found that reef structural complexity is another central property of coral reef ecosystems, especially when considering coral and algal cover, coral morphology cover, and fish and urchin density

and biomass. Habitat complexity in many marine and terrestrial ecosystems is believed to be vital for high levels of biodiversity (Kostylev et al., 2005). This is especially the case in coral reef ecosystems, often demonstrated by the significant impact structural complexity (or a lack thereof) has on maintaining diverse, abundant, and healthy fish communities (Gratwicke and Speight, 2005; Dustan et al., 2013; Rogers et al., 2014). Many past studies have examined the main sedimentary reef processes responsible for maintaining the physical foundation for complex habitats and heterogeneity in shallow-water reef systems (Ginsburg, 1956; Garrett et al., 1971; Ginsburg, 1974; James et al., 1976; Murray et al., 1982; Lidz et al., 1985; Boss and Liddell, 1987; Eberhard and Lomando, 1999). Comparatively, there is a critical gap in knowledge regarding these basic sedimentary reef processes and their effect on geomorphology and habitat complexity within mesophotic reefs.

Mesophotic reef habitat extent and significance

Somewhat arbitrarily defined by most researchers as living in waters 30-150 m deep, Mesophotic reefs are characterized as being low light and low energy environments (Lesser et al., 2009). Mesophotic coral ecosystems only receive a small percentage (0.07-5.84%) of surface photosynthetically active radiation (Kahng et al., 2010). They also can experience seawater temperatures approximately 5° C cooler than the surface (Lesser et al., 2009). Published peer-reviewed literature first used and associated the term "mesophotic" to reef environments in 2007 (Parrish and Littnan, 2007). Since that time, many more studies have been conducted, although relatively few focus on mesophotic reef geology (Fig. 1.1).

Mesophotic coral ecosystems typically form along: (1) steep geomorphologies such as high-angle continental and insular slopes from shelf breaks to nearby basins (i.e. off Belize, James and Ginsburg, 1979); or (2) gentle geomorphologies such as low-angle outer insular shelves (i.e. south of Vieques, Puerto Rico, Rivero-Calle et al., 2008), isolated banks within the mesophotic zone (i.e. Bajo De Cico, in the Mona passage, Locker et al., 2010), and seaward sloping margins (i.e. Okinawa, Japan, Yamazato, 1972; Matsuda and Iryu, 2011). A large majority of MCE research has focused on steep slope geomorphologies (Goreau and Goreau, 1973; James and Ginsburg, 1979; Hubbard, 1989; Grammer and Ginsburg, 1992; Bak et al., 2005), causing the somewhat bias impression that mesophotic reefs primarily occur at wall and slope habitats. However, these steep habitats are usually closer to land, making them more convenient locations for research.

Wave exposure, energy, and other wave characteristics have been shown to greatly control reef morphology, topographic profiles, and geomorphic structures in shallow-water coral reefs (Shinn, 1963; Adey and Burke, 1977; Geister, 1977; Roberts et al., 1977; Hubbard et al., 1981; Blanchon et al., 1997; Storlazzi et al., 2003; Hubbard et al., 2008). Although intuitive reasoning would imply mesophotic reef geomorphology is relatively homogenous, MCEs have been recorded with diverse structures that potentially contribute to high levels of biodiversity (Goreau and Land, 1974; Moore et al., 1976; Ohlhorst and Liddell, 1988; Ginsburg et al., 1991; Sherman et al., 2010; Smith et al., 2010). The drivers of mesophotic coral reef geomorphic heterogeneity are relatively unknown. Sherman et al. (2010) found upper slope south Puerto Rican mesophotic reef geomorphology was related to changes in prevailing wave exposure as well as the spatial distribution of topographic highs. The orientations of deep buttress spurs (topped with

high cover of shingle-like *Agaricia* spp. platy coral) and groove features perpendicular to the shelf edge were interpreted as resulting from previous lower sea-level reef progradation (Sherman et al., 2010).

Attempts to map MCE distributions suggest these habitats may be more common than previously thought. For example, up to an estimated 182,000 km^2 of potential MCE habitat has been predicted in the US Gulf of Mexico, Florida, and U.S. Caribbean alone (Locker et al., 2010), while an estimated 409,100 km^2 of the entire Caribbean and Bahamas, and the Gulf of Mexico have been theorized to consist of mesophotic reefs (Fig. 1.2; Ginsburg et al., 2012). Using models built on combined environmental, geophysical and benthic coverage data, Bridge et al. (2012) estimated mesophotic communities to cover over 2,000 km^2 of the Great Barrier Reef World Heritage Area (~0.59 %).

Other predictions of MCE habitat expanse, generally dependent on local geomorphology and water quality assumptions, suggest that these deep reef habitats could vastly exceed the spatial extent of shallow-water coral reef habitats and may be up to 100% underestimated in some areas (Harris et al., 2012; Moura et al., 2013). As of 2010, mesophotic reefs were still considered the least studied of all reef ecosystems (Kahng et al., 2010). At the present date, mesophotic coral ecosystems have been identified and studied throughout the world including: the Atlantic and Caribbean (James and Ginsburg, 1979; Fricke and Meischner, 1985; Lang et al., 1988; Liddell and Avery, 2000; Bak et al., 2005; Leichter and Genovese, 2006; Smith et al., 2010; Moura et al., 2013; Serrano et al., 2014; Weinstein et al., 2014); Australia (Bongaerts et al., 2011; Bridge et al., 2011; Bridge et al., 2012b; Abbey et al., 2013; Englebert et al., 2014); the

Mediterranean and Red Seas (Fricke et al., 1987; Brokovich et al., 2008; Einbinder et al., 2009; Gori et al., 2012; Bianchelli et al., 2013); Asia (Pyle et al., 2008; Breedy and Guzman, 2013; Ohara et al., 2013; Sinniger et al., 2013); and the central Pacific (Kahng and Kelley, 2007; Bare et al., 2010; Rooney et al., 2010; Boland et al., 2011). This list of studies is expected to grow substantially in the near future.

Mesophotic reefs are valued for a number of reasons such as their possible connectivity to shallow-water reefs and the importance of MCEs to the persistence of tropical reef systems (Riegl and Piller, 2003; Bongaerts et al., 2010; Slattery et al., 2011; Serrano et al., 2014). Unlike more isolated deeper mesophotic reefs (60-150 m), which contain many endemic species (Reed and Pomponi, 1997; Lesser and Slattery, 2011), shallower mesophotic reefs (30-60 m) are inhabited by numerous organisms also found in shallow-water reefs (Bak et al., 2005; Bongaerts et al., 2010). More than their deeper isolated neighbors, shallower mesophotic reefs have a greater potential for larvae connectivity with shallow-water reefs (Hughes et al., 2003; Lesser et al., 2009) or serve as refugi for shallow-water reef species threatened by local and global stressors (Glynn, 1996; Bak et al., 2005; Bongaerts et al., 2010; Slattery et al., 2011). However, recent studies have also questioned the actual premise of the refugia hypothesis as applied to mesophotic coral reefs (Riegl and Piller, 2003; Slattery and Lesser, 2012).

Geology, biology, and potential threats to mesophotic reefs

Along with macroalgae and sponges, mesophotic reefs often produce high percent covers of light-dependent scleractinian coral (Bak et al., 2005; Lesser et al., 2009; Smith et al., 2010). These coral are typically found with platy morphologies (Bare et al., 2010; Lesser et al., 2010; Sherman et al., 2010; Smith et al., 2010; Bridge et al., 2011; Luck et

al., 2013). The platy morphology is hypothesized as a zooxanthellate coral photoadaptive response to reduced illumination either from increased turbidity or deeper depths (Dustan, 1975; Fricke and Schuhmacher, 1983; Titlyanov and Titlyanova, 2002; Stambler and Dubinsky, 2005). Additionally, the platy coral morphology common to many mesophotic reefs (Fig. 1.3) is also similar to the morphology of coral extensively found throughout the fossil record of Scleractinians in paleoenvironments often interpreted as calm, deep water (Rosen et al., 2000). These paleoenvironment interpretations are partially supported by the understanding that early scleractinian reef species first appeared in the Triassic as solitary small colonies in deep, colder water (Stanley and Fautin, 2001). The scleractinian-zooxanthellae symbiosis common to most modern coral is thought to have evolved in deeper, turbid waters as well (Potts and Jacobs, 2000).

Early scleractinian corals, many with the platy morphology so common in modern mesophotic reefs, evolved a plasticity for altering algal symbiosis reliance that resulted in a vital eco-physiological adaptation for surviving major extinction events (Veron, 1995; Stanley and Fautin, 2001; Baker et al., 2004; Fautin and Buddemeier, 2004). This suggests that the evolutionary significance of modern mesophotic coral is crucial for understanding all modern coral reef evolution and related survival adaptations developed to mitigate environmental stresses (Stanley and Swart, 1995; Budd, 2000; Klaus et al., 2011; Morsilli et al., 2012; Klaus et al., 2013). Additionally, given the modern identification of MCE worldwide and large predicted expanses of unexplored MCEs (Ginsburg and Reed, 2008; Locker et al., 2010; Bridge et al., 2012a), mesophotic coral reefs probably have a long geologic history.

Many abiotic physical attributes affect the distribution, productivity, growth rates, physiology, and ecological health of photosynthetic-reliant mesophotic coral, especially carbon and sunlight intake. Some studies suggest heterotrophic feeding in coral increases at deeper depths (Muscatine et al., 1989; Mass et al., 2007), but other studies found no depth related trend to carbon acquisition (Anthony and Fabricius, 2000; Alamaru et al., 2009; Einbinder et al., 2009). Major considerations of sunlight involve photosynthetically active radiation and the spectral composition of light with depth (Dustan, 1982; Lesser, 2000; Frade et al., 2008a; Lesser et al., 2010). Beyond the optical properties of water, light availability can also be a function of the substrate slope photosynthetic components of benthic organisms reside upon, and the effect of nutrients and sedimentation on water clarity (Lesser et al., 2009).

Coral acclimation to lower light levels results from a number of adaptations such as changes in autotrophic/heterotrophic dominance (Porter, 1976; Grottoli et al., 2006; Klaus et al., 2013), differences in depth-specialization of zooxanthellae subclades (Frade et al., 2008b; Chan et al., 2009), changes in respiration resulting in decreased metabolic demand (Anthony and Hoegh-Guldberg, 2003), and adaptations in colony morphology (Kühlmann, 1983). For example, symbiotic corals in MCEs often develop (or possibly revert to) a platy morphology to maximize surface area to volume ratios for utmost irradiance (Dustan, 1975; Kühlmann, 1983). Limited light intensity is also thought to have induce the development of various photoadaptive techniques including increasing carbon fixation (Battey and Porter, 1988) and photosynthetic pigments (Dustan, 1982), and incorporating *Symbiodinium* communities more apt for deeper depths (Frade et al., 2008b; Chan et al., 2009). These techniques appear to help coral thrive in deeper water

but research in Curaçao suggested the techniques do not have a significant influence on coral growth rates (Bak et al., 2005).

Other environmental factors, such as localized and regional hydrodynamic variability, may also affect the ecological success and distribution of mesophotic reefs. Seasonal or episodic upwelling and internal wave activity can change water temperatures and nutrient and particulate organic material abundances, leading to varying impacts on MCEs (Smith et al. 2010). Tidal forcing on currents parallel to shore and increased wind stress with depth provides favorable conditions for suspension feeders in all reef systems (Kahng et al., 2010). Larval recruitment and distribution are partially controlled by hydrodynamic conditions (Holstein, 2013), potentially influencing the development of reef-scale geomorphic habitats (Weinstein et al., 2014). Interactions between abiotic and biotic properties can also effect the distribution of mesophotic reefs. Gribb (2006) found that the coral *Porites lobata* experienced colonial detachment below 50 m because basal attachment growth rates were surpassed by colony holdfast bioerosion rates.

Depth induced isolation from strong wave activity and large fluctuations in temperature generally thought to protect mesophotic reefs from common shallow-water reef anthropogenic and natural stressors (Bak et al., 2005; Armstrong et al., 2006; Rivero-Calle et al., 2008; Lesser et al., 2009). Tropical storms were also believed to cause little direct physical destruction to mesophotic reefs (summary in Bongaerts et al., 2010), but recent evidence has directly shown that high-energy storm events can rip-up coral at mesophotic depths (Harmelin-Vivien and Laboute, 1986; White et al., 2003; Bongaerts et al., 2013).

When considering land-based stressors, most mesophotic reefs appear to be geographically far enough from land sources such that they are likely undisturbed by pollution and sediment runoff (Herzlieb et al., 2005). However, a few isolated sewage discharges incidences and blooms of macroalgae adapted to low light levels have been reported in Florida (Proni et al., 1994; Lapointe, 1997; Lapointe et al., 2005a; Lapointe et al., 2005b). Storms can also have indirect negative impacts on MCE health by enabling the transport of anthropogenic derived sediment and nutrients (Hubbard, 1992; Bak et al., 2005). Sediment stress is potentially destructive to mesophotic coral by dimming already low deeper reef light levels (Locker et al., 2010) and because the dominant platy morphology of mesophotic coral is less effective for sediment removal than other coral morphologies (Bongaerts et al., 2010). Despite the identified potential damage by sediments, limited data suggests sedimentation does not substantially effect most mesophotic coral reef development, especially when the reefs are located on topographic highs (Bak and Engel, 1979; Smith et al., 2008; Sherman et al., 2010) . Sediment is often funneled off steep shelf-edge mesophotic coral reefs in adjacent narrow cuts and intervening grooves and sporadically transported down-slope during storm events (Hubbard et al., 1990; Hubbard, 1992; Sherman et al., 2010). However, Sherman et al. (2010) found that MCEs were less abundant on southeast-facing Puerto Rican slopes where wider-spacing of topographic highs compared to other slopes allowed for sediment transport over the entire low-relief slope, hindering coral development.

Climate change has global implications that could impact mesophotic reefs. Temperatures in mesophotic reefs have been found to have significant fluctuations (Bak et al., 2005), sometimes attributed to episodic transport of sub-thermocline water (Bak et

al., 2005; Leichter and Genovese, 2006; Lesser et al., 2009). These fluctuations are still relatively low when comparing long-term averages to those in the shallow reefs (Frade et al., 2008b). Temperature-related coral bleaching and diseases are thought to be more common and problematic for shallow-water coral reefs (Wilkinson and Souter, 2008), but instances of coral bleaching (Lang et al., 1988; Bunkley-Williams et al., 1991; Bak et al., 2005; Smith et al., 2010) and coral diseases (Smith et al., 2010) have been recorded in mesophotic reefs. More data from modern and ancient mesophotic reefs is still needed to better establish risks and occurrence frequencies.

Northern United States Virgin Islands (USVI)

Geology

For the present study, mesophotic sedimentary processes were investigated within distinct geomorphic habitats south of St. Thomas in the northern United States Virgin Islands (USVI). The region (Fig. 1.4) is part of the broader Puerto Rican Shelf, which contains Puerto Rico, the British Virgin Islands, and the northern USVI. These islands, constituting the northern exposed ridge of the Greater Antilles, were formed as part of the Greater Antillean Arc system when the Caribbean and North American plate collision began in the Cretaceous (Holmes and Kindinger, 1985). Subduction-induced magmatism in the Virgin Islands began approximately at the end of the Early Cretaceous and continued until the Oligocene (Pindell and Barrett, 1990). Relatively uniform development dominated the Greater Antilles Arc expanse between the Cretaceous and the Paleogene (Pindell and Barrett, 1990). This uniform development ceased in the form of collision pulses associated with Bahama platform impact, breaking apart the arc system between the late Paleocene and the Holocene (van Gestel et al., 1998).

Water Island Formation, the oldest northern Virgin Islands geologic unit recognized, consists of quartz keratophyre and spilite flows that resulted from pre-Albian submarine eruptions (Donnelly, 1964). The base of this unit has no exposure but is believed to lie above oceanic crust (Donnelly, 1989). Following a change in igneous composition represented by the Louisenhoj Formation, volcanism lessened until the late Santonian, allowing for the deposition of the Outer Brass Limestone (Rankin, 2002). Volcanism resumed in the form of the Tutu Formation, the youngest stratified unit found on St. John (Rankin, 2002). The Necker Formation, representing the youngest volcanic strata deposited in the Virgin Islands, is exposed in the British Virgin Islands and has radiometric ages between 39-35 Ma (Rakin, 2002; Jolly et al., 2006). Initial collision between the Greater Antilles Arc and the Bahama Platform has been suggested to result in north-south compression folds (Rankin, 2002). The last major tectonic activity in the Northern Virgin Islands transpired ~39 ma, related to Cayman Trough center spreading initiation (Rankin, 2002).

Tectonic activity in the Virgin Islands has been relatively subdued for the past 1.8 my, implying that Holocene reefs throughout Puerto Rico and the USVI developed during times of relatively stable tectonics, with only minor uplift between 10-30 cm (Hubbard et al., 2008). The upper sedimentary features on the shelf between the northern Virgin Islands and the Anegada Passage consist of an ~400 m thick carbonate platform. The Puerto Rico/Virgin Island platform, which connects the two island groups, was exposed during Quaternary glacial maximums (most recently ~12 ka) and is mainly composed of igneous rocks (Hubbard et al., 2008). Hubbard et al. (2008) suggested that the southern margin of the Northern USVI flooded prior to 12 ka because the margin was

relatively deep and the Atlantic was slightly higher than the Caribbean. Rapid rising sea-level and southerly tidal flow may have prevented the buildup of shallow-water Holocene reefs near the shelf edge, near where the current study is located (Hubbard et al., 2008).

From south to north, the shelf edge consists of an ~10 m relief "double reef complex," a 45 m terrace, and a 32 m terrace (Holmes et al., 2009). When present, these units (or ~1 m of sediment cover when they are not present) superimpose an acoustically transparent substrate 55 m below sea-level (Holmes and Kindinger, 1985). Holmes and Kindinger (1985) interpreted the transparent substrate as Pleistocene semi-consolidated sediment, of which the lower unit dips south and cuts horizontal reflectors under most of the 45 m terrace. The lower section is interpreted as an erosion surface feature from the most recent sea-level lowstand (~18-12 ka).

Although not the case for other parts of the Puerto Rican Shelf (such as southwest Puerto Rico and St. Croix), a critical void in knowledge regarding northern USVI reef development stems from the fact that no reef core borings from reefal deposits have been collected (for core locations taken from other areas on the Puerto Rican Shelf (see Hubbard et al., 2008). Restricted antecedent buildup attributed to rapidly eroding volcanic shorelines (Adey and Burke, 1976) was suggested to result in limited thickness of Holocene carbonate accumulation along the southeastern coast of St. Thomas and St. John (Hubbard et al., 2008).

Modern regional ecology

St. Thomas, the largest island (~83 km^2) in the northern USVI (Fig. 1.4), is surrounded by smaller islands and a diverse ecosystem of mangroves, seagrass beds, and fringing coral reefs. The north-south width of the shelf across St. Thomas is

approximately 45 km. Adjacent to the southern coast of St. Thomas is an array of shallow patch reefs surrounded by seagrass beds (Smith et al., 2008). As water depths deepen southward, mid-shelf patch reefs (15-20 m deep) periodically appear within more extensive seagrass habitats. Below 30 m, mesophotic coral form extensive reefs surrounded by substrates of primarily barren sand or pavement approximately 10 km south of St. Thomas. The Anegada Passage, with a maximum depth greater than 2.6 km, represents the southern extent of the Puerto Rican Shelf (Holmes and Kindinger, 1985).

Mesophotic reefs in the region are best developed within the Red Hind Marine Conservation District (RHMCD) and the Grammanik Bank (Smith et al., 2010). Covering an area of 44.6 km^2, the RHMCD ranges in depth from 25 to 100+ m (more than two-thirds shallower than 50 m) and supports dense coral communities dominated by the *Orbicella* spp. (formerly known as *Montastraea annularis*, Budd et al., 2012) with coral cover up to 50% (Smith et al., 2010). Less than 5 km east of the RHMCD is the Grammanik Bank, a narrow deep reef (30-40 m) 1.5 km long, which is also dominated by *Orbicella* spp. (Kadison et al., 2006). The RHMCD and Grammanik Bank are highly representative of a low-angle carbonate shelf at modern-defined mesophotic depths.

 Study site description and geomorphology

With a ban on benthic fishing and anchoring, and with collaborative support from colleagues at the University of the Virgin Islands, the RHMCD and Grammanik Bank provide ideal, easily accessible locations to study the depositional environment of a MCE. Six sites were selected for the purposes of this dissertation (Fig. 1.4, data obtained from Rivera et al., 2006 and NOAA CCMA, http://ccma.nos.noaa.gov/products/ biogeography/usvi_ nps/overview.html). The sites were selected based on the availability

of previous data (Kadison et al., 2006; Smith et al., 2007; Nemeth et al., 2008; Smith et al., 2008; Smith et al., 2010; Cherubin et al., 2011; Smith et al., 2011a). Additionally, sites were selected so the variability of sedimentary processes examined for this study could be compared between different mesophotic reef geomorphology types (Smith et al., 2010).

Site characteristics and methods used to conduct benthic surveys are displayed in Table 1.1. Spatial complexity was estimated using standard chain-link reef rugosity techniques (Risk, 1972; Luckhurst and Luckhurst, 1978; Hubbard et al., 1990). Differences between sites were tested with non-parametric statistics because site spatial characteristics were not normally distributed. One-way Kruskal-Wallis non-parametric comparisons indicated statistically significant site differences for overall coral cover, exposed consolidated substrate, and reef rugosity. Results from Kruskal-Wallis tests as well as multiple pairwise comparisons conducted with *kruskalmc*, in R package *pgirmess* (Siegel and Castellan, 1988) are displayed in Table 1. 2.

Within the RHMCD and Grammanik Banks, sites consist of MCE habitats with distinct structural characteristics (Fig. 1.5) identified based on bathymetric geomorphic classifications and biological differences (Smith et al., 2008). The upper surfaces of the reef habitats represent the main biological veneer with coral colonies often located on top of carbonate pillars varying up to 3 m in height (see Fig. 1.3a for example). All mesophotic sites primarily experience unidirectional benthic currents with almost no oscillatory current influence, except for possible (but unmeasured) long period tropical storm-generated swells (Smith et al., 2011b). Ocean models centered on the RHMCD indicate that mean currents 5-10 m above the seafloor flow in a southerly direction

(Cherubin et al., 2011). The two other sites analyzed for this dissertation were in relatively close proximity to the mesophotic reefs and served as shallow-water comparisons.

To better identify site locations, numbers were assigned by decreasing depth (with 1 being the deepest site and 6 being the shallowest). "D" for "Deep" represents mesophotic reefs, "M" indicates the Mid-Shelf site, and "S" indicates the shallowest site. The following site descriptions are organized such that they start at the shelf-break and move north toward St. Thomas.

Site D3 – The Primary Bank (Fig. 1.4b) is best observed along the shelf edge of Grammanik Bank, and represents the southernmost mesophotic habitat of the study. Within the RHMCD, this feature covers 1.4% of the area at an average depth of 42.4 m ± 2.1 SD (Smith et al., 2010). The habitat is a narrow width bank with >5 m relief and parallels the margin of the Anegada Passage for over 1 km. Habitat relief possibly represents the outer part of the double reef complex identified by Holmes and Kidinger (1985). Coral cover in 2012 (Table 1.1) was dominated by living stony coral within the *Orbicella* spp. Currents at this site are weak to moderate, dominantly north-south with stronger episodic currents towards the northwest (Smith et al., 2011b). As it resides in the Grammanik Bank, samples collected from this site were frequently labeled as "Gram."

Site D4 – The Secondary Bank (Fig. 1.4c), separated from but parallel to a deep narrow sand channel, exhibits a more continuous trend and a broader sloping northern edge than the Primary Bank. Maximum relief (>5 m above the surrounding shelf) probably represents the leeward part of the double reef complex identified by Holmes and

Kidinger (1985). Within the RHMCD, this habitat covers 25.2% of the area at an average depth of 38.2 m ± 3.1 SD (Smith et al., 2010). Coral cover in 2012 (Table 1.1) was dominated by corals within the *Orbicella* spp. Although no direct measurements were available before field sampling for this study was concluded, years of qualitative observations indicate this site experiences relatively strong, tidally driven current, with increased spring tide strength (Smith et al., 2011b). Collected samples were frequently labeled "Coll" because the local name for this site is "College Shoal."

Site D1 – The northern edge of the Secondary High Bank transitions to a basin (24.5% of the total RHMCD area) with an average RHMCD depth of 42.6 m ± 1.7 SD (Smith et al., 2010). Consisting of two different geomorphological habitats, 26.4% of the RHMCD basin is the Hillock Basin habitat and the other 73.6% is the Deep Flat Basin habitat (Smith et al., 2010). Extending more than 1 km^2 on a flat expanse, the Hillock Basin is composed of more than 10,000 coral-covered semi-conical hills and knolls rising 2 -10 m above surrounding sand flats and sparse coral cover (Smith et al., 2010). These structures may be equivalent to those labeled as "Hillocks" in deeper reefs of Discovery Bay, Jamaica (Goreau and Goreau, 1973), although this has not been independently confirmed. The particular sample site for this study (Fig. 1.4d) is located within and between several different hillock structures. Collected samples at this location were frequently labeled "S166" because the originally established name for this site was MCDS166 (Smith et al., 2010).

The Deep Flat Basin covers 18% of the total RHMCD area and is best characterized as an unbroken flat expanse. Corals were collected from this habitat by semi-randomly selecting samples from the spot that was first reached during the initial

diver descent from a generalized coordinate point obtained on the boat. Coral/pillar structures within both basin habitats are further apart than those in the High Banks. Samples collected from this site were frequently labeled "MCDFB," an acronym for "marine conservation deep flat basin." North of the RHMCD basin is the shallower (average depth of 36.6 m ± 2.3 SD) Tertiary Bank (Smith et al., 2010), likely equivalent to the 32 m terrace (Holmes et al., 2009). The Tertiary Bank was not sampled for this study.

Site D2 – Deep patch/low bank habitats located in the northeastern RHMCD are isolated from each other by unconsolidated sandy substrates with occasional algae. These features cover 5.6% of the RHMCD and have an average depth of 42.9 m ± 2.3 SD (Smith et al., 2010). This habitat is characterized as having <5 m of topographic relief with high macroalgae cover and low live coral cover compared to the previously described mesophotic coral habitats. This description is similar to other Caribbean MCEs (Fricke and Meischner, 1985; Reed, 1985; Phillips et al., 1990; Garcia-Sais et al., 2008). The coral communities appear to be ephemeral opportunists, unable to form large colonies as they attach to loose rubble substrate. No comparison was made between individual deep patches to determine potential variability in benthic coverage and species dominance or rugosity, though some additional descriptions are provided by Smith et al. (2010).

The patch selected semi-randomly for this study was labeled as the "Deep Patch," though samples collected from this location were also frequently labeled "MCDP" as an acronym for "marine conservation deep patch." Coral cover at this particular patch (Fig. 1.4e) had a relatively high abundance of *Porites spp., Agaricia spp.,* and *Manacina*

areolata. Mycetophyllia aliciae, a coral species rarely found at any of the other mesophotic sites, was also found encased by crustose coralline algae. Additionally, ~75% of rubble samples collected from the Deep Patch were classified as rhodoliths with no identifiable internal coral skeleton.

Site M5 – The Mid-shelf Patch reef site selected for our study (Fig. 1.4f) was located 1 km from the protruding southeastern most part of St. Thomas. This site has been monitored by the United States Virgin Islands Territorial Coral Reef Monitoring Program (TCRMP) since 2003. Separated from adjacent reefs by at least 1 km of unconsolidated sand and rhodolith seafloor, this isolated patch reef is 18 – 24 m below sea-level. The reef rises ~7 m above a surrounding sand apron and consists of a diverse coral community dominated by *Orbicella* spp. The local name of this location is the "Seahorse Cottage Shoal," so samples collected from this site were labeled "Sea."

Site S6 – The shallow fringing patch reef selected for our study is partially-isolated, just offshore and west of Black Point, in Perseverance Bay. Given the proximity of this habitat to Black Point, samples collected from this site were frequently labeled "BP." Throughout this dissertation, this site is referred to as the "Fringing Patch." Frequently occupied by young marine sea turtles but heavily affected by terrestrial runoff, the reef at this site consists of a sparse low coral cover community dominated by *Siderastrea siderea*, *S. radians*, and *Porites astreoides*.

Antecedent topography review

Coral recruits require some type of hard substrate for successful colonization and growth (Vandermeulen and Watabe, 1973). Therefore, initial coral larval colonization

must be considered before examining the impact of sedimentary processes on the development and maintenance of reef structure. Large-scale reef geomorphology is partially controlled by sea-level fluctuation (Tucker and Wright, 1990; Locker et al., 2010). Sea-level induced changes in geomorphology will likely be uniform for reefs parallel to shoreline and will produce a systematic change in structure in a direction perpendicular to the shoreline. Quaternary sea-level changes, which resulted in the formation of many reef deposits in the Caribbean, provide an example of this phenomenon.

Antecedent platform theory suggests that any bank (especially those created by former reef systems) located within the circum-equatorial coral reef zone is a potential site for coral reef development (Hoffmeister and Ladd, 1944). These topographies have potential for reef development by offering hard-ground surfaces for colonization, and by limiting destructive turbid bottom water and sediment interactions with potential benthic recruits (Kahng et al., 2010). Large-scale geomorphic sedimentation protection is facilitated through elevation of potential reefs above sediment transport channels, or by steep inclines, such that sediment continually transports downslope with little benthic organism interactions (Sherman et al., 2010). Besides ancient reef deposits, potential candidates for antecedent topography include salt domes, volcanic ridges, paleo-shorelines, raised terraces, and deep-shelf environments (Stoddart, 1969; Locker et al., 2010).

From seismic analysis, reef distribution has been found to correlate with antecedent topography (Purdy, 1974; Harvey and Hopley, 1982; Searle, 1983). Various independent and interrelated processes such as preferential weathering and karstification,

tectonic activity and associated changes in deposition, siliciclastic deposition, and erosion can influence the origin, lithology, and location of antecedent topography (Harvey and Hopley, 1982; Gischler and Hudson, 1998; Purdy et al., 2003). Therefore when present, the spatial distribution and vertical relief of antecedent topography have considerable potential control on the structure supporting modern mesophotic coral veneers. The topographic peaks of ancient reef structures have been shown to provide protected hard-ground habitats for potential coral colonization (Locker et al., 2010). A relic reef discovered off the coast of Barbados was found to be covered with some scattered mesophotic coral reefs (Macintyre et al., 1991). Presently, the relationship between potential antecedent topography and the mesophotic reefs south of St. Thomas have not been resolved. Hubbard et al. (2008) suggested that rapid sea-level rise and high southerly off-shelf transport would have prevented the buildup of late Pleistocene reefs. Alternatively, former reef topography may have been lost as a result of bioerosion rate increases facilitated by high nutrient levels (Adey and Burke, 1976).

New antecedent topography analysis

To examine a possible relationship between the distribution and geomorphology of USVI mesophotic reefs and antecedent topographical highs, ArcGIS 10.1, a geographical information system program, was used. Bathymetric cross-sectional profiles of different mesophotic reef habitats precisely matched up with related seismic profiles to determine if modern USVI mesophotic reefs are located atop antecedent highs. Given the high cost of conducting seismic surveys, seismic interpretation was conducted using data collected by the United States Geological Survey (USGS) in March 2009.

Of the seismic profiles conducted (Fig. 1.6), only two were useful for comparison to the mesophotic geomorphology analyzed in this study. The first profile (Fig. 1.6, line a) extends across and beyond the mapped out mesophotic habitats (Fig. 1.7a). Cutting the profile to examine just the mesophotic habitat section (Fig. 1.7b) allowed for a more accurate assessment. No resolvable structure was identified below modern surface hillock structures in the mesophotic basin (Fig. 1.7c). Despite a drop at the northern section of the Secondary Bank (Fig. 1.7d), the dominance of linear bedding in the seismic profile suggests little antecedent topographic high. Potential sloping seismic reflections align with southern Secondary Bank bathymetry, but not enough to confirm the existence of antecedent topography (Fig. 1.7e). No subsurface features were correlated with the Deep Patch habitats (Fig. 1.7f).

The second seismic profile does not directly intersect the mesophotic habitat study area but does cross over geomorphic features assumed to be extensions of adjacent study area habitats (Fig. 1.6, line b). From north to south, the deep drop-off into the Anegada Passage and two topographic highs, probably representing the Primary and Secondary Banks, are observed in cross-sectional bathymetry (Fig. 1.8). Examination of a strong seismic reflection (red line in Figure 1.8) does not appear to have significant relief correlation with the two modern mesophotic banks, except a slight potential mound below the Primary Bank. A gradual slope deeper in the subsurface (red arrows in Figure 1.8) may represent the south dipping lower units of semi-consolidated Pleistocene sediment interpreted by Holmes and Kindinger, (1985).

The analysis of two seismic profiles yielded no substantial evidence to suggest that the structure of the mesophotic reefs, as defined by their bathymetric

geomorphology, is correlated to the underlying Pleistocene antecedent topography.

However, the resolution of available seismic profiles and the lack of additional profiles

associated with the main study site prevent conclusive results. More data and habitat

mapping is needed to better address this question.
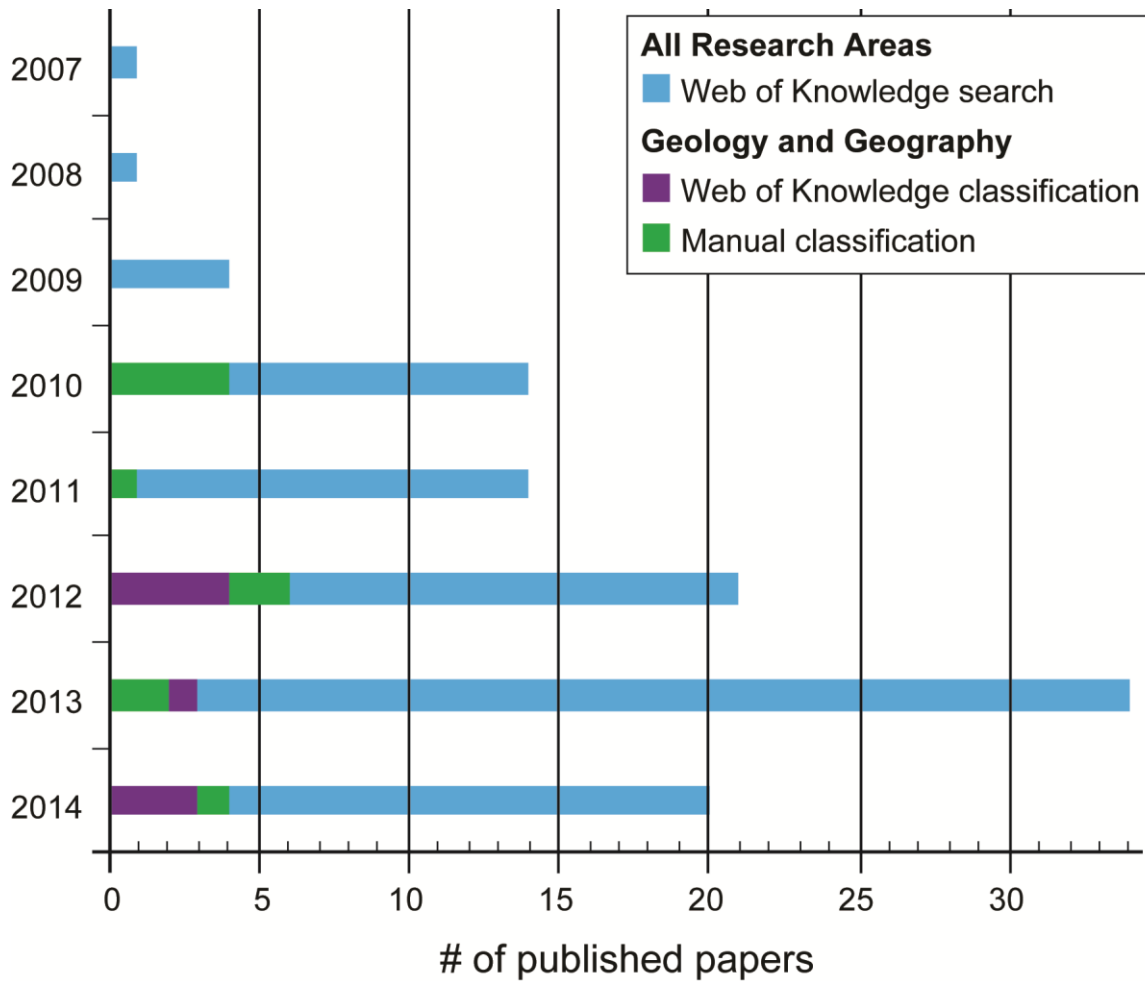
Figure 1.1 Mesophotic reef publications. Number of publications associated with mesophotic coral reef research per year, as identified using the academic search service *Web of Science* (© 2014 Thomson Reuters). A full database search was conducted on November 16, 2014. The search criteria for all categories (blue bars) entailed the phrases "mesophotic coral," "mesophotic reef," or "mesophotic coral ecosystem" were located in the publication title, abstract, author Keywords, or Keywords Plus categories. The initial search was then refined with two methods: (1) filtering the list using search program software to include only paleontology, geology, or geography research areas (purple bars); and (2) manually evaluating each of the initial 109 papers to determine which publications could be classified as relating to geology and/or geography (green bars).
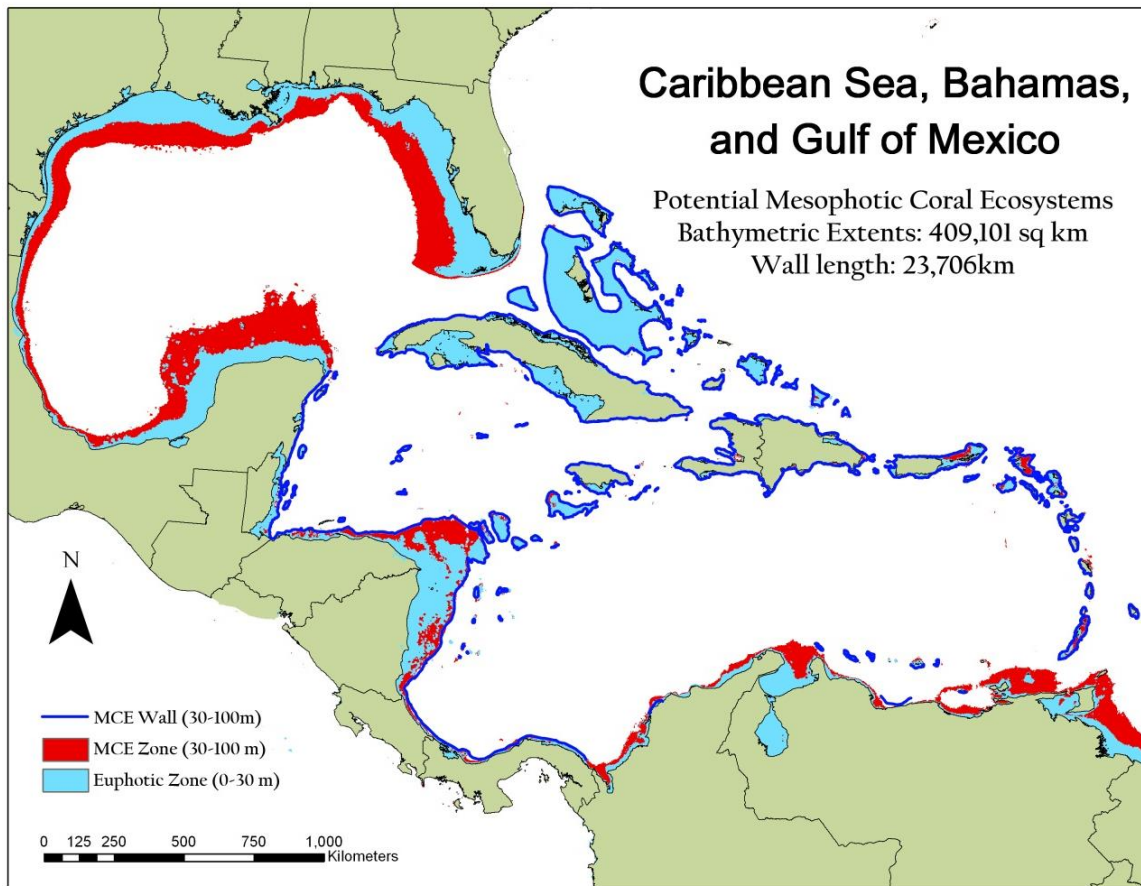
Figure 1.2 Potential Caribbean mesophotic coral reef locations. Estimated potential area coverage of mesophotic "wall" and basin habitats in the Caribbean Sea, the Bahamas, and the Gulf of Mexico (modified from Ginsburg et al., 2012). Potential mesophotic habitats were included based on locations where water conditions were known to be conducive for coral reef development and whose fine-scale bathymetry indicated depths between 30-100m.
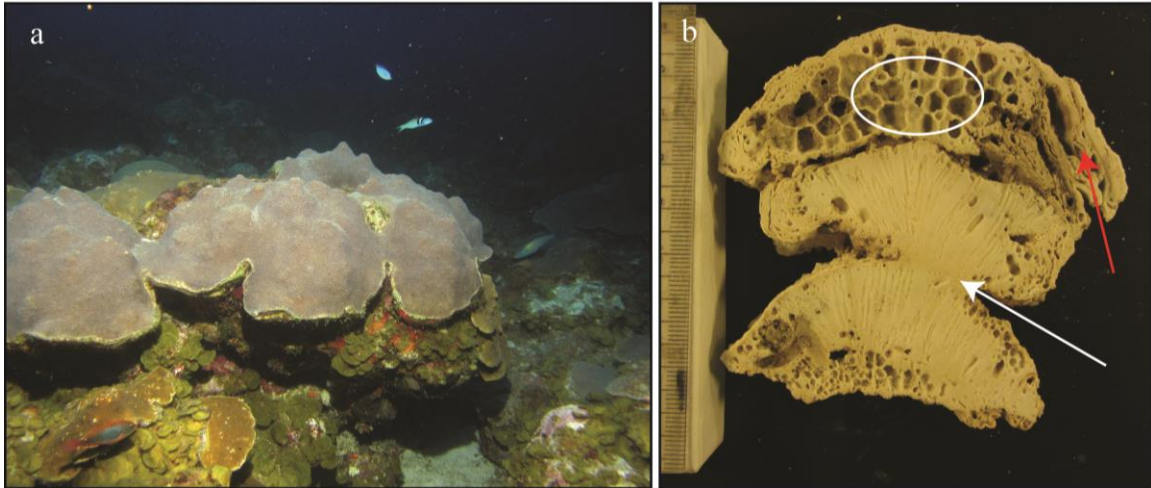
Figure 1.3 Mesophotic reef platy coral morphology. Examples of the most common coral morphology types found in mesophotic coral reefs. (a) Living platy *Orbicella annularis* species complex from the USVI Secondary Bank, ~31.0 m below sea-level (Smith et al., 2010). (b) Cross section of coral rubble dominated by the species *Stephanocenia intersepta,* collected at the USVI Hillock Basin in ~44.5 m deep water. The white arrow indicates partial coral mortality common at the site, where the coral community reinitializes skeletal growth at a later time period. The upper (youngest) section of the sample is heavy eroded by the boring sponge *Cliona* spp (white circle) and covered by secondary accretion of crustose coralline algae (red arrow). The time needed for this amount of bioerosion and secondary accretion suggests a minimum approximate exposure time of 5-10 years after death. The position of the more heavily bored, younger coral on top of the other skeletons likely prevented significant erosion of the lower skeleton by similar endolithic boring organisms.
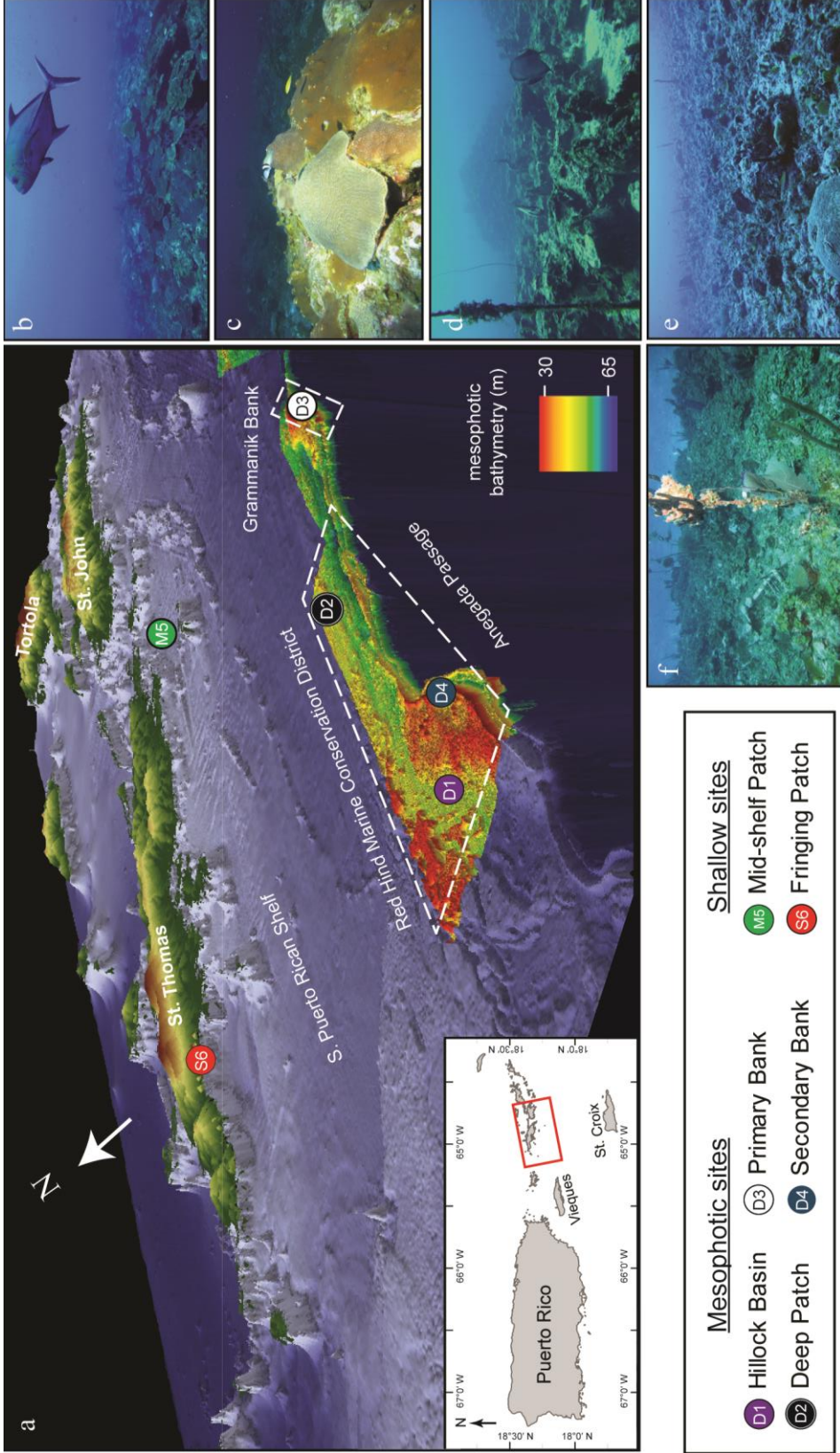
Figure 1.4. Study location. (a) South Puerto Rican Shelf 1 m resolution multi-beam bathymetry map (with 20x vertical exaggeration), with precise location identified by red box of inset map. Islands on bathymetry map are part of the U.S. Virgin Islands (St. Thomas and St. John) or the British Virgin Islands (Tortola). White dotted line-enclosed areas show extent of marine conservation areas. Locations of the six main study sites are indicated by color-labeled circles. Photos show representative reefscape of the: (b) Primary Bank; (c) Secondary Bank; (d) Hillock Basin; (e) Deep Patch; and (f) Mid-shelf Patch.
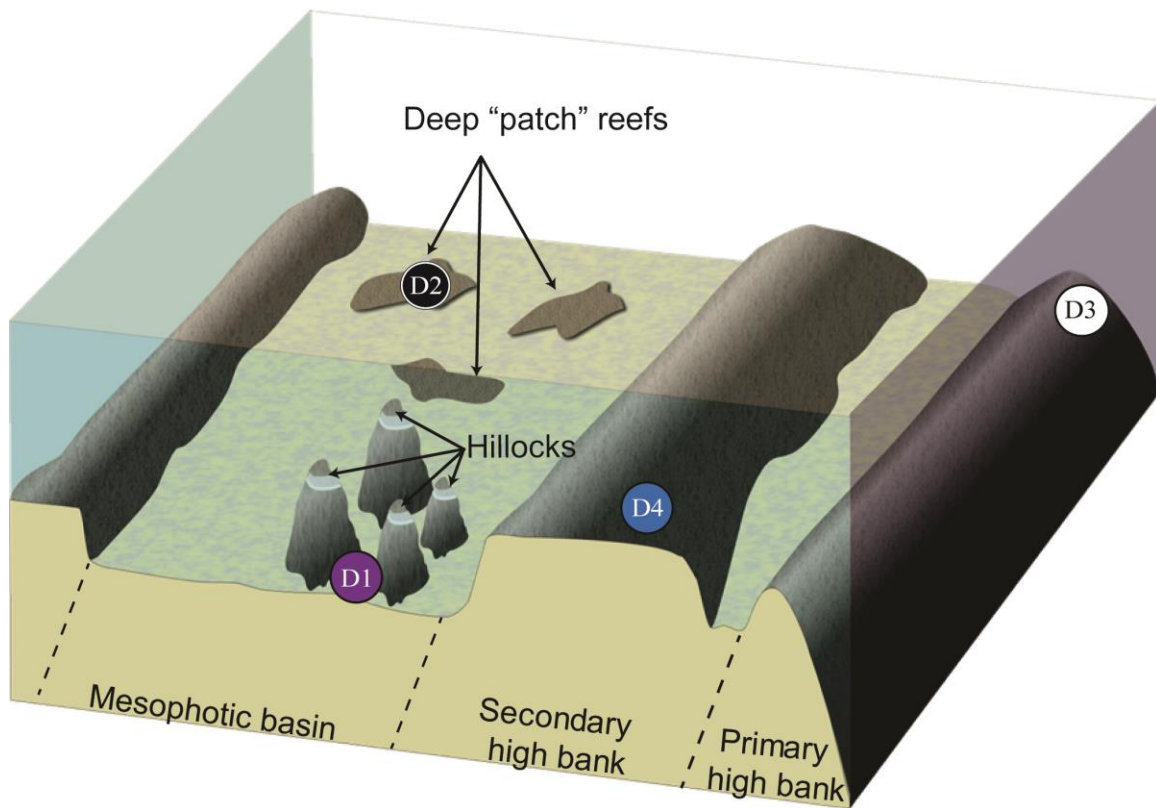
Figure 1.5. Mesophotic geomorphic habitats. Diagrammatic representation of the benthic mesophotic habitats analyzed in this study. The cartoon is not to scale but does show the relative position of each site with respect to the others. White bands on hillocks depict episodic instances of partial mortality.

Table 1.1. Study site characteristics. Bathymetry, depth, location, rugosity, and benthic coverages,[*] and rugosity from 2012. Depths in table were measured at the site locations where quadrats were installed. The relative live coral cover percent of the *Orbicella* spp. (OACX) is also indicated. The exposed substrate category consists of dead coral, rubble, boulders, pavement, and surfaces covered by macroalgae. Average benthic (number of transects displayed in table) and rugosity measurements (three transects per site) were based on independent, randomly oriented (10 m and 3 m respectively) linear transects. For statistical precision, the greatest number of individual transects available were used to find site means. Following the methodology of Smith et al. (2010), videos of linear transects were taken by the United States Virgin Islands Territorial Coral Reef Monitoring Program (TCRMP), except at the Fringing Patch (conducted by dissertation author). All benthic data sets were processed from non-overlapping still images derived from video, where the benthic percent covers for each image were estimated from ~250-400 randomly placed individual points using Coral Point Count with Excel Extensions V3.6 (Kohler and Gill, 2006). Point count analysis was conducted by TCRMP at four sites and by the dissertation author and UM undergraduate student Jessica Wingar for the Deep Patch and Fringing Patch sites. Values are reported with ± 1 standard error.

Geomorphic habitat	Site depth (m)	Location Lat.	Location Long.	Rugosity	Benthic transects	Live coral (% OACX)	% Cover G. Algae/ R. Algae	% Cover Exposed substrate	% Cover Sand
D1 Hillock* Basin	44.5	18.199311	-65.086046	1.84 ± 0.44	3	12.99 ± 4.17 (91.67 ± 0.31)	45.42 ± 1.74 15.10 ± 2.22	67.70 ± 4.47	9.99 ± 3.16
D2 Deep Patch	41.1	18.214170	-64.999010	1.13 ± 0.02	3	1.79 ± 0.81 (0.00 ± 0.00)	54.01 ± 6.56 12.36 ± 3.20	82.83 ± 3.66	0.28 ± 0.18
D3 Primary Bank	39.0	18.189156	-64.956452	2.62 ± 0.63	6	32.20 ± 2.59 (81.75 ± 0.08)	34.28 ± 1.40 5.89 ± 0.93	55.68 ± 2.26	4.07 ± 1.77
D4 Secondary Bank	30.7	18.185590	-65.076340	1.55 ± 0.14	6	33.73 ± 2.54 (88..78 ± 0.07)	36.80 ± 1.64 8.94 ± 1.03	58.31 ± 2.66	1.05 ± 0.46
M5 Mid-shelf Patch	21.0	18.294380	-64.867930	1.18 ± 0.04	42	18.26 ± 0.60 (71.47 ± 0.03)	54.20 ± 2.68 2.04 ± 0.36	73.68 ± 0.77	2.58 ± 0.52
S6 Fringing Patch	9.0	18.346450	-64.986690	1.24 ± 0.01	3	3.19 ± 0.76 (6.68 ± 0.03)	37.04 ± 3.71 0.34 ± 0.34	93.66 ± 1.53	0.11 ± 0.11

* Benthic coverage results based on surveys conducted in 2007 survey

Table 1.2. Site differences. Statistical results of one-way Kruskal-Wallis non-parametric comparison tests and related multiple pairwise comparison tests (see text). Sites with different letters indicate significant difference for the given factor. A represents the greatest value, followed by B and C, respectively.

Factor	d.f.	X^2 value	P value	Hillock Basin (D1)	Deep Patch (D2)	Primary Bank (D3)	Secondary Bank (D4)	Mid-shelf Patch (M5)	Fringing Patch (S6)
Coral cover	5	38.600	<0.001	AB	B	A	A	B	B
Exposed consolidated substrate	5	39.161	<0.001	BC	AB	C	C	AB	A
Rugosity	5	12.924	0.024	AB	AB	A	AB	B	AB
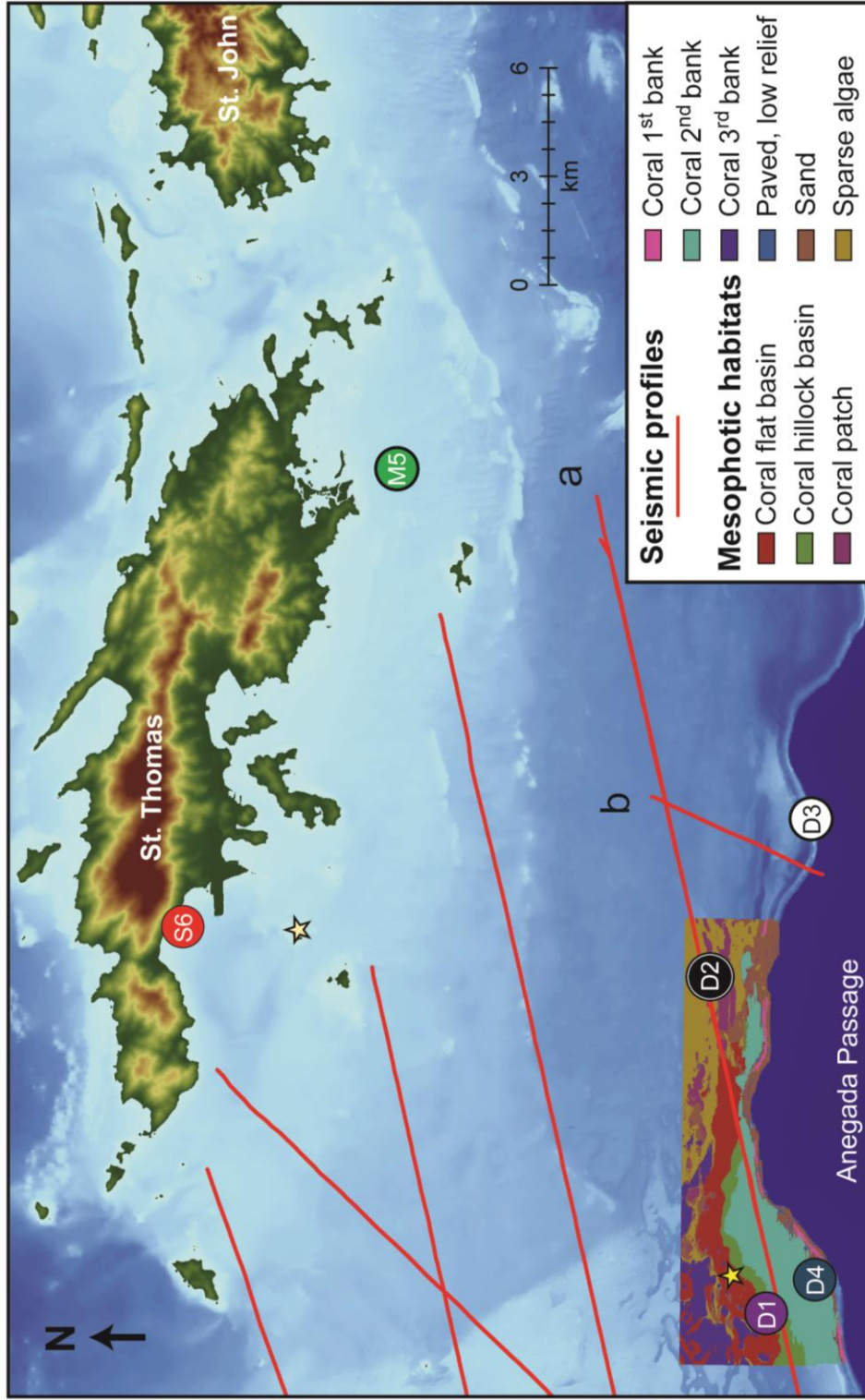
Figure 1.6. Mapping mesophotic habitats and seismic profiles. Map of North U.S. Virgin Islands, mesophotic reefs (with RHMCD benthic habitat classifications modified from Smith et al., 2010), and locations of seismic profiles (red lines) conducted by the USGS. Locations of main study sites are indicated by color-labeled circles (see Figure 1.4 key for study names). Star symbol in the mesophotic region indicates location coral samples were collected at the Flat Deep Basin. The other star indicates the location of Flat Cay, a well-known local shallow reef site (not sampled for this dissertation).
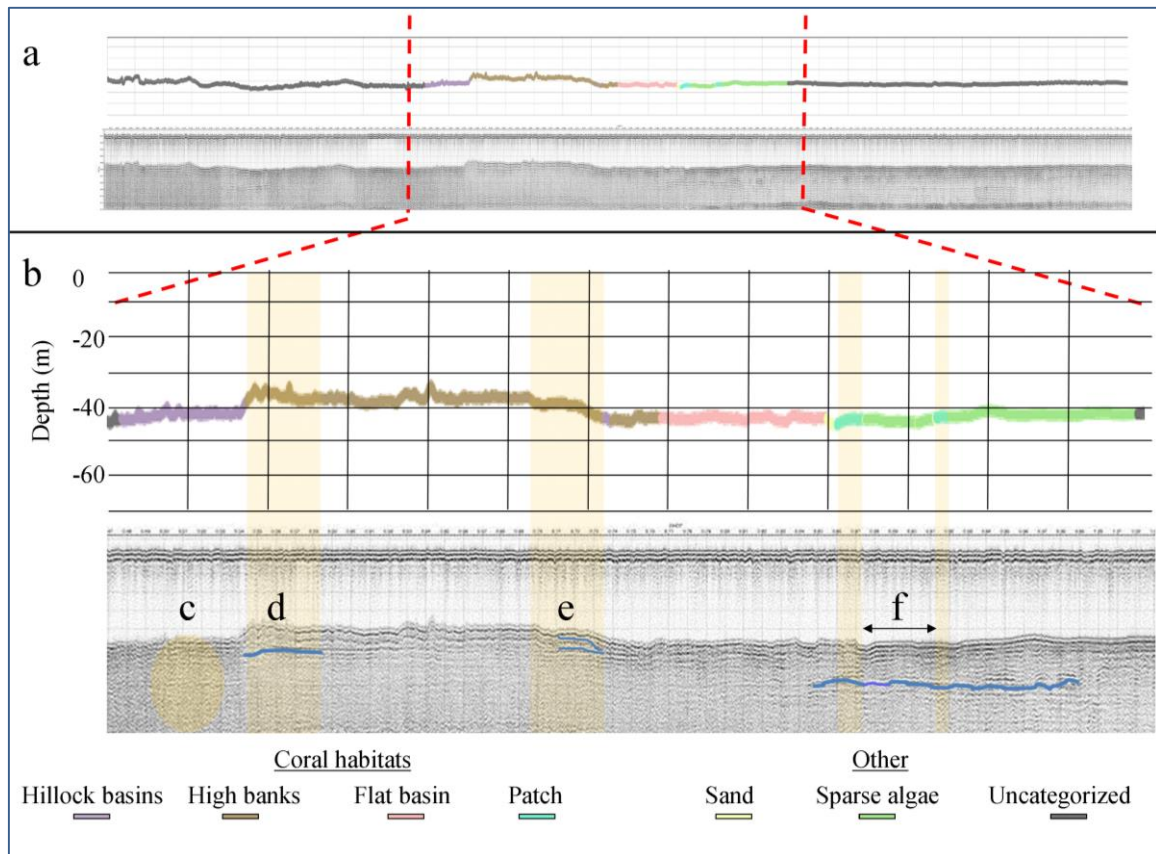
Figure 1.7. Seismic profile across mesophotic reefs. Comparison between shelf bathymetry from map (Fig. 1.4) and seismic profile (below it). (a) Entire seismic profile line "a" from Figure 1.6. (b) Section of seismic profile that aligns with mesophotic habitat coverage data. Highlighted areas (c-f) and thicker blue lines are referred to in the text.
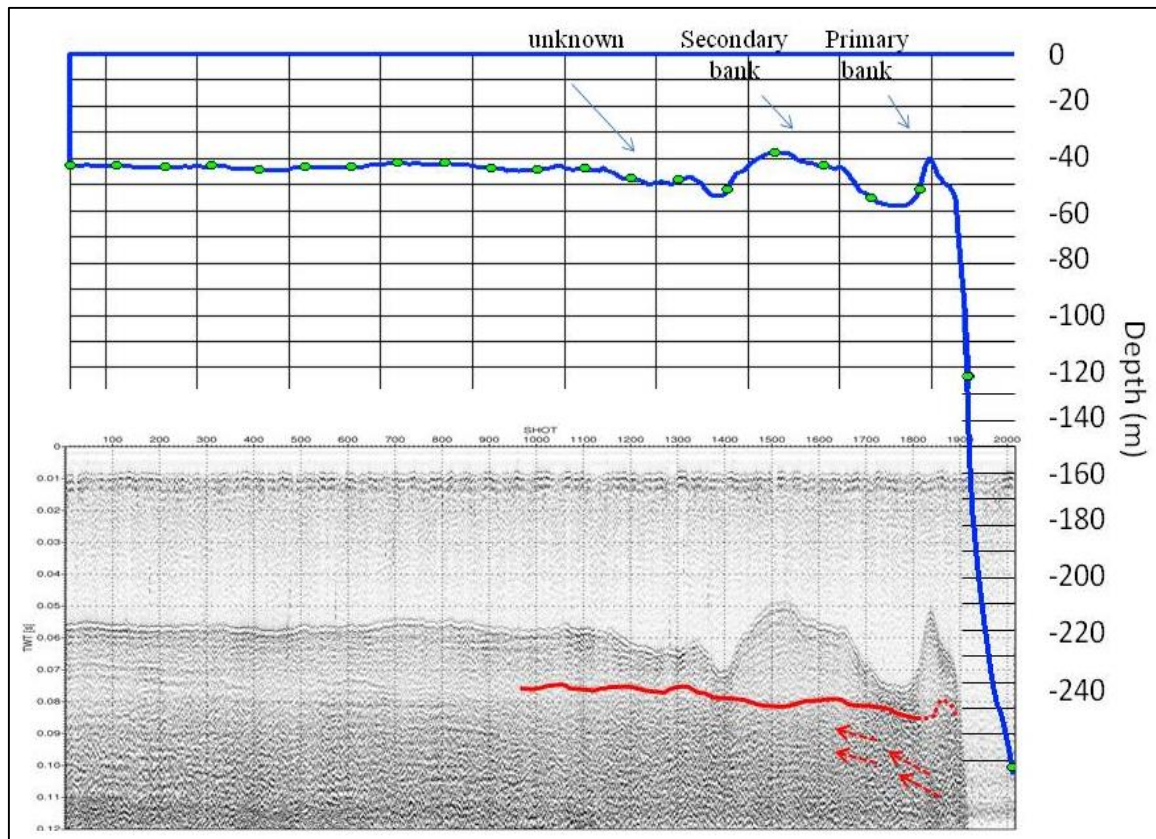
Figure 1.8. N-S seismic profile. Comparison between bathymetry (blue line on top) from digital elevation model, processed with ArcGIS software, and seismic profile of line "b" from Fig. 1.6. Green dots on line indicate locations of shot numbers used to align map with seismic scan. Red line indicates a strong seismic reflection. Additional interpretation of seismic profile is found in text.

CHAPTER 2. SEDIMENT AND CEMENTATION CHARACTERIZATION OF MESOPHOTIC REEF HABITATS

Chapter summary

Consisting of reefs with different structural characteristics, the low-angle, outer insular shelf mesophotic coral ecosystem south of the northern U.S. Virgin Islands provides an ideal location to study the relationship between habitat complexity and mesophotic coral reef sedimentary facies. Textural, compositional, and geochemical analysis of surface sediment were used to determine if sedimentary facies can distinguish different mesophotic habitats and determine the relative control biological and hydrological processes have on sediment production and deposition. Based on sedimentary characteristics, unique carbonate subfacies were identified at mesophotic reef habitats with differing geomorphology. Sediment grain composition and bulk geochemistry were found to broadly record the distribution and abundance of foundational mesophotic benthic organisms. Analysis indicated that hydrodynamic forces do not transport a significant amount of allochthonous sediment or potentially harmful terrigenous material to mesophotic reefs. Differences in bioerosion intensity and mechanism were found to predominately control size partitioning of sand grains lacking entrainment potential under maximum current velocities. Subtle differences in autochthonous grain composition and abundance indicate the relative importance and interaction of biological processes with hydrologic conditions.

Background

High coral reef biodiversity is in part a product of habitat heterogeneity and complexity. Reef building and eroding organisms such as coral, parrotfish, and crustose coralline algae (CCA) have the ability to alter habitat structural complexity, localized

hydrodynamic conditions, and overall surface area (Roberts and Ormond, 1987; Bruno and Bertness, 2001). Structural complexity increases marine ecosystem biodiversity by partitioning sub-habitats sheltered from environmental stresses that would otherwise prevent habitation by many organisms (Thompson et al., 1996) and by improving retention of propagules (Eckman et al., 1989).

In addition to shallow-water coral reefs, a direct relationship between habitat structural complexity and diversity is well known in most other aquatic and terrestrial environments (MacArthur and MacArthur, 1961; Rosenzweig and Winakur, 1969; Heck and Wetstone, 1977; Hicks, 1980). Thus, similar relationships are highly plausible for mesophotic coral reef ecosystems. Studies documenting MCE taxonomic richness (Reed and Pomponi, 1997; Cerrano et al., 2010; Bridge et al., 2012b; Breedy and Guzman, 2013) suggest biodiversity in these deeper reef systems is a significant ecosystem attribute (Lesser et al., 2009; Puglise et al., 2009; Bridge et al., 2012a).

Sedimentary facies analysis is often used to understand factors that effect the physical and biological diversity of coral reef ecosystems. These factors include hydrodynamic particle movement (Kench and McLean, 1996; Kench, 1998; Fiechter et al., 2006), biological deposition patterns, and overall carbonate accretion and reef geomorphology at different time scales (Perry et al., 2008; Rankey et al., 2011; Harris et al., 2014). Therefore, analysis of mesophotic reef sedimentary facies is needed to understand how the biological and physical processes dictating surface sediment attributes affect habitat heterogeneity and as a result, mesophotic biodiversity.

Modern carbonate sedimentary facies analysis is also a proven geological tool for studying ancient reef deposits (Ginsburg, 1974; Wilson, 1975; Abbey et al., 2013).

Specifically, facies analysis has been used for interpreting: (1) paleoecological and habitat heterogeneity evolution of analogous fossil shallow-water reef deposits (Edinger and Risk, 1994; Insalaco et al., 1997; Klaus and Budd, 2003; Hubbard et al., 2005); and (2) modern and ancient carbonate shelf and platform development (Grammer, 1991; Pomar, 2001; Aurell and Bádenas, 2004; Brandano et al., 2009; Riegl and Purkis, 2009). Cenozoic to Holocene fossil reef deposits have only recently been labeled "mesophotic" (Dill et al., 2012; Mateu-Vicens et al., 2012; Morsilli et al., 2012; Abbey et al., 2013; Novak et al., 2013; Mihaljević et al., 2014). In addition, some earlier studies have been conducted at least partially on deposits simply referred to as "deeper" or interpreted to be from specific depths and conditions similar to those that constitute the modern definition of mesophotic reefs (Mesolella, 1967; Robinson, 1969; Bosellini and Russo, 1992; Insalaco, 1996; Bosellini, 1998; Klaus et al., 2011). However, virtually no modern analog studies exist to verify and better interpret these and other ancient deep reef deposits. Therefore, detailed paleoecological interpretations of mesophotic reef depositional environments are sparse compared to shallow-water reefs. This dearth of research limits the ability to obtain a solid understanding of mesophotic coral reef evolutionary history and the origins of deep and shallow-water reef biodiversity.

Previous studies of deep reef sediment

The few studies that have been conducted with the potential to aid MCE sedimentary facies interpretation usually derive from the deepest sample collection along a transect perpendicular to the coast. These studies have been conducted in the Great Barrier Reef of Australia (Scoffin and Tudhope, 1985), the Caribbean (Hoskin et al., 1986; Boss and Liddell, 1987; Perry, 1996), and the Red Sea (Montaggioni et al., 1986).

More comprehensive deep reef sedimentary analyses are even less common (Goreau and Goreau, 1973; James and Ginsburg, 1979; Grammer, 1991).

Sediments along deep, steep-slope fore-reefs are typically composed of coarse/medium grained skeletal sand derived from varying amounts of coral, CCA, *Halimeda*, foraminifera, mollusks, and echinoderms with moderate to poor sorting (Longman, 1981; Hoskin et al., 1986). In addition, sediment mean grain size and sorting have been found to decrease with depth on the deeper Jamaican fore-reefs (Perry, 1996). Somewhat in contrast, leeward reef margin surface sediments from the central region of the Great Barrier Reef between 20-60 m deep were identified primarily as course-grained sand, but were of similar composition to sediment from other Pacific and Caribbean reefs (Scoffin and Tudhope, 1985).

Compilation of sediment data within reef environments at mesophotic depths and general assumptions about these habitats have led to implications that mesophotic reef steep-slope sedimentary deposits can mostly be characterized by one facies type. Due to a low diversity in grain producers, mesophotic depth ranges have been suggested to have less potential sedimentary facies variability than their shallow-water reef counterparts, when assigned equivalent Dunham (1962) carbonate categories (Purkis et al., 2014). However, Boss and Liddle (1987) found that overall sediment composition largely reflected reef community composition patterns, and they used this observation to delineate two different reef facies at modern mesophotic depths. Seven distinct facies were also identified from sedimentary analysis within the 60-100 m depth range of the central region of the Australian Great Barrier Reef (Scoffin and Tudhope, 1985). Regardless, discrepancies in identifying and understanding mesophotic reef sedimentary

facies and limited datasets greatly impede comparative carbonate analysis. Adding to these difficulties is the recognition that deep reef-slope facies are often the most difficult of all reef complex facies to identify in ancient deposits (Longman, 1981).

Reef cementation

The importance of submarine lithification in coral reefs is a relatively new concept, existing for only 40-50 years (Macintyre and Marshall, 1988). Since that time, subtidal lithification has been recognized in reefs globally. These include reefs near Belize (James et al., 1976; James and Ginsburg, 1979; Shinn et al., 1982), Bermuda (Ginsburg et al., 1971; Ginsburg and Schroeder, 1973), Panama (Macintyre and Glynn, 1976b), Jamaica (Land and Goreau, 1970; Mitchell et al., June, 1987), Barbados (Macintyre et al., 1991), the Red Sea (Friedman et al., 1974), and Australia (Marshall, 1986). Though lithification constitutes several processes which convert unconsolidated sediment into rock, cementation is recognized as the most important process in coral reefs (Marshall, 1983b; Tucker and Wright, 1990).

Beyond contributing to early coral reef diagenesis, reef cementation is believed to encourage reef development both by producing new available substrate for benthic colorization and by maintaining modern and ancient reef structure (Marshall, 1983b). Cements have been known to strengthen reef structure by coating branching and platy corals, filling cavities between reef framework, and forming within cavities created by boring organisms (Macintyre and Marshall, 1988). The binding of coral reefs is greatly facilitated by diagenetic cementation and biotic activity from bryozoans, bivalves, CCA, serpulid worms, foraminifera, and gastropods (Rasser and Riegl, 2002). A study in the eastern tropical Pacific found less framework cementation in reefs subjected to lower as

opposed to higher carbonate saturation states (Manzello et al., 2008). Lower cementation rates were suggested to have potentially facilitated high, previously recorded bioerosion rates (Reaka-Kudla et al., 1996), demonstrating the potential difficulties of maintaining coral reef framework rigidity in a world with higher carbon dioxide (CO_2) concentrations than those found at most modern coral reefs.

The primary mechanisms proposed for coral reef marine cementation are: (1) the physical-chemical model, where calcium carbonate supersaturation stimulates precipitation; and (2) the biological and microbial model, where microorganisms alter localized seawater chemistry to facilitate the formation of cements (Macintyre and Marshall, 1988). Reef cement mineralogy typically consists of Mg-calcite, aragonite (Macintyre and Marshall, 1988; Scoffin, 1992), and dolomite, which is rare in modern reef environments (Mitchell et al., 1987). Mg-calcite reef cements are usually the most abundant and are found as bladed spar, acicular-bladed fringes, micrite, and peloids (Marshall, 1983a; Perry and Hepburn, 2008). Aragonite reef cement usually forms as equant crystals (micrite), acicular crystals in isopachous fringes or fans, and botryoids, and it mostly occurs intra-skeletally (Marshall, 1983b; Tucker and Wright, 1990). Marine cements have been identified in all major reef habitats. Specifically, they are found in high wave-energy (agitation) areas on seaward margins (Marshall, 1983b; Macintyre and Marshall, 1988), and reefs with low sedimentation rates, high rock permeability and porosity, or slow framework accumulation rates (Lighty, 1985).

Syndepositional cementation of reef sediment is believed to be partially influenced by wave conditions (Marshall, 1983a; Macintyre and Marshall, 1988), suggesting variations in cement abundance, density, or texture may record past

hydrodynamic conditions. Relatedly, successful reef sediment facies interpretations rely on the stabilization and preservation of deposited sediments and reef framework through submarine lithification (Perry, 2000). At the least, the accuracy of reef-sediment-based paleoenvironmental and paleloecological facies interpretations requires identifying if diagenetic alterations may have resulted in misconstruing or eliminating the depositional history.

The rate of syndepositional marine cementation is also considered a fundamental question when considering reef resistance to mechanical erosion, carbonate platform development, and the evolution of porosity in carbonate systems (Marshall, 1983a; Grammer et al., 1993; Grammer et al., 1999). Geologically "rapid" cementation has been reported in shallow-water reefs (Ginsburg et al., 1971; Friedman et al., 1974; James et al., 1976), and deeper reefs (Land and Goreau, 1970; James and Ginsburg, 1979). Rates of cement growth average from 8-10 mm per 100 years along steep marginal fore-reef slopes in the Bahamas and Belize (Grammer et al., 1993). Cementation was directly observed within planted mesh sediment bags placed along the windward side of Lee Stocking Island, the Bahamas, within eight months at water depths of up to 60 m (Grammer et al., 1999). However, there is little known about cementation rates, forms, and amounts in varying mesophotic reef habitats and about the effect cementation could have on structural development.

Objectives

The mesophotic reefs of the USVI developed on a low-angle shelf margin that provides space for reefs with architecturally distinctive structures. Here, we present a detailed characterization and interpretation of the sedimentological features (sediment

composition, grain size, and cement type) found within mesophotic reef habitats with different structures. The objectives of this chapter are to: (1) categorize and compare mesophotic reef sediment composition, grain size, and basic geochemistry; (2) assess if low-gradient shelf mesophotic reef systems produce recognizable sedimentary subfacies reflective of habitats with distinct structurally characteristics; and (3) determine the significance of these potential facies differences in terms of biological and hydrodynamic processes. The ability to identify causes and indicators of habitat heterogeneity and structural complexity in modern MCEs is an essential first step in understanding the evolution, development, and maintenance of these attributes in ancient reef systems and the origins of modern coral reef biodiversity patterns (Hodgson and Smith, 1990; Flügel and Flügel-Kahler, 1992; Budd, 2000; Pomar and Hallock, 2008; Renema et al., 2008; Klaus et al., 2011; Morsilli et al., 2012).

Methods

Field sampling

In August 2011, technical research divers scooped the top 2-3 cm of sediment and water into plastic 150 ml jars at each study site (Fig. 1.4) and brought them to the surface for analysis. Each of the 28 total jars collected (three to six per site) is considered to be an independent sediment sample. At some of the sites (D2, D3), sediment was collected in the vicinity of previously deployed Nortek Aquadop Acoustic Doppler Current Profilers (ADCPs) that record hourly current velocities 1.5-2 m above the seafloor (Smith et al., 2011). ADCP measurements from a nearby reef (the Hind Bank site, from Smith et al. 2010) were used as a proxy for the Deep Patch site and were assumed to be a good representation of the site. No ADCP data were available for the Secondary Bank site but

frequent observations (Smith et al., 2011) indicate bottom velocities are similar or slightly stronger than those recorded at the Primary Bank site.

The maximum current and the mean current of all hours recorded per spring-neap tidal cycle (estimated as 15 days) were determined from ADCP measurements. For each site where ADCP measurements were available (D1, D2, and D3), the average of each spring-neap tidal cycle current velocity mean ($\overline{CV}_{mean}$) and the average of each spring-neap tidal cycle current velocity maximum ($\overline{CV}_{max}$) were calculated between February 1, 2008 and January 31, 2009. These measurements were subdivided to distinguish trends between the summer (May-November) and winter (December–April) seasons. Assuming a bed roughness length (z_0) of 0.3 mm (Soulsby, 1997), the von Karman-Prandtl law-of-wall equation (with Karman constant $\kappa = 0.4$) was first used to calculate shear velocity (u_*) for each hourly recorded current velocity. The equation was then used to recalculate $\overline{CV}_{max}$ to account for boundary layer conditions $z = 25$ mm above the seafloor so empirical relations derived by Kench and McLean (1996) could be applied. This procedure assumes all recalculated current velocities above the seafloor are only as unobstructed by surrounding topography as the original ADCP measurements, minus assumed bed roughness (z_0).

To characterize syndepositional cementation, nylon mesh bags (50 µm) filled with unaltered ooids were placed at each study site in August 2011, following a similar procedure used by Grammer et al. (1999). String was used to attach four Bahamian ooid-filled mesh bags to a rebar post, with two bags placed on the seafloor and two hung approximately 1 meter above the seafloor. Ooids were selected for their uniform carbonate texture. Prior to deployment, the surfaces of the ooids were examined with a

scanning electron microscope (SEM) to confirm the absence of cement (Fig. 2.1). Half of the mesh bags were collected in May 2012 and the remainder in May 2013. Upon collection, the bags were washed with distilled water, to remove any salt deposits, and dried.

Bulk mineralogy

Sediments from each sample jar that passed through a 2 mm mesh sieve were ground into powder with a mortar and pestle. A small amount of ground sediment from each site was saved for mineralogical and isotopic analysis. To determine the carbonate percentage of the collected sediments, ~3 g of powder from each sample were immersed in a 10% HCL solution for 24 hours (Pilkey et al., 1967). This process was repeated until no further dissolution was observed. Samples were then rinsed in deionized water three times, dried in an oven at 55°C for three days, and weighed to determine the percent of carbonate removed. The samples were then placed in a Barnstead Thermolyne furnace set at 550°C for two hours. After cooling, the reweighed value of each sample was subtracted from the pre-furnace weight to determine the amount of organic material (assumed to be removed through ignition).

The bulk carbonate mineralogy per sample was determined by assuming samples were composed entirely of aragonite, high-Mg calcite (HMC), low-Mg calcite (LMC), dolomite, and quartz (Swart and Melim, 2000). X-ray diffraction (XRD) scans between 23° and 32° 2θ (CuKa radiation) were conducted on smear mounted powdered sediment from each sample. Standard relationships between percent mineral and peak area were compared to sample peaks to determine the percentage of each mineral in the samples.

Sediment composition

To quantify sediment composition from study sites, bulk sediment samples were passed through a 2 mm mesh sieve, impregnated with resin, and thin-sectioned. Three thin sections (randomly selected from the three to six collected samples per site) were analyzed from each site. Six photographs were taken at non-overlapping locations on the thin section from each sample with an Olympus BH2 series microscope. Standard point-count analysis (Ginsburg, 1956) was conducted on each of the six photographs using the program JmicroVision (Roduit, 2008). Sediment under each point was classified based on descriptions from multiple sources (Ginsburg, 1956; Pusey, 1975; Scholle, 1978; Adams et al., 1984). Rarefaction analysis indicated that 300 points per thin section (50 randomly selected per picture) was sufficient for detailed statistical analysis (Boss and Liddell, 1987a). Using the arcsin transformation, data were corrected to meet statistical test assumptions of normality and homoscedasticity.

One-way analysis of variance (ANOVA) tests were conducted to determine significant univariate differences per site for each grain type. Specific pair-wise differences were identified using Tukey's Honestly Significant Difference (HSD) multiple comparison test. Pearson correlations were used to compare linear relationships between sediment types and depth. As mentioned in chapter 1, study site spatial benthic coverage data lacked normal distributions. Therefore, Spearman correlations were used to compare the relative percentage of major grain types (coral, green algae, and red algae) found within collected surface sediment per sample (3 per site), with the equivalent type of benthic percent cover at the site the sample was collected from. Overall differences in grain compositions were also assessed by calculating pair-wise distances between sites

with the Bray Curtis dissimilarity index, and visualized by non-metric multidimensional scaling (NMDS) of the ordination matrix with PAST statistical software (Hammer et al., 2001). All other statistical analyses pertaining to sediment composition were conducted using the program R version 3.0.3 (R Core Team, 2014).

Stable carbon and oxygen isotopes

The bulk stable oxygen and carbon isotope concentrations of each sample were determined by the common acid bath method (Swart et al., 1991). Phosphoric acid dissolution of ground-up samples (~0.5-1 mg each) produced gas analyzed with a Finnigan-MAT 251 mass spectrometer at the University of Miami Stable Isotope Laboratory. Results were corrected for isobaric interference (Craig, 1957). Stable isotopic concentrations are reported relative to the standard Pee Dee Belemnite (PDB). Replicate error analysis of internal inorganic δ^{13}C and δ^{18}O standards produced an average standard deviation less than 0.1‰. Study stable carbon and oxygen isotopic concentration data were found to be normally distributed and homoscedastic. Therefore, the statistical program R version 3.0.3 (R Core Team, 2014) was used to test for significant univariant site differences using one-way ANOVA. Multiple comparisons of significant ANOVA test results were conducted using Tukey's HSD methodology.

Grain size

Standard wet sieving techniques were used to conduct grain size analysis (Folk, 1974a). Approximately 5-20 g of sediment from each of the 28 samples were passed through a series of sieves (mesh sizes 4, 2, 1, 0.5, 0.25, 0.125, and 0.63 mm). Each sieve fraction was then dried at 55° C and weighed. Standard textural parameters (mean grain size, sorting, skewness, and kurtosis) were obtained using the program GRADISTAT

(Blott and Pye, 2001). This program uses linear interpolation on parameters obtained through a graphic method (Folk and Ward, 1957). Standard descriptive terminology was used for grain size (Friedman and Sanders, 1978) and for sorting, skewness, and kurtosis (Folk and Ward, 1957). With the statistical software program R version 3.0.3 (R Core Team, 2014), distribution normality and homogeneity of variance were confirmed, permitting one-way ANOVA tests for significant different textural parameter variance between sites. Tukey's HSD test was used for multiple comparisons if significant differences between sites were detected.

To investigate potential allochthonous sediment deposition, the settling velocity (w_s) of unconsolidated individual sediment grains of natural sand (with irregular shaped grains) hypothetically in suspension was estimated using the following empirically derived formula (Soulsby, 1997):

$$w_s = \frac{v}{d}\left[\left(10.362 + 1.049*\left[\frac{g(\frac{\rho_S}{\rho_f}-1)}{v^2}\right]^3\right)^{.5} - 10.36\right], \text{where}$$

kinematic viscosity of water $v = \frac{\mu}{\rho_f}$

dynamic viscosity (μ) = 1.08 poises

fluid density (ρ_f) = 1.023 g/cm^3 (at 40.5 m, with 27.9 C and 35.577 ppt)

grain (sphere) density (ρ_S) = 1.850 g/cm^3 (from Kench et al., 1998)

acceleration due to gravity (g) = 9.81 m/sec^2

For all three sites, fluid density (ρ_f) was calculated with a high pressure equation of state of seawater (Millero et al., 1980), using a representative depth, temperature, and salinity

of 40.5 m, 27.9 C, and 35.577 ppt, respectively.[1] The estimated settling velocities for unconsolidated fine sand grains (125 μm), very fine sand grains (104.4 μm), and sponge chip silt (with a mean diameter of 40 μm, Rützler, 1975) were calculated to be 0.677 cm/s, 0.477 cm/s, and 0.072 cm/s, respectively.

If present, unconsolidated suspended marine particles (sediment) would be expected to remain in suspension as long as the upward velocity of bottom turbulent eddies (v'_{up}) is greater than the settling velocity (w_s) of a particular grain (Bagnold, 1966). Bagnold (1966) also derived that v'_{up} is equal to 1.25 times the shear velocity (u_*). Together, these relationships imply that unconsolidated particles will remain in suspension as long as $w_s/u_* < 1.25$ (Cheng and Chiew, 1999). Therefore, the settling velocities (w_s) of hypothetical suspended particles with grain size diameters of 125μm, 104.4 μm, and 40 μm, were divided by previously calculated shear velocity values. Finally, the frequency, at different time intervals, in which currents were slow enough to permit the hypothetical particles to fall out of suspension were determined. These frequencies are considered valid when assuming associated current velocities experienced relatively little baffling from topographic obstructions for depths ≤3 m above the seafloor.

Currents of removal

Suspended particles have different properties than particles dispersed on the sea bed (McCave and Swift, 1976). To examine erosion and transport of surface sediment away from the reef study sites, a "currents of removal" approach (Kench, 1998) for

---

[1]Representative values based on average depth of analyzed sites, and average site temperature and salinity measurements obtained from semi-annual conductivity, temperature, and depth (CTD) casts taken and provided by the University of the Virgin Islands Center for Marine and Environmental Studies.

determining potential mobility (PM) was selected. This approach was chosen to reduce known shortfalls in hydrodynamic interpretation when solely applying standard grain size analysis to carbonate deposits (Gibbs et al., 1971; Komar, 1981; Kench and McLean, 1997; Smith and Cheung, 2002). To comply with PM analysis assumptions, the sieve sizes used for USVI grain size analysis were converted to equivalent spherical quartz settling velocities with the Gibb's equation (Gibbs et al., 1971). These values were then multiplied by a corrective factor of $R_D = 0.98$ (Komar, 1981), assuming an average grain density of $\rho_S = 1.850$ g/cm^3 (used for empirical relationships (Kench and McLean, 1996) from specific measurements, Jell et al. 1965). Original weights associated with the newly calculated sieve equivalent settling velocities were used to plot the mean cumulative settling velocity distribution curves for each site. Mean settling velocities were converted to the standard settling velocity chi (χ) parameter (May, 1981).

Kench and McLean (1996) defined threshold velocity as the average velocity recorded 25 mm above a flume bottom needed to move 50% of a heterogeneous reefal sediment fraction. As the hydrodynamic properties of heterogeneous sediment fractions tested were found to be very similar, Kench and McLean (1996) suggested that sediment fraction mobility could be characterized by a mean sediment settling velocity in chi (χ). The derived threshold curve from Kench and McLean (1996) is assumed to be an accurate proxy for this dissertation because the sediment used to develop the curve had similar compositional characteristics to reef sediment from the northern USVI.

Surface sediment PM was calculated using ACDP averaged spring-neap cycle maximum current velocities ($\overline{CV}_{max}$). Recalculated $\overline{CV}_{max}$ values 25mm above the seafloor were plotted as the independent variable of an asymptotic convex regression

equation fitted to the threshold curve from Kench and McLean (1996). The resultant dependent variable determines the largest mean particle settling velocity (representing a particular heterogeneous sediment fraction) that can be entrained at $\overline{CV}_{max}$. These largest mean settling velocities (in χ) were plotted as vertical lines on cumulative settling velocity distribution curves of the same site such that the vertical line intercepted the cumulative curve. The percent of settling distribution fractions above the curve/line intercept is defined as the PM of surface sediment from the site at $\overline{CV}_{max}$.

Cementation

Mesh bags were recovered at most sites both years, with the exception of: the Secondary Bank site; the year-one seafloor surface bag, and the year-two 1 m high bag from the Fringing Patch site; and the year-two seafloor surface bag from the Hillock Basin. For cementation analysis, dried ooids from the mesh bags were placed in a 1 mm sieve to isolate cemented clumps. All clumped and non-clumped sediment for each bag were weighed separately. Ooid clumps were subsampled, crushed and split in half with a mortar and pestle and razorblade, sputter coated with palladium, and mounted on individual stubs for SEM analysis. Each stub was visually examined for the presence and type of marine cement. When present, the dominant cement habit was recorded, and representative images (3-14 per stub) were taken.

For each image documenting aragonite fibrous "needle" cement, the approximately longest 30 percentile of needles meeting specific criteria were selected per image. Needles met specified criteria if: (1) the start and end points of the needle could be estimated (view was not obstructed); and (2) the angle between the full needle length was less than ~45° from parallel with the two-dimensional image plane. Using *Adobe*

Photoshop analytical tools, lines were drawn overtop of the approximated full length of each selected needle. Lengths were calculated from the SEM image scale using *Adobe Photoshop* measurement functions. For each image, the average length of the longest five needles was calculated. Site needle length values were then reported as the average of all images from the same site, year, and position (seafloor or 1 m above). The established needle selection criterion ensures that estimated needle length measurements can never be larger than the actual needle lengths. This ensures that all reported lengths represent an underestimation to some degree. Therefore, statistical analysis was not conducted.

Results

Mineralogy and bulk composition

Results reported are based on all samples collected (3-6 per site). The carbonate mineralogy of all bulk sediment samples consisted only of aragonite and HMC. Average amounts of aragonite were greatest at the Fringing Patch site (80.20% $\pm$ 0.03 SE) and least at the Deep Patch site (60.87% $\pm$ 0.02 SE). Per site average, Fringing Patch sediment had the least amount of carbonate (92.60% $\pm$ 1.60 SE) and the greatest amounts of organic and siliciclastic material, respectively (2.85% $\pm$ 0.71SE, 4.55% $\pm$ 0.92 SE). Deep Patch sediments had the greatest amount of carbonate (97.05% $\pm$ 0.31 SE) and the least amount of organic material (1.03% $\pm$ 0.15 SE). Primary Bank sediment had the least amount of clastic material (1.87% $\pm$ 0.49 SE). No statistically significant site differences were detected for any of the mineralogy or bulk composition parameters analyzed.

Grain composition

Point-count analysis of three sediment samples per site resulted in the identification of 12 sediment-type categories (Fig. 2.2a): coral; micritic grains; composite micritic grains (having the appearance of initially being more than 1 grain); mollusk; foraminifera; green algae (primarily *Halimeda*), red algae (including encrusting forms); echinoderm; bryozoan; terrigenous; carbonate mud/silt; and other (spicules, fecal pellets, worm tubes, and unidentifiable). Coral was the most common category in all samples except for the Deep Patch site, which had greater concentrations of micritic grains, foraminifera, and green algae. Terrigenous material was not found at any mesophotic sites, but did constitute more than 10% of sediment from the shallow Fringing Patch site and a trace amount from the Mid-shelf Patch site. Echinoderm, bryozoan, micritic cement, and mud/silt categories did not constitute more than 5% of the sediment from any site.

Analysis of variance indicated statistically significant differences when comparing all sites and when just comparing mesophotic sites respectively for: coral ($F_{5,12} = 15.88$, $p < 0.001$; $F_{3,8} = 47.49$, $p < 0.001$); micritic grains ($F_{5,12} = 7.92$, $p = 0.002$; $F_{3,8} = 14.67$, $p = 0.001$); foraminifera ($F_{5,12} = 16.68$, $p < 0.001$; $F_{3,8} = 30.59$, $p < 0.001$); and green algae ($F_{5,12} = 10.50$, $p < 0.001$; $F_{3,8} = 29.38$, $p < 0.001$). Significant differences were also found in the relative surface sediment abundance of red algae between mesophotic sites ($F_{3,8} = 4.06$, $p = 0.050$). Pairwise comparison results are displayed in Table 2.1. When comparing relative surface sediment grain type abundance with increasing depth, only foraminifera grains were found to correlate (with a significant, strong linear negative correlation; $n = 18$, $r = -0.86$, $p < 0.001$).

Non-metric multidimensional scaling (NMDS) ordination of the Bray-Curtis dissimilarity matrix visually indicated differences in grain composition among the study sites (Fig. 2.2b). This is supported statistically by one-way analysis of similarity (r = 0.7004, p = 0.0001). Coral, foraminifera, green algae, terrigenous material, micritic grains, and mud/silt respectively, constituted the grain types with the strongest effect on sample ordination. The Fringing Patch site was separated from other sites because of the notable abundance of terrigenous material and the greater relative amounts of mud/silt in surface sediment. Collected Deep Patch surface sediment was distinguishable because it had the greatest abundance of green algae and foraminifera-derived grains and the least relative abundance of coral-derived grains compared to surface sediment from all other analyzed site. The Primary Bank site was distinguishable from the other sites by the fact that it had a low relative abundance of mud/silt, no terrigenous material, and a moderate abundance of coral and foraminifera-derived surface sediment. Axis 1 of the NMDS ordination showed an overall gradient from sites with sediment composition dominated by coral grains (D3, D4, M5, and S6) to sites with sediment composition dominated by foraminifera, green algae, and micritic grains (D1 and D2).

The relative mean percent composition of coral and green algae grains in surface sediment per site (Fig. 2.2a) was compared to the site mean coral and green algae benthic coverage obtained through multiple linear transects (Table 1.1) using Spearman correlations. A strong overall correlation was identified between the percent coral cover and abundance of coral grains in surface sediment when all study sites were considered (n = 18, r_s = 0.743, p < 0.001). However, no correlation was found between percent green algae sediment abundance and green algae benthic cover. When only testing among

mesophotic sites, strong significant correlations were found between both abundance of coral and green algal sediment grains and benthic coral and green algae cover respectively (coral: n = 12, r_s = 0.972, p < 0.001; green algae: n = 12, r_s = 0.607, p = 0.036).

$\delta^{13}C$ and $\delta^{18}O$ isotopic composition

Results reported for stable isotopic analysis are based on all samples collected (three to six per site). Bulk surface sediment stable isotope values ranged from -2.22‰ to -0.54‰ for oxygen ($\delta^{18}O$) and from 0.93‰ to 3.62‰ for carbon ($\delta^{13}C$). Both carbonate and oxygen stable isotopes showed statistically significant differences between site means ($\delta^{18}O$: $F_{5,20}$ = 30.99, p < 0.001; $\delta^{13}C$: $F_{5,20}$ = 44.28, p < 0.001). Specific pair-wise differences are displayed in Table 2.1. Overall, a significant positive correlation was found between $\delta^{18}O$ and $\delta^{13}C$ (Fig. 3c) (n = 26, r = 0.829, p < 0.001). Furthermore, $\delta^{18}O$ and $\delta^{13}C$ values were generally related to depth, with lighter values found at shallow sites and heavier values found at deeper sites. To investigate potential relationships between bulk sediment stable isotope composition and sediment type, axis 1from NMDS ordination analysis (primarily representing relative composition of coral, foraminifera, green algae, and micritic grains) was plotted versus sample bulk carbonate and oxygen stable isotopic composition (Fig. 2.2d). Results showed significant negative correlations between axis 1 with both $\delta^{13}C$ (n = 18, r = -0.874, p < 0.001) and $\delta^{18}O$ (n = 18, r = -0.790, p < 0.001).

Grain size and hydrodynamics analyses

The site average grain size distributions and the site average of each main standard textural parameter per site are shown in Figure 2.3. Average grain size was

largest at the Deep Patch site and smallest at the Hillock Basin site, implying no correlation with depth (Fig.2.3b). All 28 samples were primarily composed of sand size particles and gravel, with trace amounts of mud (Fig. 2.3c). Site average distributions indicated that the Fringing Patch (S6) site was the muddiest, more than double the amount of mud than at the Hillock Basin (D1) and the Primary Bank (D3) sites, the next muddiest. On average, all mesophotic reef surface sediments were <4% mud.

Site average grain size distributions were unimodal at the Deep Patch and Hillock Basin sites, bimodal at the Mid-shelf Patch and the Primary and Secondary Bank sites, and trimodal at the Fringing Patch site (Fig. 2.3a). The primary grain size mode was 0.5-0.3 mm for all sites except the Fringing Patch site, which had a primary grain size mode of 1-0.25 mm, and the Deep Patch site, which had a primary grain size mode of 6-3 mm. The Deep Patch site primary grain size mode corresponded to the secondary grain size mode of all other analyzed sites with bimodal and trimodal grain size distributions (D3, D4, M5, and S6). The ternary grain size mode of the shallow Fringing Patch site was 40-20 μm.

All samples were poorly sorted except for one moderately sorted Secondary Bank sample and two very poorly sorted Fringing Patch samples. Hillock Basin samples were symmetrically to finely skewed, and mesokurtic to leptokurtic. Deep Patch samples were finely to very finely skewed, and all platykurtic. Primary Bank samples were coarsely to symmetrically skewed, and leptokurtic to very platykurtic. Secondary Bank samples were very coarsely to very finely skewed, and leptokurtic to platykurtic. Mid-shelf Patch samples were very coarsely to coarsely skewed and platykurtic to very platykurtic. Fringing Patch samples were symmetrically to finely skewed and very leptokurtic to

platykurtic. Site mean comparisons of standard sediment textural parameters indicated

statistically significant differences between each of the four main parameters (grain size:

$F_{5,22} = 5.01$, p = 0.003; sorting: $F_{5,22} = 4.73$, p = 0.004; skewness: $F_{5,22} = 7.48$, p < 0.001;

and kurtosis: $F_{5,22} = 3.36$, p = 0.021). When comparing only mesophotic sites,

significant differences between sites were still found for mean grain size and mean

sorting ($F_{3,17} = 9.93$, p < 0.001; $F_{3,17} = 4.68$, p = 0.015, respectively), but skewness and

kurtosis did not meet assumptions for ANOVA. Specific pair-wise differences between

sites for tested textural parameters are shown in Table 2.1.

The site average of each spring-neap cycle maximum current and mean hour

current between February 1, 2008 and January 31, 2009, are displayed in Table 2.2.

Under annual average tidal cycle mean current conditions ($\overline{CV}_{mean}$), little unconsolidated

sediment with diameters ≤104 μm probably deposited at any of the mesophotic sites,

assuming relatively little baffling effects (Table 2.3, none of these values are bold and

italic). Also during the same current conditions, fine sand grains (diameter = 125 μm)

were not likely to deposit at the Primary Bank site. However, under $\overline{CV}_{mean}$ winter season

conditions, fine sand grains could potentially deposit at the Hillock Basin and Deep Patch

sites for 26.87% and 29.36% of all winter hours in the measured time span, respectively.

Less than 1.3% of all hourly current measurements recorded by ADCPs at each of the

sites (D1, D2, and D3) were conducive for sponge chip deposition, assuming relatively

little baffling and that the chips were unconsolidated.

Results from the "currents of removal" approach indicated there was very low PM

(< 4%) of unconsolidated surface sediments in response to non-baffled mean current

velocities ($\overline{CV}_{mean}$) at all three mesophotic sites. However, in response to relatively little

baffling of maximum tidal current velocities ($\overline{CV}_{max}$), PM values indicated high potential entrainment (88.8% annually) of unconsolidated surface sediment at the Hillock Basin site (Table 2.4). Also, $\overline{CV}_{max}$ PM values were higher in the summer season than the winter season. A seasonal difference was not significant at the Primary Bank. Conditions necessary to move at least half of unconsolidated surface sediment (50% PM) occurred for less than 3% of the hours in the measured sampling year at the Hillock Basin (Fig. 2.4). Comparatively, 2.5% PM frequency of unconsolidated and unobstructed (minimal baffling) surface sediment at the Hillock Basin was more than four times greater than at the Deep Patch (D1: 4.49% and D2: 0.98%).

Cement form and rates

Grains in the mesh bags were found cemented into clumps at all sites after one year (Fig. 2.4a). The ratio of clump weight to non-clump weight was < 1.75 after the first year for all sites and <3.50 after two years, except for the Fringing Patch seafloor sediments, which had a ratio of 18.24. These values are relative estimates of cementation, considering that grain clumps sometimes broke up from the sieving process and a small but unknown amount of non-clumped grains fell out of the mesh bags during collection.

Examination of connections between attached ooid grains indicated four distinguishable cement types: (1) fibrous isopachous aragonite needles (Fig. 2.4b, c); (2) spheroidal clusters of needles (Fig. 2.4d, e); (3) anhedral semi-equant aragonitic minimicrite (Fig. 2.4h, i), defined as carbonate grains <1µm (Folk, 1974b); and (4) stringy elongated crystals embedded parallel to thick biofilm accumulations (Fig. 2.4f, g). Locations where cement types occurred are displayed in Table 2.5.

-Types 1 and 2

The fibrous aragonite needle cement was most common. When comparing grains from seafloor mesh bags to grains from mesh bags 1 m above the seafloor, needles were always longer in the 1 m above mesh bags, except from year 1 Mid-shelf Patch (M5) samples. The spheroidal needle clusters were only found between grain contacts after two years. For mesh bag samples 1 m above the seafloor, needles grew larger, but at a slower rate after two years (except at the Mid-shelf Patch). In addition, mesophotic needles were longer (~5 μm) than needles from shallower (M5 and S6) sites after one year (~2-3 μm), but Mid-shelf Patch (M5) needles were longest (followed by mesophotic site needles) after two years. For mesh bag samples on the seafloor, needles were always longest at the Mid-shelf Patch site (year 1: ~6 μm, year 2: ~8 μm). However, this cement type was only also present after year 1 on the seafloor at the Deep Patch (~2.3 μm). For year two seafloor mesh bag samples, Deep Patch needles were second longest (~6 μm), followed by Primary Bank (D3) needles (~5 μm). Fringing Patch needles were the shortest (~4.5 μm) for mesh bag seafloor samples after two years.

-Types 3 and 4

Minimicrite was only detected on samples collected after one year (Table 5). For both shallow sites (M5 and S6), minimicrite was identified in mesh bag samples 1 m above the seafloor (M5, S6) along with some more needle cements. When considering first year mesophotic samples, minimicrite was only found at two of three mesophotic sites (D1 and D3) and only on samples from seafloor mesh bags. The elongated

embedded needle cement (type 4) was only found after two years on the seafloor at the Primary Bank.

Besides forming at connection points between separate ooid grains, cements also formed on ooid surfaces, although the fibrous needle cement was the only type observed to completely cover entire grains (Fig. 2.4b). Secondary clusters of aragonite crystals (possibly cement type 2) were sometimes observed in patches atop of what appeared to be the first episode of cementation (Fig. 2.4b, d). Some aragonite needles were found to form along with organic biofilms (Fig. 2.5a, b) and microbial cells (Fig. 2.5c), although there was no noticeable site-specific trend. In cross-section, minimicrite-sized grains were often observed (Fig. 2.5d-e), but it was unclear if these represented early cement stages of minimicrite or an expression of the ooid interior surface.

Discussion

Results from this study show that mesophotic reef habitat heterogeneity on a low-angle shelf can be distinguished based on sedimentological data (Fig. 2.7). The deposits analyzed in the northern USVI mesophotic system would all be classified as packstones if they were lithified (Dunham, 1962). However, the subfacies identified in this study, and the habitats they represent, are still significantly distinguishable by one or more major compositional or textural properties (Table 2.1) when just comparing only grain fractions. These facies are essentially controlled through a combination of independent and interacting biological and physical hydrodynamic processes (Maiklem, 1968) over various temporal-spatial ranges. The ability to distinguish distinct mesophotic habitats and the processes controlling their physical structure requires differentiating between processes related to biological interactions and hydrodynamics (Kench and McLean,

1996). This ultimately provides a better understanding of habitat heterogeneity in the modern and analogous examples for interpreting paleomesophotic environments.

Biological subfacies controls

   -Benthic composition

      Analysis suggests that carbonate sediment composition in the USVI broadly records the abundance of major benthic species, as observed by significant correlations between both coral and green algae sediment grains and the living benthic cover of these groups. These findings are consistent with the general understanding that carbonate sand particles are largely controlled by the relative abundances of skeletal organisms in the area of deposition (Basan, 1973). Study results imply that low-angle shelf mesophotic reef sediments record basic benthic characteristics of the reef environment. These results are similar to those found along deep Jamaican fore-reefs (Boss and Liddell, 1987a; Perry, 1996). Results from the USVI also confirm and extend the depth potential of results reported by Pandolfi et al. (1996), that detailed mesophotic sedimentary composition analysis can help distinguish paleoenvironmental benthic coverage without solely relying on paleoecological coral interpretations.

      The relationship between reef sediment composition abundances and benthic cover is also reflected in the bulk sediment isotopic values. Bulk sediment carbon and oxygen stable isotopes both significantly correlate with Axis 1 of the NMDS visualization of Bray Curtis dissimilarity index ordination analysis, which primarily accounts for the relative sediment contribution of coral, foraminifera, green algae, and micritic grains (Figure 2.2d). Generally, coral sediments have the most negative isotopic values and calcareous algae have the most positive isotopic values of reefal skeletal

sediment types (Gischler et al., 2009). The Secondary Bank site, for example, with the

highest coral coverage of all sites and the highest percent of coral sediment grains, has

the lowest isotope concentrations of all the mesophotic sites (Fig. 2.2). The Deep Patch

and the Hillock Basin sites, with the lowest mesophotic coral coverages and coral

sediment percentages but the highest mesophotic green algae coverages and green algae

sediment percentages, also have the heaviest stable isotope compositions.

   -Production and erosion

   Besides sediment type abundance, grain size distributions in reef surface

sediments are also in part a product of the living benthic community population size and

sediment grain type. Reef grain size distributions commonly split into discrete size

intervals (Basan, 1973; Flood and Scoffin, 1978; Orme et al., 1978; Gabrié and

Montaggioni, 1982; Hoskin et al., 1983). The Sorby Principle, which states that intrinsic

micro-structural skeletal properties control fragmentation size, is often invoked as the

main cause for observed discrete bin sizes (Folk and Robles, 1964).

   The grain sizes of surface sediments collected in the USVI were also found to

follow similar portioning identified by previous studies in shallow-water reefs. The

primary grain population size from samples collected at analyzed study sites (0.5 – 0.3

mm) show a good correspondence with coral grit (0.5 – .25 mm), a dominant size fraction

identified in other studies (Folk and Robles, 1964; Maxwell et al., 1964; Hoskin, 1966;

Garrett et al., 1971; Hoskin et al., 1983). As coral grains were the most common

sediment type at all but the Deep Patch site (Fig. 2.2a), the identified main grain size

mode of the study sites (0.5-0.3 mm) provides additional evidence for biological control

on sediment distribution. The high abundance of coral grit versus coarse grain sand and

gravel size coral fragments implies longer seafloor exposure (Scoffin, 1992), corroborating with previous interpretations of the USVI mesophotic reefs (Weinstein et al., 2014; chapter 3).

The Deep Patch primary grain size mode corresponds well with whole *Halimeda* segments (8-4 mm; Folk and Robles, 1964), confirmed through visual inspection. This follows expectations given: (1) a greater proportion of green algae-derived surface sediment at the site compared to the other sites; (2) lower bioerosion breakdown potential (Weinstein et al., 2014; chapter 3); and (3) slower water movement compared to other sites (Table 2.3), which may prevent *Halimeda* breakdown into smaller size fractions. Furthermore, whole *Halimeda* skeleton grains are one of the quicker reef skeletal grain types to disassociate (Ford and Kench, 2012). Therefore, the identification of a great proportion of intact *Halimeda* at the Deep Patch site compared to the other sites provides evidence for little current-derived sediment agitation that would cause grains to abrade. On the other hand, visual inspection indicates that only sediment grains from the Fringing Patch site were subjected to high physical alteration.

Other biological properties such as skeletal shape and disintegration variability, diversity, and reproduction rates affect reef sediment textural characteristics and distribution (Ginsburg, 1956; Folk and Robles, 1964; Swinchatt, 1965; Stoddart, 1969; Maiklem, 1970; Garrett et al., 1971; Orme et al., 1974; Scoffin and Tudhope, 1985; Scoffin, 1992; Lidz and Hallock, 2000). These properties are also believed to be responsible for the poor grain size sorting characteristic of most reef sediments (Longman, 1981; Scoffin and Tudhope, 1985), including the analyzed USVI mesophotic reef sediment (Fig. 2.2b). Biological sediment textural control is especially noticeable in

the form of bioerosion, the dominant mechanism of sediment formation and alteration within coral reefs (Stearn and Scoffin, 1977; Scoffin et al., 1980; Hutchings, 1986; Harney and Fletcher, 2003). Parrotfish grazing is the primary mechanism for substrate modification down to upper (<35-45 m) mesophotic reef depths (Weinstein et al., 2014; chapter 3). Sand-sized fecal carbonate sediment (0.5-0.125 mm) is typically produced by parrotfish (Gygi, 1969; Garrett et al., 1971). This grain size was commonly identified in USVI reefs.

The second most common grain size mode (6-3 mm) at the shallowest four study sites (D3, D4, M5, and S6) is primarily composed of coral fragments and mollusk shells (Fig. 2.2a). Considering that recorded parrotfish biomass was highest at the four shallowest sites (Weinstein et al., 2014; chapter 3), the coral component of the secondary grain size mode at these sites is possibly attributed to the detachment of carbonate from hard substrates during parrotfish gazing. This coarser grain size, in addition to a relatively flat bathymetric profile and low structural complexity (rugosity, Table 1.1), all potentially contribute toward the significant negative skewness (Fig. 2.3) recorded at the Mid-shelf Patch site (Jordan, 1973).

Hydrodynamic facies controls

Sieve-based grain size analysis has traditionally been used to interpret sediment transport and depositional environments (Folk and Ward, 1957; Passega, 1957; Folk and Robles, 1964; Friedman, 1967). Application of this method to carbonate sediments is questionable, however, when interpreting hydrodynamic processes (Maiklem, 1968; Jindrich, 1969; Braithwaite, 1973; Kench and McLean, 1996; Kench and McLean, 1997). This results from *in situ* deposition, bioerosional modification, and the unequal hydraulic

behaviors of sediment accumulations composed of different skeleton types in the same sieve bin sizes (Folk and Ward, 1957; Poole, 1957; Jindrich, 1969; Scoffin and Tudhope, 1985; Chevillon, 1991).

To analyze USVI reef surface sediment, standard sediment sieving, the most common grain-size analysis method, was selected instead of sediment hydraulic settling behavior classification methodologies (Poole, 1957; Maiklem, 1968; Braithwaite, 1973; Wanless et al., 1981; Kench and McLean, 1996). The methodwas selected so results from this study could be compared to results from other studies in which hydraulic sediment settling methodologies may not have been used or available (Wilson, 2005; Munnecke et al., 2008; Titschack et al., 2008; Lokier et al., 2009; Spiske and Jaffe, 2009; Rong et al., 2013). The localized impacts on sediment distribution from coral reef hydrodynamics are often confounded by intricate topographic variability and energy dissipation by principle framework builders. Despite inherent difficulties modeling coral reef sediment transport and deposition, a broad understanding can be obtained when conceptualizing the net difference between sediment input (biological production, bioerosion, and transport from other sources) and output (entrainment and transport) processes.

-*Sediment additions*

Besides the biological production and bioerosion processes discussed earlier in this chapter, sediment addition to coral reefs also results from potential pelagic fallout and deposition of allochthonous sediment transported from other reefs or areas of unconsolidated sediment on the shelf. Easily distinguished from reef carbonates, terrigenous sediment provides a useful tool for deciphering broad, shelf-wide

hydrodynamic trends in coral reef. Significant terrigenous material was found

exclusively at the shallowest sites, and may suggest that some portion of the land-based

pollution from nutrients, toxins, and sediment considered in the past to be the worst USVI

coral reef stressors (Hubbard, 1987; Gray et al., 2008) may continue to impact the near-

shore reef system. However, the absence of terrigenous material in any mesophotic sites

(Fig. 2.2a) and significantly lower sedimentation rates (Smith et al., 2008) also implies

that land-based pollution sometimes associated with and transported as terrigenous

sediment has not directly affected mesophotic reef development on this low-angle shelf.

Modeling the behavior of hypothetically suspended particles above a reef and

comparison to sediment trap deposits is useful for understanding potential allochthonous

sediment deposition and the relative importance of hydrodynamic processes to

mesophotic reef subfacies development. The settling velocity of hypothetical carbonate

particles was simplified by assuming equations derived for regular quartz grains could be

applied. This assumption is considered fairly accurate because carbonate grain

hydrodynamic and sieve-sorting properties become more similar to those of quartz grains

as carbonate grain size decreases (Prager et al., 1996).

Sedimentation rates near the Deep Patch site were seven times lower than at the

Fringing Patch site (D2: 0.315 mg/cm^2/day SE = 0.037, S6: 2.315 mg/cm^2/day SE =

0.327), as indicated by analysis of sediment traps (Smith et al., 2008). Assuming similar

potential external sediment sources, sedimentation rates at the other mesophotic reefs

would relatively be comparable to those recorded near the Deep Patch. Analysis

indicated that hypothetically suspended particles with diameters ≤104.4 μm (the mean

grain diameter collected in Deep Patch sediment traps) would never deposit at any of the

mesophotic reef sites during average tidal cycle mean current conditions ($\overline{CV}_{mean}$). Still, for 25.72% of the measured hours, flow velocities were slow enough to allow suspended particles with diameters ≤104.4 μm to deposit at the Deep Patch site, provided the grains were present in the water column. Despite these frequencies, low mesophotic reef sedimentation rates imply that grains with average diameters ≤104.4 μm (including sponge chops) were either not available at neighboring sources, or that current energy was not sufficient to sustain transport from those other sources to the sites analyzed in this chapter. Results from surface sediment analysis and sediment traps (Smith et al., 2008) imply that the majority of surface sediments collected at the Deep Patch site are almost exclusively derived locally with little pelagic addition. This is presumably the case for the other mesophotic study sites and strengthens previous results from this chapter regarding the relationship between mesophotic reef benthic cover and surface sediment composition.

  -Sediment removal

   Entrainment and transport represent major processes of reef sediment erosion and removal. Average tidal cycle current mean velocities ($\overline{CV}_{mean}$) are never strong enough to entrain and transport unobstructed, unconsolidated reef surface sediment at any of the sites. This is true even at the Deep Patch (D2) site, which experiences the lowest recorded mean and maximum tidal current velocities ($\overline{CV}_{mean}$, $\overline{CV}_{max}$). The Deep Patch site also had the largest surface sediment mean grain size of the study sites. These results appear to contradict classical fluid sediment transport theory (smaller grains identify areas of reduced energy and larger grains identify areas of greater energy, Purdy, 1963), and illustrate the difficulties of applying this theory to mesophotic reef deposition.

Beyond slow current speeds, there was a relative absence of small grain sizes and a high cover of calcareous algae at the Deep Patch (D2) site compared to other examined USVI mesophotic reefs (Table 1.1). These attributes imply production rates of small carbonate grains ($\leq$ 0.152 μm) were less than the 0.98% of hours in which conditions would be able to cause at least 2.5% PM of surface sediment (Fig. 2.4). Positive skewness at the Deep Patch site also implies less sediment winnowing (Duane, 1964; Orme et al., 1974), with fine grain material trapped by more abundant, coarser sand grains (Scoffin et al., 1980).

Although $\overline{CV}_{\text{mean}}$ are never strong enough to entrain surface sediment at any of the study sites, mesophotic reef sediment, however, still has significantly different entrainment potential per habitat when considering average episodic tidal current highs ($\overline{CV}_{\text{max}}$). As measured $\overline{CV}_{\text{max}}$ entrainment potential was highest at the Hillock Basin site, interpretations based on clastic fluid sediment transport theory (Purdy, 1963) would likely imply the site is a major sediment producer and source for other depositional areas. Yet again, this logic is counterintuitive when considering the site also has the smallest unconsolidated surface sediment grain size distribution (Fig. 2.3). Calculated PM values in this study do not stem from direct *in situ* entrainment observations. Rather, they represent potentials for movement based on measured carbonate grain settling characteristics and ADPC current measurements. Therefore, PM values should be considered more as maximum potential entrainment values.

Data collected at the Hillock Basin site indicate that the addition/production of smaller grains occurs more frequently than the actual removal of these grains. This is not due to additions from transported material, as implied by low measured sedimentation rates. Observations suggest sponge boring (resulting in sponge chips) is not faster or

more common at the Hillock Basin compared to any of the other mesophotic sites (Weinstein et al., 2014, chapter 3). High PM of surface sediments was calculated at the Hillock Basin site when conditions were equivalent to the average of the maximum current velocity per tidal cycle. Specifically, conditions for 10% PM (constituting very fine sand grains and silt with diameters ≤ 0.145 mm) occurred 3.84% of the year (Fig. 2.4). However, only 24.6% of that time (0.94% of all hours measured) lasted for more than one consecutive hour in the same relative direction (less than 45° difference). Grains may just move back and forth near their original position due to oscillating current velocities. As a consequence, this movement could induce mechanical abrasion, which would also decrease grain size.

Additionally, baffling potential should be considered when making hydrodynamic sediment transport interpretations in reef environments. For example, baffling effects were noted when comparing Primary Bank sediment collected from small uncovered sand banks with sediment collected nearby, but directly under mushroom formations of living platy coral atop trunk-like columns of dead framework. Sediments collected under corals had a comparatively higher PM, indicating that sediment of relatively the same composition can slightly vary in grain size when direct baffling of coral heads dissipates current energy. Although no similar comparison was conducted at the Hillock Basin site, the complex large-scale bathymetry produced from hillock development may baffle current velocities (Roberts, 1989) enough to prevent some entrainment.

Identified relationships that defy clastic notions of sediment transport highlight the complexity of interacting sedimentary carbonate processes to making interpretations about the environment of deposition. Therefore, caution must be used when applying

interpretations from modern mesophotic reefs to analogous ancient deep reef deposits. For example, identifying high abundance of very fine grain reef sediment in ancient mesophotic reef deposits should not be the only observation used to imply a Hillock Basin-type environment. Determining the presence or absence of other factors (such as bedding structures, syndepositional cement, bioturbation, and allochthonous material) is necessary before subfacies equivalence can be inferred. These additional indicators, as well as the grain composition, would help identify if small size grains resulted from low energy and biological grain size reduction, or from oceanographic conditions such as those experienced at the Hillock Basin.

Determining the potential for sediment entrainment and transport is critical for interpreting mesophotic reef subfacies development. This is especially true for interpreting the lack of a particular grain type, such as the noticeable sponge chip void in mesophotic reef surface sediments (recognized because all average mesophotic reef surface sediments have <4% mud, Fig. 2.3). This void is not intuitive because sponge bioerosion is probably the primary modifier of framework structure on MCEs below transitional (30-35 m) depths (Weinstein et al., 2014; chapter 3). Field and hand sample observations suggest USVI mesophotic coral sponge bioerosion is either cryptic or primarily occurs on the underside of platy coral heads. Expelled chips from the osculum (Rützler and Rieger, 1973) of less-cryptic bioeroding mesophotic coral sponges have varying fall distances before deposition onto the seafloor and subsequent incorporation as autochthonous surface sediment. Calculations suggest that energy levels were almost never low enough (<1.30% of measured hours, Table 2.3) for deposition of averaged-sized sponge chips (assuming fall heights ≥25 mm and relatively little current energy

baffling). Even when oriented upward and relatively close to the seafloor, sponges still expel chips ~2-3 mm above, facilitating "resuspension" (K. Rützler, personal communication).

Though sponge chips can make up significant fractions of bulk sediment in locations with low water energy (such as lagoons, Fütterer, 1974), results indicate low potential for sponge chip accumulation on low-angle shelf MCEs, unless protected by moderate current energy baffling. A greater abundance of sponge chips is expected in cryptic spaces within coral framework, but that material does not necessarily mix into the surrounding reef surface sediment. The low abundance of sponge chips in mesophotic reef surface sediment mirrors expectations based on measured current velocities and suggest sediments from paleomesophotic deposits with similar sediment distribution voids (small amounts of sponge chips) can be used, along with other factors, to interpret the environment as experiencing moderate current flow.

Syndepositional cementation

Despite potential relationships between syndepositional cementation and the variability of local hydrodynamics (Marshall, 1983a; Macintyre and Marshall, 1988), no strong trends in either the amount or type of cementation were recognized at analyzed study sites which could contribute to overall mesophotic subfacies identification. However, study results show that low-angle shelf mesophotic coral reef habitats can be included with other tropical marine carbonate environments (shallow coral reefs (Ginsburg et al., 1971; Friedman et al., 1974), steep mesophotic reefs (James and Ginsburg, 1979), deep platform margins (Grammer et al., 1993; Grammer et al., 1999)) as locations of rapid syndepositional cementation. Additionally, identification of rapid

sediment cementation within various types of mesophotic reef habitats in the USVI supports arguments for geologically instantaneous stabilization of depositional carbonate slopes at mesophotic depths prior to the Holocene (Playford, 1980; Della Porta et al., 2003).

Cementation results from this study also indicate a high potential for rapid stabilization of reef bottom sediments (represented by mesh bags on the seafloor). Analysis also suggests rapid stabilization of sediment trapped within the reef framework above the seafloor (represented by 1 m high mesh bags) in mesophotic reefs and rapid preservation of original sediment and framework textural characteristics. These implications for high preservation potential are strengthened when coupled with results from Perry (2000) that found deep fore-reef grains suffered little diagenetic alteration before removal from the taphonomically active zone (Powell and Davies, 1990). Additionally, mesophotic reef rapid syndepositional cementation identification strengthens the possibility that MCE cements facilitate the maintenance of reef structural complexity. MCE cements could accomplish this by countering bioerosion intensity (Rasser and Riegl, 2002; Riding, 2002), and by promoting benthic colonization through the production of marine hardgrounds.

Implications

Study results indicate that biological processes wield greater control over sediment than hydrodynamic processes in the mesophotic reefs south of the northern USVI. Although showing similar episodic tendencies to their shallow counterparts, low-angle shelf mesophotic reef hydrodynamic processes appear to be less of a factor in sediment deposition when compared to shallower-water reef systems (Randazzo and

Baisley, 1995; Orpin et al., 1999; Storlazzi et al., 2004). Regardless, entrainment and deposition potentials and related noticeable absences of particular grain types and sizes highlight that hydrodynamic forces still impart some control on MCE sediment subfacies.

Overall, the low-angle shelf mesophotic reefs in the USVI can be primarily classified as local sediment production environments of deposition with initial sedimentary repository characteristics mainly controlled by biological processes. Deposits from these reefs are not likely to contribute sediment to one another. However, it is probable that the sites transport varying quantities of allochthonous sponge chips to non-reef mesophotic locations as well as off the shelf edge. Despite similar depositional environment classifications, distinct associations between deep reef habitats and sedimentary subfacies were identified in mesophotic reef habitats with architecturally different characteristics. These associations suggest the potential to record mesophotic reef habitat heterogeneity and structural complexity with associated sediment characteristics. More so, the rapid MCE syndepositional cementation identified at all studied sites implies moderate to high levels of subfacies preservation potential. Results from this study thus provide new analogues for studies of ancient mesophotic geological history and overall coral reef evolution.
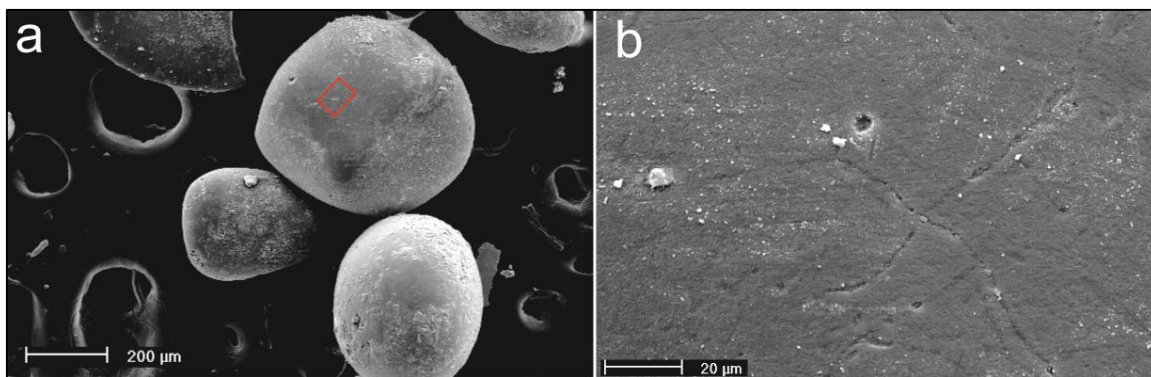
Figure 2.1. Pre-experiment ooid grains. Scanning electron micrographs illustrating pre-experiment ooid texture. (a) Smooth Bahamian ooids that were placed into mesh bags prior to site deployment. (b) Detail of red box in (a) showing a magnified view of the ooid surfaces, which are smooth with minor microbioerosion.
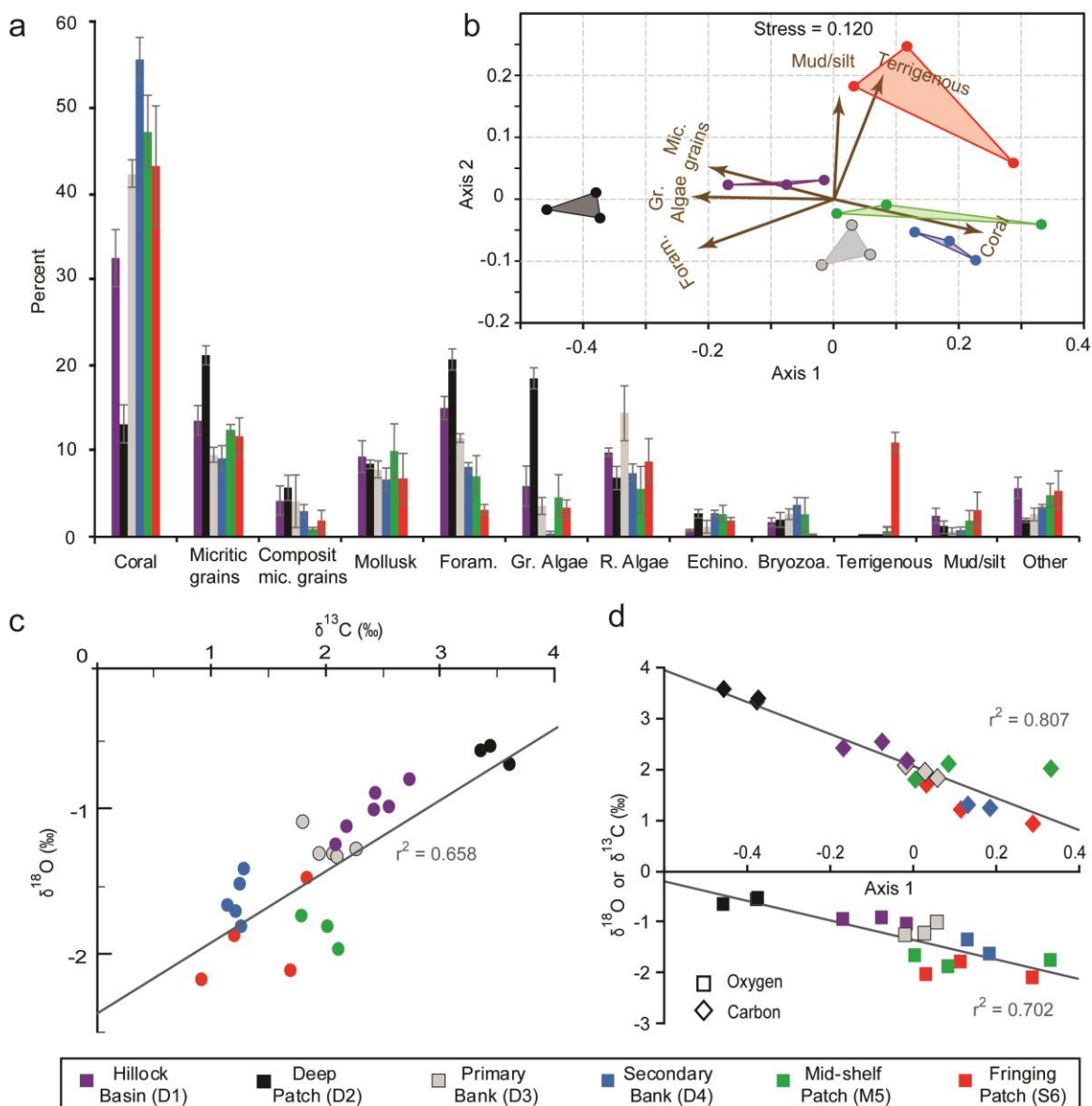
Figure 2.2. Composition of sediment from study sites. (a) Percent of constituent sediment types per site, with error bars equal to ± 1 SE. Mic = micritic, Foram. = Foraminifera, Gr. = Green, R. = Red, Echino. = Echinoderms. (b) Non-metric multidimensional scaling (NMDS) ordination, with greater visual distance between sites representing greater relative distinction. Arrow length indicates greatest relative impact of associated sediment type on driving visualization similarities within sites and differences between sites. (c) Relationship between stable carbon and oxygen isotopic composition of bulk sediment. (d) Relationship between Axis 1 from NMDS in (b), and bulk sediment stable isotopic composition of both oxygen (squares) and carbon (diamonds) of the three randomly selected samples thin-sectioned per site. Key for all graphs is located at bottom of figure.

Table 2.1. Sediment pair-wise analysis results. Outcome of Tukey's honestly significant difference multiple comparison sediment testing between sites. Each row shows all analyzed comparisons between the two specified sites from the study. Values were included when significant (p<0.05). Parentheses indicate test results for which only mesophotic sites were considered. Foraminifera are abbreviated as Foram.

	Site differences	Grain composition				Stable isotopes		Grain size		
		Coral	Micritic grains	Foram.	Green Algae	$\delta^{13}C$	$\delta^{18}O$	Mean	Sorting	Skewness
Mesophotic / mesophotic	Primary Bank: Secondary Bank	(0.045)		(0.063)	(0.030)	<0.001 (<0.001)	0.038 (0.004)			
	Deep Patch: Secondary Bank	<0.001 (<0.001)	0.001 (0.002)	0.003 (<0.001)	<0.001 (<0.001)	<0.001 (<0.001)	<0.001 (<0.001)	(0.024)	(0.030)	0.003
	Hillock Basin: Secondary Bank	0.015 (0.002)		(0.002)	0.037 (0.007)	<0.001 (<0.001)	<0.001 (<0.001)			
	Deep Patch: Primary Bank	0.001 (<0.001)	0.002 (0.002)	0.047 (0.001)	0.009 (0.002)	<0.001 (<0.001)	<0.001 (<0.001)			0.009
	Hillock Basin: Deep Patch	0.016 (0.002)	(0.035)	(0.025)	0.038 (0.007)	<0.001 (<0.001)	0.047 (0.005)	0.001 (<0.001)	(0.036)	0.008
	Hillock Basin: Primary Bank					(0.016)	(0.034)			
Mesophotic / shallow	Secondary Bank: Fringing Patch								0.018	
	Primary Bank: Fringing Patch			0.005		<0.001	<0.001			
	Deep Patch: Fringing Patch	0.001	0.014	<0.001	0.006	<0.001	<0.001			
	Hillock Basin: Fringing Patch			0.001		<0.001	<0.001		0.021	
	Mid-shelf Patch: Secondary Bank					0.003				
	Mid-shelf Patch: Primary Bank						0.002			
	Mid-shelf Patch: Hillock Basin			0.023			<0.001			
	Mid-shelf Patch: Deep Patch	<0.001	0.027	0.001	0.012	<0.001	<0.001			<0.001
Shallow	Mid-shelf Patch: Fringing Patch					0.045				0.011
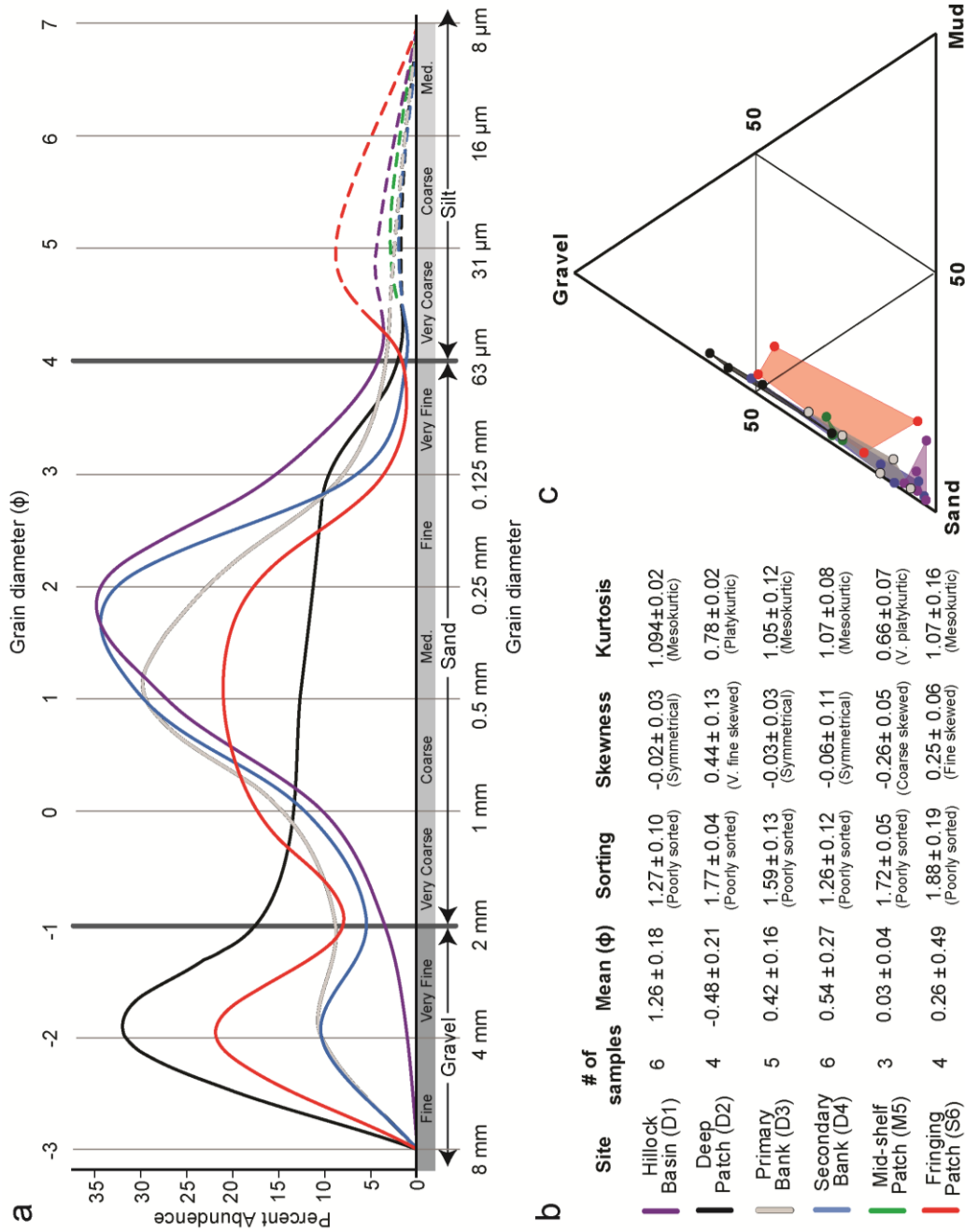
Figure 2.3. Grain size analysis. (a) Graph of average grain size distribution per site with dotted lines indicating distribution estimates after last sieve bin (63 μm). (b) Average textural parameters per site, ± 1 SE, obtained using the logarithmic graphical method (Folk, 1957). (c) Classification scheme of study sediments as a ternary diagram (Folk, 1954).

Table 2.2. Current velocity. Site average maximum current and mean current per spring-neap cycle, between February 1, 2008 and January 31, 2009. Currents are recorded every hour within each spring-neap cycle. Values are reported with ±1 standard error. Summer season from May–November, winter season from December–April.

Geomorphic habitats	Annual tidal cycle current velocity (cm/s)		Summer tidal cycle current velocity (cm/s)		Winter tidal cycle current velocity (cm/s)	
	$\overline{CV}_{max}$	$\overline{CV}_{mean}$	$\overline{CV}_{max}$	$\overline{CV}_{mean}$	$\overline{CV}_{max}$	$\overline{CV}_{mean}$
Hillock Basin (D1)	34.84 ± 4.04	7.07 ± 0.75	42.78 ± 5.59	7.87 ± 1.24	23.72 ± 3.65	5.96 ± 0.22
Deep Patch (D2)	18.83 ± 0.97	6.92 ± 0.32	20.54 ± 0.86	8.05 ± 0.20	16.45 ± 1.78	5.34 ± 0.24
Primary Bank (D3)	19.53 ± 1.45	7.22 ± 0.38	19.54 ± 1.99	7.50 ± 0.28	19.53 ± 2.23	6.82 ± 0.83

Table 2.3. Potential suspended particle deposition. Calculations of potential deposition were conducted for three representative grain-sizes. *Ave.* $\frac{w_s}{u_*}$ represents the average ratio between estimated grain settling velocity (w_s) and shear velocity (u_*), calculated using the mean current velocity per tidal cycle ($\overline{CV}_{mean}$) at each location. Bold italic text indicates when ratio is ≥1.25, implying deposition of the particle (Cheng and Chiew, 199) if relatively little baffling. Right data column indicates percentage of hours measured in which unconsolidated grains of a given size would deposit from suspension if initially present 25 mm above the seafloor. Summer season from May–November, winter season from December–April.

Geomorphic habitats	Grains (µm)	Annual tidal cycle		Summer tidal cycle		Winter tidal cycle	
		Ave. $\frac{w_s}{u_*}$	% (hours in a year) of potential deposition	*Ave.* $\frac{w_s}{u_*}$	% (hours in a year) of potential deposition	*Ave.* $\frac{w_s}{u_*}$	% (hours in a year) of potential deposition
Hillock Basin (D1)	125	1.058	58.58%	0.952	31.71%	*__1.256__*	26.87%
	104.4	0.746	36.66%	0.670	20.24%	0.885	16.41%
	40	0.113	1.27%	0.101	0.64%	0.134	0.63%
Deep Patch (D2)	125	1.081	44.95%	0.929	15.60%	*__1.402__*	29.36%
	104.4	0.760	25.72%	0.65	8.22%	0.990	17.50%
	40	0.115	0.84%	0.099	0.25%	0.149	0.59%
Primary Bank (D3)	125	1.040	38.57%	0.999	20.76%	1.098	17.81%
	104.4	0.731	21.67%	0.704	11.01%	0.773	10.65%
	40	0.110	0.50%	0.106	0.18%	0.117	0.32%

Table 2.4. Potential mobility (PM) analysis. Entrainment potential of surface sediments collected at three mesophotic reef study sites. Mean settling velocity values reported in the table were obtained in response to average spring-neap tidal cycle mean current velocity ($\overline{CV}_{mean}$) between February 1, 2008 and January 31, 2009, as recorded from Acoustic Doppler Current Profilers (ADCP) 1.5-2 m above the reef sites. Equivalent grain size indicates the largest estimated grain diameter that would likely be entrained. PM was calculated using the "currents of removal" approach (Kench et al., 1998). Summer season from May – November, winter season from December – April.

	Geomorphic habitats	Annual maximum tidal cycle average	Summer maximum tidal cycle average	Winter maximum tidal cycle average
Mean settling velocity (χ)	Hillock Basin (D1)	3.07	2.44	4.71
	Deep Patch (D2)	6.63	5.70	11.78
	Primary Bank (D3)	6.19	6.18	6.19
Equivalent grain size (mm / φ)	Hillock Basin (D1)	1.206 / -0.27	2.010 / -1.01	0.429 / 1.22
	Deep Patch (D2)	0.176 / 2.50	0.262 / 1.93	0.027 / 5.21
	Primary Bank (D3)	0.212 / 2.24	0.212 / 2.24	0.212 / 2.24
Potential mobility (%)	Hillock Basin (D1)	88.8	95.1	49.0
	Deep Patch (D2)	8.1	14.1	0.1
	Primary Bank (D3)	10.8	10.9	10.8

	Potential Mobility (PM) fraction frequency		
	2.5% PM	10% PM	50% PM
Hillock Basin (D1)	4.49 (≤ 0.050)	3.84 (≤ 0.145)	2.99 (≤ 0.436)
Deep Patch (D2)	0.98 (≤ 0.091	0.35 (≤ 0.194)	(≤ 1.823)
Primary Bank (D3)	2.63 (≤ 0.064)	1.136 (≤ 0.198)	0.10 (≤ 0.685)

Summer Winter
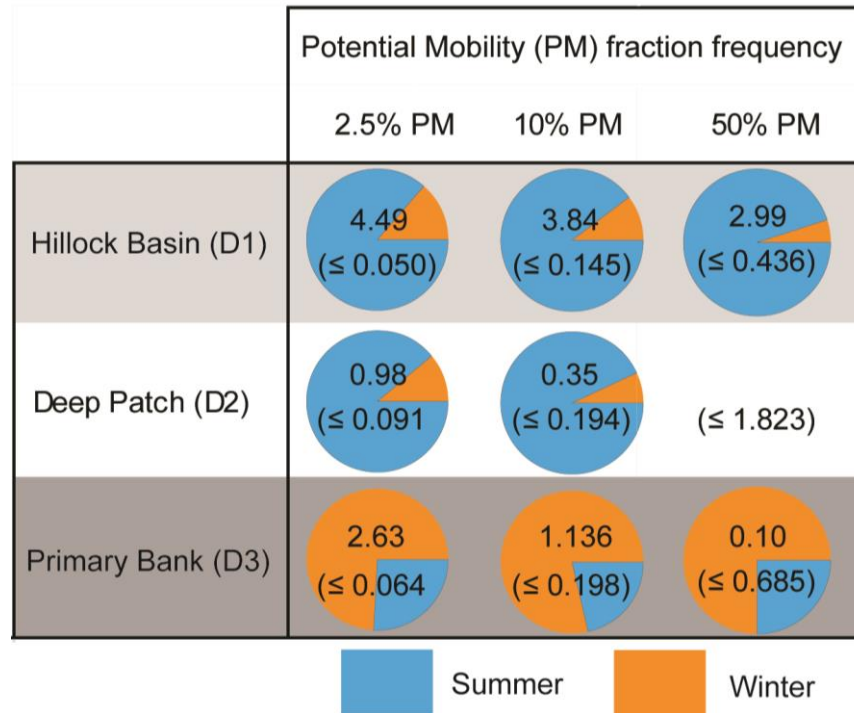
Figure 2.4. Frequency of PM. Percent of hours measured in a year for different potential mobility fractions. Values in parentheses indicate the maximum equivalent grain size that would be entrained for the corresponding PM fraction. No 50% PM graph is presented for the Deep Patch site because conditions were never met. Summer season from May – November, winter season from December – April.
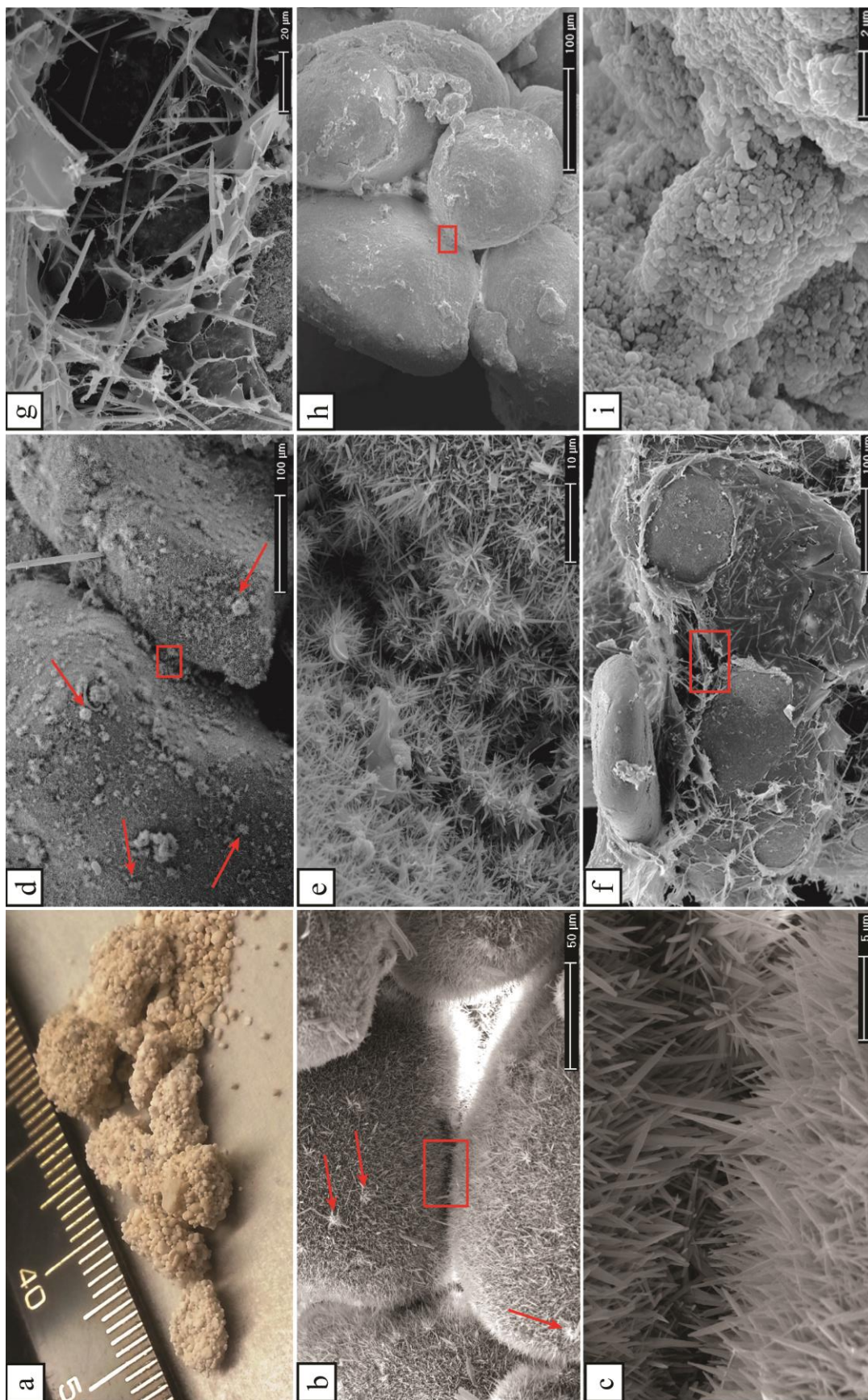
Figure 2.5. Ooid cementation. Photographs and scanning electron micrographs illustrating syndepositional cementation. (a) Clumps of cemented ooids from mesh bag. (b) SEM photomicrograph of ooid clumps after containment in mesh bag 1 m above the seafloor for 277 days at the Mid-shelf Patch site. (c) Inter-fingering fibrous isopachous aragonite cement (type 1), identified by red box in (b), near contact point between two cemented ooids. (d) Spheroidal clusters of aragonite needles (type 2) after 637 days in a mesh bag on the seafloor at the Fringing Patch site. (e) Red box in (d) showing type 2 cement formation between two adjacent ooids. (f) Elongated cement crystals embedded in thick biofilm accumulations parallel to the ooid surface (type 4). (g) Elongated crystals, like those from the red box in (f), were identified on ooids in a mesh bag after 625 days on the seafloor at the Primary Bank site. (h) Grain cementation from minimicrite cement (type 3). (i) Red box in (h) showing minimicrite cement near the contact point of two adjacent ooids found in a mess bag after 274 days on the seafloor at the Mid-shelf Patch site. Red arrows (b, d) point to secondary cement nodules on top of first generation cementation.

Table 2.5. Cement types and locations. Numbers in table indicate cement type. 1 = fibrous isopachous aragonite needles, 2 = spheroidal clusters of aragonite needles, 3 = anhedral semi-equant aragonitic minimicrite, 4 = stringy embedded crystals in thick biofilm. BF indicates when cements were found associated with biofilm interaction.

Year	Position	Hillock Basin (D1)	Deep Patch (D2)	Primary Bank (D3)	Mid-shelf Patch (M5)	Fringing Patch (S6)
1	1 m above	1 with BF	1	1	3 (and stubby 1)	1 and 3
	Seafloor	3	1	3	1	3
2	1 m above	1	1 and 2	1	1	1 (tiny) with BF
	Seafloor	N.A.	1	1 and 4	1	1 and 2
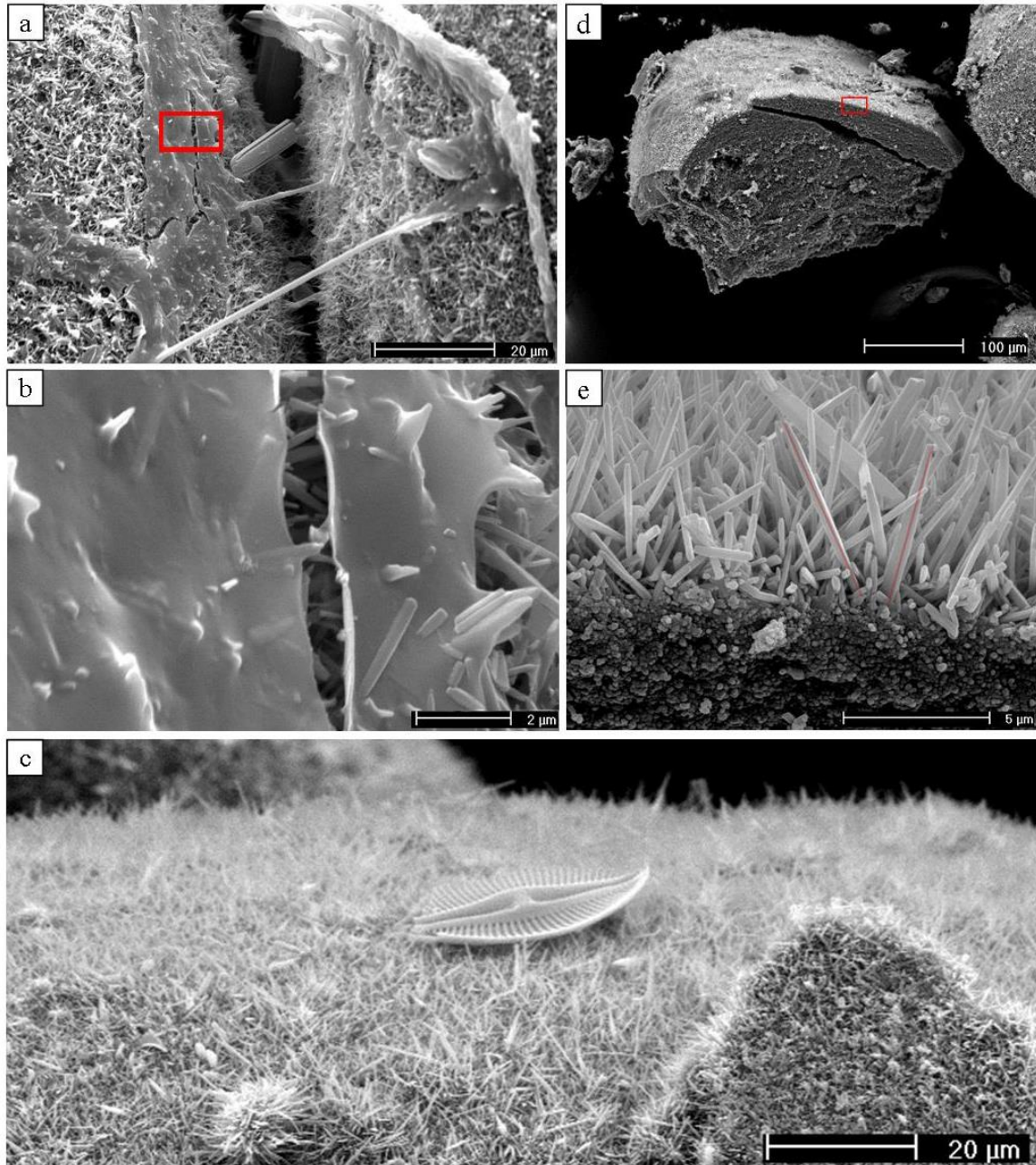
Figure 2.6. SEM micrograph cement associations. (a) Ooids coated with fibrous aragonite cement and stringy extracellular polymeric substances (EPS) connections after 289 days in a mesh bag 1 m above the seafloor at the Hillock Basin. (b) Red box from (a), showing sheet-like biofilms commonly found draped on cemented ooids. (c) Grain exposed 277 days 1 m above the seafloor at the Primary Bank showing common association between cements and biological entities such as this diatom. (d) Cross section of an ooid covered with radiating fibrous aragonite cement after 635 days in a mesh bag 1 m above the seafloor at the Deep Patch site. (e) Red box from (d) showing basal connection between fibrous cement and ooid surface, with minimicritic size crystals below. Red lines demonstrating method of measuring fibrous "needle" cement length, following criteria discussed in text.
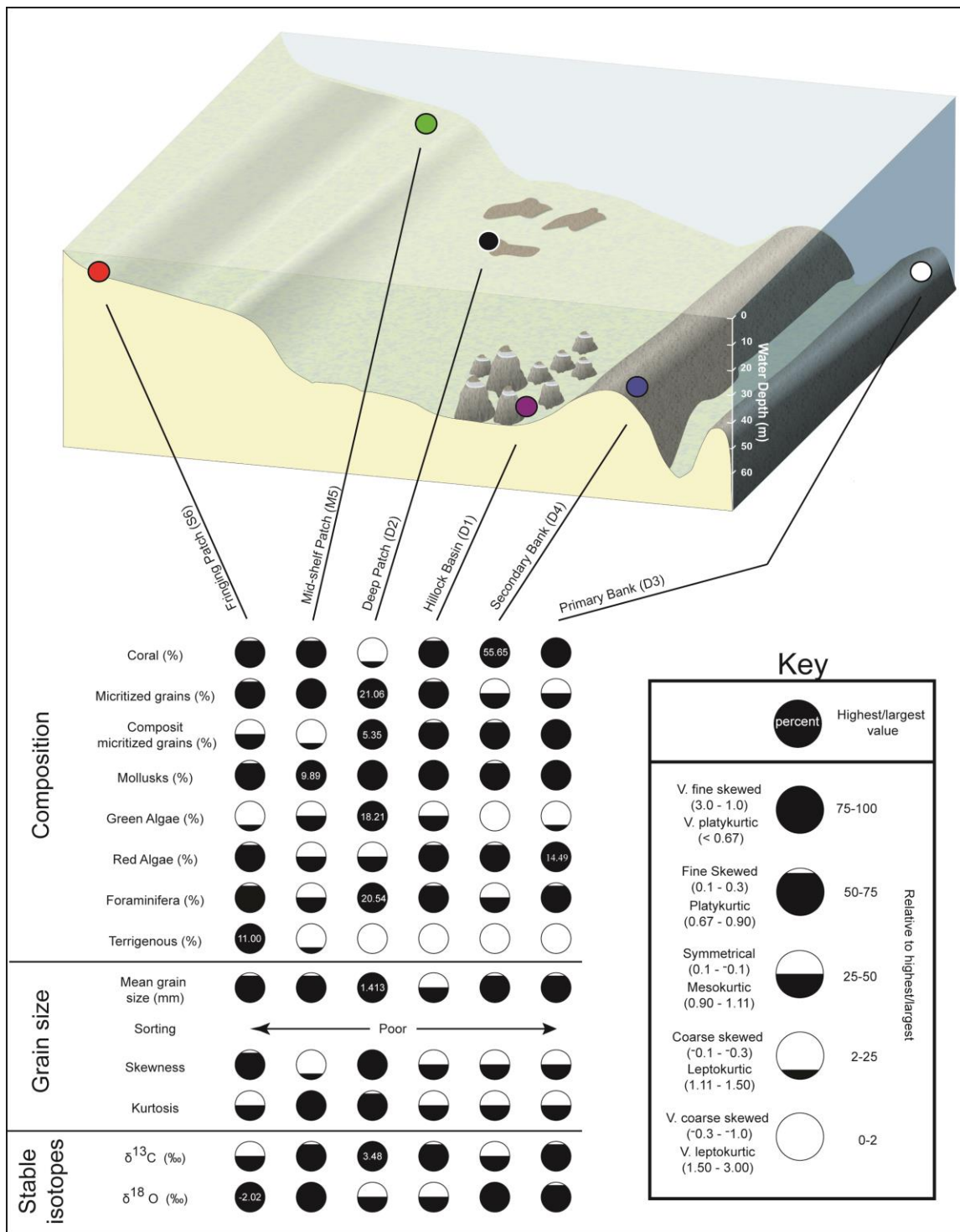
Figure 2.7. Subfacies summary. Cartoon showing benthic habitat and geomorphology of study sites and summary diagram showing the distribution of different sedimentary metrics tested and used in this study to distinguish different sediment facies. Number on solid black circles indicates the highest site value for the category of interest and the other circles indicate the relative percent compared to the largest category value.

CHAPTER 3. MESOPHOTIC BIOEROSION: SUBSTRATE MODIFICATION IN THE DEEP REEFS OF THE U.S. VIRGIN ISLANDS

Chapter summary

Mesophotic reef corals build complex structures that provide habitat for diverse ecosystems. Whereas bioerosion is known to impact the development and persistence of shallow reef structures, little is known regarding the extent of mesophotic bioerosion or how it might affect deeper reef geomorphology and carbonate accretion. Originally pristine experimental coral substrates and collected coral rubble were both used to investigate the variation and significance of mesophotic coral reef bioerosion south of St. Thomas, U.S. Virgin Islands. Bioerosion rates were calculated from experimental coral substrates exposed as framework for 1, 2, and 3 years at four mesophotic habitats with structurally distinct characteristics (between 30-45 m) as well as at a mid-shelf patch reef (21 m) and a shallow fringing patch reef (9 m). The long-term effects of macroboring were assessed by examining coral rubble collected at all sites.

Overall, differences in bioerosional processes were found between shallow and mesophotic reefs. Increases in bioerosion on experimental substrates (amount of weight lost) were related to both decreasing seawater depth and increasing biomass of bioeroding parrotfish. Significant differences in coral skeleton bioerosion rates, ranging from -19.6 to 3.7 g/year, were found between the transitional mesophotic reef zone (30-35 m) and the upper mesophotic reef zone (35-50 m) after two years of exposure. The shallowest site from the upper mesophotic reef zone exhibited substrate weight changes parallel to those at shallower sites after three years of exposure. Total coral rubble macroboring coverage was greater at most deep sites compared to shallow-water reef sites. Bioerosional grazing was found to dominate initial substrate modification in reefs 30.7 m

and shallower, whereas sponges are believed to act as the main time-averaged, long-term substrate bioeroders in reefs between 35-50 m. Comparison of site composition suggests that mesophotic bioerosion will vary depending on the interaction of subtle differences in bioerosional patterns on the amount, location, and type of substrate available for erosion and the duration both coral rubble and *in situ* coral framework are exposed on the seafloor. These variations may exaggerate pronounced structural differences in mesophotic reef habitats, even for sites with similar recorded bioerosion patterns of the same substrate type.

Background

Bioerosion, a major control on the architectural integrity of a reef (Hubbard, 2009), plays an important role in the formation and maintenance of reef relief and structural complexity through the production, modification, and transport of the main sedimentary elements of a reef (Scoffin et al., 1980; Hutchings, 1986; Glynn, 1988; Kiene and Hutchings, 1994; Glynn, 1997). At a very basic level, bioerosion is thought as a primary variable in the reef growth equation (Sammarco, 1996). When bioerosion rates exceed framework growth rates, the reef will eventually be destroyed (Stearn and Scoffin, 1977; Ginsburg, 1983; Scoffin, 1992). To that end, bioeroding organisms are key factors regulating the amount of reef destruction and/or preservation in the geologic record (Hutchings, 1986; Glynn, 1997). Studies of carbonate budgets assess the impact of bioerosion on reef geomorphology (Glynn, 1997; Edinger et al., 2000; Perry and Hepburn, 2008), but direct observations of bioerosional modification to reef geomorphology are rare. In one example, increased coral skeleton bioerosion rates compared to low carbonate production rates at Champion Island, Galapagos, were

believed to be responsible for observed rapid structural destruction (Reaka-Kudla et al., 1996). These increased rates were hypothesized to result from environmental changes induced by the 1982-1983 E1 Nino Southern Oscillation. Reaka-Kudla et al. (1996) suggested that these changes led to increased benthic algal cover and the availability of cryptic habitat, facilitating a biomass increase of the bioeroding sea urchin *Eucidaris thouarsii*.

Caribbean reefs have experienced significant declines in architectural complexity in the past four decades (Alvarez-Filip et al., 2009; Bozec et al., 2014). Changes in annual live coral cover were found to relate in part to architectural complexity (Alvarez-Filip et al., 2011a). Coral bleaching was not found to be a short-term major influence on the reef structural changes, but physical impacts, such as hurricanes and reef bioerosion appeared to be major drivers of widespread decline in reef architectural complexity (Alvarez-Filip et al., 2011c). Bioerosion also influences other elements of reef structure by increasing reef susceptibility to physical damage through mechanical erosion (Scott and Risk, 1988; Sammarco and Risk, 1990), and by eroding coral known to dissipate coastal wave energy (Sheppard et al., 2002; Koch et al., 2009).

The impact of bioerosion, beyond the mere removal of carbonate, has also been suggested to have positive consequences for reef growth. Increased reef growth has been associated with moderate to higher levels of parrotfish (Brock, 1979) and echinoid grazing (Sammarco, 1980; Sammarco, 1982). This association is thought to result from reduction of superior competitive algae (Ogden and Lobel, 1978) and the creation of space for new coral recruits (Sammarco, 1980). Further research suggests most negative impacts of carbonate removal by parrotfish are insignificant compared to the positive

effects of parrotfish herbivory on coral recruitment and growth (Mumby, 2009). There is also speculation that some degree of bioerosion may actually facilitate and maintain high levels of ecological biodiversity through small-scale, local intermediate disturbances (Connell, 1978; Hutchings, 1986). The boring of framework also seems to help restore coral reefs by increasing fragmentation and cementation of remaining colonies (Tunnicliffe, 1981; Scott et al., 1988; Guzman, 1991). Given the impact bioerosion has on so many reef processes, Acker and Risk (1985) suggested that ignoring bioerosional processes will probably result in a highly incomplete facies model.

From a mesophotic reef bioerosional standpoint, the limited studies to date suggest that there is much more substrate infestation in deeper reef-fronts (15-50 m) then other geomorphologies, and that sponges are the main contributors to this bioerosion (Goreau and Hartman, 1963; Perry, 1998; Greenstein and Pandolfi, 2003). The results of these studies in turn propose that bioerosion group diversity is lower in deeper reefs compared to shallower reefs (Perry and Hepburn, 2008). Studies comparing changes in bioerosion with depth (some only using minimal deep sites) have found that grazing rates generally decrease with increasing depth (Scoffin et al., 1980; Kiene and Hutchings, 1994; Steneck, 1994; Bruggemann et al., 1996; Brokovich et al., 2010). Identifying a relation for infaunal boring is more ambiguous, but studies testing sponge boring and overall boring abundances and bioerosional rates imply macroboring decreases with increasing depth (Moore and Shedd, 1977; Kiene and Hutchings, 1993; Vogel et al., 2000).

The results of most relevant studies to date, when complied, lead to the general understanding that total bioerosion decreases with increasing depth (Kobluk and Kozelj,

1985; Kiene and Hutchings, 1994; Chazottes et al., 1995; Vogel et al., 2000).

Successional bioerosion patterns have been suggested to induce some of these observed

and hypothesized relationships (Kiene and Hutchings, 1994). On a larger spatial scale,

Hubbard (2009) hypothesized slow bioerosion rates in deep reefs as the main process

responsible for the rejection of the traditional reef accretion theory (Schlager, 1981;

Macintyre, 1988; Bosscher and Schlager, 1992). However, no study has

comprehensively or quantitatively analyzed how bioerosion rates change along a

complete depth gradient (Hubbard, 2009), particularly including sampling from multiple

mesophotic reef habitats. Consequently, little is known regarding the potential variability

of bioerosional processes across a heterogeneous mesophotic reef shelf, and the inherent

implications of such differences to shelf and ecosystem habitat development.

The purpose of this chapter is to determine how bioerosion rates and bioeroding

organism distributions vary between MCE habitats of different geomorphology and with

shallow-water reef counterparts. This chapter describes a two-pronged approach to

studying bioerosion in mesophotic reef habitats by: (1) comparing time-averaged

macroboring of coral rubble; and (2) calculating bioerosion rates of experimental coral

substrates exposed for one, two, and three years. Bioerosional analysis constitutes a large

portion of this dissertation and is now a highly researched topic in coral reef science.

However, with so little known about mesophotic bioerosion, a detailed knowledge of the

processes was needed to permit accurate interpretations of new deep-reef data.

Therefore, an extensive literature review of bioerosion geological history, classification,

methodology, interaction between groups, and controls on bioerosion rates is provided in

the appendix. Alternatively, a short summary is provided along with results from the first two years of this study by Weinstein et al. (2014).

Objectives

The primary objective of this chapter is to determine how general trends in bioerosion and bioaccretion, bioerosion rates, and spatial distributions of bioeroding groups vary between mesophotic habitats with different structural characteristics and with shallow-water counterparts. The working null hypotheses for this chapter are that: (1) boring sponges will not be the dominant macroborer group at all study sites; and (2) bioerosion rates and abundance distributions will be homogeneous between different MCE habitats. To test these hypotheses, the amount of grazing, macroboring, and accretion was quantified using experimental substrates. Coral rubble was also analyzed to provide a longer-term perspective.

Methods

Coral rubble macroboring

In August 2010, technical research divers utilizing decompression and tri-mix techniques conducted an opportunistic collection of exposed random-sized rubble (~3-30 cm in diameter) south of St. Thomas, USVI (Fig. 1.4). Rubble was defined as hard substrate unattached to the underlying reef framework (Rasser and Riegl, 2002). Each sample collected was soaked overnight in a dilute bleach solution (~1:3 bleach to water), rinsed in fresh water, and sun -dried for two days. Dried coral rubble were cut into slices approximately parallel to the primary growth axis (Fig. 3.1a) and identified to species. Cut samples identified as coralline algae rhodoliths (primarily from the Deep Patch site,

Fig. 3.1b) were not included in any subsequent analyses. From the six reef sites, 44 useable coral rubble samples were analyzed (4-8 samples/site, Table 3.1). Digital photographs were taken of each cut surface, and point-count analysis was used to determine spatial coverage and abundances of macroborings (Perry, 1998; Macdonald and Perry, 2003).

Three randomly selected, non-adjacent surfaces were evaluated for each sample using Coral Point Count with Excel Extensions V3.6 (Kohler and Gill, 2006). Point count results from each of the three slices were averaged. Excavations produced by endolithic boring organisms were identified using published descriptions (Pang, 1973; Rützler, 1974; Bromley, 1978; Rice and Macdonald, 1982; Scott and Risk, 1988; Macdonald and Perry, 2003). Classification was restricted to the categorical groups of sponges, worms (polychaete and sipunculan), bivalves, others (boring gastropods and cirripedias), and unknown (boreholes too modified for identification). When considering group abundances, results were adjusted to eliminate the unknown category from all sites. One-way analysis of variance (ANOVA) tests were conducted to identify significant differences in rubble excavation and Tukey's honestly significant difference (HSD) tests were used to conduct multiple comparisons between sites. Potential relationships between rubble excavation percent and depth were tested with Pearson Correlations. Statistical analysis was performed in R Version 2.15.0 (R Core Team, 2014).

Bioerosion grazer abundances

Though not a direct indicator of grazing bioerosion rates (Bruggemann et al., 1996; Mumby, 2006), biomass data from the USVI Territorial Coral Reef Monitoring Program (TCRMP) study (Nemeth et al., 2008; Smith et al., 2011a) can still be used as a

proxy for the potential influence of parrotfish grazing on mesophotic bioerosion. Within each habitat, 4 - 82 visual census transects were completed by an experienced observer to determine parrotfish biomass. Transects were 25 x 4 m belts, with the exception of transects at the shallow Fringing Patch site, which were 30 x 2 m belts. Each transect was 12-15 minutes in duration, during which parrotfish were counted and assessed for size. Sizes were estimated into the following bins: 0-5, 6-10, 11-20, 21-30, 31-40, and 41+ cm, where fish above 41 cm were sized to the nearest cm. Biomass of each parrotfish was calculated from the middle of the size bin, given the formula and length-to- weight parameters of Bohnsack and Harper (1988). For TCRMP study sites, including the Primary and Secondary Banks, the Mid-shelf Patch, and the shallow Fringing Patch, transects immediately surrounding the location of the experimental substrates were performed between 2003 and 2011. For the Hillock Basin and Deep Patch study sites, data were taken from Smith et al. (2010) and included sites within 5 km that had similar characteristics to the experimental substrate sites (i.e., similar geomorphology and benthic structure).

The biomass of *Sparisoma viride* and *Scarus vetula*, the two primary Caribbean bioeroding parrotfish present at the study sites (Bruggemann et al., 1996; Cardoso et al., 2009), was used for bioerosion analysis. Bioeroding parrotfish biomass for each site was calculated as the average of all transects, each calculated by adding *S.viride* biomass to the adjusted biomass of *S. vetula*. The biomass of *S. vetula* was divided by 7 because of reports that the daily bioerosion rates of *S. viride* are 3-10 times higher than those for *S. vetula* (Bruggemann et al., 1996). One-way Kruskal-Wallis non-parametric comparisons

using JMP version 10.0 (SAS Institute Inc, 2012) were used to determine variability of parrotfish biomass between sites.

Experimental substrate weight change

The experimental design used to determine bioerosion rates was modified from Kiene (1988). By-product cores drilled through healthy, massive *Orbicella faveolata* (formerly known as *Montastraea faveolata*) colonies 2 m deep in the Florida Keys (Hudson, 1977). These were used to create unaltered experimental coral substrates that all shared similar material properties such as density and porosity. Following visual inspection to eliminate previously eroded substrate (Fig. 3.2a), 9.4 cm diameter cylindrical coral skeleton cores were cut into 216 individually labeled pristine coral substrates approximately 2 cm thick (Fig. 3.2b). The average height and diameter of all disks were recorded, and the surface area of the top ($\overline{SA}_t$), bottom ($\overline{SA}_b$), and side ($\overline{SA}_s$) of each disk were summed to find the total initial surface area ($\overline{SA}_i$) for each disk. After holes were drilled through the centers, disks were washed, dried in an oven for two days at 55° C, individually weighed, and photographed (Fig. 3.2b).

Each disk was mounted to a PVC quadrat (~ 50 cm X 10 cm). A nylon bolt and washer were inserted through the disk hole followed by a nylon spacer below the disk, allowing both sides of the substrate to be available for erosion (Fig. 3.2c). The remaining bolt below the spacer was then threaded through holes drilled in the PVC. The disk and nylon attachments were locked in place with a nylon nut screwed to the bolt sticking out below the PVC (Fig. 3.2c, green arrow). Sets of 12 randomly selected disks were mounted to 1 of 18 quadrats, with the PVC location of each individual sample label recorded (Fig. 3.2c, yellow arrow pointing to number 6 for example). Notches were cut

into the arbitrary selected top long frame of the PVC in 1 of 3 positions and marked with a zip-tie (Fig. 3.2c, purple arrow). This was done to distinguish between quadrats installed at the same sites and indicate PVC orientation relative to recorded disk sample label locations. Quadrats with experimental substrates were designed to simulate newly available bare coral framework and blend with the surrounding reef (Fig. 3d).

In August 2010, divers used reinforced steel and sledge hammers to anchor (between corner holes such as indicated with brown arrow in Figure 3.2c) quadrats with the coral disks parallel to the seafloor (Fig. 3.3a). Three quadrats were installed at each site. The first quadrat at each site was installed at a semi-randomly selected location based on where divers first dropped onto the reef. The other two quadrats were attached to the seafloor approximately 10 m apart in random directions from each other. Divers mapped out the location of each quadrant to assist with locating them in the future. To provide experimental replication and utilize a randomized blocking design, three randomly pre-selected disks from each quadrat were scheduled for collection approximately once a year for three consecutive years. A final collection was originally scheduled for 10 years after deployment to provide more temporal resolution for future studies. However, by the third collection year, the remaining (10 year) substrate disks at some sites appeared heavily grazed. Although these samples may be removed before the planned 10-year interval, they remain at their respective sites as of December 2014.

The 1st -3rd substrate disk collections occurred Aug. 2011 (Fig. 3.3b), May 2012 (Fig. 3.3c), and May 2013 (Fig. 3.3d), using PVC cutters to cut the nylon bolts (Fig. 3.3d). To avoid mislabeling, samples were stowed, in the order of collection, in PVC storage containers (see arrow in Fig. 3.3b) specially designed to avoid "human" erosion

during transport back to the surface, often after 30 minutes of required decompression. Collected substrate samples were washed with a hose to remove internal eroded material from cryptic locations and soaked in a weak bleach solution for up to two days before being air-dried. Prior to weighing, samples were oven dried at 55° C for an additional two days. A small number of samples were eliminated from analysis because of damage during transport or incorrect documentation (Table 3.1).

Differences in mean weight change, which represents net carbonate "production" per substrate disk, were compared with a nested two-way factorial ANOVA. The ANOVA was conducted in JMP 10.0 (SAS Institute Inc.) with year of collection and site as crossed factors and quadrat nested within the site factor. Data were transformed with a natural logarithm to meet assumptions of homogeneity of variances. Significant site differences among substrate weight change means within factors were tested with Tukey's Post-Hoc honest significant difference (HSD) test. The relationship between substrate weight change and other explanatory variables was tested in R Version 2.15.0 (R Core Team, 2014) with Pearson Correlations and linear regression.

Year 3 bioerosion and accretion analysis

To quantify the relative contributions of substrate weight change from bioeroding groups and secondary accreting organisms, a digital analysis approach, modified from Kiene (1988), was applied for the experimental substrates collected after three years of exposure. The first step entailed calculating the percent each carbonate removing process (grazing, macroboring, and microboring) contributed to the weight change of each substrate disk (initial disk weight pre-experiment minus final disk weight). Next, the percent of each process was multiplied by the initial disk mass prior to exposure to

estimate the amount of material removed from the substrate disk (in g) by each process. Specifically, three main bioeroding processes were measured: (1) total grazing (Tg_m), calculated as the total material removed by perimeter grazing (PG_m), top grazing (TG_m), and bottom grazing (BG_m); (2) total macroboring ($Tmac_m$), calculated as the sum of total carbonate removed by bivalves (B_m), worms (W_m), sponges (S_m), vermetid gastropods (V_m), and others (O_m); and (3) total microboring ($Tmic_m$).

To quantify perimeter grazing percentages, photographs of each eroded disk top and bottom were taken, with the camera lens approximately parallel to the disk surface (top or bottom). After outlining the outer eroded substrate edges as seen in the photograph using Adobe Photoshop (Fig. 3.4a, solid orange line), the program NIH image J was used to calculate the difference in initial and final projected surface area (ΔP_{SA}) for each disk (Fig. 3.4a, area between solid and dotted orange line). The term "projected surface area" is used because this value represents a two-dimensional surface area estimate of a three-dimensional object, with the outer most parts of the disk anywhere along its height making up the edges used to calculate the area. Theoretically, the top and bottom projected surface areas are should be equal, but were not due to photographic distortion. Therefore, the greater of the two surface areas (top or bottom) was used to represent the projected surface area because this value could not be overestimated when using the described technique. The ΔP_{SA} for each disk was used to find the projected percent of original surface area removed by grazing ($\Delta P_{SA}/\overline{SA}_t$ or $\Delta P_{SA}/\overline{SA}_b$), and was then multiplied by the initial disk weight to provide an estimated value of the total material removed by perimeter grazing (PG_m).

Although the two-dimensional projected disk photographs enable quantification of perimeter grazing (PG_m), this method cannot detect material removed by on the top and bottom parts of the disk that do not extend to the edge of the rock (Fig. 3.4, red arrow). Therefore, non-projected top and bottom grazing surface area represents the amount of removed outer substrate material not previously accounted for by ΔP_{SA} (Fig. 3.4c, brown and grey areas). To determine the percent of carbonate removed by top and bottom grazing, as well as by macroboring, each collected disk was cut into eight triangular slices (Fig. 3.4b) radiating from the disk center (Kiene, 1988a). To prevent optical distortion, each non-adjacent slice face was digitally imaged with a flatbed scanner (Fig. 3.4b inset). The theoretical (if they were cut before deployment) cross-section surface area sum of eight pre-experiment slices ($\bar{T}_{SAi}$) was calculated as eight times the product of the initial average disk radius and height and recorded.

All bio-modification features (macroborings and top and bottom grazing) were identified and digitally outlined on each slice of a disk set (Fig. 3.4c). On each slice, a line parallel to the theoretical disk height was drawn at the outermost intersection point of the remaining substrate (Fig. 3.4c, black line). The intersection of that line delineated what was defined as top grazing and bottom grazing. Using *Adobe Photoshop* measurement functions, the surface areas (in mm^2) of each feature per slice were calculated. For each feature type identified, the calculated surface areas from all eight disks were summed to give a total value for the sample. Sum surface areas were calculated for top and bottom grazing (GT_{SA8} and GB_{SA8} respectively), as well as for the macroboring of bivalves (B_{SA8}), worms (W_{SA8}), sponges (S_{SA8}), vermetid gastropods (V_{SA8}), and others (O_{SA8}). Each value was then divided by $\bar{T}_{SAi}$ to approximate the

present of each bio-modification feature (with the exception of perimeter grazing) per substrate disk. These percentages were then multiplied by the initial disk weight to determine the mass of carbonate removed from the disk by macroboring processes (B_m, W_m, S_m, V_m, O_m) and grazing processes (PG_m and TG_m added to the previously calculated PG_m).

Total weight removed by microboring ($Tmic_m$) was not directly measured, but was still believed to contribute to overall weight change. Therefore, microboring rates were needed to approximate the impact of this bioerosion group on overall experimental substrate weight change. The most applicable data currently available come from research conducted along the windward side of Lee Stocking Islands, in the Bahamas (Vogel et al., 2000). Using micritic limestone experimental substrates, Vogel et al. (2000) measured mean microbioerosion rates on a 2 m deep *Acropora palmata* dominated reef ($\bar{B}_{micro_2} = 0.21$ kg m^{-2} y^{-1}) and on an adjacent 30 m deep shelf-edge reef ($\bar{B}_{micro_{30}} = 0.12$ kg m^{-2} y^{-1}). Values from the 2 m site ($\bar{B}_{micro_2}$) were used for experimental substrate microboring estimates at the two shallowest USVI sites and values from the 30 m site ($\bar{B}_{micro_{30}}$) were used for equivalent estimates at the mesophotic sites. The amount of carbonate removed by microboring for each disk ($Tmic_m$) was estimated as the product of the depth-appropriate rate ($\bar{B}_{micro_{depth}}$) and the projected final surface area ($\overline{SA}_t$ or $\overline{SA}_b$), divided by the duration of disk exposure. The projected surface area, not the entire disk surface area, was used because microbioerosion tends to occur on the top surfaces of substrate where light is accessible.

Total disk bioerosion weight removed ($TB_m = Tmac_m + Tg_m + Tmic_m$) was then subtracted from the final measured weight of the disk to provide an estimate of total disk

weight gained by accretion (TA_m). The average of TB_m (and similarly the average of TA_m) for each disk collected from the same quadrat were calculated and considered the base sampling unit (for which standard error was calculated from). The values from each triplicate quadrat set were used to calculate the site average carbonate mass removed by bioerosion ($\overline{BM}_{xs}$) and the site average carbonate mass gained by secondary accretion ($\overline{AM}_{xs}$).

Results

Coral rubble

The average amount of macroboring excavation by site (Fig. 3.5) was highest in coral rubble collected from mesophotic sites closest to the Anegada Passage (43.0-46.1%) and lowest at the deep patch site (18.7%), where many samples were encased by coralline algae (Fig. 3.1b). A one-way analysis ANOVA indicated significant differences in the average percentage of rubble excavated by macroborers collectively between all sites ($F_{5,43}$= 6.248, p < 0.0003). Tukey's (HSD) pairwise indicated macroboring significant differences between D1, D3, and D4, with S6, and between D1, D3, and D4, with D2.

Sponge borings, which showed significant differences between sites ($F_{5,43}$= 3.465, p = 0.012), were the most abundant at all sites, ranging from 88.5% at the Primary Bank to 47.0% at the shallow Fringing Patch site (Fig. 3.5). Worms were the next most common macroborers at all sites, except at the Deep Patch site. Compared to the other sites, the shallow Fringing Patch reef coral rubble had the most diverse macroboring assemblage (sponges, worms, bivalves), and the largest amount of gastropod and barnacle borings (18.7%). Assemblage diversity was lower at the Mid-shelf Patch site and lowest

at the mesophotic sties. The Pearson Correlation showed little apparent relationship (n = 6, r = -0.329, p = 0.524) between the average amount of coral rubble excavated by macroborers per site and site depth because the Deep Patch site was an outlier (Fig. 3.6). Removal of the Deep Patch site from analysis, however, resulted in a very strong correlation (n = 5, r = -0.967, p = 0.007).

Parrotfish and Diadema antillarum *abundance*

Transect surveys showed the site-average biomass of the bioeroding parrotfish, *S. vetula* and *S. virde* ranged from 0 g/100m^2 at the Deep Patch site to 578.17 g/100m^2 at the secondary Bank site (Fig. 3.7). Excavating parrotfish biomass was significantly different between study sites (Kruskal-Wallace, df = 5, X^2 = 15.23, p < 0.0094). While no significant differences between means were detected by Tukey's HSD comparison, a trend of increasing biomass at the shallow sites (M5, S6) and the Secondary Bank (D4) was detected. *Diadema antillarum* was only identified at three of the study sites, and mean densities never surpassed 2 per 100 m^2 (shallow Fringing Patch = 1.15±0.74 SE, n = 61; Mid-shelf Patch = 0, n = 75; Primary Bank = 0, n = 75; Secondary Bank = 0, n = 72; Hillock Basin = 0, n = 6; Deep Patch = 0, n = 4, Smith et al., 2012).

Substrate bioerosion

The weight change of coral substrates provides a proxy for framework carbonate modification through bioerosion and encrustation. To directly compare bioerosion at different locations, uniform substrates with similar material properties were used to eliminate substrate composition different as a variable. However, these also induced limitations, as the substrates were not composed of the dominating mesophotic coral but of a shallow coral with material properties different than that of coral naturally found at

the mesophotic sites. Therefore, all conclusions from the resulting data should be considered specific for the particular substrate used.

Analysis revealed significant differences in substrate weight change between sites (Fig. 3.8) among various factors (df = 23, F = 7.30, p < 0.0001). Comparison of means showed that the site, year, and nested quadrat factors were all significantly different among groups, whereas year and the year*site interaction were not significant (Table 3.2). This indicated that weight change was not consistent across sites and that the rate of weight change increased from year one to year two, and year two to year three, except at the Deep Patch site. The significant nested quadrat factor also indicated that experimental quadrats behaved differently within the sites, suggesting inter-site differences in bioerosion potential.

Experimental substrates at the two shallower sites and the shallowest mesophotic site had negative rates of average substrate weight change (weight loss) not significantly different from each other. In contrast, the Deep Patch and the Hillock Basin sites primarily experienced small weight gains not significantly different from one another (or from the Primary Bank for year one to year two), but were significantly different from the shallower sites. By the third year, the small amount of net erosion experimental substrates from the Hillock Basin site was substantially differences from any of the other sites. Additionally, the Deep Patch site remains different from the others as the only site with significant net accretion. The trend at the Primary Bank site was similar to that of the deepest sites (D1 and D2) after one year, and began to deviate more after two years (though not a statistically significantly difference). However, the Primary Bank site experimental substrate bioerosion trend shifted group clusters by year three, with similar

rates compared to the other shallower sites. Experimental substrate bioerosion rates (Fig. 3.8, slope of lines equal rates of change) at the Secondary Bank site and the shallow Fringing Patch site slowed down after year two compared to the respective rates recorded for them earlier. These were also no longer the sites where collected experimental substrates experienced the mean greatest weight change (which was at the Mid-shelf Patch after year 3). Rates of substrate loss increased between years two-three for all other sites, except the Deep Patch site, which appeared to have relatively little net change between year two and three.

Inspection of sliced experimental substrates revealed few macroborings in the first year and only slightly more in the second year, with bivalves and worms primarily responsible for the macroborings observed at all sites. There was also significantly more colonization of bio-accreting calcareous organisms on experimental substrates collected from the reefs in the upper mesophotic reef zone (compared to substrate disks from the shallower sites. Based on these results, it was decided that a more in-depth examination was not as imperative for year one and two samples, but was still conducted for samples exposed for three years.

When examining the relative contributing elements responsible for the measured final average substrate weight change per site after three years of exposure, secondary accretion was observed to add material relatively uniformly, regardless of location and depth (Fig. 3.9). However, the relative proportion of substrate removed by bioerosion versus carbonate grained by secondary accretion is not uniform. Generally, the ratio decreases with depth (Fig. 3.9). At all sites, grazing bioeroders were found to remove significantly more substrate than any other bioerosion process. Per site, perimeter

grazing was always significantly higher than the other two grazing measurement types (top and bottom), and bottom grazing was always the lowest (Fig. 3.10).

Carbonate removal by macroboring processes was found to be relatively minor (Fig. 3.9). The greatest amount of experimental substrate removed by macroboring was at the shallowest site (S6). Potentially related, bivalve boring dominated at the Fringing Patch site and was greater at that location than any other by 61.2 %. The study average relative worm component of macroboring was greater than the other groups by 50.3 %, implying worms may be slightly more dominant (in terms of amount of boring) within the study areas when substrate is exposed for a short (3-year) time span. No other major trends in relative macroborer contributions were identified.

To better understand patterns of substrate modification, the average weight change at each site was compared to: (1) water depth; (2) coral rubble macroboring; and (3) grazer biomass. A strong correlation was found between average substrate weight change and water depth ($n = 6$, $r = -0.866$, $p = 0.026$) after one year of exposure (Fig. 3.11). The relationship becomes less obvious after two years of exposure ($n = 6$, $r = -0.744$, $p = 0.090$). However, removing the Secondary Bank samples from this testing greatly increased the correlation ($n = 5$, $r = -0.966$, $p = 0.008$). No statistically significant correlation could be confirmed after three years ($n = 6$, $r = -0.668$, $p = 0.147$).

No significant correlation was identified between the rate of average experimental substrate weight change and average coral rubble macroboring per site (year one: $n = 6$, $r = 0.055$, $p = 0.918$; year two: $n = 6$, $r = -0.137$, $p = 0.796$; year three: $n = 6$, $r = -0.271$, $p = 0.603$). Also, a linear regression relationship between the rate of experimental substrate weight change and average measured bioeroding parrotfish biomass per site (Fig. 3.12)

was not significant after one year of exposure (n = 6, R^2 = 0.656, p = 0.051). However,

the a linear relationship between the same variables was significant after two and three

years of exposure, with the measured bioeroding parrotfish biomass explaining a

moderately high amount of weight change variability (year 2: n = 6, R^2 = 0.684, p =

0.042; year 3: n = 6, R^2 = 0.752, p = 0.025).

Discussion

Grazing and parrotfish

Three years of substrate weight change data (Fig. 3.8) indicates major differences

in bioerosional patterns at mesophotic habitats with distinctive structural characteristics.

Although sites analyzed for this study do not span the entire mesophotic range,

comparison between study mesophotic reef sites and with shallow-water counterparts

generally indicates that initial bioerosion of exposed substrate decreases with depth.

These results are consistent with previous shallow-water reef studies (Stearn and Scoffin,

1977; Kiene, 1988b; Chazottes et al., 1995; Tribollet et al., 2002).

The limited quantity of macroborings observed in all experimental substrate disks,

even after three years of exposure, suggests that most substrate weight change resulted

from grazing and bioaccretion. Minimal *D. antillarum* detection and the moderate

relationship between excavating parrotfish biomass and substrate weight loss (Fig. 3.12)

form the basis for two main conclusions. (1) Parrotfish grazing is the dominant initial

bioerosion method of shallow-water coral reefs down to the upper mesophotic zone in the

northern USVI. (2) A reduction in parrotfish grazing is partially responsible for the low

substrate bioerosion rates of mesophotic reef communities in the middle to lower depths

of the mesophotic reef zone. Similar trends have been found in the Red Sea (Brokovich

et al., 2010), the Great Barrier Reef (Kiene and Hutchings, 1994), and the Netherlands Antilles (Bruggemann et al., 1996; Perry et al., 2012).

Macroboring

Many previous studies have shown that fresh carbonate substrate requires a minimum exposure time of two-five years before macroborers site differences are observed (Hutchings et al., 1992; Kiene and Hutchings, 1993; Kiene and Hutchings, 1994; Chazottes et al., 1995; Peyrot-Clausade et al., 1995; Hassan, 1998; Pari et al., 2002; Tribollet et al., 2002). Therefore, coral rubble offers the best record of long-term macroboring modification within a reef. The sampling design and analytical techniques of coral rubble for this study were partly developed to minimize some of the known taphonomic uncertainties associated with coral rubble analysis (see chapter 1 for examples of specific uncertainties). A random sampling of mesophotic coral rubble in reefs with similar coral species distributions (except the Deep Patch) ensured that on average, the same types of skeleton substrates were analyzed (Table 3.1).

Although rubble seafloor exposure time is unknown, a substantially greater average number of macroborings were identified in mesophotic rubble than in all experimental substrate disks analyzed. This observation implies that mesophotic coral rubble has been exposed to bioerosional processes for at least 10-20 years, and suggests they could have been exposed considerably longer. An example of this is seen when comparing the number of borings identified in an experimental substrate exposed for ~3 years at the Hillock Basin (Fig. 3.4c) with that of coral rubble from the same location (Fig. 3.1a). The studied northern USVI mesophotic reefs were identified as experiencing low rates of sedimentation (Rothenberger et al., 2008), relatively little transport of gravel-

sized sediment and allochthonous sediment (see chapter 2). The sites are also located on bathymetric highs along a very gradual slope over 10 km from the shore (Fig. 1.4). Therefore, the mesophotic sites are unlikely to harbor allochthonous downslope transported rubble or experience significant burial. These observations also advocate that mesophotic coral rubble analyzed in this study was relatively *in situ*, had a long potential exposure time, and a high probability of being collected from the original taphonomic "active" zone (not buried then re-exposed). These arguments are partially supported by the suggestion that slower growth rates of deeper coral lead to lower sedimentation rates (Pandolfi and Greenstein, 1997).

Coral rubble analysis in the USVI showed that the average percent of exposed rubble carbonate removed by macroborers usually increased for denser mesophotic corals (excluding those found at the Deep Patch site). This trend is reasonable considering bioerosion is thought to increase with longer exposure time (Scoffin et al., 1980), an intuitive idea since organisms would have more time to erode the substrate. These results do not contradict the conclusion from this study that total initial bioerosion decreases with depth because, as several studies have shown, grazing initially removes much more carbonate than macroboring (Kiene and Hutchings, 1994; Chazottes et al., 1995; Reaka-Kudla et al., 1996; Perry et al., 2012). Using dead coral framework and coral rubble, studies in Jamaica found that macroboring infestation was highest in deep fore-reefs compared to the shallower fore-reefs (Perry, 1998; Macdonald and Perry, 2003). Other non-experimental substrate studies documented greater macroboring in deep reef-fronts than shallow reef-fronts (Goreau and Hartman, 1963; Pandolfi and Greenstein, 1997; Greenstein and Pandolfi, 2003). Contrary to these studies and to coral rubble

macroboring trend results from the northern USVI, carbonate removal by macroboring in experimental substrate exposed for three years was greatest at the shallowest two sites (M5 and S6) analyzed. The reason for these seemly different patterns is related to exposure time and concurrent grazing, and grazing intensity.

Grazing intensity has been suggested to partially regulate macroboring community succession by creating new available substrate for macroborer recruitment (Kiene and Hutchings, 1994); however it is uncertain if this is more beneficial for recruitment of coral or bioeroders. Regardless, Sammarco et al. (1987) found that different levels of grazer accessibility alter the composition of bioerosional communities. Macroboring communities mature with increasing substrate age, starting as immature communities of small, short-lived worms, followed by longer-lived larger worms, sipunculans, mollusks, and finally by mature boring sponge communities (Hutchings et al., 1992; Kiene and Hutchings, 1994; Hutchings, 2008). With higher sedimentation rates, faster coral growth rates, and more storm disturbances and branching coral, the time-average age of shallow-water reef coral rubble is likely to be much younger than deep rubble (Perry and Hepburn, 2008). This younger reef rubble may explain why macroboring was greatest in mesophotic coral rubble with dense skeleton but initial experimental substrate macroboring was greatest at the shallow Fringing Patch site. Over longer time spans (coral rubble exposure time compared to the length of experimental substrate deployment), macroborers have a greater potential to infiltrate dense mesophotic rubble.

Results from our study indicate that the coral rubble macroboring community is primarily mature at the mesophotic reef sites, intermediate at the Mid-shelf patch, and

immature at the shallow Fringing Patch site. Rapid substrate grazing, along with a suggested shorter exposure time probably prevent the duration needed to establish mature bioerosional communities at the Fringing Patch. On a short-time scale, the higher rates of grazing more common in shallow-water reefs than mesophotic reefs may enable greater macroborer access to fresh substrate. The advantage is not long-lasting through because rapid grazing may eventually remove previously macrobored substrate initially facilitated by grazing. This would remove traces of abundant macroborings that were observed to be more characteristic of dense mesophotic rubble. And because mesophotic rubble in the USVI is presumed to have longer potential exposure time than rubble from shallow-water reefs, the rubble is further available for additional macroboring penetration (and grazing, but this does not seem to be as intense for deeper reefs). This explains the discrepancy between the short term experimental results and the time-averaged pattern observed by coral rubble analysis.

The distinct shallow and deep macroboring pattern differences in rubble and recently exposed substrate are slightly harder to distinguish at the transitional boundary between shallower and mesophotic reefs. At the Secondary Bank, for example, coral rubble macroboring patterns were similar to patterns at other mesophotic sites (D1, and D3). However, the Secondary Bank also harbored the greatest parrotfish biomass and had the greatest experimental substrate weight loss in the first two years compared to the other sites. We speculate that processes differentiating shallow and mesophotic bioerosion are less defined at the Secondary Bank, where the deepest shallow-water conditions meet the shallowest mesophotic depths. The high recorded parrotfish biomass might result from the fact that the Secondary Bank is a marine protected area and

experiences fast bottom currents, facilitating high productivity attractive for parrotfish (Smith et al. 2012). Primary Bank results from year three, indicating a greater increase in average weight loss compared to all other sites (Fig. 3.8), might represent a shift to bioerosion patterns more similar to reefs at or shallower than the transitional zone.

Although parrotfish grazing appears to be the primary initial bio-modifier of reef framework down to the transitional mesophotic reef zone (30-35 m), data suggests macroborer-initiated erosion is the main process responsible for most reef framework modification in the upper mesophotic reef zone (35-50 m). This trend is reasonable when considering the lack of grazing disturbance and longer assumed rubble exposure time in the deeper mesophotic study sites. Pacific experimental substrate studies found no boring sponges for up to one and a half to three years (Davies and Hutchings, 1983; Kiene, 1988; Chazottes et al., 1995). However, they predicted longer exposure time would allow for boring sponge recruitment, given the identification of extensive sponge excavations in nearby coral heads. With similar coral rubble observations in the northern USVI (Fig. 3.1a), sponge erosion in mesophotic experimental substrates would likely increase more than other types of macroboring or grazing with time. Although sponge macroboring was still not the dominant mesophotic bioerosion type after three years of exposure (Fig. 3.9), qualitative observations noted that the relative percent of sponge bioerosion was higher after three years than the previous collection years.

Previous studies have implicated sponges as the most common and destructive coral macroborer group (Hein and Risk, 1975; Risk et al., 1995; Glynn, 1997; Holmes, 1997). These studies, reasonable assumptions, and USVI macroboring and parrotfish biomass data suggest sponges are the chief macroborers responsible for long-term

substrate modification in and below the upper mesophotic coral reef zone. This is suggested despite the short three-year exposure time that allowed for immature bioerosional community development. Whereas the same outcome would initially be true for coral rubble (such that sponge dominance in erosion might not be apparent), sufficient time eventually the dominant endolithic boring group could infiltrate. A longer time span would also allow for multiple generations of sponge bioerosion to erase nearly all traces of the initial immature community (Focke and Gebelein, 1978; James and Ginsburg, 1979). This may also explain northern USVI study results, that coral-rubble macroboring group-diversity decreased with depth (Perry and Helpburn, 2008).

Bioerosion variability between mesophotic habitats

Despite significant initial substrate bioerosion rate differences between the two shallowest and the two deepest mesophotic study sites from this study, bioerosion analysis does not provide evidence to suggest these differences either result from or cause variability in mesophotic geomorphology. Homogeneous experimental substrates were used to limit variables and focus primarily on bioerosion. But in actuality, composition and amount of available substrate is not always similar for nearby mesophotic reefs, as best observed at the rhodolith-rich Deep Patch site sparsely covered with live coral. The only non-rhodolith skeletal rubble samples retrieved after multiple collections were of *Manacina areolata* and *Mycetophyllia aliciae*, coral with skeletal densities much lower than the coral rubble collected at other mesophotic sites. This skewed Deep Patch rubble analysis results towards low levels of macroboring, as endolithic sponges are able to remove more carbonate from denser coral than from less dense, more porous coral (Highsmith, 1981; Highsmith et al., 1983; Schonberg, 2002). Additionally, Deep Patch

coral rubble was often encased in coralline algae (Fig. 3.1b). Encasement of this nature creates a protective coating believed to block endolithic surface access holes and limit macroboring infiltration beyond the coralline algal layers into the coral (Bromley, 1978; Peyrot-Clausade and Bruno, 1990). Encasement protection of coral substrate may also just be a result of penetration potential. Within a dead coral colony (or a living colony, to a lesser degree), the probability of macroboring excavation drops considerably the further carbonate is located from the coral outer surface (see Glynn, 1997).

Over long time scales, subtle differences in mesophotic bioerosion patterns possibly increase small-scale structural reef complexity. And although larger-scale distinct geomorphic mesophotic habitat structures may not predominately result from differences in bioerosion directly, we propose that the mesophotic bioerosion impact on maintaining or at least exaggerating differences in habitat geomorphology will depend on how the interaction of somewhat similar bioerosional conditions change for habitats that vary in composition and other parameters (Perry and Hepburn, 2008). Differences in reef orientation, substrate exposure time, and benthic recruitment patterns change the amount of coral rubble and *in situ* coral framework available for bioerosion and new coral larval recruitment (Perry and Hepburn, 2008). The amount of available substrate for erosion and colonization can vary between mesophotic sites (Table 1.1) and can be influenced by environmental disturbances, potentially impacting the overall effect of bioerosion (Pang, 1973; Highsmith et al., 1983; Kiene, 1988).

For example, coral skeleton examined from the Hillock Basin site verified a history of multiple die-off events (see Fig. 1.3b). This was probably related to intercostal mortality syndrome (IMS), an abiotic extreme disease documented as preferentially

occurring at the Hillock Basin compared with other mesophotic sites (Smith et al., 2010). Surveys after the outbreak showed significantly more substrate availability in the Hillock Basin site than even at the shallowest reef sites. Therefore, a possible scenario for mesophotic reef hillock development is that episodic disease events (or other stressors) produce available dead substrate, which promoted coral colonization and vertical hillock accretion. Meanwhile, lower initial bioerosion rates and slow water currents (Smith et al., 2010) may have prevented rubble from breaking off the hillocks into the surrounding sand. Formation of a more homogeneous reef geomorphology may become more difficult without new coral rubble-deposited areas for coral colonization between the hillocks. An alternative scenario for lateral homogenous mesophotic reef extension may depend partially on if bioerosion creates new coral rubble without eroding it away completely. Faster currents recorded at the Primary and Secondary Banks (Smith et al., 2010) and similar cover of available exposed substrate (Table 1.1) may partially explain the maintenance of similar trending lateral bank geomorphology. However, the double reef bank geomorphology also partially or completely results from earlier shallow-water reef growth when sea-level was lower than present (Holmes and Kindinger, 1985).

Finally, the importance of secondary accretion in mesophotic reef development is suggested by results from northern USVI experimental substrate analysis. This is especially true given the fact that coral growth rates in these environments are much slower than in shallow-water coral reefs (see chapter 4). Although secondary accretion on experimental substrate was comparatively homogenous, regardless of site location and depth (Fig 3.9), the relative high amount of secondary accretion compared to bioerosion suggests that seemingly slower growing mesophotic reef communities could have net

positive carbonate accretion. This explains why the Deep Patch site, a low relief habitat

that appears to have less primary productivity but similar secondary accretion patterns as

other sites, is still able to maintain a slow-glowing but stable habitat relief. However,

more mesophotic reef research regarding benthic recruitment patterns, rubble production,

and habitat composition, and longer mesophotic sponge bioerosion rates are needed to

fully assess the mesophotic reef "slow but steady" accretion effectiveness towards

maintaining structurally sustainable habitats.
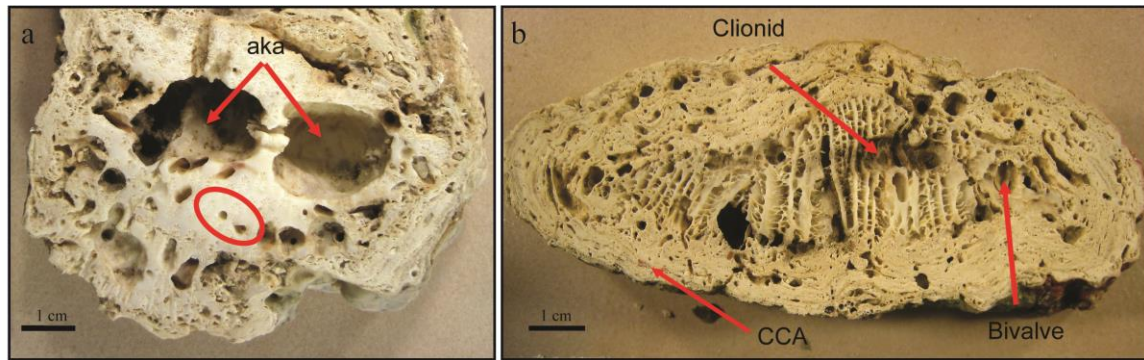
Figure 3.1. Macrobored mesophotic coral rubble. (a) *Stephanocoenia intersepta* rubble from the Hillock Basin site, bored by polychaete or sipunculan worms (red circle), and by the sponge genus *Aka brevitubulatum*. (b) Porous *Mycetophyllia aliciae* rubble encased by crustose coralline algae (CCA) and with preserved macroboring Cliona sponge and bivalve borings.
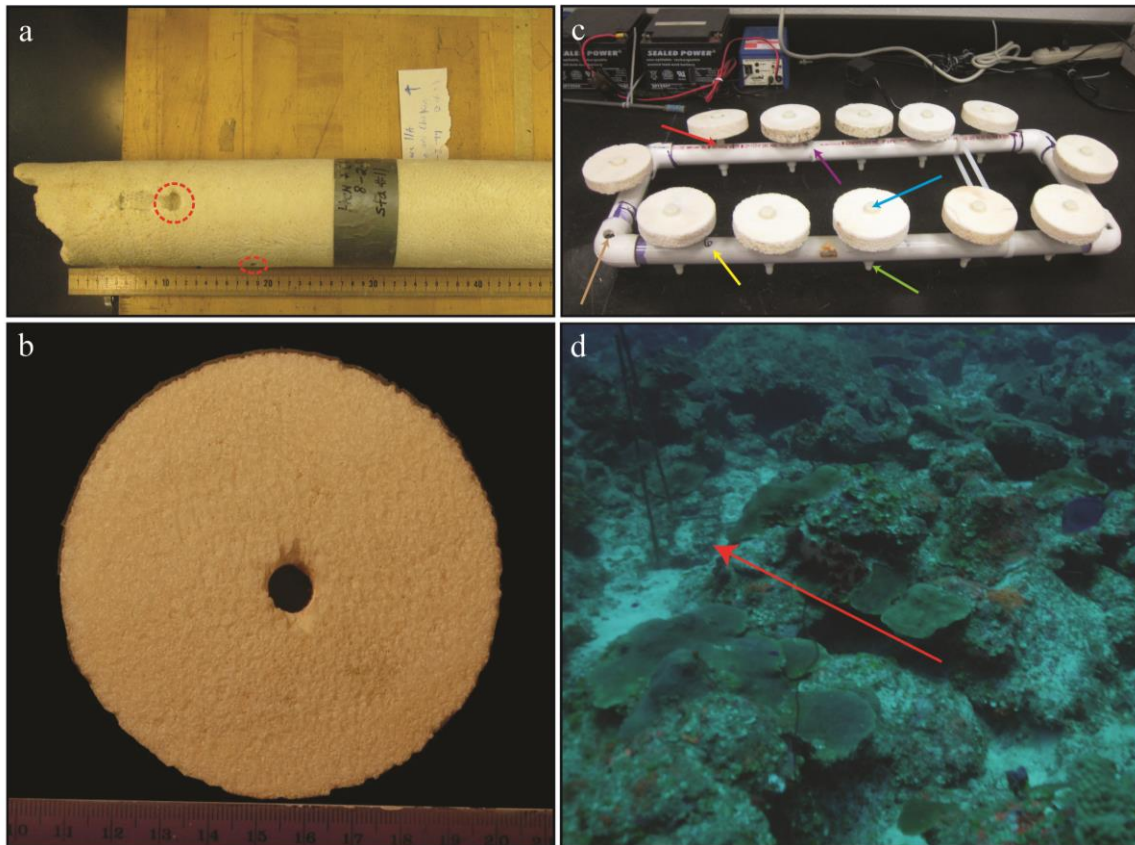
Figure 3.2. Experimental coral substrates. (a) Core taken from pristine living massive *Orbicella faveolata* coral 2 m below sea-level in a Florida Keys reef (Hudson, 1977). Red circles indicate areas of previous macroboring, which were identified and not used for experimental substrates. (b) Example of experimental substrate "disk" before experiment. (c) Randomly selected substrates were mounted to PVC quadrats prior to deployment. Blue arrow points to example of nylon bolt head, red arrow points to example of nylon spacer location, green arrow points to example location of nylon nut used to lock disks to the PVC, with the remaining bolt tail below (see text). Purple arrow points to location where zip-tie wraps around notch in quadrat top, used for identification and orientation. Yellow arrow points to numbers used to identify the mount location of each individual substrate disk prior to deployment. Brown arrow points to corner holes rebar was inserted through to anchor quadrats. (d) Quadrats and disks (indicated by red arrow) quickly became nearly indistinguishable from the rest of the reefscape, providing a fair representation of exposed substrate.
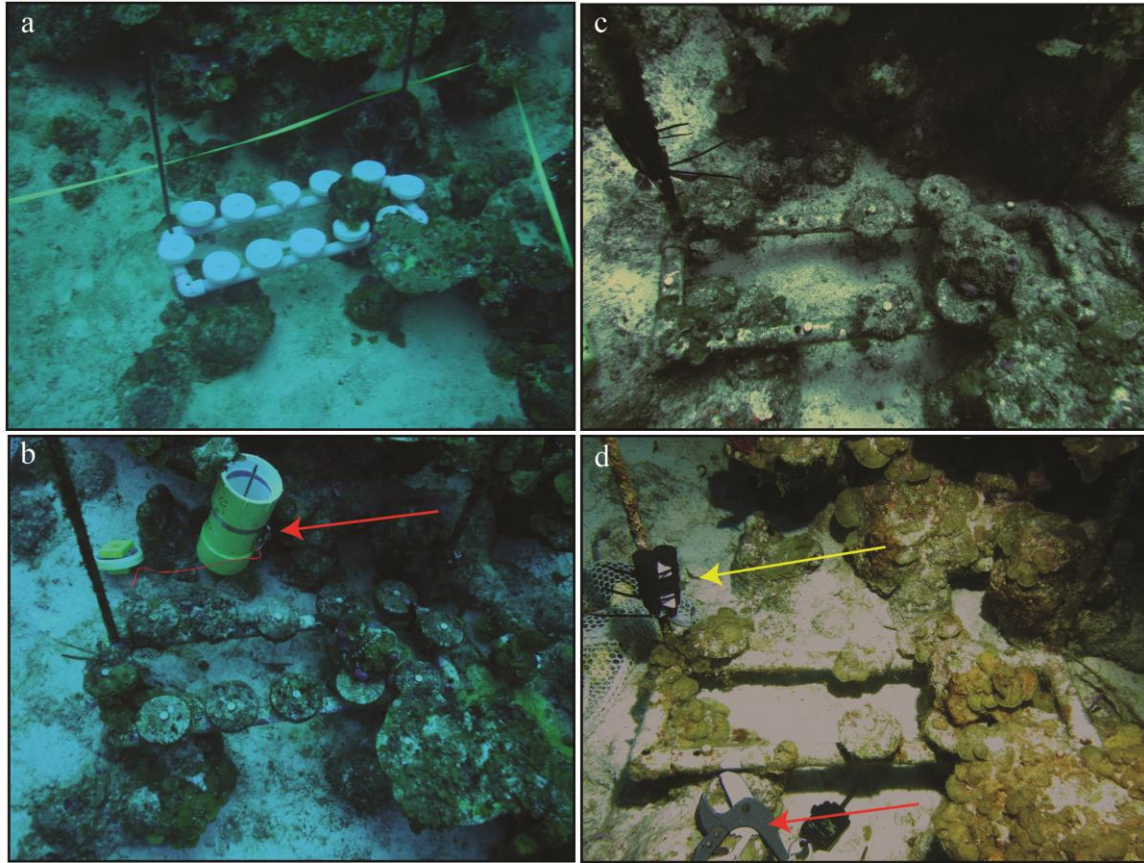
Figure 3.3. Deployment and exposure. Quadrat 2 from the Hillock Basin. (a) Instillation occurred on Aug. 28, 2010. The same quadrat was sampled (b) 352 days later (red arrow points to disk collection container), (c) 637 days later, and (d) 990 days later (red arrow points to PVC cutter used to cut nylon bolts and remove substrates, yellow arrow indicates a temperature logger. Three substrate disks were removed each collection period for analysis. Pictures after 352 days (b) and after 990 days (d) were taken before substrates were removed and the picture after 637 days was taken after the yearly substrate removal.

Table 3.1. Rubble and disk sample sizes. Table shows the number of experimental substrates collected from each quadrat during each collection period, and the number of coral rubble samples analyzed in which the indicated species was the dominant "nucleolus" coral skeleton of the rubble sample. Chapter 3 text explains why there were deviations from the planned collection of three substrates per quadrat each year. Underlined values indicate samples from a quadrat that was found toppled over before year one collection and put back in place. Analysis indicated this did not have a significant affect.

Geomorphology and depth (m)	Number of substrates				Number of rubble samples (by dominant coral species)											
	Quad. #1	Quad. #2	Quad. #3	Total	*Orbicella franksi*	*Orbicella annularis*	*Montastraea cavernosa*	*Agaricia spp.*	*Porites porites*	*Porites. astreoides*	*Stephanocoenia intersepta*	*Manicina areolata*	*Mycetophyllia aliciae*	*Siderastrea siderea*	*Dichocoenia stokesi*	Total
D1 Hillock Basin (44.5)	2, 3, 3	3, 3, 3	2, 3, 3	25				3		2	2					7
D2 Deep Patch (41.1)	1, 3, 1	3, 3, 3	3, 2, 3	22								3	1			4
D3 Primary Bank (39.0)	2, 3, 3	3, 3, 3	3, 3, 3	26	1		1	3		3	3					11
D4 Secondary Bank (30.7)	3, 3, 3	3, 3, 3	3, 3, 3	27	1	1		2	2	1						7
M5 Mid-shelf Patch (21.0)	3, 3, 3	3, 3, 3	2, 3, 3	26		1	1	1						1	1	5
S6 Fringing Patch (9.0)	3, 3, 4	3, 3, 3	3, 3, 3	28	1	2		3	1	2						9

Grazing
- ■ Perimeter (dark purple)
- ■ Top (brown)
- ■ Bottom (gray)

Macroboring
- ■ Bivalve (green)
- ■ Worm (dark blue)
- ■ Sponge (teal)
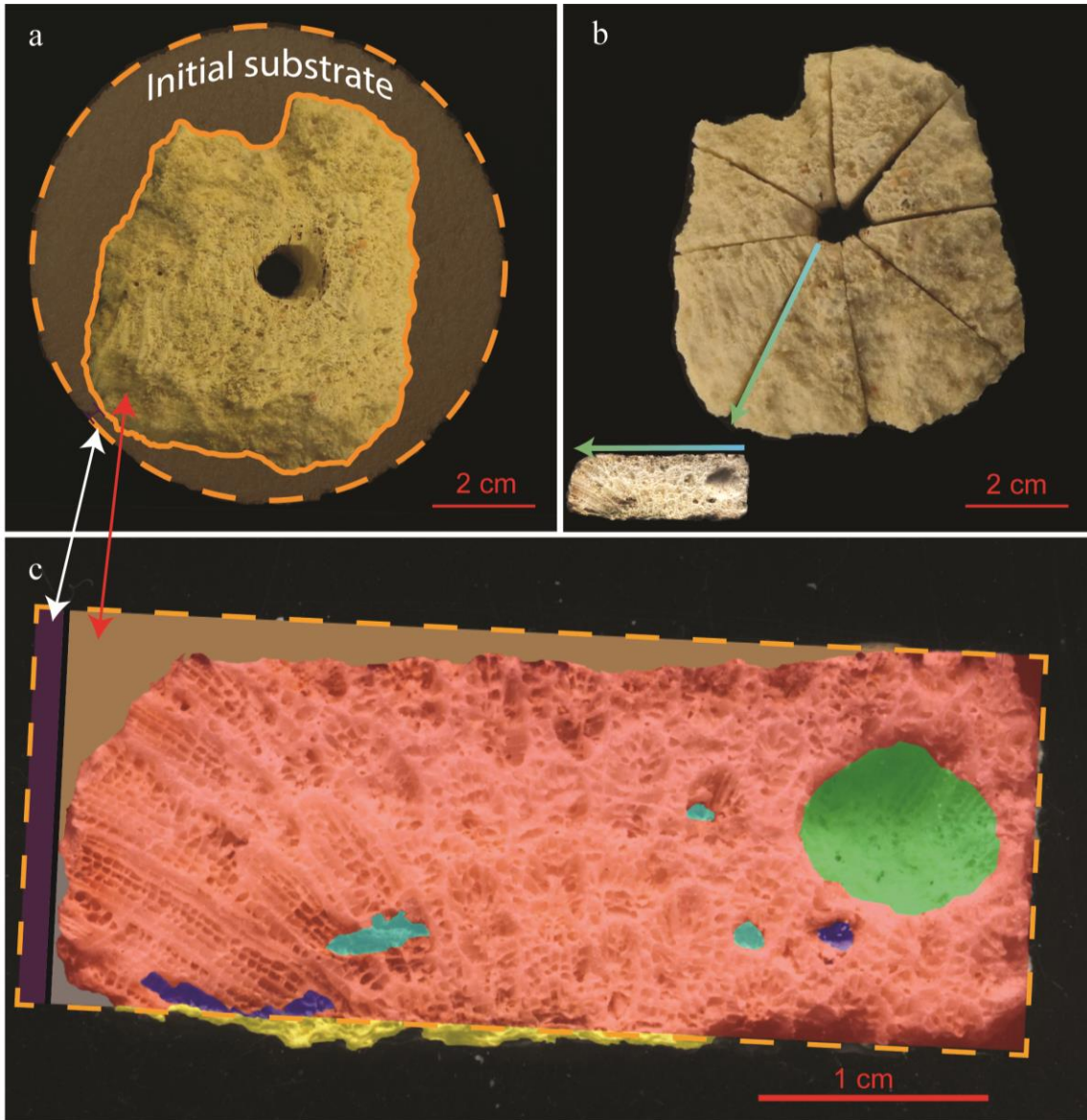
Accretion
- ■ (yellow)

Other
- ■ Original substrate (salmon)
- - - Initial surface area/ Original disk projection
- — Eroded projected edge

Figure 3.4. Components of substrate weight change. (a) Example comparison between experimental substrate prior to deployment and after three years of exposure. The area between the orange dotted and orange solid lines provides a visual representation of the projected perimeter difference (ΔP_{SA}). Purple lines indicate the distance between the original and eroded disk edge at one location. (b) Sample cut into eight triangular slices. Arrows indicate location of the inset image, with matching colors pointing towards the outer edge of the substrate. (c) Magnified view of previous inset slice, showing map of all bioerosion features. Purple area indicates slice cross sectional view of ΔP_{SA} (white arrow) and its equivalent location on (a). The cross sectional ΔP_{SA} is defined as the area between the initial height outer edge of the theoretical pre-experimental slice (orange box) and the first parallel line that intersects the outermost remaining substrate. Top and bottom grazing account for material removed that is not detected from projection method. The key shows which colors are associated with the surface area of different macroboring features. Red arrow shows an example of top grazing not detected by the projection method. Accretion is identified, but the surface areas are not used in calculation, which is instead based on the remaining weight (see text).
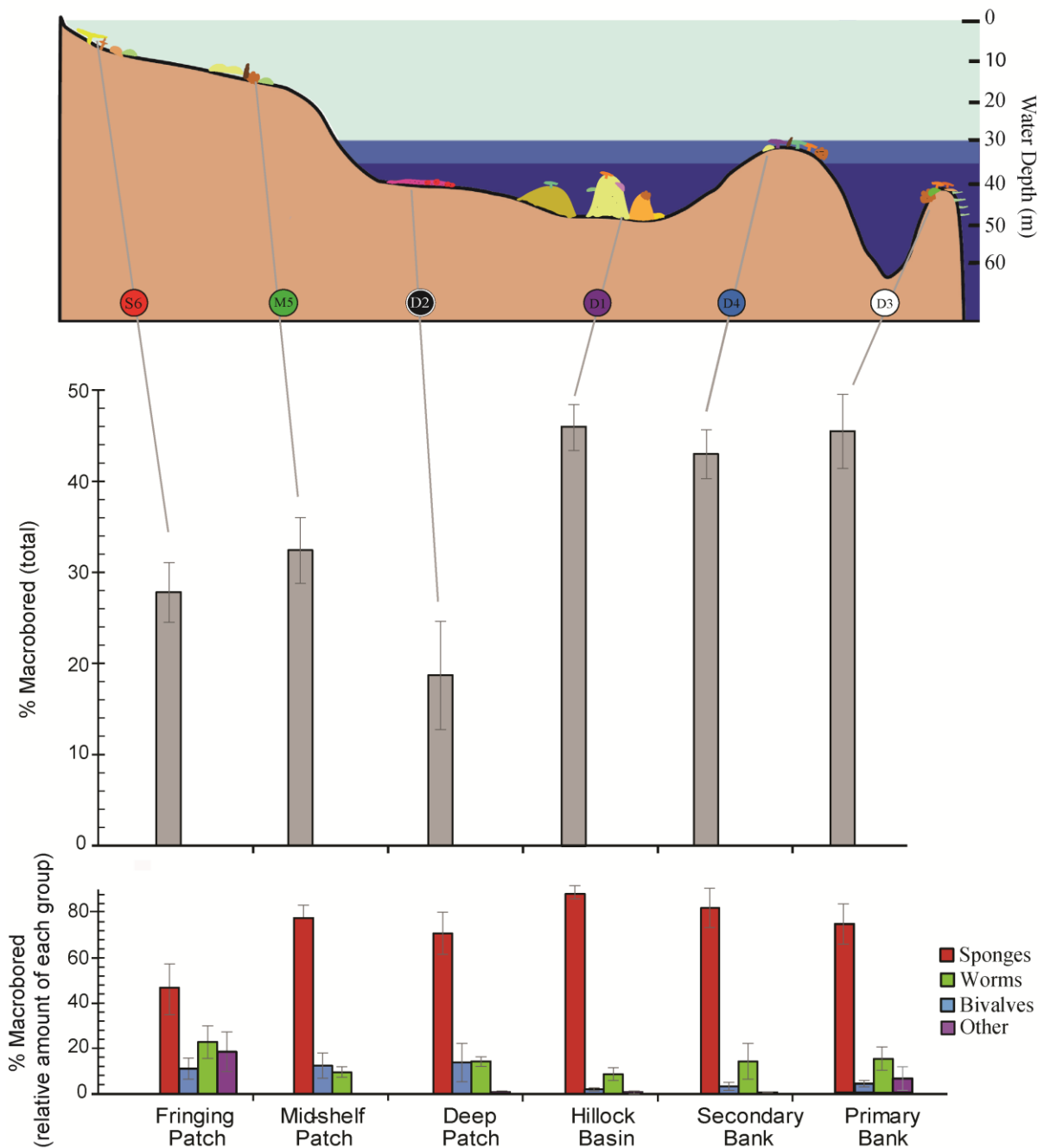
Figure 3.5 Coral rubble macroboring. Schematic cross section of southern Puerto Rican Shelf, indicating the location of each study site and corresponding values of averaged percent of total macroboring (upper graph) and percent abundances of macroboring groups per site (lower graph). Error bars equal ± 1 standard error.
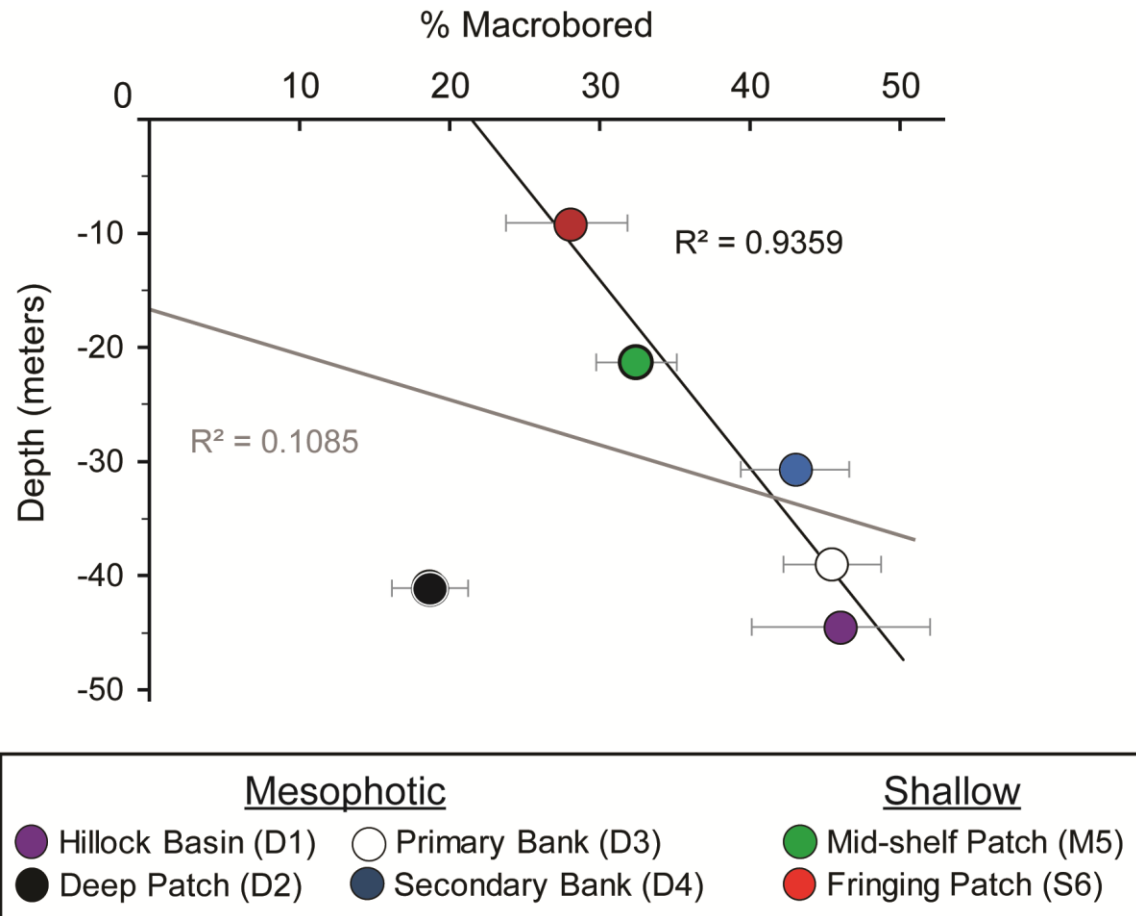
Figure 3.6. Rubble boring versus depth. Relationship between water depth and site average percent coral rubble excavated by macroborings. Error bars equal ± 1 standard error.
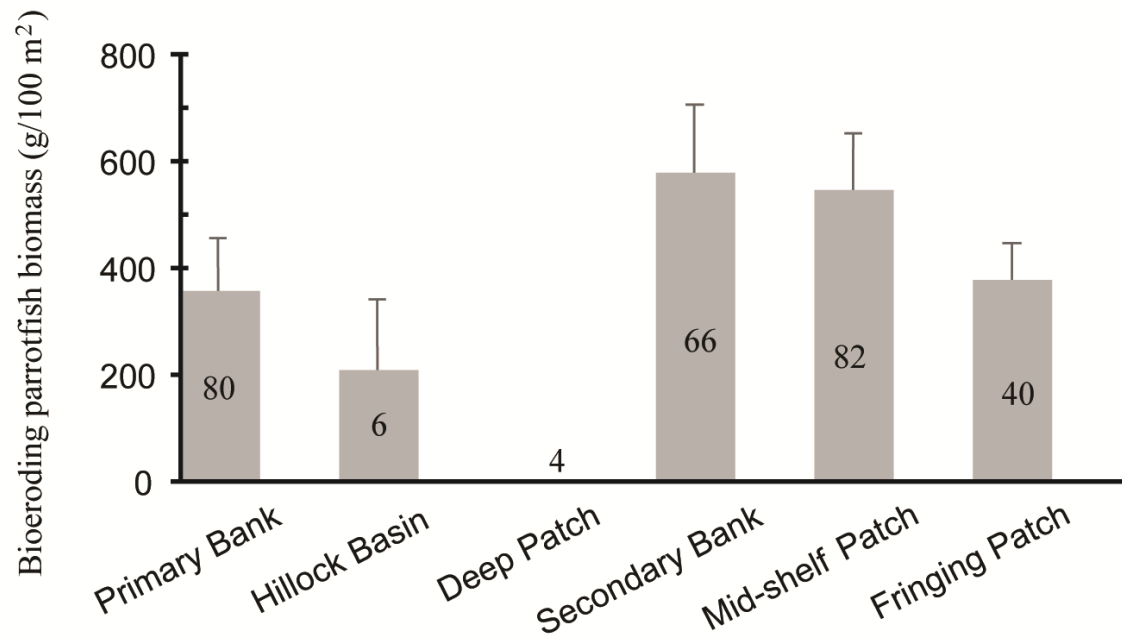
Figure 3.7. Parrotfish biomass. Average biomass, per site, of bioeroding parrotfish, *Sparisoma viride* and *Scarus vetula*. Values displayed on each bar provide number of transects used to calculate site mean. Error bars equal ± 1 standard error.
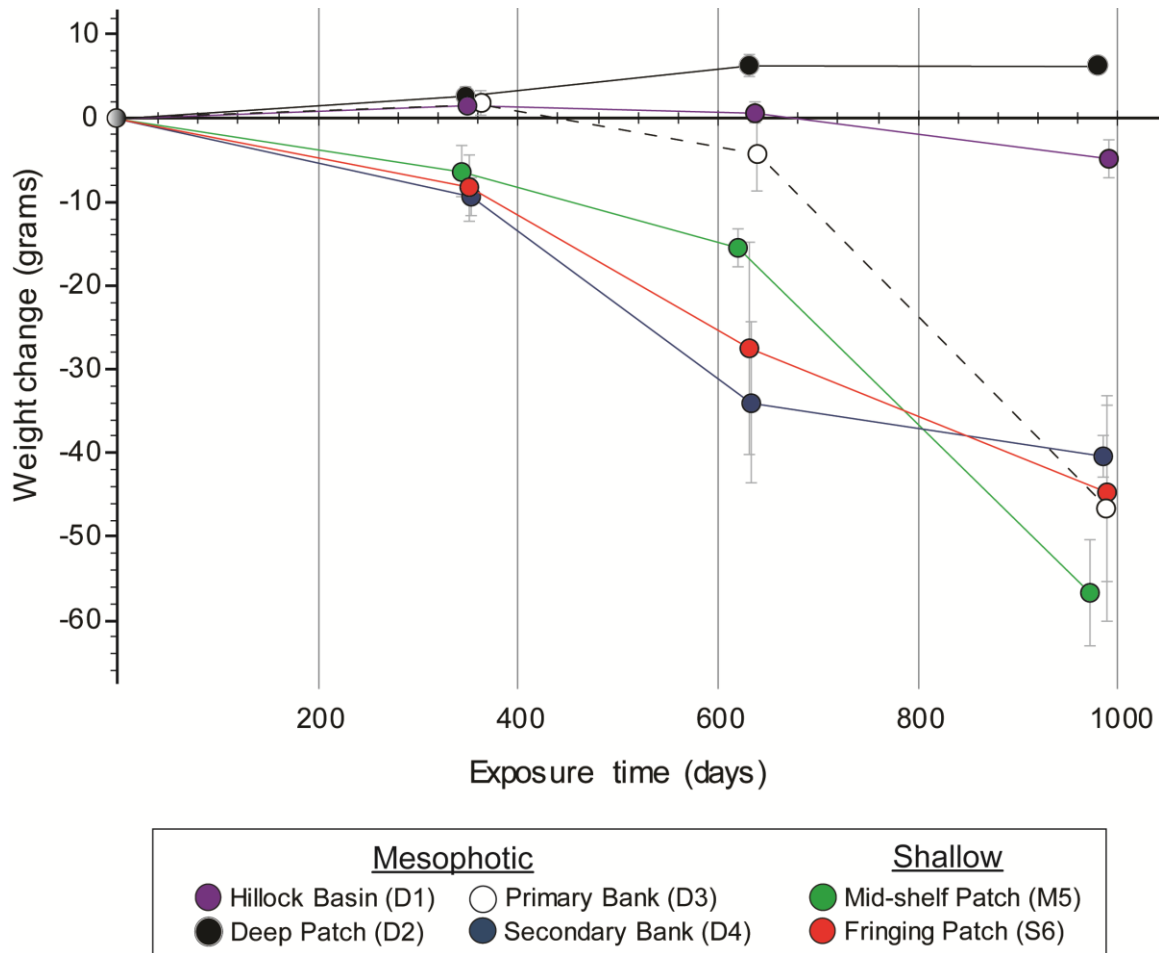
Figure 3.8. Weight change of experimental substrates with time. Error bars equal ± 1 standard error of the average from each quadrat. Slope of the lines provide rates of bioerosion between installation date and year one, year one and year two, and year two and year three. Specific rate for year three would be represented by a line from the origin to the year three points.

Table 3.2. Substrate weight change statistical analysis. Results of a nested two-way factorial ANOVA, comparing the weight change with collection year and site factors and quadrat nested within site factor. Post-hoc results are given for the site factor. Sites with different letters were significantly different.

Factor	d.f.	F value	p value	Secondary Bank	Shallow patch	Mid-shelf Patch	Primary Bank	Hillock Basin	Deep Patch
Quadrat	12	3.48	<0.0004						
Year	1	9.54	0.0028						
Site	5	21.27	<0.0001	A	A	A	B	B	B
Year*Site	5	1.81	0.1198						
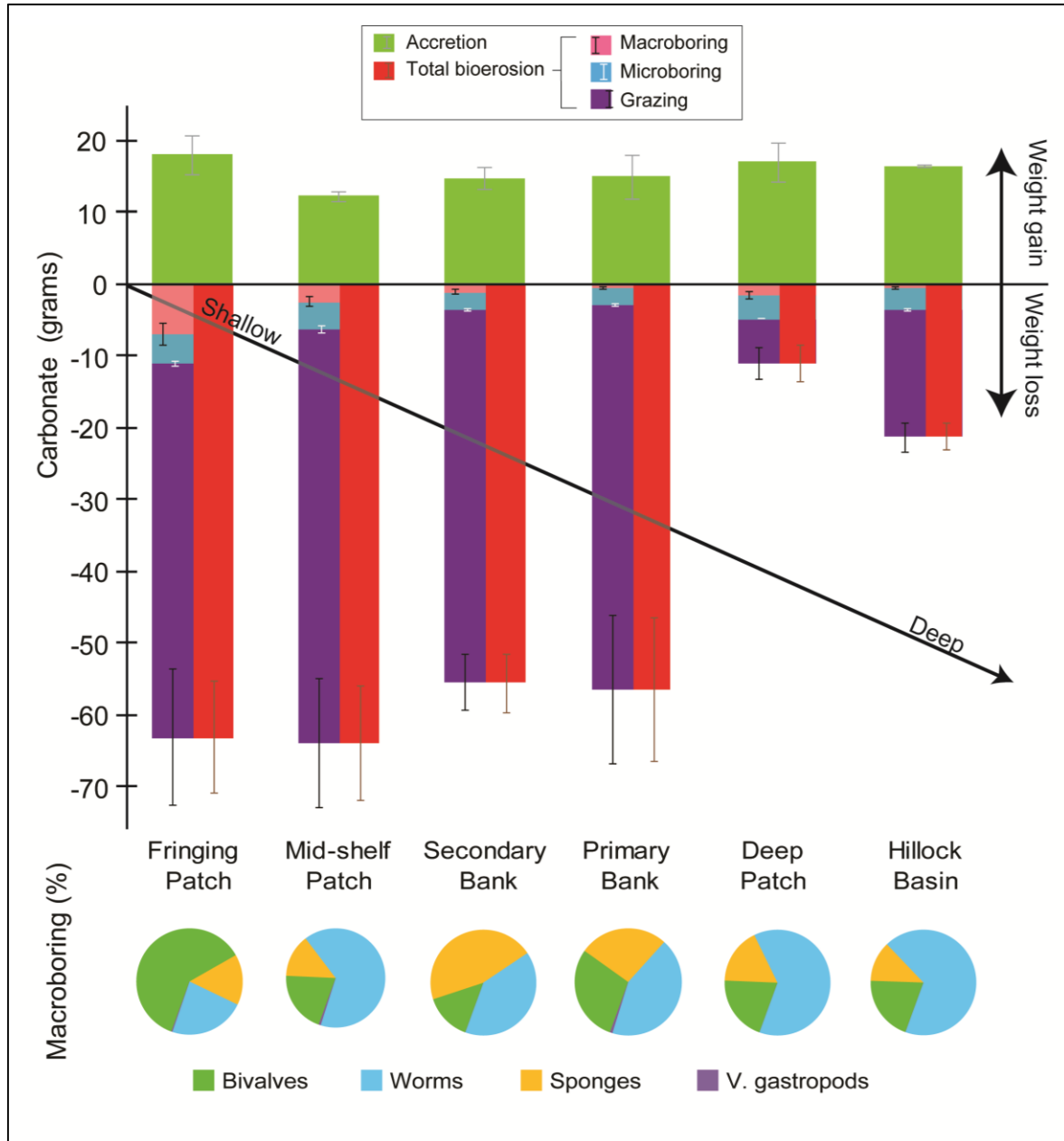
Figure 3.9. Components of year three disk weight change. Graph shows the contributions of varying bio-modifying groups to the final site average experimental substrate weight. Bar graph compares accretion of carbonate (positive) to removal of carbonate (negative). Pie charts display the relative percent each macroboring group contributed to the macroboring portion of total bioerosion. Error bars equal ± 1 standard error of the average from each quadrat.
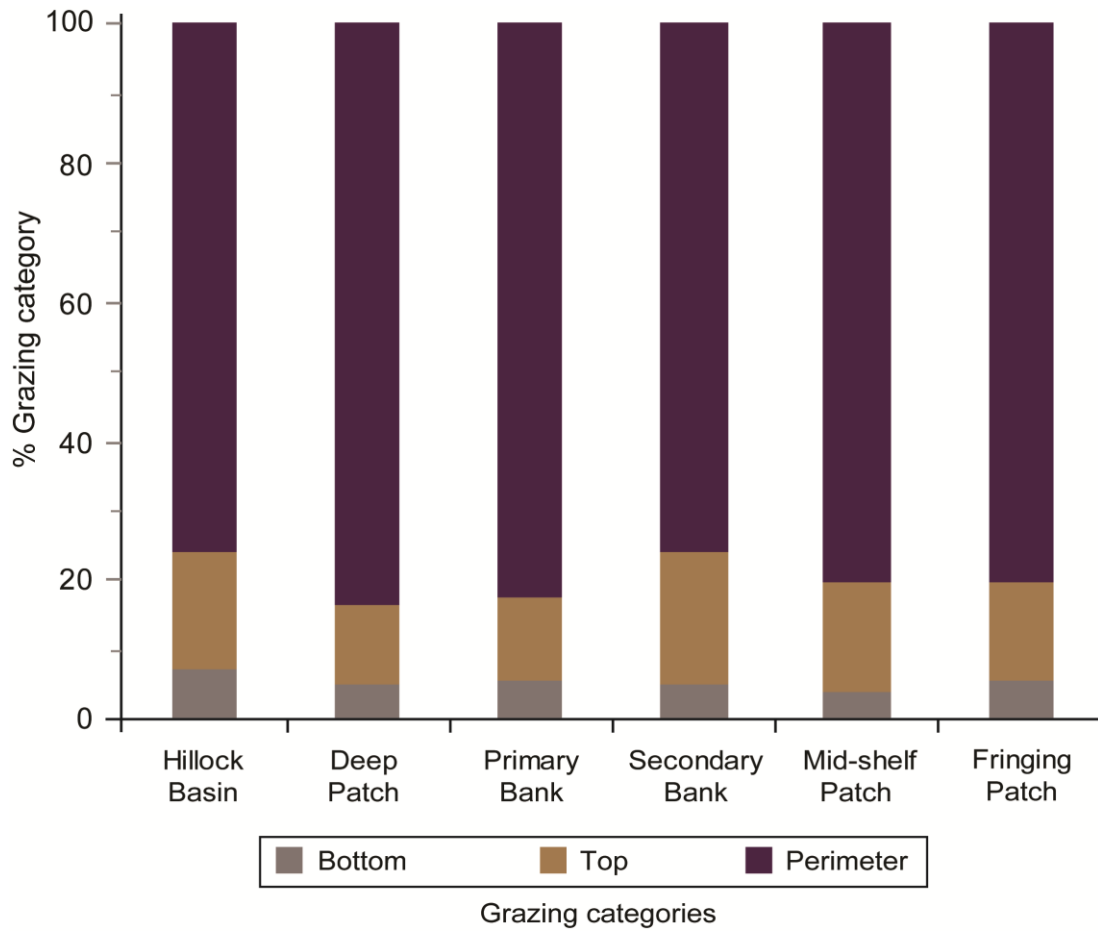
Figure 3.10. Experimental substrate grazing. Relative percent of the three grazing categories measured, by site.
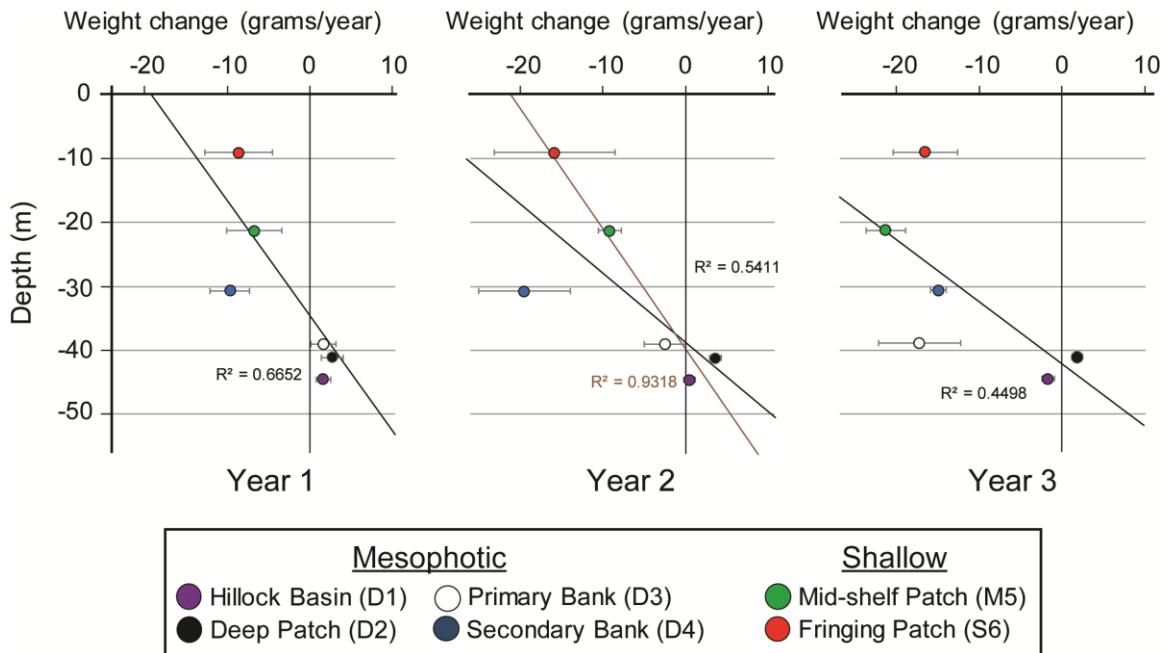
Figure 3.11. Bioerosion rate versus depth. Relationship between rates of substrate weight change and seawater depth after substrate exposure for one, two, and three years. Brown year two trend line indicates best fit when not including Secondary Bank site. All error bars equal ± 1 standard error. Vertical axes all have same interval spacing.
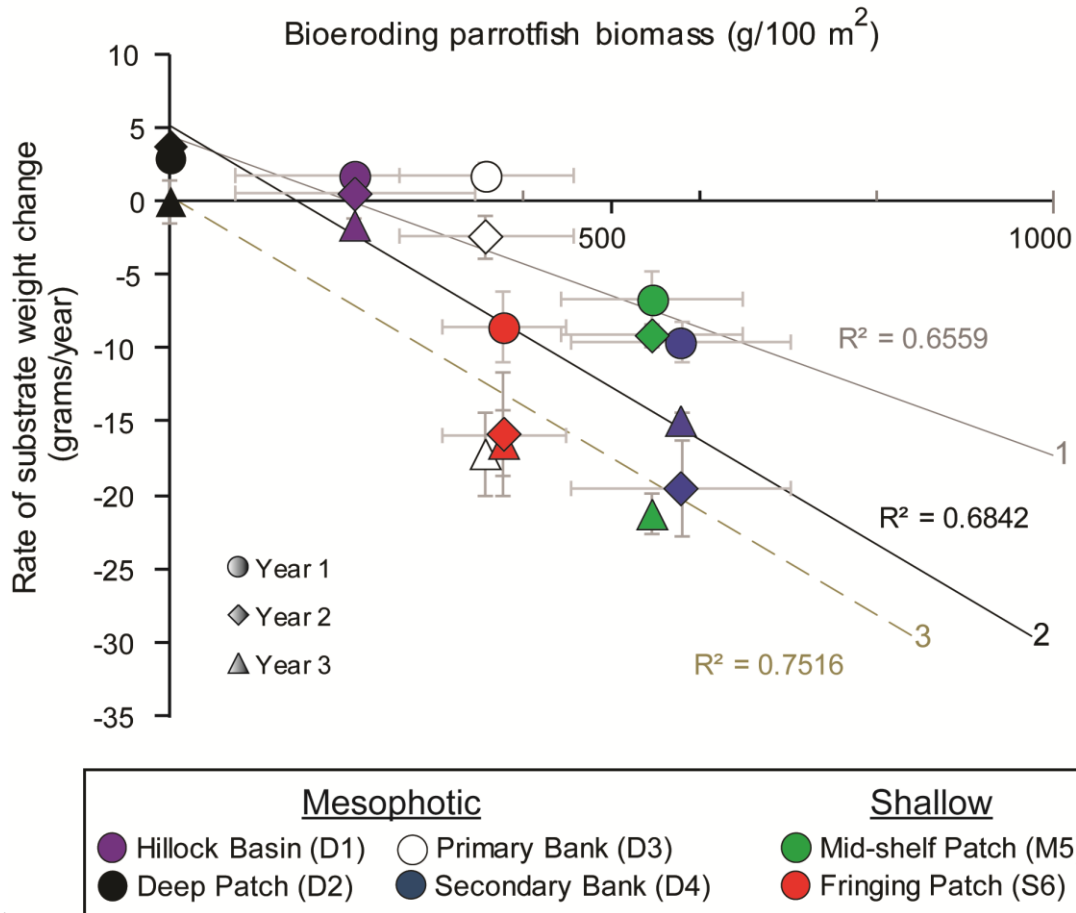
Figure 3.12. Bioerosion rate versus parrotfish biomass. Comparison between mean bioeroding parrotfish biomass and rates of substrate weight change at each site after one (circle), two (diamond), and three (triangle) years of exposure. Vertical and horizontal error bars equal ± 1 standard error. Number next to trend line corresponds to year.

CHAPTER 4. LIVING MESOPHOTIC FRAMEWORK: RATES OF CORAL GROWTH, BIOEROSION, AND SECONDARY ACCRETION

Chapter summary

Growth rates of the Caribbean reef coral, *Orbicella annularis,* decrease with increasing water depth as a result of increasing light attenuation with depth. Reliable rates for coral growth deeper than 35 m are rare, however, and no study has measured coral growth rates from multiple habitats within a regional mesophotic reef setting. Furthermore, no study has simultaneously compared mesophotic coral growth rates with rates of secondary accretion by encrusting organisms or macroboring rates of living mesophotic coral framework colonies. Towards this end, live platy samples of the *O. annularis* species complex were collected at three south Puerto Rican Shelf mesophotic reef habitats with varying structural characteristics at depths of 30-45 m. Rates of coral growth were determined by standard X-radiographic and buoyant weight techniques. Secondary accretion and framework bioerosion were determined by point count analysis.

Average linear extension rates of mesophotic coral, confirmed by stable isotopic analysis, were found to be 0.799 mm/yr $\pm$ 0.03 SE. Though slower than rates measured previously at depths now defined as "mesophotic," and considerably slower than shallow-water reef counterparts, results from this study still fit previously established standard *O. annularis* growth rate versus depth models. Secondary bio-modification processes did not show significant variation with site and were relatively insignificant compared to coral calcification rates. Significant variability in calcification rates between different mesophotic reef sites, which do not correspond directly to depth differences, have notable implications to long-term carbonate basin development, best examined through carbonate budget analysis.

Background

Interpretation of density band growth patterns as annual occurrences in the carbonate skeletons of hermatypic scleractinian coral (Knutson et al., 1972) greatly advanced the field of sclerochronology (Helmle and Dodge, 2011). Beyond providing a methodology for quantifying multiple parameters of coral growth, the measurement of coral density bands provides a tool to improve the study of coral growth ecology, paleoclimatology, environmental climate change, and coral reef sedimentology. Coral "density bands" are produced by bulk density deviations of skeletal material, skeletal thickening variances, spacing of skeletal elements, and overlapping of skeletal structures (Le Tissier et al., 1994; Helmle et al., 2011).

Hydraulic drills, which minimize impact on living colonies and obtain long linear records, are commonly used to obtain coral cores. Often, these cores are sectioned into thin slabs parallel to the coral primary growth direction and exposed to X-rays for X-radiography or X-ray computed tomography. Based on these methods, some coral species have been shown to accrete repeating successions of low-density (dark) skeletal material and high-density (light) skeletal material, which produce linear "density bands" perpendicular to the primary coral growth axis (Knutson et al., 1972; Dodge and Thomson, 1974; Barnes and Lough, 1989; Helmle and Dodge, 2011). X-ray and gamma densitometry methods have also been found helpful to measure coral bulk density (the skeleton distribution of calcium carbonate). Other techniques used to measure skeletal density including mercury displacement (Dustan, 1975), buoyancy weighing, and computerized tomography (Dustan, 1975; Highsmith, 1979; Dodge and Brass, 1984; Barnes and Devereux, 1988).

Three main parameters are typically used to quantify coral growth (for review, see Dodge and Brass, 1984): (1) linear extension rates (distance from top of one light band to the next, in cm/year when assuming the cycle repeats annually); (2) bulk skeletal density (g/cm^3); and (3) calcification (a unit area measure of calcium carbonate mass, as a product of extension and density, in $g/cm^2/year$). As no single parameter is a good predictor of the other two, the use of all three parameters is needed to fully define coral growth and potential density variations (Dodge and Brass, 1984; Helmle and Dodge, 2011). For example, some coral in St. Croix, USVI where found to have similar extension rates, but differing calcification rates and density (Dodge and Brass, 1984). Dodge and Bass (1984) suggested that although the extension may be similar, the corals with lower calcification may be lacking in bulk material to sustain structural framework.

Simultaneous direct coral growth staining measurements (MacIntyre and Smith, 1974; Hudson, 1982; Wellington and Glynn, 1983) and radiometric dating techniques (Dodge and Thomson, 1974; Moore and Krishnaswami, 1974; Druffel, 1981) have verified that the repetitive sequence of high and low density bands in some massive coral species has an annual frequency. As a result, most studies interpret coral density bands as being annual in nature (Helmle and Dodge, 2011). Other studies, however, have questioned the accuracy and interpretation of coral X-radiography (Le Tissier et al., 1994), and suggested the assumption of annual coral growth bands for some coral species may be oversimplified, incorrect, or related to different timescales such as lunar cycles (Buddemeier, 1974; Brown et al., 1986; Barnes and Lough, 1989). In addition, some types of density bands may be stress related (Hudson et al., 1976; Dodge and Brass, 1984; Leder et al., 1991; Wórum et al., 2007).

Coral growth characteristics resulting in alternating density bands are determined by the variability of environmental attributes (Barnes and Lough, 1989; Barnes and Lough, 1992; Helmle et al., 2011). These include differences in: (1) temperature (Hudson et al., 1976; Highsmith, 1979); (2) light intensity (Knutson et al., 1972; Wellington and Glynn, 1983); (3) sedimentation (Dodge and Brass, 1984; Barnes and Lough, 1999); (4) latitude (Dullo, 2005); and (5) rainfall and cloud cover (Lough and Barnes, 1989). Recent studies have also predicted that ocean acidification and global warming will hinder carbonate accretion by limiting coral growth and recovery from bleaching events, leading to increased global degradation of coral reefs (Hoegh-Guldberg et al., 2007; Baker et al., 2008). Although these stresses have been shown to affect coral density band development (Cantin et al., 2010; Fabricius et al., 2011; Crook et al., 2013), results from a study in the Florida Keys did not find expected ocean acidification-driven declines in calcification rates over a 60-year period (Helmle et al., 2011). These results led Helmle et al. (2011) to suggest localized, high seasonal variability of aragonite saturating states could counter expected decline (Helmle et al., 2011).

Along with characteristic species zonation with depth, corals also exhibit variations in growth rates with increasing water depth (Baker and Weber, 1975; Highsmith, 1979; Dodge and Brass, 1984; Huston, 1985; Bosscher and Meesters, 1993; Lough and Cooper, 2011). However, few studies responsible for our broad understanding of coral growth rate variation with depth obtained reliable rates for coral growing deeper than 35 m. Studies with the coral *Porites* spp. in the Rea Sea down to 52 m did find that coral growth rates continue to decrease with depth (Klein et al., 1993; Rosenfeld et al., 2003). Another coral study in the same region showed that the size of

Leptoseris fragilis decreases with depth from 100-150 m, but growth rates (0.2 -0.8 mm/year) did not have significant depth differences between 90-120 m (Fricke et al., 1987). Grigg (2006) found that growth rates of *Porites* spp. in Hawaii decrease with depth, and also observed a 50 m accretion cessation resulting from higher rates of colony holdfast bioerosion compared to growth rates of coral basal attachments.

Massive Indo-Pacific *Porites* and Atlantic *Orbicella* represent the two coral genera most used for studies of coral density bands (Dávalos-Dehullu et al., 2008). *Orbicella* (formerly *Montastraea* for some species of the group*,* Budd et al., 2012) has been recognized by some to be one of the most important reef-building coral in the Atlantic (Goreau, 1959). Caribbean coral studies using various techniques have found that linear extension and calcification rates decrease and skeletal density increases with increasing depth. The results of these studies include a limited number of sites that sampled *Orbicella annularis* at upper mesophotic steep shelf depths such as: 36.6 m in St. Croix, USVI (Hubbard and Scaturo, 1985); 44.1 m in Barbados (Runnalls and Coleman, 2003); and 45 m in Jamaica (Dustan, 1975). However, none of these studies have examined growth rates on low-angle shelf mesophotic reefs or identified potential variability in mesophotic growth rates from habitats with varying geomorphological characteristics at similar depths.

As coral colonies grow, so does the potential for bioeroding organisms to remove carbonate from either older, interior skeleton now void of polyps, or directly from the living colony surface. Although bioerosion or living coral colonies has been observed in shallow-water coral reefs (Randall, 1974; Scott, 1988; Le Campion-Alsumard et al., 1995; Schönberg and Wilkinson, 2001; Tribollet and Golubic, 2011), little is known

regarding the magnitude in which bioeroders remove carbonate from living mesophotic coral colonies. Subsequently, no Caribbean studies have directly compared rates of mesophotic primary (coral) framework growth and secondary accretion additions versus erosion rates of live coral colonies.

Objectives

The objectives of this chapter are to quantify coral growth and erosion rates at three mesophotic reef habitats with distinctive architectural characteristics. The null hypothesis for this chapter is that the sum of mesophotic coral framework linear extension rates and secondary accretion minus living substrate bioerosion rates at each tested habitat are equal, and that linear coral extension rates in mesophotic coral reefs are equal to the growth rates of similar species in shallow-water coral reefs. This hypothesis was tested by interpreting X-radiograph exposures of mesophotic coral to obtain linear extension rates, and by point count analysis of secondary accretion and bioerosion (specifically macroborings) on mesophotic coral skeleton slabs. The overall goal for this chapter was to determine how the magnitude and variability of mesophotic reef coral framework growth and bio-modification potentially contributes to carbonate shelf accretion and the maintenance of habitat heterogeneity.

Methods

Field collection and sample preparation

In August 2011, technical divers collected samples from three mesophotic reef sites (Fig. 1.4): (1) the Deep Flat Basin (43.3 m); (2) the Primary Bank (39 m); and (3) the Secondary Bank (30.7 m). Samples were collected from the Deep Flat Basin to maximize sample collection within the limited field time available. However, with no

distinctive boundary between the Deep Flat Basin and the Hillock Basin, rates of framework growth and bio-modification were assumed to be similar. At each site, 10-20 live coral samples, approximately 5-10 cm in diameter (Fig. 4.1), were removed from independent, semi-random opportunistically selected mesophotic reef colonies of OCAX with a hammer and chisel, taking the utmost care to minimize any adverse impact to the colony and the overall environment.

Samples were taken from colonies with the platy morphology type that is dominant at mesophotic reef depths (Smith et al., 2010). The OCAX was chosen because it is the primary framework builder at each of the mesophotic sites sampled for this chapter (Table 1.1). The species was also chosen to enable comparison with results from other studies in the Caribbean, which also commonly measured coral from the genus *Orbicella* (Dustan, 1975; Hubbard and Scaturo, 1985; Huston, 1985; Bosscher and Meesters, 1993; Runnalls and Coleman, 2003). Colony interiors were too dense to remove without harming the coral so samples were taken along the colonies' outer edges, representing the youngest portion of the colony. Samples were placed in a mesh bag, brought up to the surface and transported to the Rosenstiel School of Marine and Atmospheric Science (RSMAS) at the University of Miami.

The samples were soaked in a 50% solution of a commercial bleach product for one day, rinsed in distilled water for one day, dried in an oven for two days at 55° C. Samples large enough for precision sectioning were cut into slices approximately 2-5 mm thick with a slab circular saw normal to the primary coral growth axis. Preliminary analysis indicated that mesophotic samples were denser than coral of the same species previously examined using similar methodology (Barnes and Devereux, 1988; Helmle et

al., 2011). Therefore, thin slices (only one corallite wide) were needed to ensure X-ray penetration.

Colleagues working at the Nova Southeastern Oceanographic Center[2] produced X-radiographs of sliced samples using a methodology modified from Helmle et al (2011). Slices were placed on Kodak Industrx film 1.5 m away from an X-ray machine set to70kV and 15mA, and were exposed for 10 seconds. After manually developing the film, X-ray negatives were digitized using a medical X-ray scanner with scaling parameters: x-axis = 104.1668 pixels/cm; y-axis = 141.6254 pixels/cm. The need to cut thin coral slices resulted in X-radiographs displaying large density differences between adjacent corallite (porous, low density individual polyp skeleton cups) and coenosteum (dense skeletal area between corallites) pairs (Fig. 4.2). X-rays penetrate deeper into shallow-water, less dense coral, permitting previous similar, but shallower-water studies to use thicker slices with multiple rows of staggered corallites (Barnes and Devereux, 1988; Helmle et al., 2011). The images produced from these thicker slices provide a more spatial averaged density profile of the entire coral, unlike the vertical pattern parallel to growth direction observed in images produced for this study (Fig. 4.2).

Linear extension

Resolution of density bands were not always possible, resulting from the high bulk skeletal density of the samples. Therefore, the following procedures were performed on the five slices (each from a different coral colony) from each site with the best image resolution. Lines were traced over corallite high density bands (using *Adobe*

[2]X-rays, film development, and image digitization were overseen by Dr. Keven Helmle and were conducted by Dr. Helmle and Dustin Marshall at the Nova Southeastern University Oceanographic Center. http://www.nova.edu/ocean/overview/faculty-staff-profiles/kevin_helmle.html

Photoshop), where the greatest exposure of repetitive bands could be identified (Fig. 4.2a). Distance between adjacent bands was assumed to represent one annual cycle (Hubbard and Scaturo, 1985). Tracing continuous density bands between neighboring corallites was not possible because of the high luminance contrast between coenosteums and corallites. To measure maximum coral extension rates, Coral X-Radiograph Densitometry System (*CoralXDS,* Helmle et al., 2002), was used to select transects (rectangular selection boxes on digitized X-ray images) on coral X-radiographs where potential density bands had been mapped (Fig. 4.2a, white box). Transects were set to be less than one corallite thick and oriented parallel with the growth axis of the corallite being analyzed. Set to the extension/luminance mode, *CoralXDS* converts pixels from the digitized X-radiograph (representing relative X-ray penetration) into gray scale luminance values (0-255). The program then averages luminance values over the transect width and plots a luminance curve (where local curve peaks correspond with high luminance/high density and local troughs correspond with low luminance/low density) as a function of distance along the transect (Fig. 4.2b).

Two methods offered by *CoralXDS* ("2nd derivative" and "half range") were used to digitally delimit high-density and low-density bands that most closely matched previous visual trace estimates (Fig. 4.2a). The "2nd derivative" method calculates a cubic spline curve (smoothing was set to 0.1) from each transect luminance curve and plots the corresponding second derivative. The user then selects the horizontal axis value of a second derivative bounding luminance maximum line. Intersection of the threshold line and the second derivative delimited band locations and band thicknesses along the analyzed transect. The "half range" method (in which a starting neighborhood value of

0.05 cm was selected for all transects) identifies adjacent density maxima and minima on original, unsmoothed luminance curves. *CoralXDS* then delimits density band locations at designated maxima peaks and calculates the length between bands as the mean distance between adjacent max/min points. Initial "half range" results were compared with the original density band traces of the same corallite to determine the need to add or remove additional maxima, minima, or both.

To obtain precise band measurements for each transect, the "2nd derivative" method was first used and the "half range" method was subsequently used if output from the first method did not reflect original trace estimates. For visual reference, the selected band delimits of each transect were plotted on the digitized X-radiograph (Fig. 4.2b) and compared directly with previous visual estimates. These steps were then repeated on two to four adjacent corallites. Finally, high density bands from adjacent corallite transects were manually connected (Fig. 4.2c). A computer screen-shot was taken of the two individual transect luminance curves that best matched the location where selected representative coral slices were micro-drilled for isotopic analysis. The two images were imported into the program "Plot Digitizer" so that fine intervals of the luminance curves would be comparable with isotope sampling intervals.

Correlated corallite annual density band measurements from each corallite (calculated with *CoralXDS)* were averaged for each connecting year line to determine the slice extension length of each year. The annual extensions were then averaged to obtain the sample average linear extensions rate ($\Delta\overline{LE}$). Assuming the top of each X-ray slice represents September 2011 (when the samples died), the distance between the top of the coral and the first identified density band was measured and used with the average

$\Delta\overline{LE}$ to estimate the year each high density band was formed (Fig. 4.2c). However, it should be noted that specific year selection was an approximation and should not be considered definitive. Annual extension rates per approximate year were plotted simultaneously per site to compare variation. The software program R version 3.0.3 (R Core Team, 2014) was used to test for significant differences between site linear extension rates using one-way analysis of variance (ANOVA). Post hoc multiple comparisons of means were carried out with Tukey's HSD test.

Bulk density and calcification

A modified buoyant weight technique was used to obtain the bulk density of analyzed samples (Davies, 1989; Bucher et al., 1998; Smith et al., 2007). This method can be less accurate than the gamma densitometry methodology for coral growth studies because measurements correspond with the entire slice, and not solely with selected portion of the slice used for linear extension analysis. However, the X-radiograph gamma densitometry methodology suggested by *CoralXDS* and others (Chalker and Barnes, 1990; Helmle et al., 2002) was deemed to be unreliable to measure the density of samples collected for this study. This was decided because *CoralXDS* program limitations prevented exact, equal selections of corallite and coenosteum pairs within a single transect, resulting in skewed density measurements.

Following the buoyant weight technique, slices were first placed on a scale to measure dry weight (DW_{clean}). More slices were used to measure density than were used to obtain linear extension rates because the buoyant weight technique was not limited by resolution. This allowed for more accurate representative average density calculations. To form a water-tight barrier, slices were immersed in molten paraffin wax (set at 110°

C, Smith et al., 2007) with triceps for approximately five seconds before being pulled out, allowing wax coating to solidify. Once fully dry, wax-coated samples were reweighed (DW_{wax}). The buoyant weight (BW_{wax}) of each waxed slice was measured in an enclosed tub of seawater.[3] Temperature and salinity were measured simultaneously and used to calculate seawater density (ρ_s) for each slice (Millero and Huang, 2009). The following equations (Bucher et al., 1998) were then used to calculate the total enclosed volume ($V_{enclosed}$) and slice bulk density (BD):

$$V_{enclosed} = (DW_{wax} - BW_{wax}) * \rho_s$$

$$BD = DW_{clean} / V_{enclosed}$$

Slice bulk density measurements from the same sample were averaged to determine the sample average bulk density. Before bulk density analysis was conducted, three samples were destroyed through analysis, so the densities for those samples were estimated as the site average bulk density ($\overline{BD}$). Bulk density values assigned to their associated sample were multiplied by the sample $\Delta\overline{LE}$ to obtain the sample average calcification rate (ΔC). Identification of differences between sites, and subsequent multiple pair-wise comparisons were determined with one-way ANOVA and Tukey's HSD testing, respectively, using R version 3.0.3 (R Core Team, 2014).

Stable isotopic analysis

To provide additional corroboration of X-radiograph results, a random representative slice was selected from both the Secondary Bank (sample: Coll. 7) and the Deep Flat Basin (sample: MCDFB.4) for stable isotopic analysis. Samples were drilled

---

[3]This analysis was conducted primarily by Leah Chomiak at the RSMAS at the University of Miami Experimental Hatchery, under the supervision of Dr. Christopher Langdon, who provided lab resources.

every 50 µm along the thecal wall, parallel to the growth axis, in close proximity to locations of previous luminance analysis. Using a low-speed microdrill with a 0.5 mm diamond drill bit and a plunge depth of 50 µm, five to eight drill passes were made to collect enough material for isotopic analysis. Drilling began seven to-eight mm from the top of the last living coral growth horizon, with subsequent drilling conducted incrementally upward to the surface of the coral. Samples were analyzed for $\delta^{13}C$ and $\delta^{18}O$ with an automated carbonate device (Kiel III) connected to a Finnigan-MAT 251 mass spectrometer. Precision and accuracy, calculated from standards run along with samples (n = 22), were 0.07‰ and 0.06‰, respectively for $\delta^{13}C$ (n=96), and 0.14‰ and 0.13‰ for $\delta^{18}O$ (n=95).[4]

Wavelet power spectrum analysis was used to compare the periodicity of corresponding stable isotope compositional trends and luminance as a function of time (expressed as distance (mm) along the coral) for both selected coral slices. This was performed with the Morlet wave (Torrence and Compo, 1998) and a modified MATLAB script. Before analysis, each data series were detrended and equally spaced at 0.05 mm, corresponding to actual sampling intervals for isotope and luminance analysis. Co-variation in the stable isotope ($\delta^{13}C$) and luminance paired data sets were calculated using cross wavelet transform (CWT). Wavelet semblance analysis on isotopic and luminance data were performed following the continuous wavelet transform method (Cooper and Cowan, 2008) using a modified MATLAB script.[5]

---

[4]Microdrilling and mass spectrometer analysis were conducted by Sharmila Giri in the Stable Isotope Laboratory at the University of Miami RSMAS (http://mgg.rsmas.miami.edu/groups/sil/index.htm).
[5]WPS and CWT analysis were conducted by Arash Sharifi at the University of Miami RSMAS.

Framework bioerosion and secondary accretion

To determine the spatial area removed by bioerosion and added by secondary accretion (Fig. 4.3), two non-adjacent slices from seven to eight samples per site were analyzed using a modified point count analysis (Perry, 1996; Macdonald and Perry, 2003; Weinstein et al., 2014). Material removed by grazing and microboring was not quantified. Dry slices were digitally scanned to produce unaltered two-dimensional digital image projections. More slices were used for this analysis than were used to obtain linear extension rates because there was no similar resolution issue with this technique, allowing for more accurate averages. Using the program Coral Point Count with Excel Extension V3.6 (Kohler and Gill, 2006), points were randomly distributed upon the digitized slice image and were identified as framework, macroborings, secondary accretion, or "void" (points placed outside the calcification areas or not on the intended two- dimensional image projection). Percent area of macroboring and of secondary accretion was calculated as the sum of macroboring points or secondary accretion points, divided by the sum of macroboring and framework points. Results from each sample pair were combined to determine the sample average for each parameter. The results were multiplied by the associated sample $\Delta \bar{C}$ (when available) or the overall site $\Delta \bar{C}$.

The results provide a minimum macroboring and secondary accretion rate because this methodology assumes constant rates of these processes, regardless of the amount of substrate available. For example, if a coral grew for three years without any erosion, followed by three years with constant macroboring activity followed by three more years with a macroboring hiatus, the rate of change for macroboring carbonate removal

reported using the described technique provides the percent macroboring divided by nine years, not three years, resulting in a smaller value. Statistical comparison between overall macroboring versus secondary accretion rates of all sites (percent surface area cover times sample primary framework $\Delta \bar{C}$) was calculated with a Welch's t-test. Testing for significant differences between sites was made with a one-way Kruskal-Wallis non-parametric comparison. Statistical analysis was conducted with R version 3.0.3 (R Core Team, 2014).

Results

Mesophotic coral growth

  X-radiographs of thinly sliced, platy *Orbicella spp.* coral skeletons collected in the transitional and upper mesophotic reef zone (30-50 m) displayed closely spaced density bands that were often difficult to resolve, a feature also noted by Hubbard and Scaturo (1985). When obtaining rates from samples with distinguishable bands, the overall average linear extension rate of all mesophotic samples measured for this study was calculated to be 0.799 mm/year ± 0.03 SE. Within the same site, linear extension rates (ΔLE) were found to vary between samples (Fig. 4.4-4.5). One-way ANOVA indicated significant site differences for ΔLE ($F_{2,12}$ = 10.48, p = 0.002), with group differences explaining 64% (R^2 = 0.636) of the variance. Overall comparison between annual linear extension with time showed individual coral sample annual growth rates measured from the same sites generally experience simultaneously similar variations from the site average (Fig. 4.6).

  Calcification rates (ΔC) were detected with statistically significant differences between sites ($F_{2,12}$ = 7.28, p = 0.009), but skeleton bulk density had no significant

differences between sites ($F_{2,19}$ = 1.702, p = 0.209). Site means and standard errors are presented in Figure 4.7. Coral analyzed from the Secondary Bank (shallowest mesophotic site) had the fastest average linear extension and calcification rates ($\Delta\overline{LE}$ = 0.90 mm/yr ± 0.03 SE; $\Delta\bar{C}$ =1.81 kg m^{-2}yr^{-1}± 0.06 SE). Trends were the opposite for coral from the second shallowest mesophotic site, the Primary Bank, which had the lowest average linear extension and calcification rates ($\Delta\overline{LE}$ = 0.69 mm/yr ± 0.04 SE; $\Delta\bar{C}$ = 1.44 kg m^{-2}yr^{-1} ± 0.09 SE). Post hoc comparisons using Tukey's HSD revealed that $\Delta\overline{LE}$ and $\Delta\bar{C}$ from the Secondary Bank were significantly faster than rates at the Primary Bank ($\Delta\overline{LE}$: p_{adj} = 0.002, $\Delta\bar{C}$: p_{adj} = 0.007), but that neither parameter was significantly different between the Flat Deep Basin and the other sites.

Luminance and stable isotopic comparison

An example of wavelet power spectrum (WPS) analysis conducted for this study is displayed in Fig. 4.8, where global spectrums with the most significant power are shown on the right-side graphs. When graphed as a function of time (with time expressed as distance for the purposes of these data), luminance curve major periodicities (Secondary Bank sample: T = 1.7 mm, Deep Flat Basin sample: T = 2.0 mm) had some correlation with associated isotopic curves (Secondary Bank sample: T = 1.5, Deep Flat Basin sample: T = 1.84 mm) obtained from the same corallites, with isotope periodicities having only a slight (0.16 – 0.2 mm) lag. However, these results did not provide enough information to indicate the strength and sign (positive or negative) of the correlation, and were based on the entire data sets available, not just where both data types overlapped spatially on the sample.

When regenerating the luminance data with a sampling interval of 0.05 mm (to correspond to the isotope sampling interval) and only testing overlapping segments of the signals, additional results were obtained. Cross wave transforms (CWTs) displayed positive amplitudes (indicated by reds and yellows in CWT panels) at the start and end of the Secondary Bank coral luminance time series (Fig 4.9a) but adjacent negative amplitudes (purples and blues in CWT panels) at the same locations on the Secondary Bank $\delta^{13}C$ time series (Fig. 4.8b). The opposite pattern was observed when examining the same CWT panels from the Flat Deep Basin time series. However, the major importance is that the co-related proxy for coral growth has noticeably opposing amplitudes. These differences are reflected in the semblance plot (Fig. 4.8c), where the dominating blue coloration indicates a strong negative correlation (-1) between luminance and $\delta^{13}C$ for the analyzed samples.

Macroboring and secondary accretion

Grazing and microboring were assumed to remove minimal quantities of carbonate from living coral framework samples collected on northern USVI mesophotic reefs for a number of reasons. First, few grazing organisms in the USVI are believed to remove distinguishable amounts of carbonate from living coral colonies (see Appendix for more extensive review). Examination of the living surface of collected samples indicated no major signs of parrotfish corallivory that would remove underlining skeleton (Fig. 4.1). Additionally, no clear indicators of parrotfish grazing (such as typical grazing scars) were observed on the non-living outer surfaces of collected. Examination of individual cut slices indicated the presence of green bands, indicative of (Fig. 4.3, red arrows) moderate abundance of the microboring cyanobacteria *Ostreobium quekettii*.

Despite identifying these bands in a portion of samples analyzed, it was assumed that lower mesophotic reef light attenuation would prevent these organisms from dissolving a significant amount of skeletal carbonate from the collected samples. However, more research into mesophotic reef microboring processes is needed to confirm this assumption.

Preliminary precision analysis of two samples from each site suggested that 207 points were needed to calculate bio-modification surface area percentages within a 95% confidence interval. Additionally, 400 points were found sufficient to accurately determine the macroboring slice percentage (Fig. 4.9). Although secondary accretion was only found on one of the six randomly selected preliminary slices, results imply that the 400 point assumption is also sufficient. For overall living framework skeleton modification, Welch's t-test indicated rates of macroboring carbonate removal are significantly faster than rates of secondary carbonate accretion (t_{23}= -6.7188, p <0.001), but both are slow compared with primary coral framework calcification. Although mean macroboring and secondary accretion rates were lowest at the Primary Bank (Fig. 4.10), no significant site differences were found between framework macroboring rates (Kruskal-Wallace, df = 2, X^2 = 0.63, p = 0.729) or between secondary accretion rates (Kruskal-Wallace, df = 2, X^2 = 2.16, p = 0.340).

Ultimately, the unit area net rate of carbonate (by mass) directly contributing to framework production of living mesophotic coral colonies can be understood when comparing the two carbonate framework accretion processes (primary calcification and secondary accretion) with macroboring (Fig. 4.11). When summing these parameters, but only including those samples where both linear extension and bio-modification rates

were measured on the same slice, statistical testing showed that the average summation of framework carbonate change ($\sum \bar{C}$) is statistically different between measured mesophotic sites ($F_{2,10} = 10.86$, p = 0.003). Post hoc comparisons with Tukey's HSD test indicated specific $\sum \bar{C}$ differences between samples from the Primary Bank site and samples from both the Secondary Bank ($p_{adj} = 0.005$) and the Deep Flat Basin ($p_{adj} = 0.007$). However, if site average $\Delta \bar{C}$ were used for calculations of samples where carbonate modification measurements were conducted but linear extension rate measurements were not, ANOVA did not find any significant site differences in average site framework carbonate summations ($F_{2,20} = 2.493$, p = 0.108).

Discussion

Comparison to other studies

As expected, the linear extension rate of *Orbicella* spp. calculated in this study were all less than rates calculated for the same species at shallower, non-mesophotic reef depths (Dustan, 1975; Hudson, 1982; Dodge and Brass, 1984; Barnes and Devereux, 1988; Bosscher and Meesters, 1993; Helmle et al., 2011). Also, USVI mesophotic extension rates generally fit within standard models (Fig. 4.12) of decreasing coral growth rates with depth (Bosscher, 1992; Hubbard, 2009). However, significant differences detected in mesophotic coral calcification rates at relatively similar depths indicate fine-scale deviations from the standardized models, with potential impacts on the overall carbonate budget of mesophotic reefs. Also, with the exception of a few 36.6 m deep samples with recorded growth rates of 0.60- 0.70 mm/yr (Hubbard and Scaturo, 1985), the linear extension rates calculated in this new study were less (more than 0.5 mm/yr greater, Fig. 4.12b) than most other measurements of the same coral species at

similar depths (Baker and Weber, 1975; Dustan, 1975; Hubbard and Scaturo, 1985; Huston, 1985; Bosscher, 1992). The fine-scale deviation from standard models and the lower than expected growth rates suggest a closer examination of both methods and driving factors is needed to confirm the validity of measured results and offer specific implications.

Coring mesophotic samples was deemed unpractical given financial, logistical, and technical restraints, leading to potentially less accurate results than standard core-based techniques (see next section for details). However, it must also be noted that no previous study has used coring techniques to acquire samples from depths as deep as those in this study. Growth rates recorded from the same species by the only other study (Dustan, 1975) to acquire samples from deeper than the transitional mesophotic reef zone (>35 m) were based on only one year of alizarin staining observations and by using a mercury displacement bulk density technique (45 m: $\overline{LE}$ = 1.63 mm/yr (n = 7), $\overline{BD}$ = 1.650 g/cm^3 (n = 1)).

Coral linear extension and density series usually vary somewhat from year to year (Dodge and Brass, 1984; Lough and Barnes, 1989; Castillo et al., 2011; Helmle et al., 2011; Kwiatkowski et al., 2013), a trend also observed with mesophotic UVSI coral samples (Fig. 4.5-4.6). Therefore, it is quite possible that measurements from Dustan (1975) may have been from a slower year. In addition, mesophotic high density growth bands (see Fig. 4.13a), and live growth surfaces (Fig. 4.13b) show how large variability in horizontal extent could possibly skew linear growth measurements when taken from a single alizarin stain line (see Fig. 2 top, from Dustan, 1975). Finally, coral calcification rates from this most recent study may be slower than those from earlier studies (Baker

and Weber, 1975; Dustan, 1975; Hubbard and Scaturo, 1985; Huston, 1985; Bosscher, 1992) because those measurements represented conditions 20-40 years earlier. And since that time, ocean acidification as well as global climate change-induced coral bleaching have been predicted to hinder carbonate accretion and calcification (Hoegh-Guldberg et al., 2007; Baker et al., 2008). Instances of coral bleaching (Lang et al., 1988; Bunkley-Williams et al., 1991; Bak et al., 2005; Smith et al., 2010) and coral diseases (Smith et al., 2010) have since been recorded in mesophotic reefs.

Analysis of modified standard coral growth techniques

The deeper depths and higher densities of corals collected from the USVI for this study, compared to those of shallower reefs, required procedural modification from more standard X-radiograph coral growth study techniques (Barnes and Devereux, 1988; Helmle et al., 2011). By using coral hand samples instead of cores, shorter amounts of coral could be collected (i.e. less representative time records). The irregular hand sample shapes produced difficulty cutting samples into uniform slices. This was especially problematic because slices needed to be cut even thinner than what is used for more standard shallow-water studies so that X-rays could penetrate through the denser mesophotic skeletons. Uniform thickness is necessary when making gamma densitometry density measurements and was therefore another reason the buoyant weight technique was used.

Irregular slice thickness can cause localized luminance deviations (usually identified and easily handled when doing linear extension measurement techniques) and non-uniform resolution of resolvable density bands along the entire slice lengths (Hubbard and Scaturo, 1985). Therefore, intervals used to calculate overall sample mean

growth rates could not always be selected from the same year span or be based on the same number of years (Fig. 4.5 - 4.6). Sampling from different year intervals could cause slight error with overall measurements when considering the previously mentioned fact that coral growth rates often vary from year to year. However, cumulative mean linear extension rates (Fig. 4.14) as a function of number of years incorporated into the measurement show that individual sample rate variability become considerably more consistent after four to five years of measurements. Also, site cumulative mean linear extension rates (solid orange line in Figure 4.14) evened out significantly after three years. Similarly, examination of sample cumulative standard error (SE) with number of measurements (Fig. 4.15) indicated SE generally declines as more years are added to the measurements.

Within the maximum 16-year time span examined, we could obtain annual extension rates for 55% of the annual cycles (132 of 240 years). The time interval with the most number of potential cycles showing bands (90% of available substrate) was between 2007 and 2005. When mean calculations were restricted to just those years, ANOVA indicated statistically significant differences for linear extension rates ($F_{2,12}$ = 6.12, p = 0.015) and calcification rates ($F_{2,12}$ = 4.87, p = 0.028). Tukey's HSD post-hoc comparisons revealed that $\Delta\overline{LE}$ from the Secondary Bank was significantly different than $\Delta\overline{LE}$ at the Deep Flat Basin and the Primary Bank (p_{adj} = 0.047, p_{adj} = 0.017, respectively), but that the only statistically significant difference in calcification rates was between the Primary and Secondary Bank (p_{adj} = 0.028). Restricting the years analyzed provides results that have greater significant differences than when using all available data (same significant results plus significant differences in $\Delta\overline{LE}$ between the Secondary

Bank and the Deep Flat Basin). Regardless, trends to more consistent averages as more sampling years are added (Fig. 4.14 – 4.15) appear to justify using the maximum amount of recovered data, increasing the overall statistical power of results to detect significant differences.

Another possible error when examining the X-radiographs produced for this study is that what was identified as high density bands resemble coral dissepiments in size and position (Fig. 4.2). It could be argued that our measurements then are merely based on dissepiment identification. However, studies have shown that annual density variations recorded in the coral genus *Montastraea* are directly associated, to some extent, with dissepiment thickening (Dodge et al., 1993; Dávalos-Dehullu et al., 2008).

Isotopic analysis considerations

The cyclical coral stable oxygen and carbon isotopic composition curves identified in two representative samples coarsely verify assumptions of annual density band formation and relative density band spacing used to calculate linear extension rates (Fig. 4.4). This verification is useful because the methodology used for stable isotopic analysis in this study was independent from the X-radiographic methodology used. Previous independent studies have shown that carbon and oxygen stable isotope trends from coral skeleton can have equivalent annual periodicity (Weber et al., 1976; Fairbanks and Dodge, 1979). Generally, coral stable oxygen isotope variation is influenced by temperature and seawater isotopic composition as a function of numerous properties such as precipitation, salinity, and water mass transport (Carriquiry et al., 1994). On the other hand, coral stable carbon isotope composition is influenced by a complicated set of coral-

algal metabolic interactions generally thought to act as a "light meter" (Weber, 1974; Swart, 1983; Grottoli and Wellington, 1999).

Beyond just showing cyclical patterns, wavelet analysis allowed for the direct identification of strong negative correlations between stable carbon isotope composition and skeletal density (measured by luminance) variation (Fig. 4.8). Correlations between mesophotic skeletal density variations and stable isotope composition were more readily apparent for $\delta^{13}C$ than $\delta^{18}O$. The reasons for this observations are likely that: (1) the annual temperature fluctuations at mesophotic depths do not vary enough in amplitude to produce strong temperature signals (see temperature data from Smith et al., 2010); and (2) $\delta^{13}C$ has been shown to have depth-related anomalies such that samples from deeper (15 m instead of 1 m) samples show two to three times greater amplitude fluctuations in carbonate isotope composition (Carriquiry et al., 1994). Although negative correlations (out-of-phase relationships) between high density bands and $\delta^{13}C$ have been identified in other studies (Emiliani et al., 1978; Fairbanks and Dodge, 1979; McConnaughey, 1989; Klein et al., 1992; Carriquiry et al., 1994), just as many studies have documented in-phase relationships (see list of other studies and review in Barnes et al., 1995; Barnes and Lough, 1996). This lack in a consistent relationship indicates the reasons and processes controlling potential correlations between stable isotopic composition and density band formation are not fully understood. Regardless of these inconsistencies and the use of just two samples for isotopic analysis (due to limited availability of time and funding), the results from wavelet analysis and additional qualitative observations are thought to justify the mesophotic coral growth rate conclusions from this dissertation.

Greater implications of mesophotic coral growth rates

Results from this study provide the first spatially-extensive data set of mesophotic coral growth rates in the Caribbean. Analysis shows that the mesophotic samples analyzed in this study generally fit within proposed models of coral growth rate reduction with depth (Bosscher, 1992; Hubbard, 2009). However, longer mesophotic coral records are needed to determine if the slower $\Delta\bar{C}$s measured in this chapter (compared to studies conducted 20-40 years ago, Baker and Weber, 1975; Dustan, 1975; Hubbard and Scaturo, 1985; Huston, 1985; Bosscher, 1992) resulted from worsening atmospheric and oceanic conditions such as global climate change or ocean acidification.

Statistically significant different calcification rates were identified in coral living on neighboring mesophotic reef habitats with varying structural characteristics. Rates do not vary enough to produce noticeably distinctive carbonate accumulations over short time scales. However, subtle differences in carbonate production implicate a potential long-term mechanism for the creation of heterogeneous reef geomorphology needed to maintain the heath and stability of both shallow and deep marine ecosystems, including recovery from both anthropogenic and natural disturbances (Maragos et al., 1996; Lenihan et al., 2008; McClain and Barry, 2010). Therefore, substantial time-scale dependent carbonate accumulation differences are possible along broad sloping carbonate shelves with mesophotic reef systems such as those on the Puerto Rican Shelf. This has direct implications for our general understanding of mesophotic reef carbonate basin development and sea level change.

The slow rates recorded in this study also provide some support to the traditional carbonate shelf theory (that reef accretion decreases with depth, Schlager, 1981;

Macintyre, 1988; Bosscher and Schlager, 1992). This support is increased when considering that measured direct framework bioerosion rates were not quick enough to balance out deep and shallow-water reefal carbonate accretion, as suggested by Hubbard (2009). However results from this chapter do not account for benthic coverage and only considered the fate of coral carbonate covered by living polyp communities. Also, regardless of the implications identified in this discussion, the actual geomorphological implications depend on the three-dimensional spatial coverage of carbonate framework in the mesophotic reef habitats, as well as other carbonate altering processes within the reef system. These various processes are best addressed in the form of a carbonate budget.

Figure 4.1. Mesophotic coral framework collection. Living samples of *Orbicella* spp. after collection with dive weights for scale. Samples were placed under dock to shade them before transport to Miami.
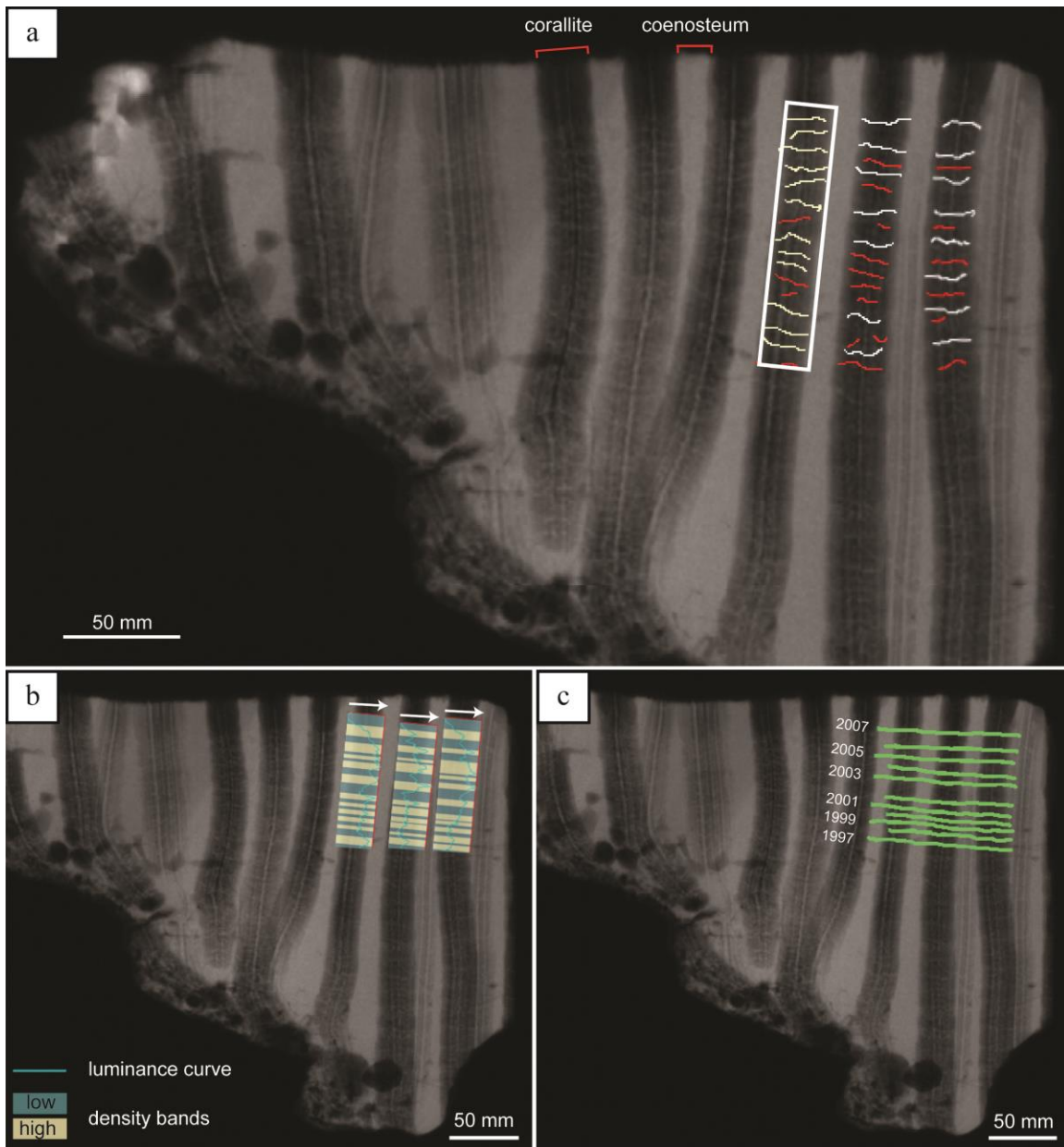
Figure 4.2. Mesophotic X-radiograph analysis. Negative X-rays of a platy mesophotic *Orbicella* spp. coral subsample collected from the Deep Flat Basin. X-ray color variation differentiates between high (light) and low (dark) density. The thin slices needed for analysis resulted in the vertical strip pattern because corallites are significantly less dense then their surrounding coensteums (see chapter text for more details). (a) Definite (white) and potential (red) visually identified high density bands on separate corallites. White rectangle transect indicates the spatial extent of one corallite selected for analysis. (b) Scaled *CoralXDS* luminance scan results atop location of analyzed corallites (area selected with transects). Arrows point in direction of increasing luminance. (c) Interpretation of connected colony-wide density bands expressed on adjacent analyzed corallites, with approximate year of formation indicated.
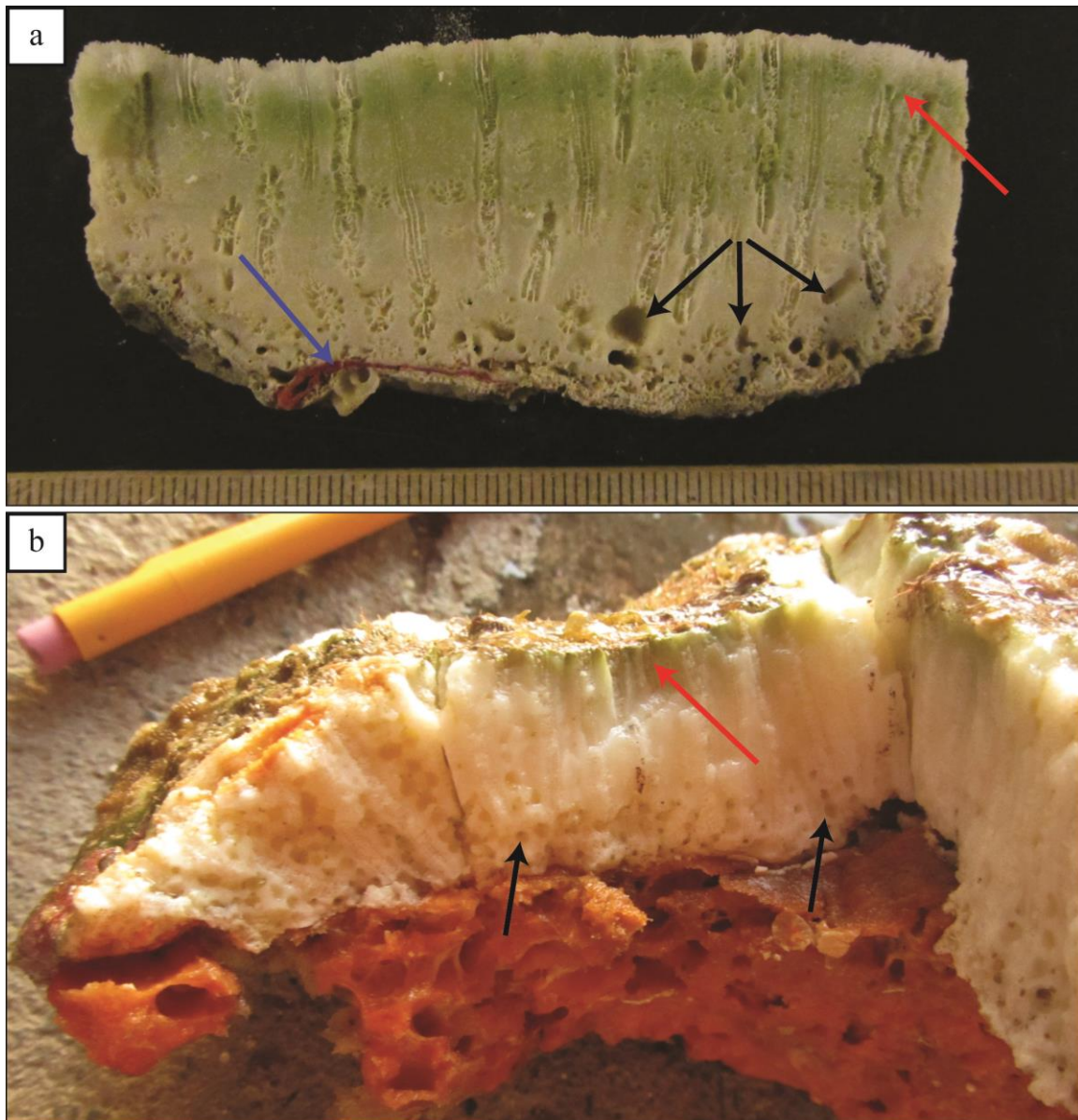
Figure 4.3. Mesophotic framework bioerosion and secondary accretion. (a) Sample from *Orbicella* spp. colony collected from the Flat Deep Basin. The black arrows show examples of "living framework" macroboring and the blue arrow provides an example of "living framework" secondary carbonate accretion, all on the lower side of the coral. (b) Different collected mesophotic *Orbicella* spp. sample with bioeroding sponge still attached to the underside of the colony in which no protective coral tissue cover was present. Above the orange sponge, tiny eroded chambers are observed within the coral skeleton (black arrows for example) and provide a helpful *in situ* example of cryptic sponge macroboring processes. Red arrows in both images identify microboring cyanobacteria community of *Ostreobium quekettii*.
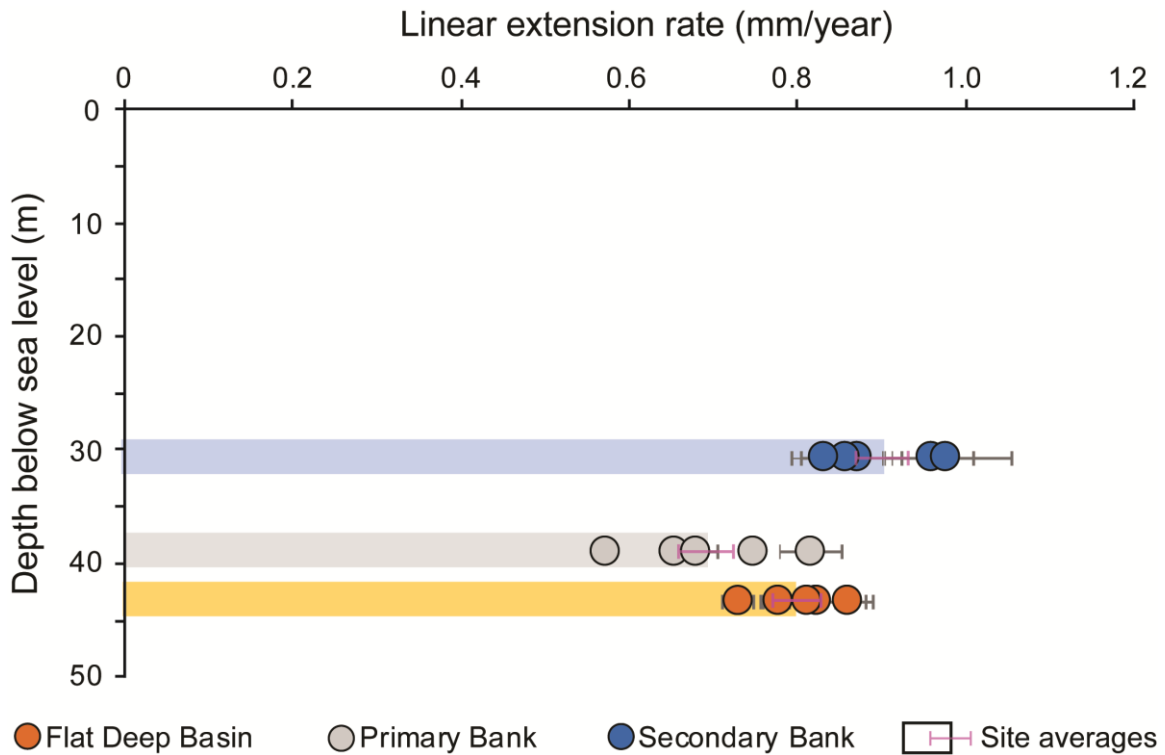
Figure 4.4. Linear extension rates with depth. Results for each analyzed sample based on 3-5 adjacent corallite transects per sample. See chapter text for specific methodology. The extension rate recorded for each sample is calculated as the average distance between subsequent representative high density bands. Error bars equal ± 1 standard error.
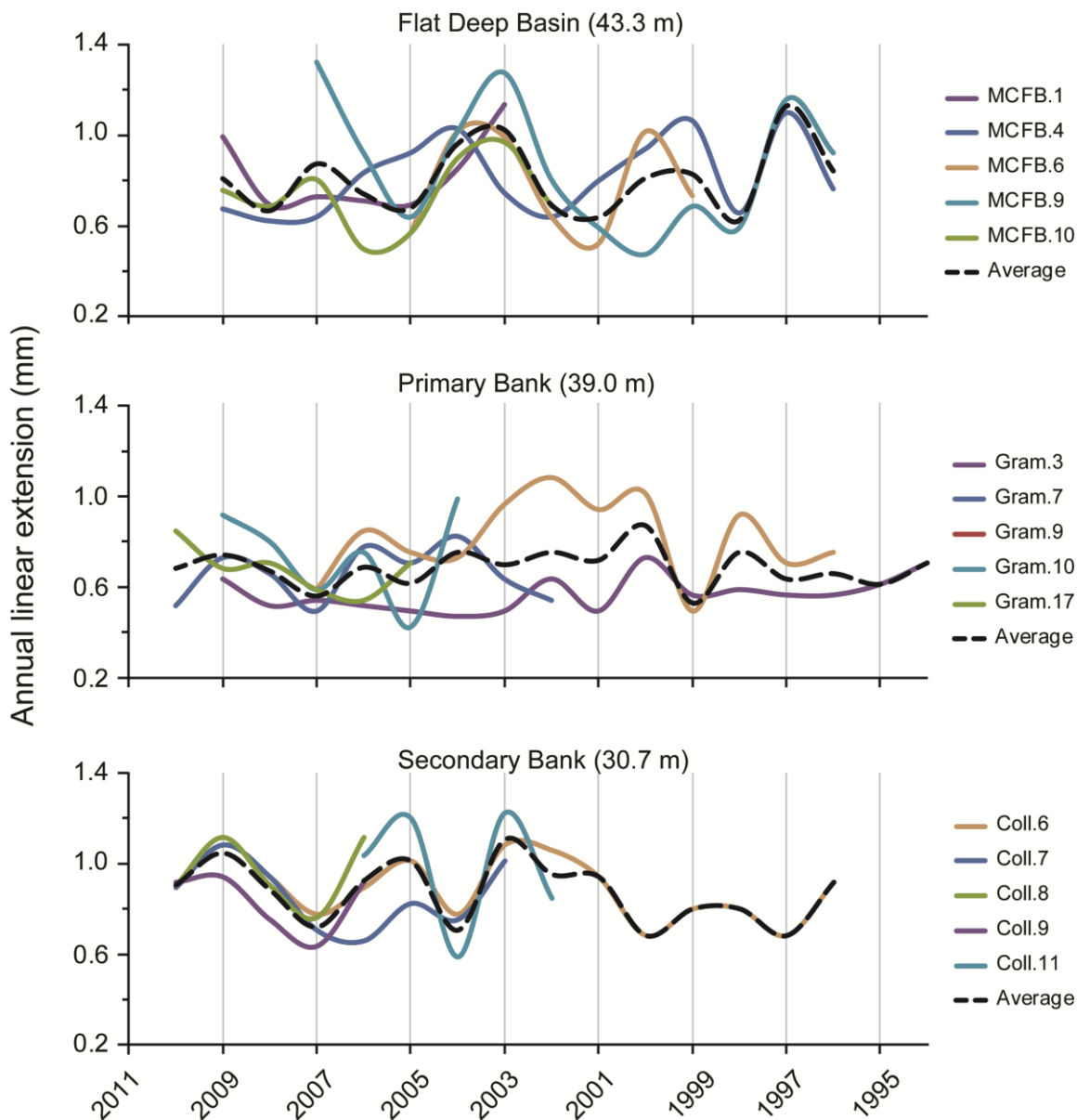
Figure 4.5. Linear extension rate variation with time. All mesophotic *Orbicella* spp. samples analyzed by site, plot to compare annual linear extension variation during individual years of growth. Curve colors correspond to specific sample results at a given site. Dotted black lines are overall site average trends.
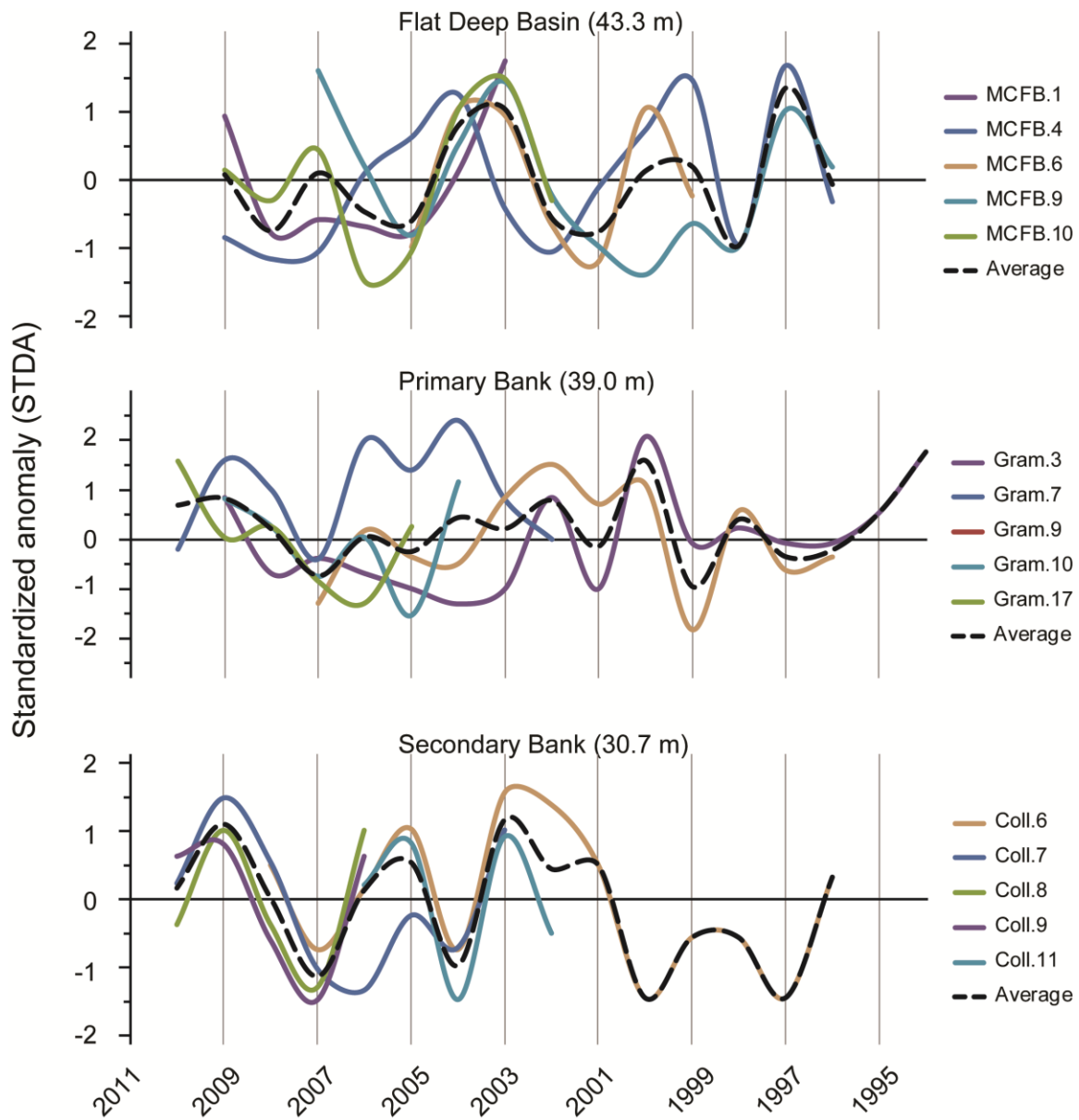
Figure 4.6. Coral growth in standardized anomaly (STDA) units. Same plot as Figure 4, but converted to STDA (annual deviation from the mean, divided by standard deviation) as is common convention (for example, see Helmle et al., 2011).
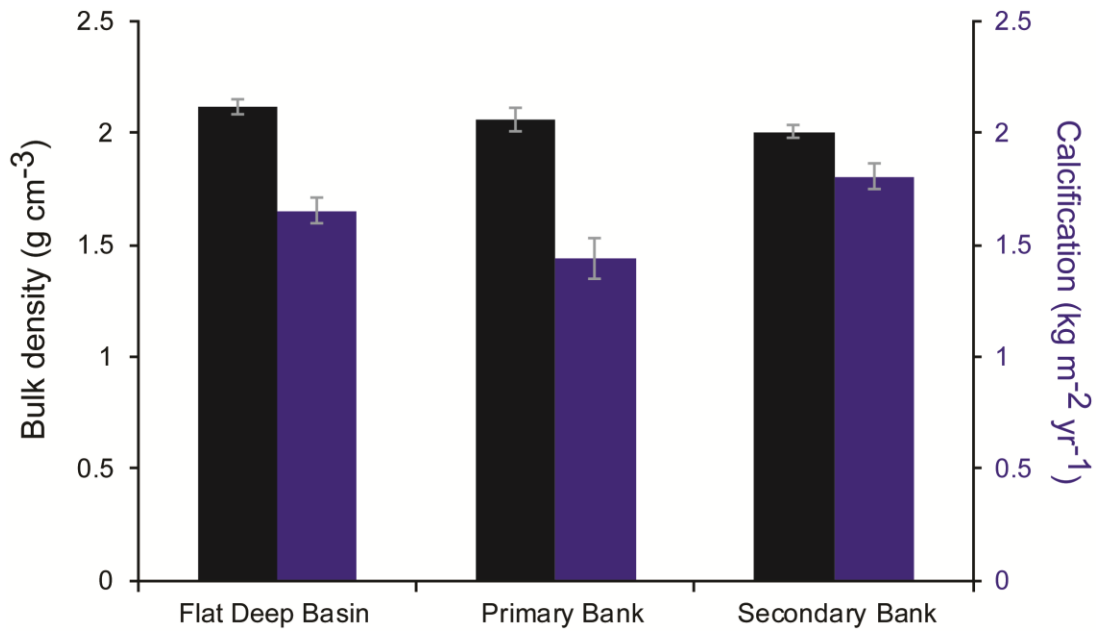
Figure 4.7. Mesophotic coral bulk density and calcification. Bulk density averages ($\overline{BD}$) from buoyant weight method. Mean calcification (displayed in units commonly used for carbonate budget analysis) are calculated as bulk density multiplied by mean linear extension rate (Fig. 4.4). Error bars equal ± 1 standard error.
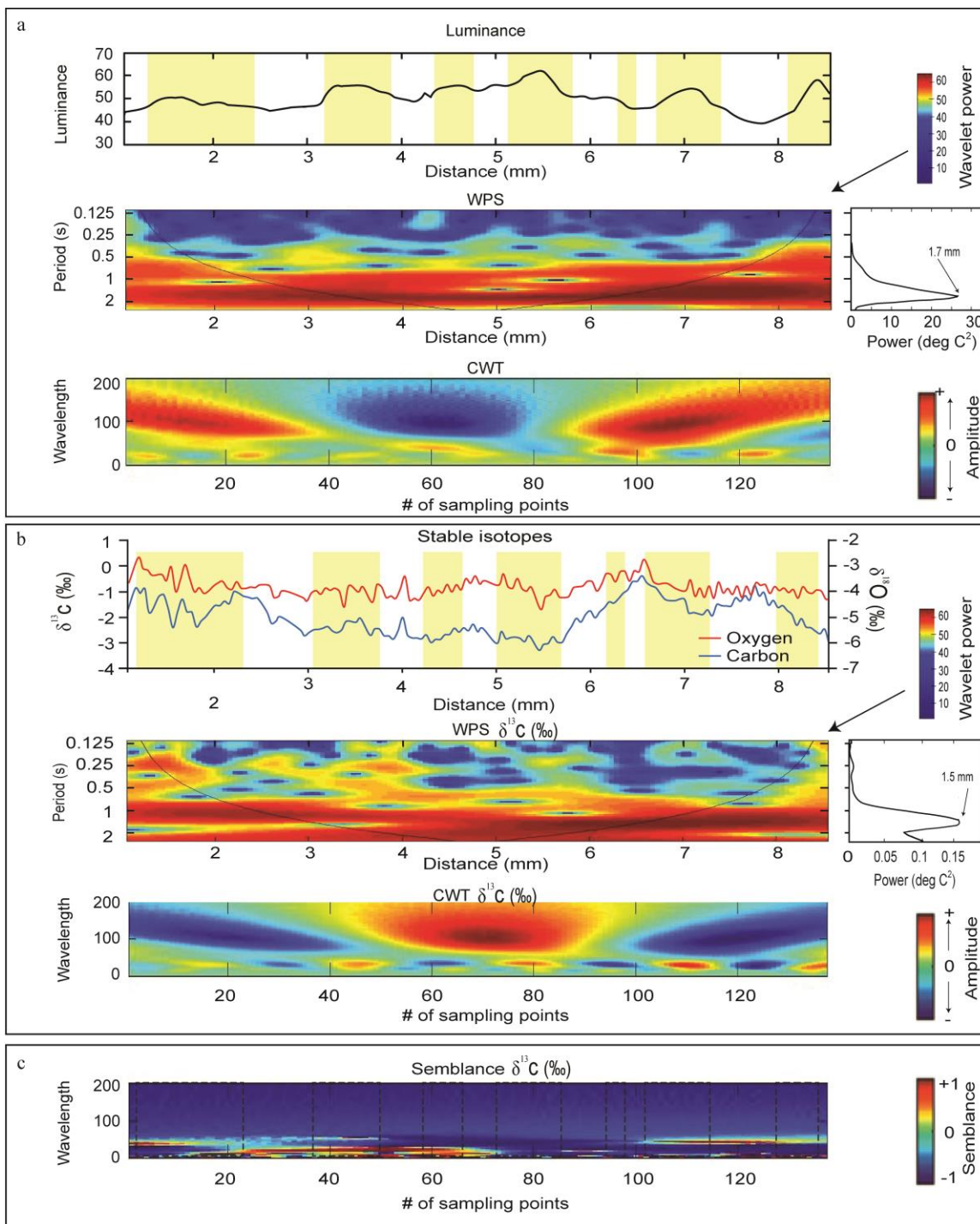
Figure 4.8. Wavelet analysis of Secondary Bank coral. Data from same corallite (a) luminance and (b) stable isotope trends. Upper graphs (a, b each) show original time series (as distance in mm), middle graphs display wavelet power spectrum (WPS) results (notice stable isotopes have different axes), right-side graphs indicate global frequencies with the most significant power spectra, and bottom graphs display cross wavelet transform (CWT) analysis (see text). (c) Time series CWT comparison between isotope and luminance analysis. Vertical boxes/dotted lines show high density bands, determined from luminance analysis. WPS and CWT δ18O curves not included due to low semblance.
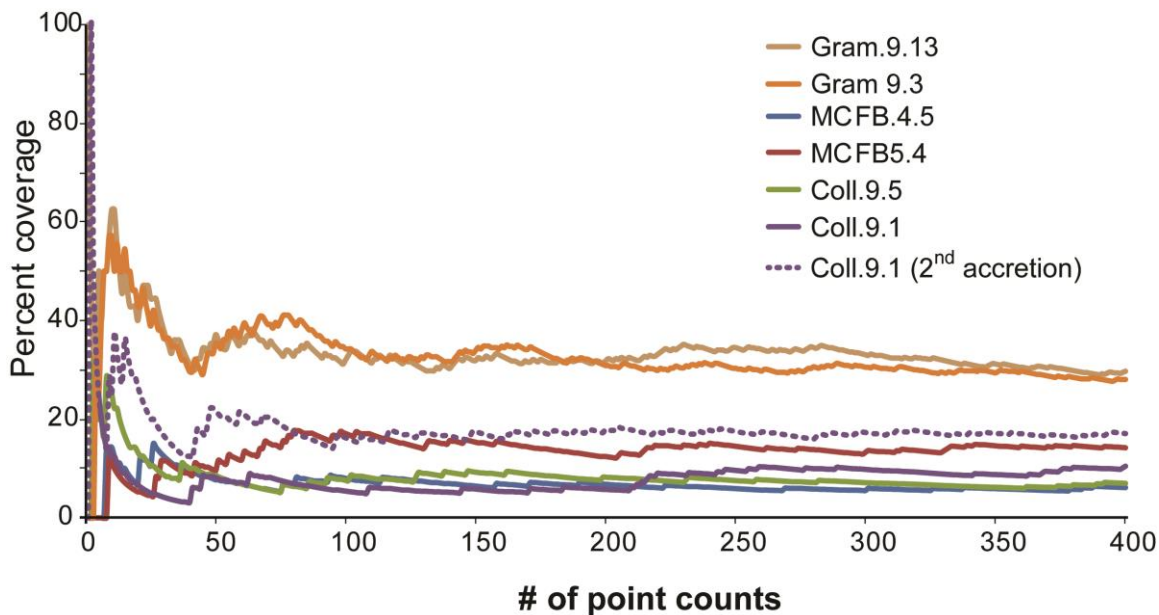
Figure 4.9. Data points needed for bio-modification analysis. The percent of slice surface area occupied by macroborings (or encrusted over by secondary accretion, as indicated by the dotted line), as a function of the total number of points used for point count analysis.
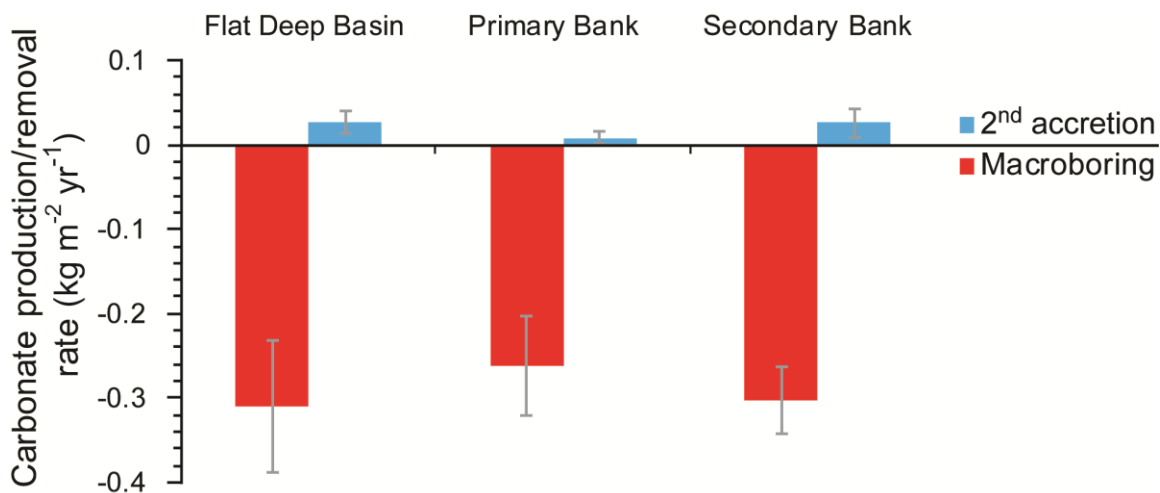
Figure 4.10. Living mesophotic coral framework bio-modification rates. Comparison between mean rates of *Orbicella* spp. framework macroboring and secondary accretion. Values are fairly insignificant compared to primary coral calcification rates (Fig. 4.7).
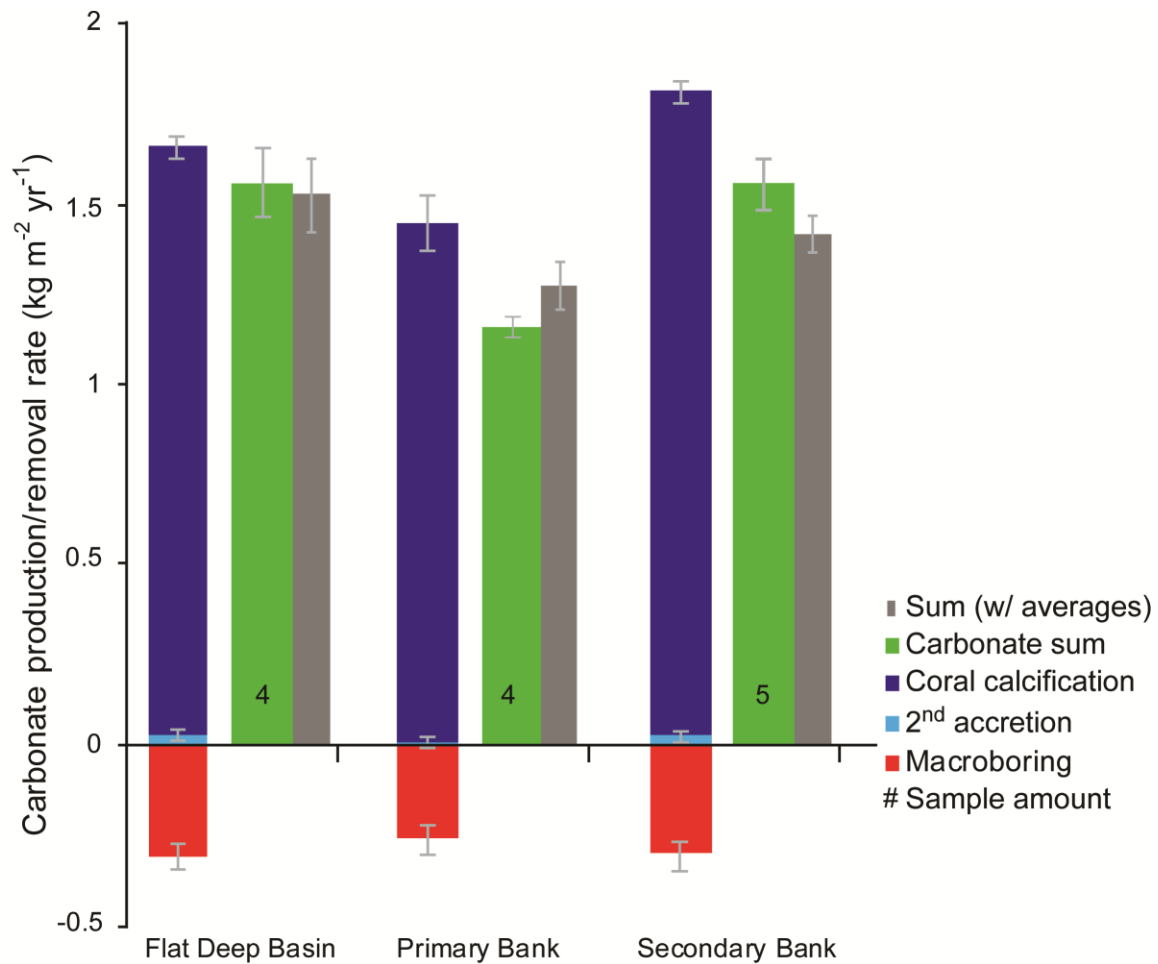
Figure 4.11. Mesophotic coral framework calcification and bio-modification rates.
Rates of primary *Orbicella* spp. calcification, per site, plotted with macroboring and secondary accretion rates. Green left bars show the summation of all three processes when only using specific corresponding data sets, with the number indicating how many samples had this attribute. The grey bar shows the summations if site average calcification rates were used to augment calculations for samples that had direct measurements of framework modification but not liner extension rates. Error bars equal ± 1 standard error.
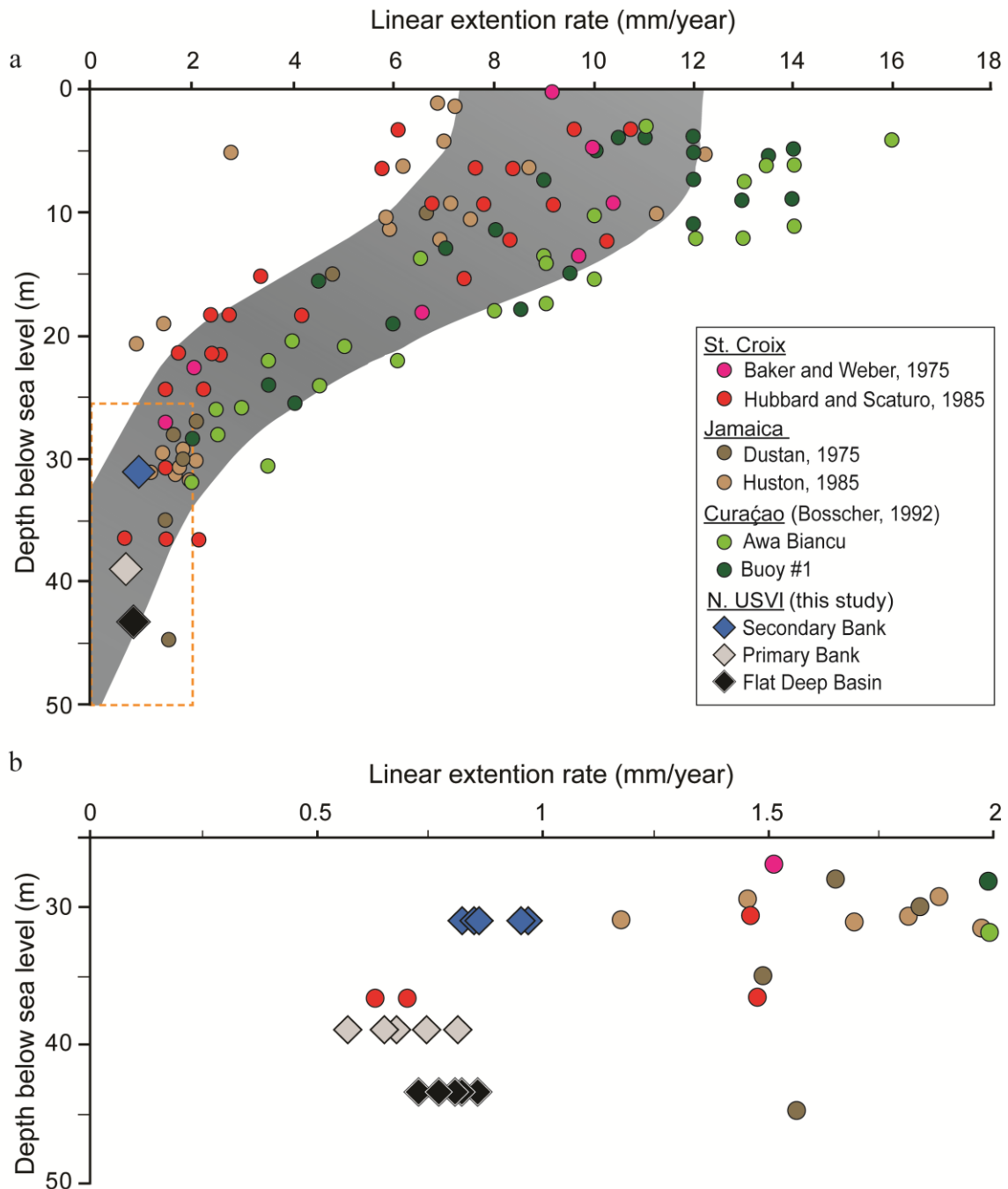
Figure 4.12. Study comparisons between linear extension rates. (a) Comparison of *Orbicella* spp. linear growth rates measured from this study with other Caribbean measurements of coral defined as *Montastrea annularis*. Shaded area represents the predicted range of *M. annularis* growth rates (Hubbard, 2009). Orange dotted line indicates location of lower graph. (b) Magnified view of measured growth rates between 20-50 m. Data from current mesophotic study are displayed for each sample measured.
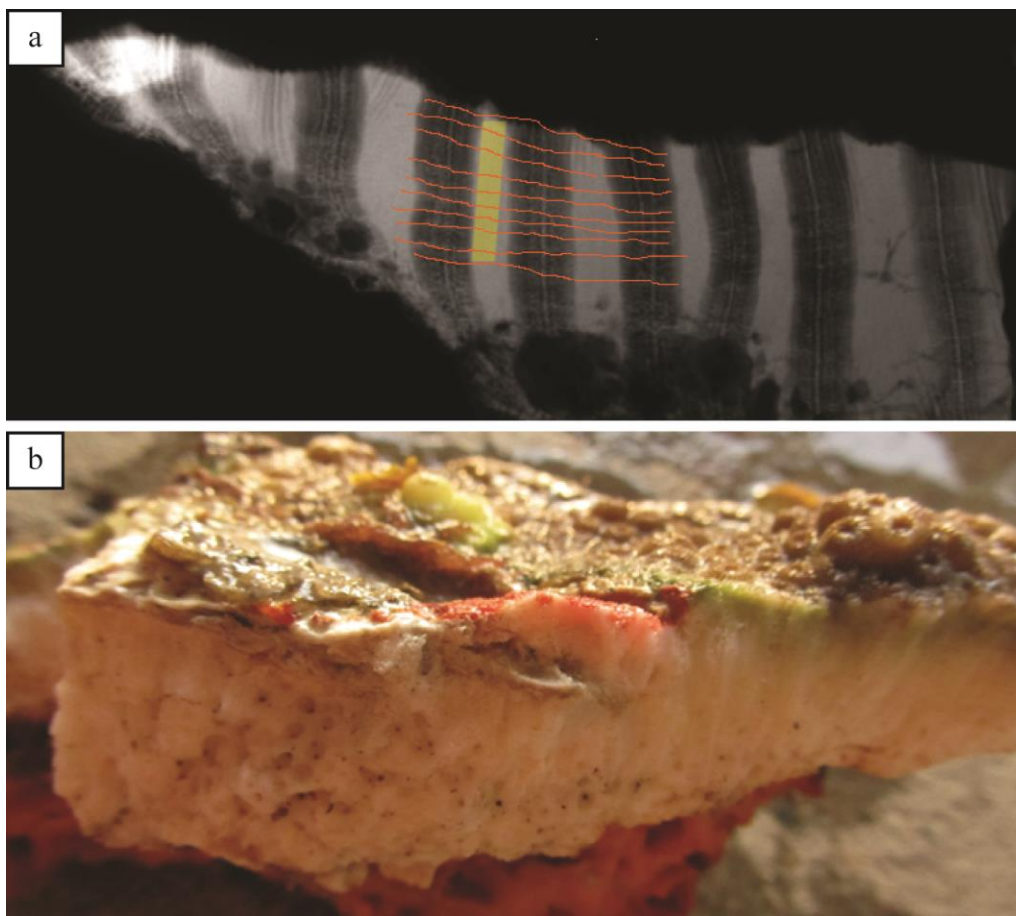
Figure 4.13. Growth horizon variability. (a) *Orbicella* spp. sample from the Secondary Bank, showing irregular growth high density band horizons (orange). Yellow box indicates micro-drilling location of for isotopic analysis. (b) Recently collected live sample with top surface showing the same irregular growth horizon.
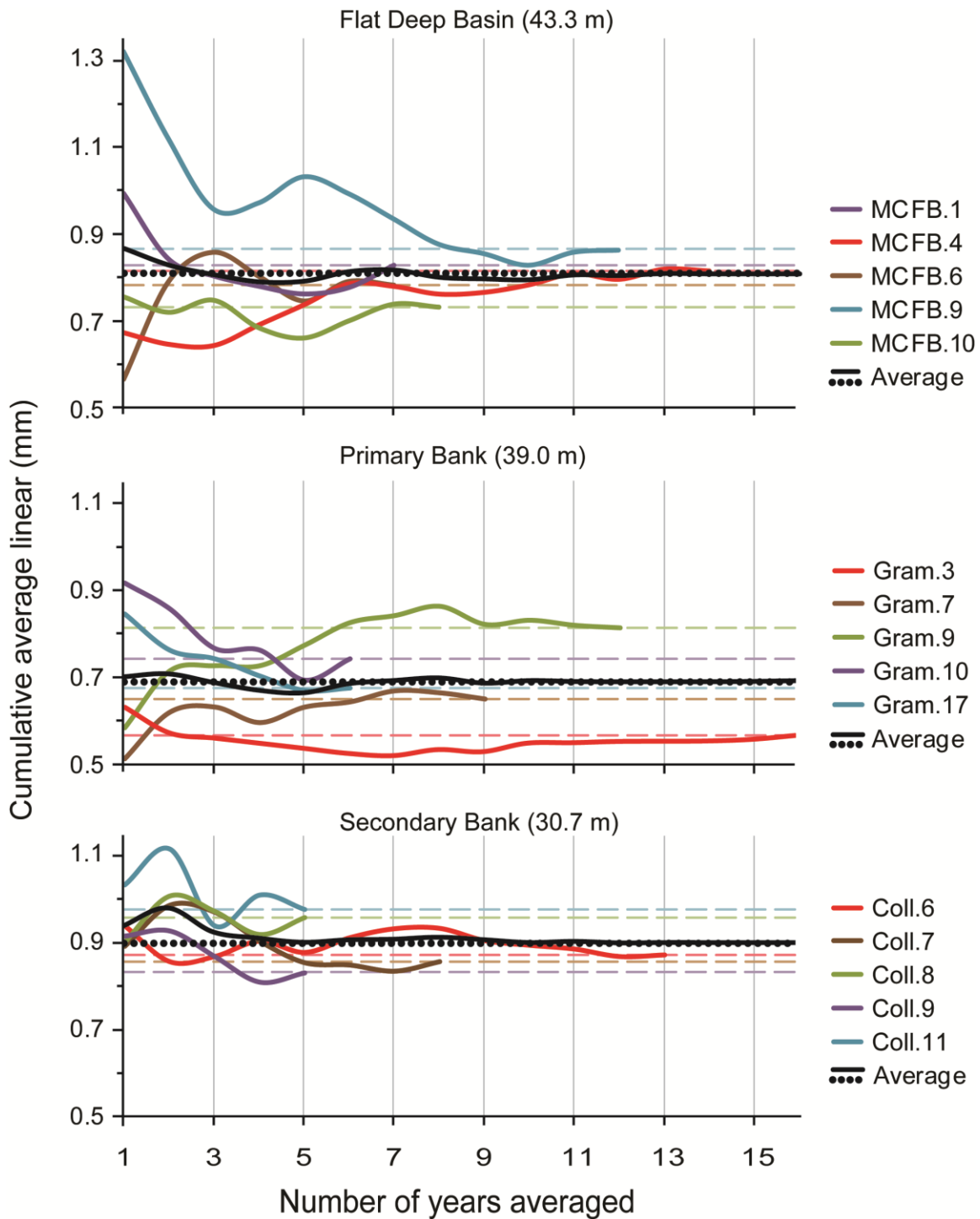
Figure 4.14. Cumulative mean linear extension rates. For each indicated study site, graphs show the cumulative individual sample average mean linear extension rate change as a function of number of years included in the calculation. Colored dash lines indicate overall sample mean linear extension rates used for analysis in this study, and black dotted lines indicate the respective average mean linear extension value for each site. Solid black line represents the site cumulative average mean linear extension rate (when including all samples) as a function of number of years included in the calculation.
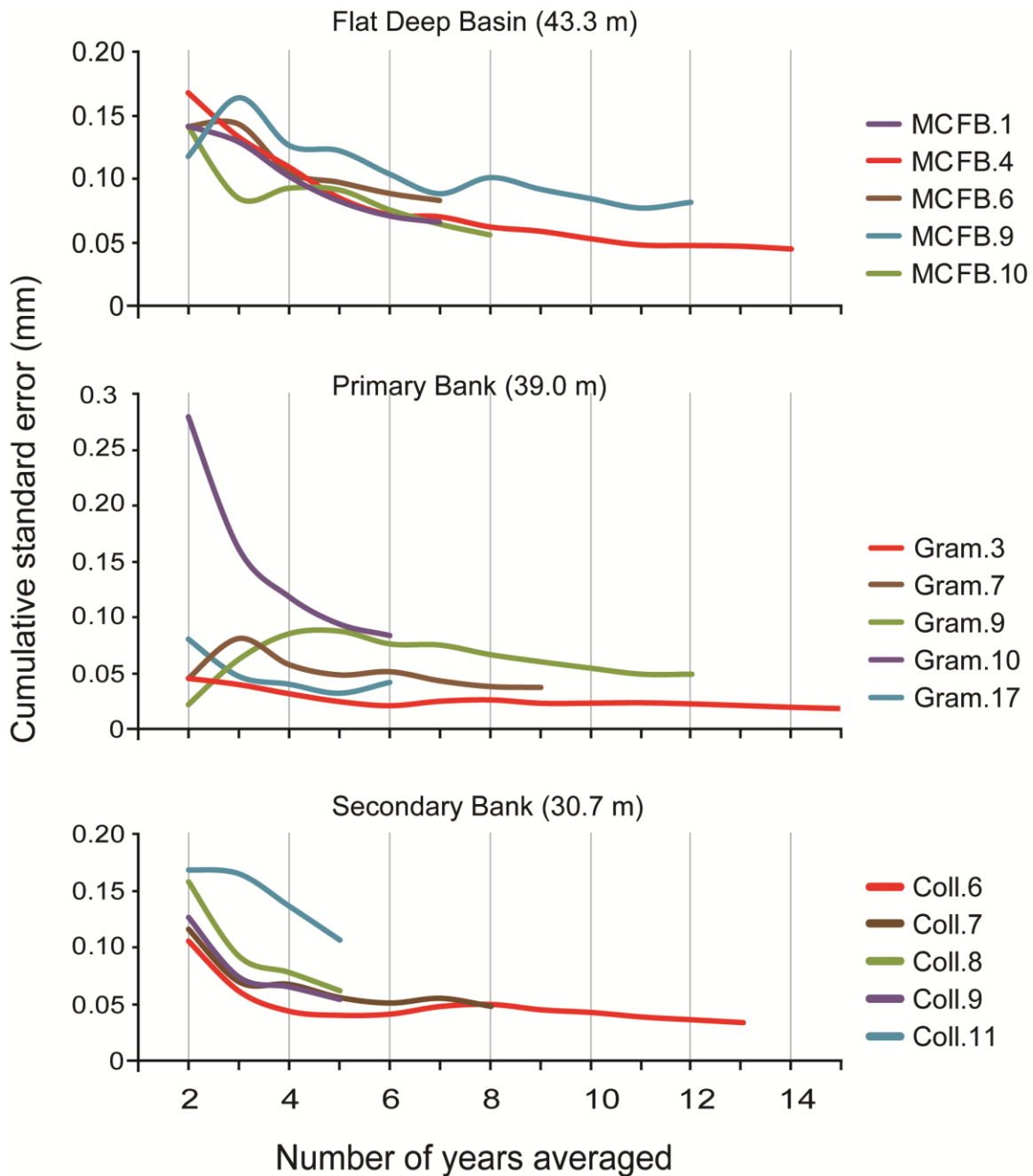
Figure 4.15. Cumulative mean linear extension standard error. For each indicated study site, graph shows the cumulative standard error of sample mean annual linear extension rate (grouped by site) with number of years included in the measurement.

CHAPTER 5. CARBONATE BUDGET ANALYSIS OF MESOPHOTIC REEF HABITATS WITH DIFFERENT STRUCTURAL CHARACTERISTICS

Chapter summary

As indicated from shallow-water coral reef carbonate budget analysis, reef geomorphology and long-term reefal carbonate accretion are determined by the balance of local carbonate constructive and destructive sedimentary processes. Despite the recent influx of publications addressing mesophotic coral reef physiology and ecology, little is known regarding the fundamental sedimentary processes that construct, maintain, and alter mesophotic reef framework and how these processes interact to determine the sustainability and structural integrity of mesophotic reefs. A modified census-based carbonate budget model was therefore developed to address the identified knowledge deficiency and to compare implications of the interrelated sedimentary processes examined in the previous chapters of this dissertation.

To formulate site specific mesophotic carbonate budgets, bioaccretion and bioerosion rates obtained from experimental coral substrates exposed for 3 years, and growth versus bio-modification rates framework-building coral colony carbonate skeletons were scaled by habitat-specific benthic abundances and spatial coverage. Despite variability, all examined mesophotic sites were found to be in states of net positive geomorphic production, with one site further classified as being in a precarious equilibrium stasis. Calculated net production rates were lower than estimates rates in the recent past, potentially a result of discrete, climate-change related stress events. This suggests mesophotic reef structural sustainability may be less immune to worsening environmental conditions degrading global shallow-water coral reef health then once though. On a larger temporal scale, results suggest mesophotic coral reef accretion was

173

not the sole, primary driver of shelf-scale topographic relief on the Puerto Rican Shelf. However, estimated accretion rates suggest variability of mesophotic reef "slow, but steady" carbonate accumulation during some portion of the past 6 ka years greatly contributed to habitat-scale relief and complexity essential for maintaining biologically diverse, healthy ecosystems.

Background

Reefs are three-dimensional, physically accreted, carbonate production and deposition centers. The development and maintenance of coral reef structural integrity is greatly dependent on net carbonate production and accumulation rates. Assortments of often related biological, chemical, and physical processes add and remove calcium carbonate from a reef system. These processes also cycle carbonate within a reef, until the carbonate is deposited as different physical states (e.g. skeleton, cement, sediment) within the geomorphic constructional sedimentary reef landforms (Perry and Hepburn, 2008). Regardless of how rapidly coral colonies grow, the cumulative effect of early diagenetic carbonate cycling constructive and destructive processes (Scoffin, 1992), dictate net calcium carbonate reef accumulation, reef accretion, and overall reef geomorphology (Perry, 1999). Still, accretion of a reef will not occur if destructive processes dominate.

The earlier chapters in this dissertation focused on specific processes that modify the physical aspects of mesophotic coral reefs, using habitats with different structurally characteristics as the basis for inquiry. Within these chapters, the overall cumulative objective of this dissertation, to determine the variability of fundamental mesophotic reef sedimentary processes, was addressed. Also, the magnitude and variability of these

processes were considered in terms of promotion, maintenance, and destruction of habitat heterogeneity and structural complexity, and of short-term ecosystem health. Results from these earlier chapters may also have greater implications when making paleo-mesophotic reef interpretations, and examining mesophotic reef evolution and potential relations to the origins of coral reef biodiversity. Despite the merits of examining each component of reef sedimentology individually, reef carbonate budget analysis provides a useful method to quantitatively compare the relationships, feedbacks, and relative contributions of major sedimentary components. This provides means to evaluate mesophotic reef structural complexity and sustainability, and mesophotic reef accretion and preservation potential from multiple perspectives.

The carbonate budget of a reef is defined as the summation of carbonate produced from primary and secondary calcareous secreting organisms, sediment production, cementation, and sediment transport into the reef, minus carbonate losses associated with biological and physical erosion, sediment export, and dissolution (Chave et al., 1972). The net calcium carbonate accumulation within a reef when considering all processes attributable to reef carbonate cycling, is classified as either constructive or destructive (Scoffin, 1992). Perry et al. (2008b) proposed that a carbonate budget should provide a tangible, all-inclusive measure of the functional geomorphic status of a reef. Most studies that monitor the health of coral reef systems mainly focus on ecological changes. However, there is a clear distinction, from a temporal standpoint, between the health of the thin ecological veneer of a coral reef and the ability of the underlying coral framework to maintain the integrity of the reef structure (Edinger et al., 2000).

The study of carbonate budgets may also be applied to understanding carbonate shelf development. Traditional reef accretion theory was primarily established based on relationships between calcification rates and light attenuation. The theory states that reef accretion decreases with depth (Schlager, 1981; Macintyre, 1988; Bosscher and Schlager, 1992). However, studies of Holocene reef cores from the Caribbean determined that there is insufficient evidence to support the traditional reef accretion theory (Gischler, 2008; Hubbard, 2009). Using a carbonate budget analysis approach, other studies concluded that reef accretion is highly dependent on cementation, encrustation, and bioerosion, and ultimately questioned the previously stated traditional theory of reef accretion and depth (Stearn and Scoffin, 1977; Scoffin et al., 1980; Harney and Fletcher, 2003; Mallela and Perry, 2007; Perry et al., 2008b). The results of these studies prompted Hubbard (2009) to suggest that differences in bioerosion with depth may partially explain why the proven coral growth—light intensity association does not result in the theorized decrease in reef accretion with depth.

The carbonate budget analytical approach was first developed to provide a more quantitative method for studying carbonate sedimentology and interpreting coral reef lithological evolution (Macintyre et al., 1974). Though the concept is simple, no carbonate budget technique can fully account for the numerous large to subtle environmental and sedimentary variants interacting simultaneously on varying spatial scales. In general, there are three main carbonate budget approaches. These include techniques that evaluate: (1) net sediment accumulation rates (Land, 1979; Hubbard et al., 1990; Ryan et al., 2001); (2) hydrochemical spatial variations (Smith and Kinsey, 1978; Kinsey, 1985; Campion-Alsumard et al., 1993; Langdon and Atkinson, 2005); and

(3) calcification and bioerosion rates applied to census-based benthic surveys (Chave et al., 1972; Scoffin et al., 1980; Eakin, 1996; Harney and Fletcher, 2003; Perry et al., 2012). Because these approaches rely on distinct assumptions and provide varying perspectives over different temporal and spatial scales, the accuracy and reliability of a particular budget approach depends on the specific research question the budget is being used to address (Perry et al., 2012). Carbonate budget analysis has increased scientific knowledge on a wide range of topics such as: (1) initial development and long-term accretion of reefal carbonate shelves (Stearn et al., 1977; Hubbard et al., 1990); (2) temporal impacts of ecological phase-shifts on reef geomorphology (Perry and Hepburn, 2008); (3) coastline evolution relationships with reef structure (Harney and Fletcher, 2003); and (4) potential impacts of terrigenous runoff and impending reef stressors on reef ecological health and longer-term structural sustainability (Scoffin et al., 1980; Eakin, 2001; Mallela and Perry, 2007; Browne et al., 2013).

Objectives

Despite the valuable information gained from carbonate budget analysis, no study has compared the relative importance of different major mesophotic reef sedimentary processes and how these processes contribute to mesophotic reef growth and accretion, community stability, and temporal variations in habitat productivity. Therefore, the objective of this chapter is to calculate modified census-based carbonate budgets that would systematically address these overarching broad concepts and provide new data for interpreting traditional reef accretion theory. The other objective of this chapter is to use the carbonate budget approach as a platform to outline the major results and conclusions of this study and address the previously established overarching dissertation goal: to

determine the significance and variability of the key sedimentary processes involved in the development, maintenance, and destruction of mesophotic reefs. Finally, suggestions are offered for future mesophotic sedimentology research of both modern and ancient deposits.

Approach philosophy

The availability and use of multiple techniques and ideologies hinders comparisons between different carbonate budget studies. To resolve this issue, generate larger and more easily accessible datasets, and provide a relatively simple standardized methodology, Perry et al. (2012), developed a rapid, non-destructive census-based carbonate budget approach in a similar fashion to the AGRRA protocol (Lang, 2003). The *Reefbudget* approach (Perry et al., 2012) was thus selected as the best starting base for carbonate budget analysis of northern USVI mesophotic reef habitats. However, multiple factors associated with data availability, research goals, and research constraints (examined in discussion section) led to deviations from *Reefbudget* baseline procedures when necessary or when deemed possible to obtain more accurate, location-specific results. The outcome of these changes was a new model (Fig. 5.1 and associated equations in Table 5.1) derived to calculate a "hard substrate carbonate budget" and estimate a total carbonate budget of different mesophotic reef habitats and shallow-water comparisons on the South Puerto Rican Shelf.

The reason for distinguishing a "hard substrate carbonate budget" was because the original *Reefbudget* methodology simplifies carbonate budget calculations by indirectly assuming all bioeroded carbonate is removed from the system. Actually, only the physical state of the eroded carbonate changes (especially since macro-bioerosion is

dominated by mechanical modification compared to carbonate dissolution, Glynn, 1997).

This simplification incorporated into *Reefbudget* methodology was probably

implemented to maintain a rapid-survey, user-friendly approach. Since the publication of

the original *Reefbudget* approach (Perry et al., 2012), additional papers have been

published by *Reefbudget*-affiliated authors that minimize the fore mentioned

simplification (Browne et al., 2013; Perry et al., 2013). A model was also created (and

provided much supplementary material) which allows for the input of 115 different

variable means and standard deviations and appears to greatly improve the accuracy and

relevance of the overall budget method (Kennedy et al., 2013). However, these materials

were not available during the planning and implementation of this current dissertation,

and for most of the analysis. Therefore, the model was not used in place of the hard

substrate carbonate budget developed for this dissertation. After calculating the hard

substrate carbonate budget, additional measurements and characteristics were included to

develop estimated complete carbonate budgets.

Methods

Model generation

Hard substrate carbonate budgets were calculated from data collected at four

mesophotic reef habitats (Primary Bank, Secondary Bank, Hillock Basin, and Deep

Patch), as well as at the Mid-shelf Patch and Fringing Patch reef sites (Fig. 1.3) between

August 2010 and May 2013. Unless otherwise stated, the same methodology was used

for all habitats analyzed. To calculate carbonate budgets, results from prior chapters

were considered, and supplemented, when necessary, with data from other studies (using

values obtained from locations, species, and depths similar as possible to those of this

current study) compiled and made available by *Reefbudget* (Perry et al. 2012, available at

http://geography.exeter.ac.uk/reefbudge). The derived model was used to implement

these data and ultimately calculate mean hard substrate net carbonate production rates

($\Delta\overline{NP}_{HS}$) for each habitat.

The hard substrate budget $\Delta\overline{NP}_{HS}$ is defined as the sum (Eq. (1)) of the total mean

primary carbonate production ($\Delta\overline{PP}_T$) and secondary carbonate production rates ($\Delta\overline{SP}_T$),

collectively referred to as the rate of gross hard substrate carbonate production, minus the

mean total bioerosion rate of hard substrate ($\Delta\overline{BH}_T$). These carbonate reef states were

calculated from what were considered the five most attainable and important site specific

average rate categories of the implemented carbonate budget model. The three

constructive rate budget categories include: (1) primary (scleractinian) carbonate

production ($\Delta\overline{PP}_{coral}$); (2) secondary carbonate production on living framework

($\Delta\overline{SP}_{frame}$); and (3) secondary carbonate production on exposed consolidated substrate

($\Delta\overline{SP}_{ecs}$). Countering these are two destructive rate categories: (1) macro-bioerosion of

living framework ($\Delta\overline{Bmac}_{frame}$); and (2) total bioerosion of exposed consolidated

substrate ($\Delta\overline{Bt}_{ecs}$). Although the mean primary carbonate production rate is calculated

from a single carbonate budget category, (Eq. (2)), the site mean secondary carbonate

production and mean total bioerosion rates each consist of two budget categories (Eq. (3)

and (4) respectively). Summation of the main hard substrate carbonate budget categories

enables classification of the major carbonate reef geomorphic production states on a

continuum defined by three end-member states; primary net production, secondary net

production, and net erosion (Perry et al., 2008b).

Benthic coverage and rugosity

Major spatial variables for this study include: (1) percent cover of each jth calcifying coral specie; (2) percent coverage of each jth component of exposed consolidated substrate (ECS); and (3) habitat spatial complexity (estimated by standard chain-link reef rugosity techniques, Risk, 1972; Luckhurst and Luckhurst, 1978; Hubbard et al., 1990). ECS includes dead coral, rubble, boulders, pavement, bedrock, and surfaces covered by macroalgae. These variables were obtained from reef surveys conducted in 2012 (except benthic data at Hillock basin, measured in 2007) by the United States Virgin Islands Territorial Coral Reef Monitoring Program (TCRMP) (Smith et al., 2011b). Survey methodology and results are provided in Table 1.1. Benthic and substrate coverage data were based on analysis of 3-64 independent video transects (Fig. 5.1d). Data from these transects, in terms of mean benthic or substrate percentage cover ($\overline{PC_j}$), were multiplied (Eq. (5)) by average reef rugosity ($\bar{R}$) to calculate what we defined as the mean "spatial cover index" ($\overline{Si_j}$). This value is considered a proxy for reef three-dimensional surface area (Perry et al., 2012).

Primary coral carbonate production

By design, the derived carbonate budget model for this study considered primary production to result from all scleractinian corals found at a particular site and not just coral exclusively defined as framework building, like methods used by some other carbonate budget studies. Species specific mean extension rates ($\overline{LE_j}$) and mean coral bulk densities ($\overline{BD_j}$) were first input into a modified version of the *ReefBudget* "benthic data entry" spreadsheet. Site specific *Orbicella* spp. values (Fig. 4.4 and 4.7) were used when appropriate, while $\overline{LE_j}$ and $\overline{BD_j}$ values were selected from which ever Caribbean

survey of the same (j^{th}) coral type, obtained from *ReefBudget* compiled data, was

conducted at the most equivalent water depth. The species mean calcification rate ($\Delta\bar{C}_j$),

defined as the product of $\overline{LE}_j$ and $\overline{BD}_j$ (Eq. (6)), was multiplied (Eq. (7)) by $\overline{PC}_j$ to obtain

the species mean planar production rate ($\Delta\bar{p}_j$). The sum of $\Delta\bar{p}_j$ for all j^{th} species provided

the overall site sum rate of mean planar production ($\sum\Delta\bar{p}_j$). Finally, the site $\Delta\overline{PP}_{coral}$

(equal to $\Delta\overline{PP}_T$) was calculated as the product of $\sum\Delta\bar{p}_j$, and the site average rugosity (Eq.

(8)). This same process was also carried out individually for the platy coral *Orbicella*

spp. type using $\overline{LE}_{OACX}$, $\overline{BD}_{OACX}$, and $\overline{Si}_{OACX}$, to calculate $\Delta\overline{PP}_{OACX}$ to make it readily

available (Fig. 5.1i).

Living framework secondary accretion and macroboring

       As noted previously, the platy *Orbicella* spp. is the dominant framework building

coral found in the mesophotic reefs of the Red Hind Marine Conservation District

(RHMCD) and the Grammanik Bank (Smith et al., 2010). Carbonate budget aspects of

living mesophotic coral bio-modification were only calculated for *Orbicella* spp. at three

sites (Primary Bank, Secondary Bank, and Hillock Basin). Methods for this are

continued from the previously calculated $\Delta\overline{PP}_{OACX}$. Average rates obtained by point

count analysis (Fig. 4.10) were used to determine the average percent framework

secondary accretion surface area coverage ($\overline{SAC}_{2nd}$) and the average percent framework

macroboring surface area coverage ($\overline{SAC}_{mac}$) for the three sites (Fig. 5.1j). Similar to

Browne et al. (2013), secondary production (accreting) was defined as carbonate secreted

by non-scleractinian organisms such as CCA, bivalves, gastropods, worms (polychaetes

and sipunculids), foraminifera, bryozoan, and other less common organisms. These

values ($\overline{SAC}_{2nd}$ and $\overline{SAC}_{mac}$) were then multiplied by $\Delta\overline{PP}_{OACX}$ to obtain the secondary

carbonate production rate on living framework ($\overline{SP}_{frame}$) and the macroboring rate of living framework ($\Delta\overline{Bm}_{frame}$), (Eq. (9) and (10), respectively).

Exposed consolidated substrate secondary accretion and bioerosion

The final two major carbonate budget categories, calculated simultaneously, rely on experimental substrate results (see chapter 3 and Weinstein et al., 2014). Though collected after approximately 1, 2, and 3 years of exposure (with an additional set currently still exposed at the sites), the experimental substrates collected after 3 years were deemed to record data most representative of bioerosion rates from any given random moment in time. The first step was to use the year 3 collection site average carbonate mass gained by secondary accretion ($\overline{AM}_{xs}$) and the site average carbonate mass removed by bioerosional processes ($\overline{BM}_{xs}$) from chapter 3 (Fig. 5.1m, n). As previously noted, $\overline{BM}_{xs}$ was obtained by averaging the quadrat mean experimental substrate carbonate mass loss (initial substrate dry weight minus final dry weight, less contributions from secondary accretion). This value includes removal by macroboring, microboring, and grazing processes. A similar procedure was used to calculate $\overline{AM}_{xs}$. These mass averages were divided (Eq. (11) and (12)) by the site average experimental substrate initial surface area ($\overline{SA}_i$) and the sample specific total exposure duration (t_t), measured in days but converted to years (Fig. 5.1o), to acquire the mean normalized total experimental substrate bulk area secondary production (accretion) rate ($\Delta\bar{a}_T N_{xs}$) and the mean normalized total experimental substrate bulk area bioerosion rate ($\Delta\bar{b}_T N_{xs}$). Finally, these normalized rates were multiplied (Eq. (13) and (14)) by the site exposed consolidated substrate (ECS) spatial coverage index ($\overline{Si}_{ecs}$) to obtain the site mean total

exposed substrate secondary production rate ($\Delta\overline{SP}_{ecs}$) and the site mean total ECS

bioerosion rate ($\Delta\overline{Bt}_{ecs}$). Important and subtly acknowledged is the fact that

$\Delta\overline{Bmac}_{frame}$ only applies to macroboring organisms but $\Delta\overline{Bt}_{ecs}$ applies to all types of

bioerosion (grazing, macroboring, and microboring).

Complete total carbonate budget

      More precise calculations were carried out for the Primary Bank, Hillock Basin,

and the Deep Patch sites because hydrodynamic data was available, and this enabled

more accurate estimates of grazer eroded potential reincorporation. A complete

estimated carbonate budget was also calculated at the Secondary Bank by assuming that

the site experiences hydrodynamic conditions similar to the neighboring Primary Bank

site. Similar assumptions from Perry et al. (2013) were also used for estimating the

complete carbonate budgets of the two shallowest reefs. Modification of the hard

substrate carbonate budget to estimate a complete habitat-specific reef budget used the

additional equations found in Table 5.2. These equations required average rates such as:

exportation of bioeroded exposed consolidated substrate ($\Delta\overline{EB}_{ecs}$); non-coral sediment

production by calcifying organisms ($\Delta\bar{P}_{sed}$); sediment dissolution ($\Delta\bar{S}_{dis}$); and gross hard

carbonate production ($\Delta\overline{GP}_T$), which still equals the sum of primary and secondary

carbonate production rates (Eq. (15)). The export rate of hard substrate bioeroded

material ($\Delta\overline{EB}_{ecs}$) equaled (Eq. (16)) the total hard substrate bioerosion rate ($\Delta\overline{BH}_T$)

minus the total hard substrate bioeroded material retention rate at the site ($\Delta\overline{RB}_T$). The

final calculated value (Eq. (17)) for this section was the estimated complete budget net

carbonate production rate ($\Delta\overline{NP}_C$).

Additional sedimentation input was not included in the model. This decision was made based on the significantly low sedimentation rates documented near the Deep Patch mesophotic site (0.315 mg/cm2/day, Smith et al., 2008) and a low predicted probability that sediment collected in these sediment traps derived from carbonate produced at other locations (see chapter 2). Therefore, most sediment within the traps just constitutes sediment locally produced, and hence do not add additional material to the carbonate budget. Although the same approach was taken for the shallower reef control sites (M5 and S6), these assumptions are less probable and could not be confirmed without hydrodynamic data from these sites.

I. *Macro/microbored retention*

Even when implementing specific experiments designed to directly calculate $\Delta\overline{RB}_T$, the accuracy of the measurements are still arguably limited. Because these types of experiments were beyond the original dissertation parameters, $\Delta\overline{RB}_T$ values per site were estimated using methods similar to Eakin (1996). To estimate the specific mean total rate of bioeroded exposed consolidated substrate ($\Delta\overline{Bk}_{ecs}$) directly attributable to each major (kth) bioerosional process (Eq. (18)), the site mean ($\Delta\overline{Bt}_{ecs}$) was multiplied by the grazing, macroboring, and microboring bioerosion proportion (Pg_{xs}, $Pmac_{xs}$, and $Pmic_{xs}$, respectively). Phototrophic and organotrophic microorganisms are thought to penetrate substrate by dissolving skeletal carbonate (Tribollet and Golubic, 2011). Therefore, the entire portion of total hard substrate bioerosion rates attributed to microboring was not included as part of sediment retention (thus all this material is considered to be removed for this carbonate budget model). Although macroboring produced sediment of exposed consolidated substrate were primarily composed of very

fine and smaller grains, $\Delta\overline{Bmac}_{ecs}$ was estimated to be complete retained at all sites. This assumption was made as a result of the highly cryptic nature of these organisms and because 98% of substrate bored by clionid sponges (often the dominate macroboring type of mature bioeroding communities, as noted in chapter 3) is believed to transform into sponge chips (Hutchings, 1986), with only the remaining amount potentially removed from partial dissolution caused by sponge carbonic anhydrase regulation of secreted acid (Pomponi, 1979). Some confirmation of this assumption came when experimental substrates were washed before dry weight measurements and sediment was continually removed through multiple washing treatments. Alternatively, as discussed in chapter 2, hydrodynamic conditions at the mesophotic sites were almost never low enough to permit sediment produced from live framework bioerosion (primarily on the lower "bottom" side of platy mesophotic coral colonies) to deposit, so $\Delta\overline{Bmac}_{frame}$ was never added to the retention rate of hard substrate bioeroded material.

II. *Grazed sediment retention*

Although areas with intense bioerosional grazing are known to produce coarser sediments (medium to fine grain) than areas with less grazing activity (Gygi, 1975; Scoffin et al., 1980; Sammarco et al., 1987; Chazottes et al., 2004), these areas still produce sediment of all size classes. For the purposes of this carbonate budget model, half of parrotfish grazing-produced sedimentation is assumed to consists of very fine grained sand and larger (diameter $\geq$ 125 μm) that immediately falls out of the organism's mouth or fall as various size chunks of carbonate broken by parrotfish activity. Multiplying this sediment fraction (Eq. (19)) by 100 minus the percent of potential deposition time (under annual mean current velocities) of very fine sand grains and larger

$(PD_{\geq 125}$; found in Table 2.3), provides an estimated retention rate for this particular size fraction $(\Delta Rg_{\geq 125})$. These calculations inevitably assume that although this process may still immediately entrain smaller grain sizes, the amount would be relatively insignificant and can be ignored for this model.

The other half of sediment produced by parrotfish, that which is smaller than very fine grained sand, is assumed to be reintroduced through defecation in the water column. Eakin (1996) estimated parrotfish spend 50% of time within the reef. Therefore, multiplying the defecated fraction by half the value of $PD_{\geq 125}$ (Eq. (20)) provides the retention rate of defecated parrotfish eroded, exposed consolidated substrate $(\Delta Rg_{<125})$. After completing these procedures, all aspects of sediment retention are summed together to calculate the total bioeroded retention rate (Eq. (21)). Lacking similar hydrodynamic data at the shallowest two sites, it was assumed that 50% of all carbonate removed from the hard substrates by grazing was retained within the complete carbonate budget (Perry et al., 2013).

III. *Non-coral sediment production and sediment dissolution*

To calculate total rates of non-coral direct sediment production $(\Delta\overline{Pt}_{\text{sed}})$, the mean percentage of each jth sediment type $(\%sed_j)$ found in collected surface sediment (Fig. 2.2a) was multiplied by the "best estimate" calcification rate of the organism $(\Delta C_j$; converted into units of kg m^{-2} y^{-1}). Individual organism calcification rates were based on compiled values presented by Hart and Kench (2007), which were obtained through a detailed literature search. The calculation was repeated for coralline algae, *Halimeda*, foraminifera, and mollusks, the dominant non-coral sediment producers from the region (Fig. 2.2a). Incorporating this step into the overall budget model is conceptually depicted

in Figure 5.1s. Finally, the products of each of the mentioned sediment types were summed together and multiplied by the average percent cover of sediment at the site (Eq. (22), obtained from benthic survey results, Table. 1.1). The sediment percent cover was not scaled by rugosity because these areas were almost entirely flat, and would have a rugosity approximately equal to one. Although the majority of surface sediments were dead and not actually calcifying, results from chapter 2 indicate that the sediment composition can generally serve as an approximate indicator of the relative abundance of those organism types on the reef. Because these smaller-scale calcifying organisms are not really included when conducting video transects, this method seemed to provide a good approximation to the amount of carbonate these calcifying organisms may be contributing.

The rate of sediment dissolution ($\Delta \bar{S}_{dis}$) was calculated as the product of mean site sediment coverage obtained from benthic surveys (Table. 1.1) and 0.21 kg m^{-2} y^{-1} (Eq. (23)), an average of multiple in situ experimentally derived net dissolution/calcification rates of carbonate sediment substrate (see compiled list by Eyre et al., 2014; Yates and Halley, 2003). Again, the percent cover of sediment was not scaled by rugosity for the same reasons for calculating $\Delta \overline{Pt}_{\text{sed}}$. After converting estimated mesophotic sedimentation rates to units of kg m^{-2} y^{-1}, components are available to calculate the estimated complete budget net carbonate production rate ($\Delta \overline{NP}_C$).

Reef accretion

After estimating complete carbonate budgets at different mesophotic habitats and shallow counterparts, results were analyzed in terms of long-term reef accretion. The estimated complete net carbonate production rate ($\Delta \overline{NP}_C$) at each site, as well as assumed

values for reef density (ρ_{reef}) and porosity (ϕ_{reef}), were inputted into a previously

established theoretical relationship (Kinsey, 1985; Hubbard et al., 1990; Browne et al.,

2013) to calculate estimated rates of reef accretion:

$$RA_{site} = \frac{\overline{\Delta NP}_{\text{CaCO}_3} \times \rho_{\text{CaCO}_3}}{(100 - \phi_{\text{reef}})} \times 100,$$

in units of mm/yr.

Results

 Multiple repeated experiments and observations used to calculate the results

discussed earlier in this dissertation facilitate correct statistical analysis. However, the

samples used to calculate these previous variables were not exclusively related to

individual benthic/structural surveys. Although the site average of calculated variables

and site average rugosity could have been applied to the results of each individually

conducted transect, this would artificially create a larger number of samples that standard

statistical analysis would incorrectly assume to be independent. Therefore, carbonate

budget categories and production states were calculated from the site averages of the

independently calculated variables, scaled by the site average spatial cover index, which

provided one representative value per site and significantly reduced the degrees of

freedom. As a result, standard statistical analysis was not conducted. However,

comparison of site results is still considered to provide meaningful information because

all datasets were generated from multiple samples and surveys. Calculated intermediate

and final values for all site specific hard substrate major carbonate budget categories are

displayed in Table 5.3 and corrective values and results for site specific estimated

complete carbonate budgets are displayed in Table 5.4.

Net carbonate production rates

Comparison between all individual site carbonate budget results (Fig. 5.2) indicated variability between carbonate cycling processes. Estimated complete net carbonate production rates were always greater than hard substrate budget net production rate from the same site, but with different ranges. Despite similarities in hard substrate carbonate production states, results indicated that sites with less gross production also had less bioerosion, and sites with greater gross production had more hard substrate bioerosion removal, especially for mesophotic sites (Fig. 5.3). Hard substrate carbonate budget states were predominately static, though they all trended towards net production, except at the shallow Fringing Patch, where the only significant net erosional carbonate budget state was identified in the study. Carbonate budget net production rates were always greatest at the Mid-shelf Patch ($\Delta\overline{NP}_{HS}$: 1.197 kg m^{-2} yr^{-1} ± 0.220, $\Delta\overline{NP}_C$: 1.623 kg m^{-2} yr^{-1} ± 0.241), implying that all mesophotic site net production rates were contained between the study range set by the two shallowest sites.

Of the four mesophotic sites analyzed in this study, the greatest hard substrate net carbonate production rate, $\Delta\overline{NP}_{HS}$, was recorded at the Secondary Bank (0.339 kg m^{-2} yr^{-1} ± 0.183 SE). The greatest estimated complete budget net carbonate production rate, however, was recorded at the Primary Bank (1.050 kg m^{-2} yr^{-1} ± 0.597 SE), and was well within the boundaries of a primary net accretion classification. The corrections for estimated complete carbonate budgets resulted in three of the six sites being classified as net primary carbonate production states (the Hillock Basin site could also be classified in a net primary/secondary carbonate production state). The Deep Patch site was the only one where gross production rates were dominated by secondary accretion processes, but

was still classified in a static state due to overall low net production rates. Despite this low rate, the overall 2012 mean mesophotic reef estimated complete carbonate budget net production rate indicated that, on average, the examined deep reefs were definitively net constructional ($\overline{\Delta NP_{C_{site}}}$ = 0.672 kg m^{-2} yr^{-1} ± 0.165 SE).

No direct correlations were determined when comparing hard substrate net carbonate production rates to such individual habitat parameters as depth, coral cover, and rugosity (Fig. 5.4a), or when compared with specific measurements of bioerosional processes (Fig. 5.5a). However, a potential relationship did exist when only considering mesophotic sites. Closer analysis of each individual carbonate budget category is needed to better understand the cause and implications of net carbonate production variability between sites.

Gross carbonate production (constructive budget components)

Primary coral carbonate production ranged from a maximum of 2.022 kg m^{-2} yr^{-1} ± 0.211 SE at the Mid-shelf Patch (with the Secondary Bank having the greatest mesophotic rate of 1.117 kg m^{-2} yr^{-1} ± 0.154 SE) to just 0.144 kg m^{-2} yr^{-1} ± 0.095 SE at the Deep Patch (Fig. 5.3), a range of 1.878 kg m^{-2} yr^{-1}. Secondary carbonate producer accretion rates had a shorter range than primary production (0.224 kg m^{-2} yr^{-1}), with a maximum of 0.423 kg m^{-2} yr^{-1} ± 0.106 SE at the Primary Bank to a minimum of 0.199 kg m^{-2} yr^{-1} ± 0.009 SE at the Mid-shelf Patch. For the three sites where recently dead mesophotic *Orbicella* spp. skeleton was examined, living framework secondary accretion ($\Delta \overline{SP}_{frame}$) was greatest at the Secondary Bank (0.255 kg m^{-2} yr^{-1} ± 0.031 SE), however this category never constituted more than 5.5% of the mean gross carbonate production. Although coral accounted for a larger percent of the site gross carbonate production rates

than secondary accretion at all sites except at the Deep Patch, the two processes were almost equal at the Hillock Basin and the shallow Fringing Patch. Regardless, the trend from least to greatest gross carbonate production rates followed that of the primary carbonate production. Live coral cover appeared to have some correlation with gross carbonate production, but not with depth or rugosity (Fig. 5.4b). Gross product also showed high potential correlation with bioeroding parrotfish biomass.

Total bioerosion (destructive HS budget components)

Of the three main end-member carbonate budget production states (primary net production, secondary net production, and net carbonate elimination), hard substrate bioerosion rate ranges were found to be intermediary (1.528 kg m^{-2} yr^{-1}) but closer to primary production ranges than those of secondary accretion. Carbonate rates of removal from the hard substrate carbonate budget were greatest at the Primary Bank (1.717 kg m^{-2} yr^{-1} ± 0.394 SE) and lowest at the Deep Patch (0.189 kg m^{-2} yr^{-1} ± 0.019 SE). Grazing (Pg_{xs}) primarily through parrotfish bioerosion, was found to be significantly greater than any other bioerosion process at all sites (Fig. 5.3). More than 90% of total bioerosion rates were attributable to grazing processes at the three sites with the highest gross carbonate production rates (Mid-shelf Patch, Primary Bank, and Secondary Bank). Though still dominant, grazing was found to contribute slightly less to overall bioerosion rates at the shallow Fringing Patch and the Hillock Basin sites, and significantly less at the Deep Patch site (57.66 % of total bioerosion rate). Total bioerosion rates described the line of best fit with depth better than $\Delta\overline{NP}_C$ or gross carbonate production rates (Fig. 5.4c). There was also possible correlation between total bioerosion rates and bioeroding parrotfish biomass (Fig. 5.5c), although the potential relationship coefficient of

determination (R^2) was less than between gross carbonate production rates and parrotfish biomass (Fig. 5.5b).

Long-term reef accretion estimates

To put hard substrate carbonate budget results into a longer-term geological context and compare it with other studies, potential reef accretion rates (RA_{site}) were estimated at the different habitats as functions of the complete estimated site net carbonate production rate ($\Delta\overline{NP_C}$). Following similar logic from other studies (Browne et al., 2013), reef density was assumed to be that of carbonate ($\rho_{CaCO_3} = 2.9$ g cm^{-3}) and consolidated subsurface reef porosity was estimated at 50%. The greatest accretion rate was found at the Mid-shelf Patch (1.115 mm/yr $\pm$ 0.166 SE). Calculations of estimated accretion rates are provided in Table 5.5. Assuming past conditions were similar to those recorded in this study, the negative $\Delta\overline{NP_C}$ at the Fringing Patch prevents calculating an accretion rate for this shallower depth carbonate producing system. The slowest accretion rate was measured at the Deep Patch site (0.221 mm/yr $\pm$ 0.070 SE), the site with the lowest rugosity and coral cover. When considering the mesophotic sites, estimated reef accretion at current conditions was highest at the Primary Bank (0.715 mm/yr $\pm$ 0.412 SE), and the average of the four studied mesophotic sites was 0.463 mm/yr $\pm$ 0.114 SE. If assumed that conditions remain constant with no additional rate adjustments, it would take approximately between 53-186 ka for the examined mesophotic deposits to accrete to present sea-level.

Discussion

Results from this study are intended to apply a new geological perspective toward answering various unknown critical mesophotic reef habitat questions, often with

implications to larger-scale reef management, such as: (1) what are the expected baselines of mesophotic reef geomorphic carbonate potential and their specific relationships to ecosystem health; (2) have there been a significant negative impact of expected baseline mesophotic reef conditions to recent changes in global ocean conditions, and if not, how vulnerable is mesophotic reef structural sustainability; and (3) what contributions have mesophotic reefs made to overall carbonate shelf development? A large problem with answering these questions stems from the fact that, unlike the better understanding we have for shallow coral reefs (Dustan and Halas, 1987; Goreau, 1992; Jackson, 1997; Greenstein et al., 1998; Knowlton and Jackson, 2008), pre-industrial baseline conditions for mesophotic reefs are unknown. Additionally, with a relative lack of modern and ancient mesophotic geological data (see chapter 1), and a need both to improve the accuracy of carbonate budget models and especially to understand specific carbonate budget production state residence times and related interactions (Perry et al., 2008a), results from this dissertation can only begin to answer the proposed questions with relative speculation.

Despite these difficulties, these questions were explored by examining the plausibility of two proposed MCE scenarios. Specifically, that recently conducted carbonate budget analysis results of different northern USVI mesophotic reef habitats most likely represent: (1) pre-industrial baseline carbonate production rates for low-angle shelf mesophotic reef systems, implying relative protection from conditions currently degrading shallow-water reefs; or (2) net carbonate production mesophotic rates have been reduced compared to what would be expected of pre-industrial conditions, by some degree of the same stressors previously mentioned. A corollary to the correctness

of the first scenario is if mesophotic reef baseline conditions represent what shallow-water reef baselines might have been like, or if mesophotic reef carbonate production state trends are governed by different properties than their shallow counterparts and result in different trends. While the actual scenario currently being played out probably resides somewhere between these two-end members, questioning the probability of these two different scenarios is vital for future mesophotic coral reef research and management.

Local implications from carbonate budget analysis

With results indicating that the mesophotic hard substrate carbonate budgets of all habitats analyzed are presently in precarious stasis equilibriums (mesophotic circles depicted in Figure 5.2), the geomorphic state of examined mesophotic habitats with seemingly distinctive structural attributes appears relatively homogeneous. To some degree, this implies framework/rubble structural complexity is barely maintained, yet production rates are large enough so that none of these deep reefs are net erosional. Detailed analysis of carbonate cycling processes shows that these similar potential geomorphic states result from significantly different mechanistic budget "pathways," with large site differences between constituent carbonate budget components (Fig. 5.3). Regardless, calculated gross carbonate production rates were all greater than those predicted for Atlantic reefs 30-40 m below sea-level (0.1 kg m^{-2} yr^{-1}, Vecsei, 2001).

The story is quite different when considering the potential retention of eroded sediment within the habitat complex. Revised "complete" carbonate budget estimates show that both the Primary and Secondary Banks unambiguously have primary net positive carbonate production states (diamonds in Fig. 5.2). The higher accretion rate at these shelf-edge mesophotic reef deposits could partially result from active shelf break

currents and terrestrial separation assumed to support high coral cover at Cayman Island shelf-edge reefs (Roberts et al., 1977).

These results also agree with conclusions from similarly conducted shallow-water coral reef carbonate budget studies which indicated that Caribbean reefs usually revert to negative carbonate production states when live coral cover drops below 10% (Perry et al., 2013). Four of the six sites analyzed for this dissertation had greater than 10% coral cover as well as arguably related positive net carbonate production (Fig. 5.6a). The Hillock Basin could possibly be excluded from this finding, given that its current geomorphic state edges the arbitrarily set border between net positive and static equilibrium. The increase in net carbonate production rates from the hard substrate carbonate budgets to the revised "complete" carbonate budgets were primarily attributed to significant rates of bioeroded sediment retention, where the greatest mesophotic reef value was estimated at the Primary Bank site (0.943 kg m^{-2} yr^{-1} $\pm$ 0.426 SE). Comparatively, results from the Hillock Basin, the site with the highest non-coral direct sediment production rate ($\overline{Pt}_{\text{sed}}$) and sediment dissolution rate ($\Delta \bar{S}_{dis}$), indicates that $\overline{Pt}_{\text{sed}}$ and $\Delta \bar{S}_{dis}$ parameters were relatively insignificant to the overall complete carbonate budget calculation ($\overline{Pt}_{\text{sed}}$: 0.023 kg m^{-2} yr^{-1} $\pm$ 0.009 SE, $\Delta \bar{S}_{dis}$: 0.021 kg m^{-2} yr^{-1} $\pm$ 0.007 SE).

The discovery of significant estimated complete carbonate budget heterogeneity implies a potential relationship between this measured attribute and with the high habitat and structural heterogeneity documented in the northern USVI mesophotic reef system (Smith et al., 2010). These results also have important implications for the mesophotic coral reef refugia hypotheses (Glynn, 1996; Riegl and Piller, 2003; Bongaerts et al.,

2010), especially because, like the Fringing Patch site analyzed in this study, a significant decline in shallow Caribbean reef coral cover and resilience has been documented and is predicted to continue (Hughes, 1994; Gardner et al., 2003; Wilkinson and Souter, 2008; Alvarez-Filip et al., 2011c; Perry et al., 2013; Bozec et al., 2014). Carbonate budget analysis from this current study suggests that, unlike the "flattening" trend of shallow Caribbean coral reefs (Alvarez-Filip et al., 2009), MCEs will continue to at least maintain, if not add to, the architectural complexity and habitat heterogeneity vital for the high mesophotic biodiversity suggested as a vital attribute of these deeper reef systems (Reed and Pomponi, 1997; Lesser et al., 2009; Puglise et al., 2009; Bridge et al., 2012b).

Results from this study also indicate that secondary production can help supplement low primary production rates to maintain net positive production states when relatively low grazing intensity allows sessile epilithic colonization to proceed unperturbed. Higher secondary accretion and potentially related lower relative grazing bioerosion were clearly observed at the Deep Patch site (the only mesophotic site that net erosional budgets were informally predicted) and to a lesser extent at the Hillock Basin and shallow Fringing Patch sites (Fig. 5.4). These organisms are thought to strengthen the reef structure (Gherardi and Bosence, 2005; Perry et al., 2008b), promote cementation (Scoffin, 1992), and retain, bind, and stabilize loose framework components (Rasser and Riegl, 2002), ultimately improving potential framework preservation. However, secondary carbonate production-dominated net accretion geomorphic states appear considerably less common in classical "coral" reef habitats (Fig. 5.7), and were close to, but not exclusively documented within, USVI mesophotic sites.

Mesophotic reef temporal variability

Potential mesophotic temporal carbonate production state transitions were investigated by applying site-specific rate calculates, based on measurements and observations spanning the duration of this dissertation, to available transect benthic survey data conducted in 2003 (from the Primary and Secondary Bank and Mid-shelf Patch sites). Following this proposed methodology inevitably introduces additional assumptions and related variability, such as assuming coral cover has changed between the 10 year span of the benthic surveys, but rugosity and site normalized rates of carbonate cycling remain constant. However, this approach was seen as the only way to examine potential temporal trends, especially considering that almost no comparable mesophotic coral reef datasets from sedimentary analyses have been generated. The additional assumptions are also implicitly accepted by many published carbonate budget studies, which apply relationships (such as parrotfish biomass and length measurements to predict grazing rates indirectly) and calcification rates that were often generated from locations and time periods different than those for which the carbonate budget was being calculated for (Perry et al., 2012). Finally, results obtained from 2003 benthic surveys are almost definitely underestimates, considering that rugosity tends to increase with increasing coral cover and that environmental conditions in 2003 were more likely to be the same or more conducive for calcification that the rates obtained in 2012.

Analysis of all comparable available data indicates that Primary and Secondary Bank mesophotic reef habitats have experienced significant declines in net carbonate production rates since 2003 (Fig. 5.7). The calculated temporal decline results from a moderate reduction of live coral cover at both sites (reduced by ~29%) and a somewhat

related increase in available, exposed consolidated substrate accessible to bioeroders. Although coral cover at the Primary and Secondary Banks had similar averages each year, the higher 2003 net carbonate rate at the Secondary Bank compared to the Primary Bank showed a greater temporal decline than the Primary Bank. This outcome primarily resulted from the larger relative increase in exposed consolidated substrate at the Primary Bank (26.70% increase) compared with changes at the Secondary Bank (7.79% increase), prompting higher rates of grazing, especially as parrotfish biomass is greater at the Secondary Bank (Fig. 3.7).

One possible interpretation, taking the proposed mesophotic reef carbonate budget scenarios into mind, is that the temporal decline in observed net carbonate production rates is merely a result of small fluctuations in the long-term, naturally variable, carbonate cycling processes. Detecting a temporal decline merely could result from coincidence and random selection of the only two years used for comparative temporal analysis (maybe rates were lower in 2006 for example, but we did not examine data from that year). However, if this were the case, it would be especially coincidental that the temporal comparison done for the three sites (Primary and Secondary Bank and Mid-shelf Patch) all showed significant, yet similar rate declines.

A more reasonable interpretation can be made when evaluating documented ecological disturbances between the nine-year time intervals. The northern Antilles were heavily impacted by a severe seawater warming event in 2005 (Donner et al., 2007; Manzello et al., 2007), resulting in high coral cover reduction of shallow-water USVI coral reefs (Miller et al., 2006; Whelan et al., 2007). This event coincided with a large increase of mesophotic reef "old partial mortality" and likely caused increased mortality

(and related coral cover reduction) throughout the USVI MCEs (Smith et al., 2010).

Intermediately, high levels (nearly 100%) of coral bleaching at the Mid-shelf Patch site

were also recorded, as well as high bleaching levels that occurred there in 2010 and 2011

(Smith et al., 2011b). Also, an extreme disease event, referred to as the intercostal

mortality syndrome (IMS), was documented in 2007 and found to preferentially impact

mesophotic reefs in the RHMCD basin habitats, inducing higher coral mortality (Smith et

al., 2010). Despite the availability of Hillock Basin and Deep Patch site benthic coverage

data before the IMS event, it is highly probable that this stressor may be reflected in the

relatively low net carbonate production rates measured in 2008 at the Hillock Basin site

and in 2012 at the Deep Patch site.

These types of shorter-term ecological stress events do not necessarily influence

the geomorphic performance of a reef in terms of the ecological services they provide.

This is because these processes often act on different timescales and different reefs show

significant variability in terms of their resistance to substrate degradation (Perry et al.,

2008b). This contradiction is known to occur on different reefs (Mallela and Perry, 2007;

Banks et al., 2008), although other studies have also demonstrated rapid, somewhat

simultaneous parallel ecological disturbances and decreasing structural complexity

(Eakin, 1996; Reaka-Kudla et al., 1996; Edinger et al., 2000; Lewis, 2002). Therefore,

these mesophotic reef stressors, possibly related to worsening regional sea water

conditions, could still be reflected in the temporal reduction of net carbonate production

rates (Perry et al., 2008b). The bigger question then returns to whether these local

disturbances are relatively minor in geomorphic timescales (longer than the 10 years

compared).

Results from this study has shown that, at least when analyzed with census-based techniques, moderate changes in coral cover and related cover of available exposed hard substrate can significantly alter net carbonate production rates (if all other factors are presumed to be the same). Although it appears clear that the mesophotic coral reefs have not fully regained lost coral cover, it is unknown if they are in a recovery process or still greatly affected by previous and/or new environmental stressors. Subsequently, it cannot be gaged if the geomorphic production states determined in this dissertation reflect that of a recovering or fully recovered MCE or demonstrate alarming parallels with the suggested decline in carbonate production of neighboring shallower coral reef habitats of the Caribbean (Perry et al., 2013). The answer to this question and further evaluation of the two proposed scenarios requires a closer comparison of carbonate budget methodology to understand how well conclusions from other studies can be applied to these deep reef systems for interpretation.

Comparisons to other carbonate budget studies

Despite the large spectrum of assumptions required for the developed carbonate budget model, interpretations derived from direct comparisons between study sites, such as those discussed above, are deemed fairly accurate. This is because all study sites were subjected uniformly to the same assumptions, uncertainties, and potential errors, as well as similar temporal durations and environmental conditions, a phenomenon similar to interpretations derived from experimental coral substrates in chapter 3. When making larger-scale ecological and geological interpretations, based on comparisons between this study and others, caution must be used primarily because results from other studies were obtained using a variety of methods and assumptions on different spatial scales. This

point is particularly relevant when claiming results from the northern USVI plot within the intermediate array of recorded values obtained from most other carbonate budget studies (Fig. 5.7). Similarly, caution must be used when interpreting that the general results from this study –that coral reef geomorphologic potential, generally range between static and primary net production states, are consistent with results from most other studies.

Regardless, northern USVI carbonate budget results still plot among the overall range of other studies limited to recent (within the last five years of this dissertation) shallow Caribbean reef census-based carbonate budgets conducted on 101 transects using comparable methodology (Perry et al., 2013), the methodology that USVI analysis was largely based on. Although 63.2% of the shallow Caribbean reef averages were definitively in net productional carbonate budget states (>0.5 kg m^{-2} yr^{-1}), only nine transect censuses (8.91%) recorded net carbonate production rates greater than 5 kg m^{-2} yr^{-1} (Perry et al., 2013). These observations were consistent, regardless of depth and habitat type (Fig. 5.8), and were used with statistical modeling to suggest that live coral spatial extent (most commonly approximated by transect percent coverage) significantly influences the geomorphic carbonate production state of shallow Caribbean coral reefs (Perry et al., 2013).

Although a clear signal was found, the apparent trend may result from the methodology used. Almost every assumed or calculated production (or erosion) rate for carbonate budget analysis, using methods equivalent to *ReefBudget,* are results scaled by coral cover and rugosity surveys, such that strong "correlations" are almost inevitable. On the other hand, the methodology was implemented precisely because all processes are

greatly dependent on their actual spatial distribution, implying that theoretical

relationships between production rates and coral cover are fairly accurate.

More than half of the reefs examined for this dissertation generally fit within the

relationship Perry et al., (2013) determined between coral cover and net carbonate

production (Fig. 5.6a). The main exception to the trend stems from an

"underperforming" status of the mesophotic bank sites to the model. This implies that

despite some similarities, the net carbonate production of a mesophotic reef may be more

reliant on slightly different factors than those of shallower coral reefs, such that the

carbonate budgets of these systems have a separate set of governing principles. Though a

similar, but exclusively mesophotic relationship may exist compared to what has been

proposed for shallow Caribbean reefs (Perry et al., 2013), no other carbonate budget data

is presently available to include with data from this study that could be used to verify this

possibility using statistically significant linear mixed effect models (Fig. 5.6b).

Another possible explanation for the discrepancy pattern of the Primary and

Secondary Bank net carbonate production rates compared with predicted shallow

Caribbean reef budget effects could be that some of the environmental stressors (such as

climate change, ocean acidification, and diseases), presumably responsible for overall

shallow-water coral reef Caribbean gross carbonate production rate decline (Perry et al.,

2014), have larger negative affects on the net carbonate production of mesophotic reefs

than previously thought. With no baseline data, this possibility is feasible regardless of

the relatively high levels of mesophotic coral cover compared to their shallow-water

counterparts (Bak et al., 2005; Smith et al., 2010). As such, our temporal mesophotic

reef carbonate budget analysis showed that this scenario is highly probable, at least for shorter time frames.

The interpreted decline in shallow-water Caribbean coral reef gross carbonate production rates (3.5 kg m^{-2} yr^{-1} average at the transect level, Perry et al., 2013) is especially apparent when compared to coarsely obtained region shallow fore-reef estimates (10-17 kg m^{-2} yr^{-1}), which were based on previous Caribbean reef dominance of branching *Acropora* species prior to the impact of modern day reef stressors (Vecsei, 2001). This comparison is relevant to mesophotic carbonate budget analysis in that the highest gross carbonate production rates calculated by Perry et al., (2013) were recorded on reefs dominated by massive *Orbicella spp.* colonies (Fig. 5.6), the same species (though different morphology) that also dominates mesophotic reefs within the RHMCD and the Grammanik Bank (Table 1 and Smith et al., 2010).

Another important comparison stems from study results that positive production rate magnitudes closely mirror rate magnitudes of carbonate bioerosion (Fig. 5.3). A similar observation was made at 19 different shallow-water reefs contained within the exclusive economic zone of four different Caribbean countries (Perry et al., 2014). Perry et al., (2014) noted that bioerosion rates were 75% less than those previously recorded in the Caribbean prior to modern coral reef degradation, still resulting in low, but positive average net carbonate production rates (mean of all 101 transects was 1.514 kg m^{-2} yr^{-1} ± 0.331 SE). These rates, considered to be indicative of future carbonate budget reef shifts towards negative net carbonate production (Perry et al., 2013), were still greater than the mean calculated for northern USVI mesophotic reef carbonate budget net production rates (0.661 kg m^{-2} yr^{-1} ± 0.165 SE). As observed through temporal mesophotic reef

carbonate budget analysis, a likely explanation for these similar mirroring dual trends in carbonate cycling rates could be the expected relationship between live coral cover and the cover percentage of exposed available substrate (as live coral cover decreases, exposed available substrate tends to increase). Given the amount of data currently available, another way to interpret results of mesophotic carbonate analyses, as well as providing predictions of mesophotic reef contributions to greater carbonate shelf development, is to consider long-term accretion potentials of these deep reefs.

Potential reef accretion and Holocene reef development

A subsequent byproduct of the central long-range goal of this dissertation involves questioning the significance of mesophotic reef deposition on the carbonate properties of the shelf (thickness, variability, rate, etc.) and subsequently any geomorphological contributions in terms of habitat development, maintenance, diversification, and sustainability. However, this significance is highly dependent on the relative spatial and temporal scales in question, such as on the order of: (1) accretion of the entire carbonate shelf; (2) habitat-scale relief of the reefs compared to surrounding non-reef substrate; and (3) smaller scale structural complexity within the reef itself. Therefore, each scale must be addressed to fully determine the greater implications of potential past mesophotic reef accretion and future production.

From the various available Caribbean Holocene sea-level curve projections (see Hubbard, 2009, for a summary of existing models), it was determined that the mesophotic reefs analyzed in this study could have existed at mesophotic reef-like depths for approximately six thousand years. With this assumption and when only considering carbonate budget estimates based on 2012 benthic survey results, the maximum accretion

height expected at any of the mesophotic sites would be at the Primary Bank (Table 5.5, 4.34 m ± 2.47 SE). Thus, from a general shelf-scale perspective, 6 ka was not enough time to produce the observed elevation difference between mesophotic sites (> 5 m). This implies significant topographic relief prior to sea-level reaching mesophotic depths.

Some additional evidence to support this conclusion derives from the work of Holmes and Kindinger (1985). *Acropora palmata* coral fragments from a 1 m core described as taken from the St. John "shelf edge" reef were calculated to be older (7,600 yr, by ^{14}C and ^{230}Th/^{238}U dating) than the 6 ka proposed window needed for significant mesophotic reef accretion (Holmes and Kindinger, 1985). With *A. palmata* known to typically grow in shallow water (4-6 m below sea-level), Holmes and Kindinger (1985) deduced that topographic relief found at the shelf edge was a product of earlier (before 7.6 ka) growth, when sea-level was lower. This would imply there has not been much mesophotic reef buildup in the past 6 ka. The shallow-water branching coral that had likely lived where the modern-day mesophotic deposits now reside are known to produce significant amounts of carbonate (see Perry et al., 2008 for review). As such, it is highly possible that reef growth prior to 7 ka could have produced some or all of the topographic relief that has been used to partially categorize the different mesophotic reef habitats.

Interpreting the development of individual mesophotic habitat relief compared to surrounding substrate is even less clear. When solely making interpretations from mesophotic reef net carbonate production rates based on the 2012 benthic surveys (Table 5.5), results imply that even if the mesophotic reef habitats had been accreting at a relatively constant rate since 6 ka, mesophotic coral still could not have accounted for all of the relief (> 5 km, as defined in chapter 1) used to define the Primary and Secondary

Banks, or for hillock structures at the Hillock Basin site that are presently greater than 2 m in height. These values may lead to the suggestion that the uniquely different habitat structures found within the northern USVI mesophotic reefs are a product of antecedent topographic relief, potentially from earlier shallow-water reef accretion when the sea level was lower, with a small to moderate additional carbonate accretion "topping" by deeper current mesophotic communities making little to possibly moderate additions to overall relief.

On the other hand, the development of the Deep Patch site could have resulted mainly from its slow to moderate accretion rate potential, despite its low relief. This potentially different geological history could account in part for the substantially different benthic coral community (and possibly other species inhabitants, though biodiversity analysis was not a goal of this study) that currently thrives at this particular site. Additionally, when considered on a localized, transect-length spatial scale, visual observations and documentation (Weinstein et al., 2014; Smith et al., 2011b; Smith et al.,2010) clearly indicate that that variability in growth rates, mortality events, and bioerosional patterns significantly contribute to finer structural complexity (see Fig. 1.3c for an example of topographic complexity with various specialized locations for species habitation).

Another result that must also be considered though, especially when developing longer-term predictions from carbonate budget analyses that rely on 2012 benthic coverages, is the fact that this study has shown how, even over a short time period, there are potential temporal differences inducing oscillation of overall rates with time. Net carbonate production rates ($\Delta\overline{NP_C}$) obtained through the application of 2003 benthic

survey results (Table 5.6, top half) implied a greater potential for higher accretion rates then when calculating $\Delta \overline{NP_C}$ based on 2012 benthic surveys. Also, as noted earlier, these values are believed to be an underestimate of net production. Rugosity usually increases with increased coral cover (Alvarez-Filip et al., 2011b), but 2003 net carbonate production was initially calculated by applying 2012 rugosity rates. Therefore, if rugosity in 2003 was estimated based on derived coral cover and rugosity relationships for *Orbicella* spp. dominant reefs (Alvarez-Filip et al., 2011b), estimated accretion values could have had even greater potential rates (Table 5.6, bottom half). Additionally, 2012 rugosity at the Primary Bank was greater than what would have been expected, given the particular coral cover, so Table 5.5 also displays accretion estimates for a corrected Primary Bank rugosity with an additional 15% increase.

These results indicate there was at least some possibility that mesophotic habitats developing along the same shelf could have had considerably different accretion rates. Over the 6 ka time scale, when sea-level was such that coral at the study sites would still be in mesophotic conditions, these corrected calculations indicate that a significant potential was available for the USVI mesophotic reef system to account for a portion or even a large majority of the mesophotic reef architectural heterogeneity that currently distinguishes the studied modern reef system. Additionally, ocean conditions in 2003 were still worse than what has been suggested for prior to modern industrialism and as such, imply that even greater accretion differences were possible, assuming modern mesophotic reef production is impeded, compared to earlier times. Finally, as discussed earlier, although 2003 benthic survey results were not available from the Hillock Basin and Deep Patch sites, net carbonate production rates would probably be greater than what

was recorded for 2012, as coral cover and rugosity values are probably still recovering from the 2007 IMS (Smith et al., 2010).

However, some caution is needed when making interpretations based on these projected rates for longer time periods. Table 5.5 provides reasonable values for mesophotic reef accretion given the scenarios proposed in this discussion, but still only provides what was possible. Just because these reefs may have had the ability to create these structural differences in the timeframe allotted, it does not mean that this situation was what happened. For an example similar to results from other research (Holmes and Kindinger, 1985), mesophotic coral initiation at the study sites examined may have occurred more recently than 6 kya, such that they would not reach the estimated values in Table 5.5 when accreting at constant rates. Even if the coral did begin to grow 6 kya, there is no evidence as of yet to support an assumption that accretion rates were consistent during that entire time period.

As is usually the case, the Holocene history of reef accretion along the southeast Puerto Rican Shelf was probably more complex. Observations of modern mesophotic reef relief and spatial abundance, calculated potential net carbonate production rates, and comparisons with data that may or may not be applicable to the particular location of study lead to the suggestion that reef accretion since the last seafloor exposure probably resulted from a combination of the hypothetical situations presented. It is highly probable that more than 6 ka ago, there was some degree of shallow-water coral reef development on the edge of the Puerto Rican Shelf where the Primary Bank site currently resides. However, because this assumption is based on a general understanding of reef accretion developed for shallow-water reef systems and on the unconfirmed location and

extent of previous data, it is also suggested that this development was likely to be patchy in distribution, and not creating a fully developed reef crest along the entire edge of the bank. Since 6 kya, potential net carbonate accretion rates led to the suggestion that there was also variable, patchy mesophotic coral growth accretion, essentially building on topographic highs and filling in gaps left by the earlier reef system. This would add some degree of habitat-scale relief to reef-dominated sections of the shelf, and continue to form or exaggerate structural complexities important for the development of a highly diverse mesophotic ecosystem.

Conclusions

The complex structure of coral reefs provides vital ecosystem services that are crucial for sustained environmental health (Dryden et al., 2012; Graham and Nash, 2013) and for the sustainability of the current global economy and food supply (Dalzell et al., 1996; Moberg and Folke, 1999; Pandolfi et al., 2005; Brander et al., 2007). The global decline in shallow-water coral reef health (Gardner et al., 2003; Hughes et al., 2003), and the relative implications for the theory of mesophotic refugia and connectivity (Glynn, 1996; Lesser et al., 2009), have led to an increased scientific interest in mesophotic coral reef habitats (Puglise et al., 2009). While recent technological advances in deep sea diving (Pyle, 1998; Lesser et al., 2009; Lombardi and Godfrey, 2011) have permitted increased research of MCE biology and ecology (see Kahng et al., 2014, for a thorough review), there has been a critical gap in the knowledge and understanding of mesophotic reef depositional processes and their effect on the ecology and structural sustainability of the ecosystem. This dissertation thus represents one of the first comprehensive modern sedimentary analyses of mesophotic reef systems.

Based on sedimentary characteristics, unique, carbonate subfacies were identified within mesophotic habitats with distinctive structural characteristics, implying a parallel relationship between facies distribution, structural complexity, and habitat heterogeneity. Relatedly, the sediment composition and bulk geochemistry of low-angle mesophotic reefs were found to broadly record the distribution and abundance of foundational benthic communities. Relative hydrodynamic weakness confirmed a lack of transported allochthonous sediment, including potentially harmful inundation of terrigenous material to low-angle shelf MCEs. Rapid cementation identified at all deep habitats indicated that subfacies and associated interpretations for biological and hydrodynamic functioning could be preserved over time and thus provide a new analogue for studies of ancient mesophotic geological history and overall coral reef evolution.

Analysis of experimental coral substrates and coral rubble provided additional validation of the suggested hypothesis that bioerosion decreases with depth, a phenomena largely related to decreases in parrotfish biomass. Bioeroding sponges were suggested to be the dominant modifiers of mesophotic coral reef substrate. Depending on differences in substrate availability, location, exposure duration, and type, subtle differences in bioerosion patterns are likely to increase the small-scale structural complexity of mesophotic reef habitats. The bioerosion rate magnitudes were also found to closely parallel carbonate production rates in mesophotic reefs regardless of reef geomorphic habitat type.

The growth rates of mesophotic coral from the USVI fit within previously proposed models, indicating that coral growth rates decrease with increasing depth. However, statistically significant differences in calcification rates of mesophotic coral

suggest another potential long-term mechanism for enhancing the heterogeneity of mesophotic reef geomorphology. All mesophotic sites were found to have net positive geomorphic production states, although some sites were probably in precarious equilibrium stasis. Additionally, temporal calculations in carbonate budget analysis suggest that mesophotic reefs have had high net carbonate production in the past and may be affected by degrading environmental conditions known to impact shallower coral reefs.

On a larger spatial and temporal scale, it was shown that USVI mesophotic reef accretion could not have produced the significant topographic variations observed in the different mesophotic reef habitats. Carbonate budget calculations reliant on the most recent benthic coverages also indicate mesophotic coral reef accretion had little impact on current local relief. However, a higher calculated accretion potential for mesophotic reefs prior to modern coverages and uncertainty with previous research lead to the suggestion that that the characteristic, heterogeneous structural relief of USVI mesophotic reef habitats is a combined product of earlier (before 7 ka) patchy distributed shallow-water reef accretion augmented by slow but steady mesophotic reef deposition. Although this study provides some of the first predictions of long-term mesophotic reef carbonate shelf development, based on empirically derived data, further research is needed to better constrain detailed accounts of mesophotic shelf accretion. Collection of site-specific rotary cores, correlated with more accurate seismic data, would greatly assist in deciphering the accretion history of mesophotic reefs. Additionally, although this study provided new data useful for managing mesophotic reef systems and understanding functional aspects of mesophotic reef geomorphological variation and potential,

additional studies of mesophotic reef systems are needed to better determine the role of sedimentology in the development, sustainability, and potential destruction of mesophotic coral reef ecosystems.
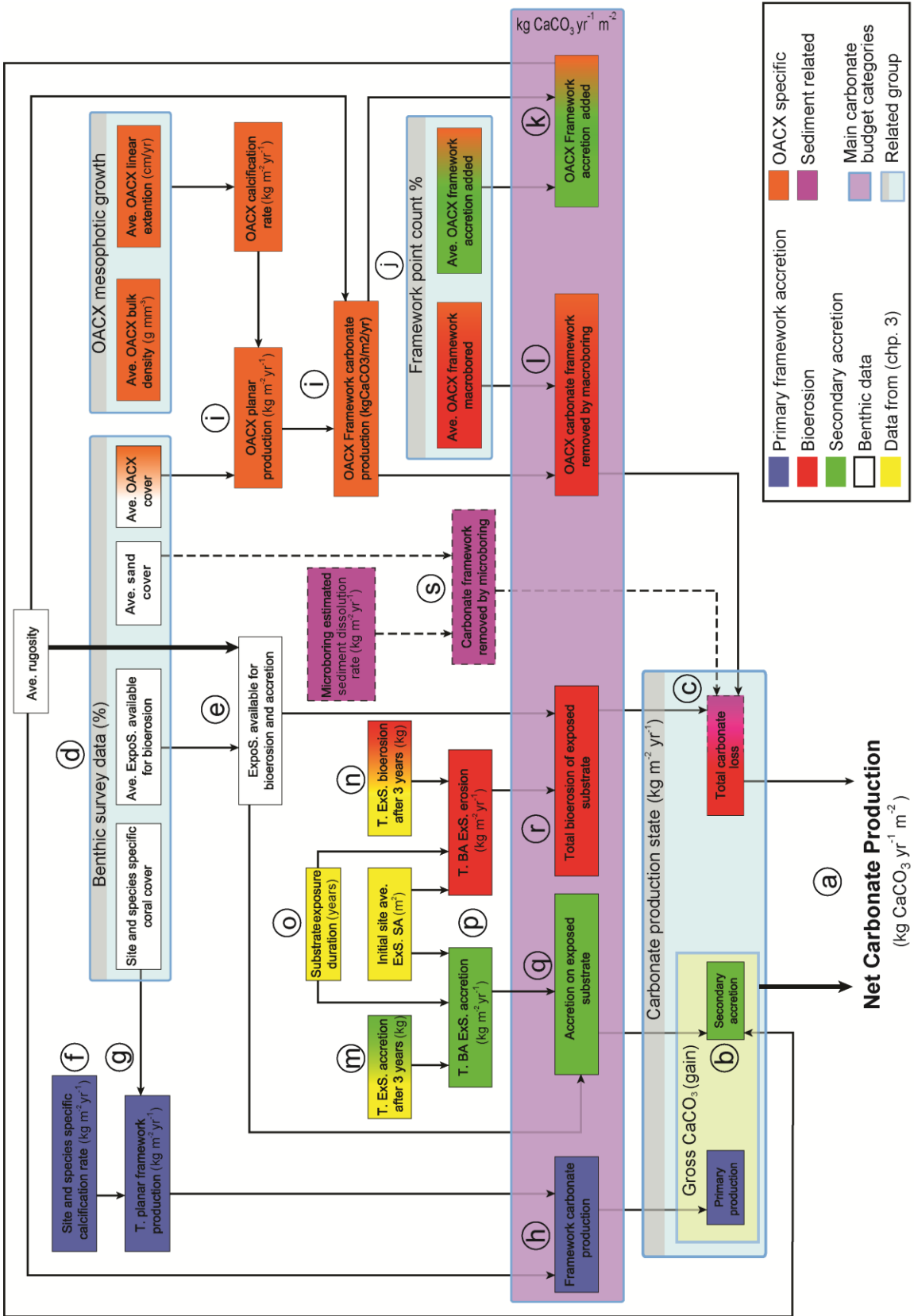
Figure 5.1. Mesophotic reef habitat carbonate budget flowchart. Diagram of the developed carbonate budget model. The arrow or set of arrows pointing from one or multiple boxes and/or "related groups" make up the set of values used to calculate the "receiving" resultant variable. Thicker arrows that span over related groups indicate they are not used in calculations for what they span over. Dotted lines represent additions to the original "hard substrate carbonate budget" model (see discussion section). Letters denote specific equations associated with the adjacent mathematical expression (as seen in Table 5.1) and variables referenced in the chapter text, or both. T. = total, BA = bulk area, SA = surface area, ExS. = experimental substrate, ExpoS. = exposed substrate, OACX = *Orbicella* spp.

Table 5.1. Equations and variables for hard substrate carbonate budget model. All variables represent mean rates reported in standard units of kg m⁻²yr⁻¹, except equation 5, which is dimensionless.

Eq. #	Variable	Equation	Variable name (means)	Flowchart step[a]
1	$\overline{NP}_{HS}$	$= (\overline{PP}_T + \overline{SP}_T) - \overline{BH}_T$	Net CaCO₃ production rate	a
2	$\overline{PP}_T$	$= \overline{PP}_{coral}$	Total site primary CaCO₃ production rate	-
3	$\overline{SP}_T$	$= \overline{SP}_{frame} + \overline{SP}_{ecs}$	Total site secondary CaCO₃ production rate	b
4	$\overline{BH}_T$	$= \overline{Bmac}_{frame} + \overline{Bt}_{ecs}$	Total site hard substrate bioerosion rate	c
5	$\overline{Si}_j$	$= \overline{PC}_j \times \overline{R}$	Spatial cover index	e
6	$\overline{C}_j$	$= \overline{LE}_j \times \overline{BD}_j$	Calcification rate	f
7	$\overline{p}_j$	$= \overline{C}_j \times \overline{PC}_j /100$	Planar production rate	g
8	$\overline{PP}_{coral}$	$= \sum \overline{p}_j \times \overline{R}$	Primary CaCO₃ production rate	h
9	$\overline{SP}_{frame}$	$= \overline{SAC}_{2nd} \times \Delta\overline{PP}_{OACX}$	Secondary CaCO₃ production rate on living framework	k
10	$\overline{Bmac}_{frame}$	$= \overline{SAC}_{mac} \times \Delta\overline{PP}_{OACX}$	Macroboring rate of living framework	l
11	$\overline{a}_T N_{xs}$	$= \dfrac{\overline{AM}_{xs}}{(t_t \times SA_i)}$	Normalized total bulk area experimental secondary accretion rate	p
12	$\overline{b}_T N_{xs}$	$= \dfrac{\overline{BM}_{xs}}{(t_t \times SA_i)}$	Normalized total bulk area experimental substrate bioerosion rate	p
13	$\overline{SP}_{ecs}$	$= \overline{a}_T N_{xs} \times \overline{Si}_{ecs}$	Secondary carbonate production rate on exposed consolidated substrate	q
14	$\overline{Bt}_{ecs}$	$= \overline{b}_T N_{xs} \times \overline{Si}_{ecs}$	Total bioerosion rate of exposed consolidated substrate	r

[a] associated with Fig. 5.1

Subscript code: HS = hard substrate, T = total, $frame$ = reef framework, ecs = exposed consolidated substrate, j = specific coral species, $2nd$ = secondary production processes, $OACX$ = *Orbicella* spp., mac = macroboring, xs = exposed substrate, t = exposure duration (days), i = initial.

Table 5.2. Equations and variables for complete carbonate budget model. All variables represent mean values and all are reported in standard units of kg m^{-2}yr^{-1}. Subscript code found in Table 5.1 and below. "Large grained" implies sediment with an intermediate diameter size greater than 125 μm.

Eq. #	Variable	Equation	Variable name (means)
15	$\overline{GP}_T$	$= \overline{PP}_T + \overline{SP}_T$	Gross hard carbonate production rate
16	$\overline{EB}_{ecs}$	$= \overline{BH}_T - \overline{RB}_T$	Exportation rate of bioeroded ECS
17	$\overline{NP}_C$	$= \overline{GP}_T + \overline{Pt}_{sed} - (\overline{EB}_{ecs} + \bar{S}_{dis})$	Complete net carbonate production rate
18	$\overline{Bk}_{ecs}$	$= \overline{Bt}_{ecs} \times P(k)_{xs}$	Hard substrate bioerosion rate directly attributed to process k
19	$Rg_{\geq 125}$	$= (\overline{Bg}_{ecs_{all}} / 2) \times (100 - PD_{\geq 125})/100$	Retention rate of "larger grained" parrotfish eroded ECS
20	$Rg_{<125}$	$= (\overline{Bg}_{ecs_{all}} / 2) \times (PD_{\geq 125} /100) / 2$	Retention rate of defecated parrotfish-eroded ECS
21	$\overline{RB}_T$	$= Rg_{<125} + Rg_{\geq 125} + \overline{Bmac}_{ecs}$	Total Retention rate of bioeroded ECS
22	$\overline{Pt}_{sed}$	$= \overline{PC}_{sed} \times \sum_j (\%sed_j \times C_j)$	Total normalized non-coral direct sediment production
23	$\bar{S}_{dis}$	$= \overline{PC}_{sed} \times 0.21$ kg m^{-2} y^{-1}	Normalized sediment dissolution rate per site

Subscript code: C = complete budget, dis = dissolution, sed = reefal surface sediment.

Table 5.3. Hard substrate carbonate budget results. Results obtained through model implementation, included for sites where benthic coverage data was available in 2003. Bold text headers indicate values for the five main carbonate budget categories. Italicized cells indicate the three categories used in ternary space diagram displays. Bold values show final budget product. All values are presented in standard units of kg m^{-2}yr^{-1}. Negative values indicate the process is a destructive component. Empty spaces exist where no data was available and was considered of little importance (see text). Values include ± 1 standard error. Variable abbreviations are provided below table.

*Based on 2007 benthic survey. ECS = Exposed consolidated substrate, OACX = living *Orbicella* spp.

Geomorphic Habitats	**ECS Bioerosion**	**ECS Accretion**	**OACX Macroboring**	**OACX Accretion**	***Primary Production***	*Total Bioerosion*	*Gross Production*	Net Production
2012 Benthic Survey								
Hillock Basin*	-0.44 ± 0.11	0.35 ± 0.09	-0.07 ± 0.03	0.01 ± 0.00	0.43 ± 0.16	-0.51 ± 0.11	0.78 ± 0.18	**0.27 ± 0.22**
Deep Patch	-0.19 ± 0.02	0.30 ± 0.02			0.14 ± 0.10	-0.19 ± 0.02	0.44 ± 0.10	**0.25 ± 0.10**
Primary Bank	-1.55 ± 0.39	0.42 ± 0.11	-0.17 ± 0.06	0.00 ± 0.00	1.57 ± 0.40	-1.72 ± 0.39	1.99 ± 0.42	**0.27 ± 0.57**
Secondary Bank	-0.89 ± 0.09	0.24 ± 0.03	-0.14 ± 0.03	0.01 ± 0.01	1.12 ± 0.15	-1.03 ± 0.09	1.37 ± 0.16	**0.34 ± 0.18**
Mid-shelf Patch	-1.02 ± 0.06	0.20 ± 0.01			2.02 ± 0.21	-1.02 ± 0.06	2.22 ± 0.21	**1.20 ± 0.22**
Fringing Patch	-1.37 ± 0.07	0.40 ± 0.02			0.44 ± 0.15	-1.37 ± 0.07	0.84 ± 0.15	**-0.53 ± 0.16**
2003								
Primary Bank	-1.14 ± 0.30	0.31 ± 0.08	-0.26 ± 0.09	0.01 ± 0.01	2.09 ± 0.54	-1.40 ± 0.31	2.40 ± 0.54	**1.00 ± 0.62**
Secondary Bank	-0.82 ± 0.09	0.22 ± 0.03	-0.19 ± 0.03	0.02 ± 0.01	2.45 ± 0.26	-1.01 ± 0.10	2.69 ± 0.26	**1.68 ± 0.28**
Mid-shelf Patch	-0.83 ± 0.06	0.16 ± 0.01			6.52 ± 2.40	-0.83 ± 0.06	6.69 ± 2.40	**5.85 ± 2.40**
	$\overline{Bt_{ecs}}$	$\overline{SP_{ecs}}$	$\overline{Bmac_{frame}}$	$\overline{SP_{frame}}$	$\overline{PP_{coral}}$	$\overline{BH_T}$	$\overline{GP_T}$	$\overline{NP_{HS}}$

Table 5.4. Complete carbonate budget additions and results. Additional data used to convert from hard substrate carbonate budget to the estimated complete carbonate budget. All values are rates of change. When no units are displayed, values are given in terms of g m⁻²yr⁻¹. Total retention column is not the sum of the two columns before it (see Table 5.2 for more detail). Empty spaces exist where no approximate hydrodynamic data was available; an alternative method was used (see text). Values are presented with ± 1 standard error.
*Based on 2007 benthic survey. ECS = Exposed consolidated substrate.

| Geomorphic Habitats | ECS Retention | | | Total Bioeroded ECS Exportation (kg m⁻²yr⁻¹) | Total sediment non-coral production | Sediment Dissolution | Complete net production (kg m⁻²yr⁻¹) |
	"Large"	Defecated	Total (kg m⁻²yr⁻¹)				
2012 Benthic Survey							
Hillock Basin*	77.1 ± 22.2	54.5 ± 15.7	0.14 ± 0.03	0.30 ± 0.11	27.3 ± 9.0	21.0 ± 6.6	**0.49 ± 0.22**
Deep Patch	30.0 ± 13.2	12.3 ± 5.4	0.07 ± 0.02	0.12 ± 0.02	1.0 ± 0.6	0.6 ± 0.4	**0.32 ± 0.10**
Primary Bank	453.7 ± 164.0	142.4 ± 51.5	0.61 ± 0.17	0.94 ± 0.43	13.5 ± 6.4	8.6 ± 3.7	**1.05 ± 0.60**
Secondary Bank	257.1 ± 37.9	80.7 ± 11.9	0.35 ± 0.04	0.54 ± 0.10	2.3 ± 0.8	3.1 ± 1.0	**0.83 ± 0.19**
Mid-shelf Patch			0.43 ± 0.10	0.60 ± 0.12	4.5 ± 1.7	5.4 ± 1.1	**1.62 ± 0.24**
Fringing Patch			0.42 ± 0.13	0.95 ± 0.15	0.2 ± 0.2	0.2 ± 0.2	**-0.11 ± 0.21**
2003							
Primary Bank	332.6 ± 122.2	104.4 ± 38.4	0.45 ± 0.13	0.69 ± 0.32	Same data used from corresponding 2012 site		**1.72 ± 0.63**
Secondary Bank	237.3 ± 36.8	74.5 ± 11.6	0.33 ± 0.04	0.50 ± 0.10			**2.19 ± 0.28**
Mid-shelf Patch			0.35 ± 0.08	0.49 ± 0.10			**6.20 ± 2.40**
	$\overline{Rg}_{\geq125}$	$\overline{Rg}_{<125}$	$\overline{RB}_T$	$\overline{EB}_{ecs}$	$\overline{Pt}_{sed}$	$\overline{S}_{dis}$	$\overline{NP}_C$
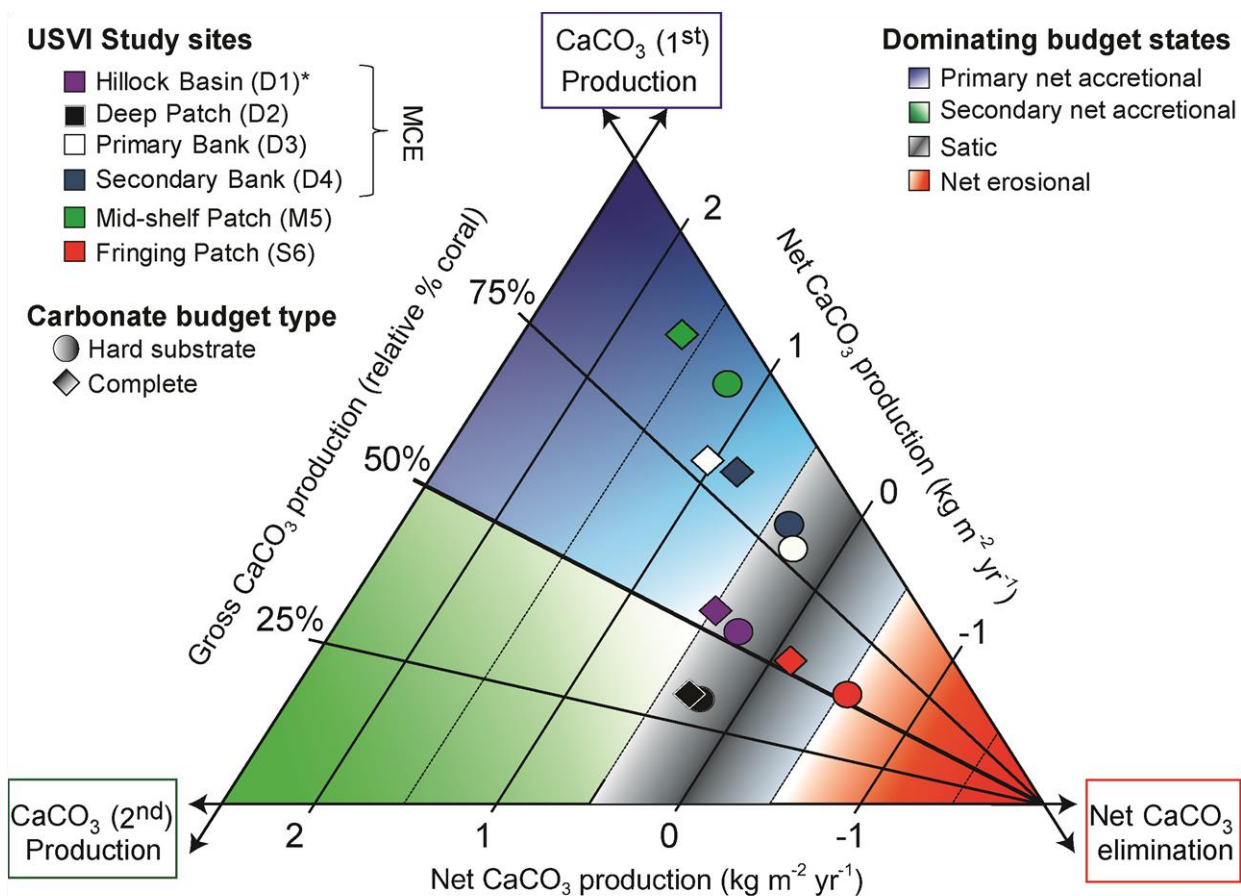
Figure 5.2. USVI coral reef carbonate production states. Ternary space conceptual approach (Perry et al. 2008) of how carbonate cycles through the different reef habitats in various carbonate production states. Triangle apices show end-member carbonate production states. Net carbonate elimination is "total bioerosion" for hard substrate carbonate budgets (circles) and exported and dissolved sediment for complete carbonate budget estimates (diamonds). Right and bottom axes denote net carbonate production for the carbonate budgets of each habitat. The position along each net carbonate production "axes line" (equal net carbonate production along entire length of line) between the top and bottom of the triangle corresponds to the relative percent of the total gross carbonate production rate attributed to primary scleractinian production (compared to secondary production). A 'stasis' region (Perry, 2008) is arbitrarily defined between 0.5 and -0.5 kg m^{-2}y^{-1}.
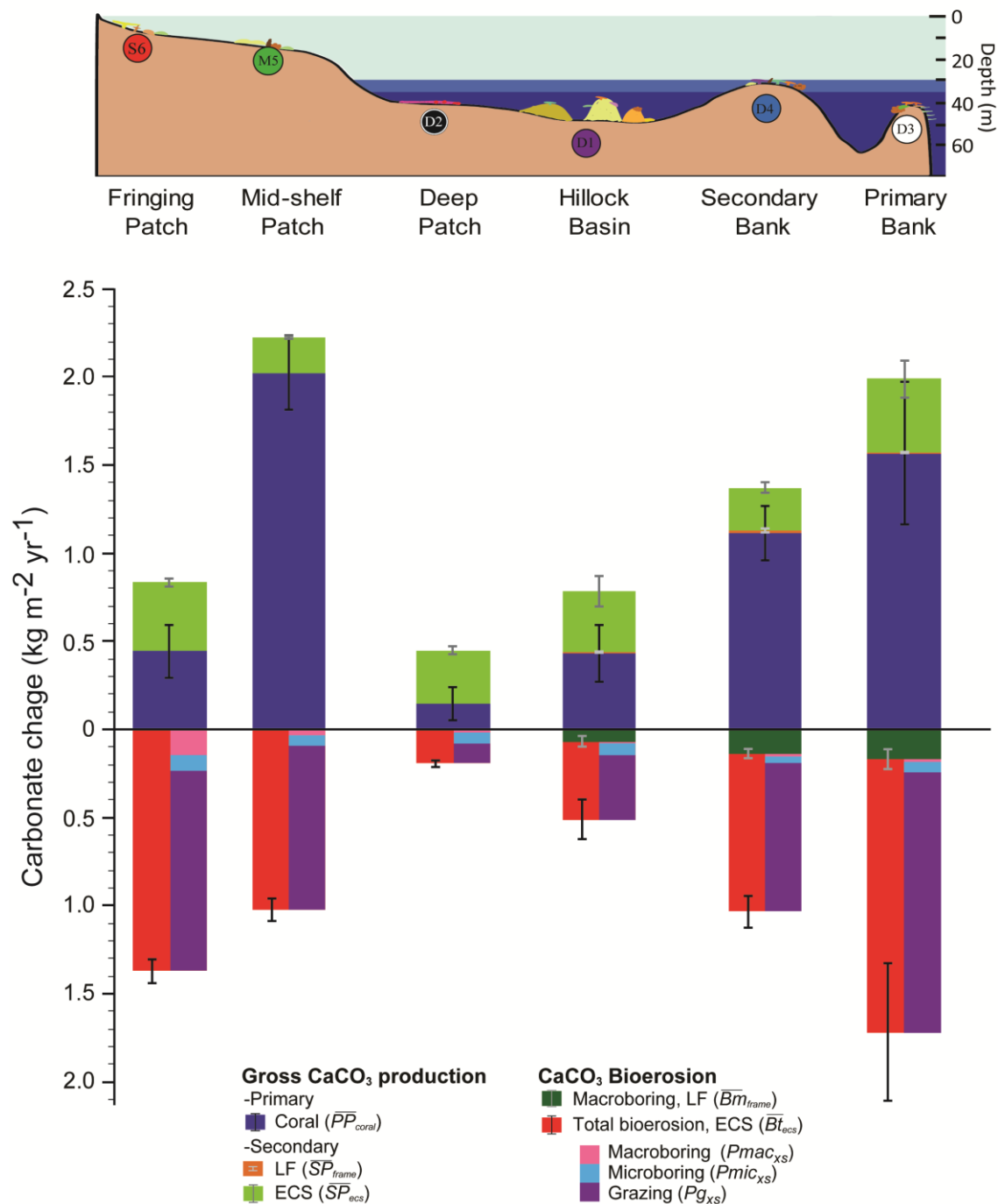
Figure 5.3. Main coral reef hard substrate carbonate budget categories.
Comparison between constructive (gross carbonate production) and destructive (carbonate bioerosion) processes calculated on living framework (LF) and exposed consolidated substrate (ECS), matched to theoretical cross-section across the southern Puerto Rican Shelf. Relative contributions of the three constituents of total ESC bioerosion are shown compared to that group total. Error bars equal ± 1 standard error and their specific group correspondence is shown in the key. Full names of variables in the key are found in Table. 5.1 – 5.2).
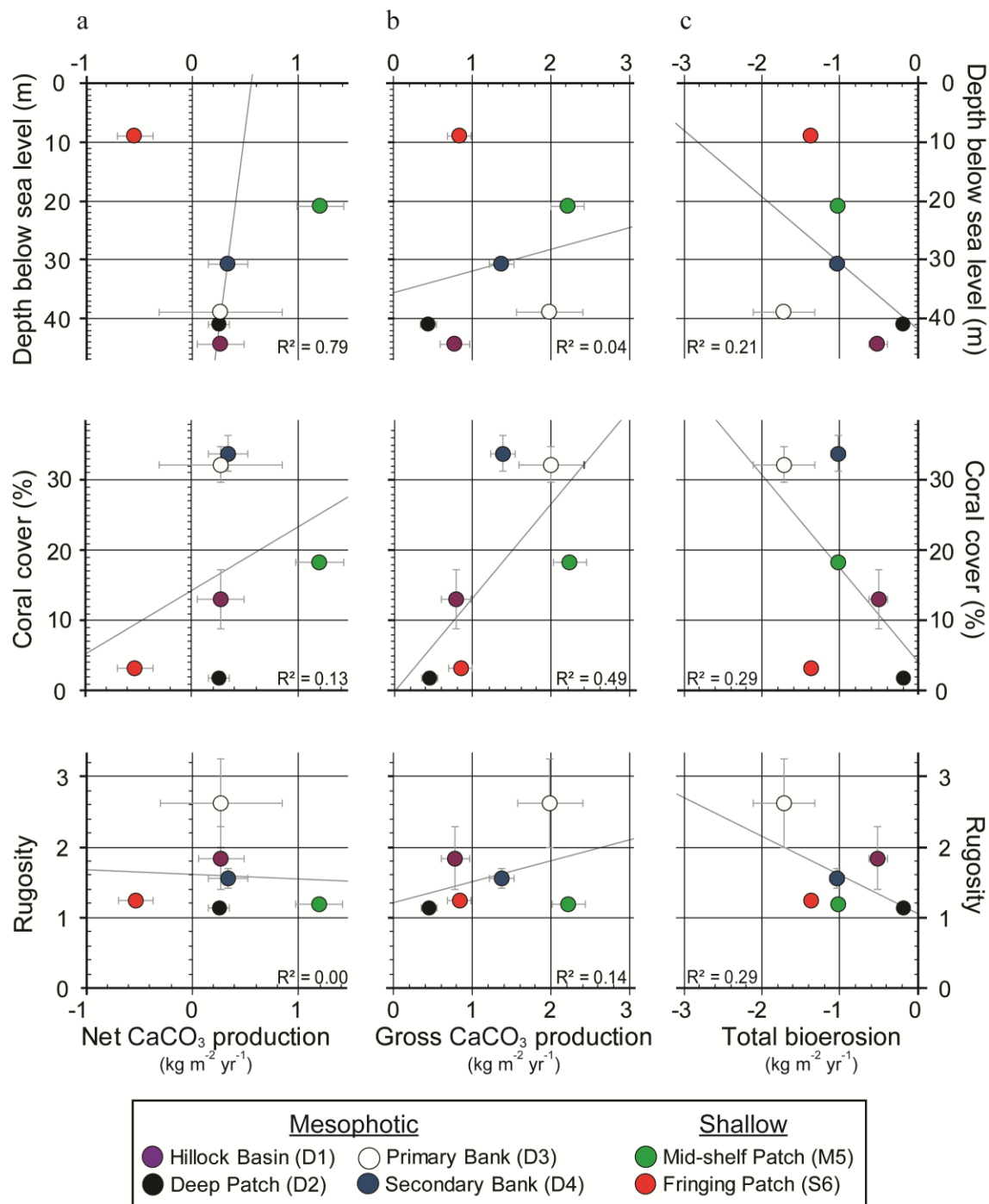
Figure 5.4. Carbonate production states versus depth and benthic factors.
Comparing depth and ecological spatial relationships with: (a) net carbonate production (for hard substrate carbonate budget); (b) gross carbonate production; and (c) total bioerosion. Plots are aligned such that vertical axes and horizontal axes share the same values, respectively. Error bars represent uncertainty calculated by standard error propagation, using ± 1 standard error of each measured variable needed to calculate the production state value. R^2 shows how well the line of best-fit describes all sites (except for the depth graph of (a), where the line was only plotted for mesophotic sites).
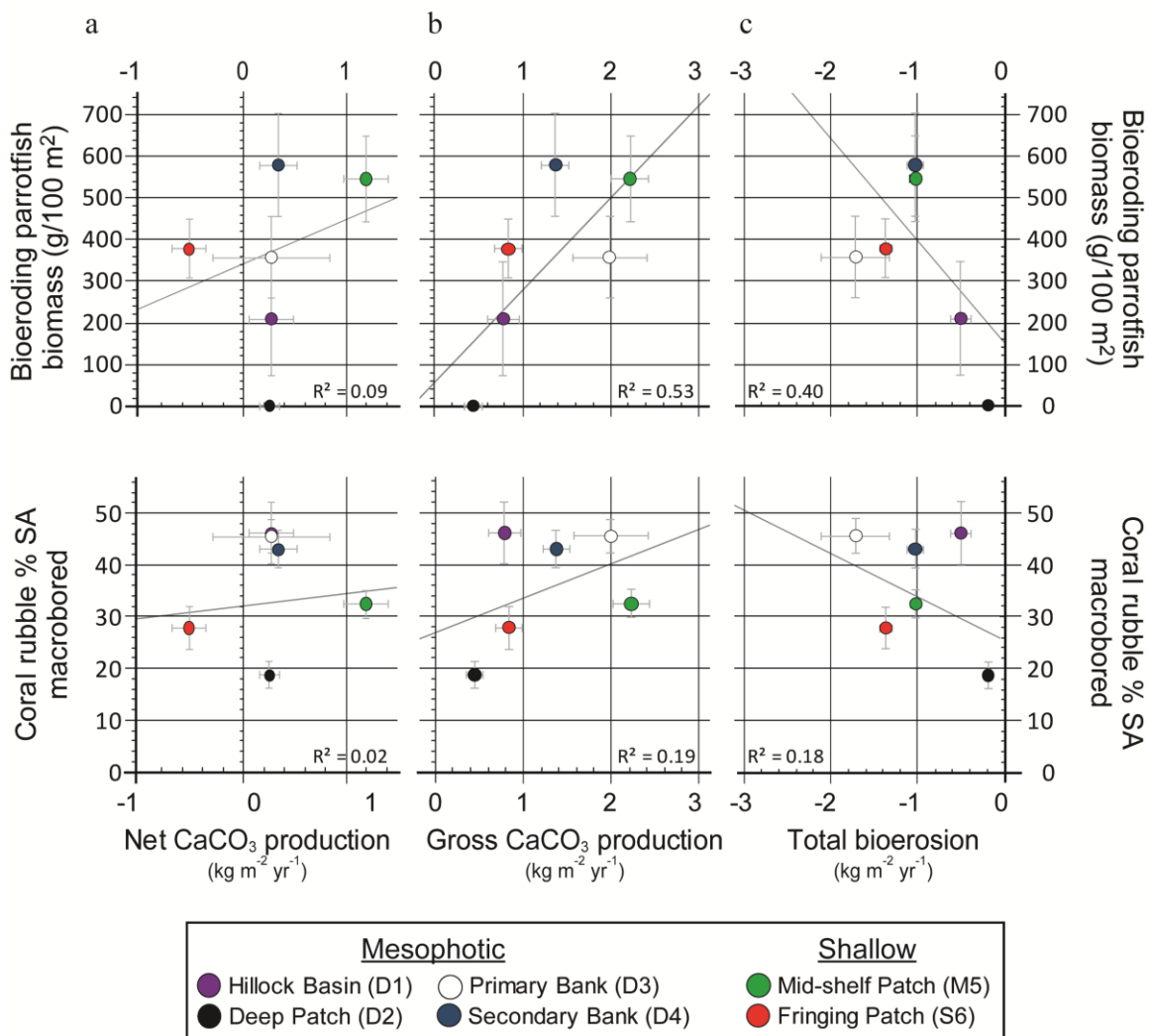
Figure 5.5. Carbonate production states versus bioerosion. Comparisons between different metrics of bioerosion with: (a) net carbonate production (for hard substrate carbonate budget); (b) gross carbonate production; and (c) total bioerosion. Plots follow the same design scheme, error bar calculations, and trend line properties (trends fit to all six sites for ever graph in this site).

Table 5.5. Mesophotic reef accretion. Estimated rates of reef accretion, calculated for all study site habitats (except the Fringing Patch, which had overall net erosion). Values are presented with ± 1 standard error. *Based on 2007 benthic survey.

Geomorphic habitats	Approx. reef accretion rate (mm/yr)	Time until present sea-level (yr)	Calculated 6 ka vertical accumulation (m)
Hillock Basin*	0.33 ± 0.15	133026	2.01 ± 0.89
Deep Patch	0.22 ± 0.07	185632	1.33 ± 0.42
Primary Bank	0.72 ± 0.41	53862	4.34 ± 2.47
Secondary Bank	0.57 ± 0.13	53553	3.44 ± 0.77
Mid-shelf Patch	1.12 ± 0.17	18775	6.71 ± 1.00
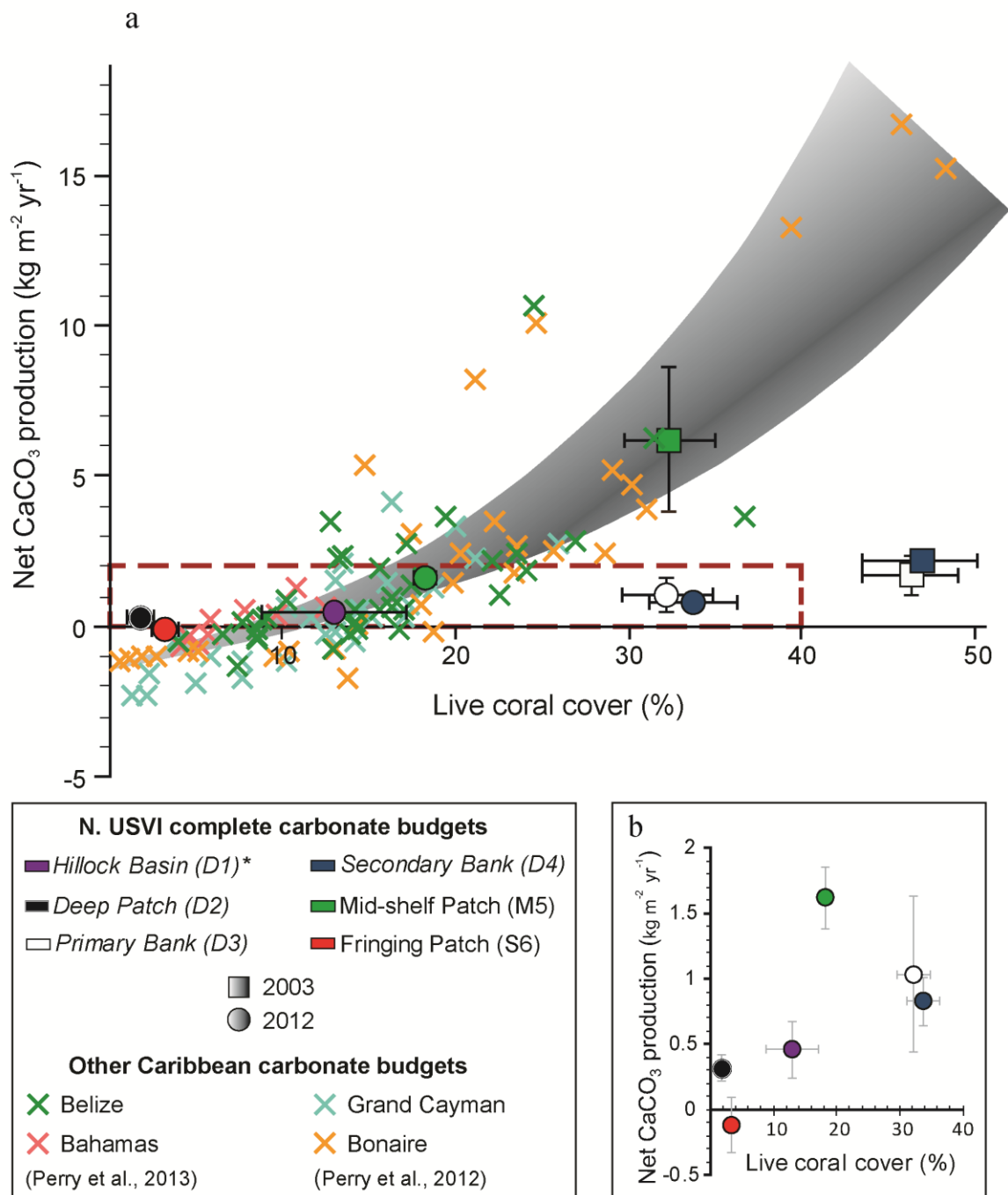
Figure 5.6. Caribbean net carbonate production versus depth. (a) Comparison between live coral cover and carbonate budget net production rates calculated for this study (showing results of estimated complete budgets) and from 101 individual reef transects, grouped by the 4 countries in which they were conducted (Perry et al., 2013). Shaded area depicts the 95% confidence interval best fit regression for *Orbicella* spur and grove reefs from the 19 reefs examined by Perry et al. (2013). Red dotted box indicates location of (b) inset graph specifically showing the relationship between specific study sites. *Italicized* site names in key indicate mesophotic reefs. Error bars equal ± 1 standard. *Results based on benthic surveys conducted in 2007 (Smith et al., 2007).

226
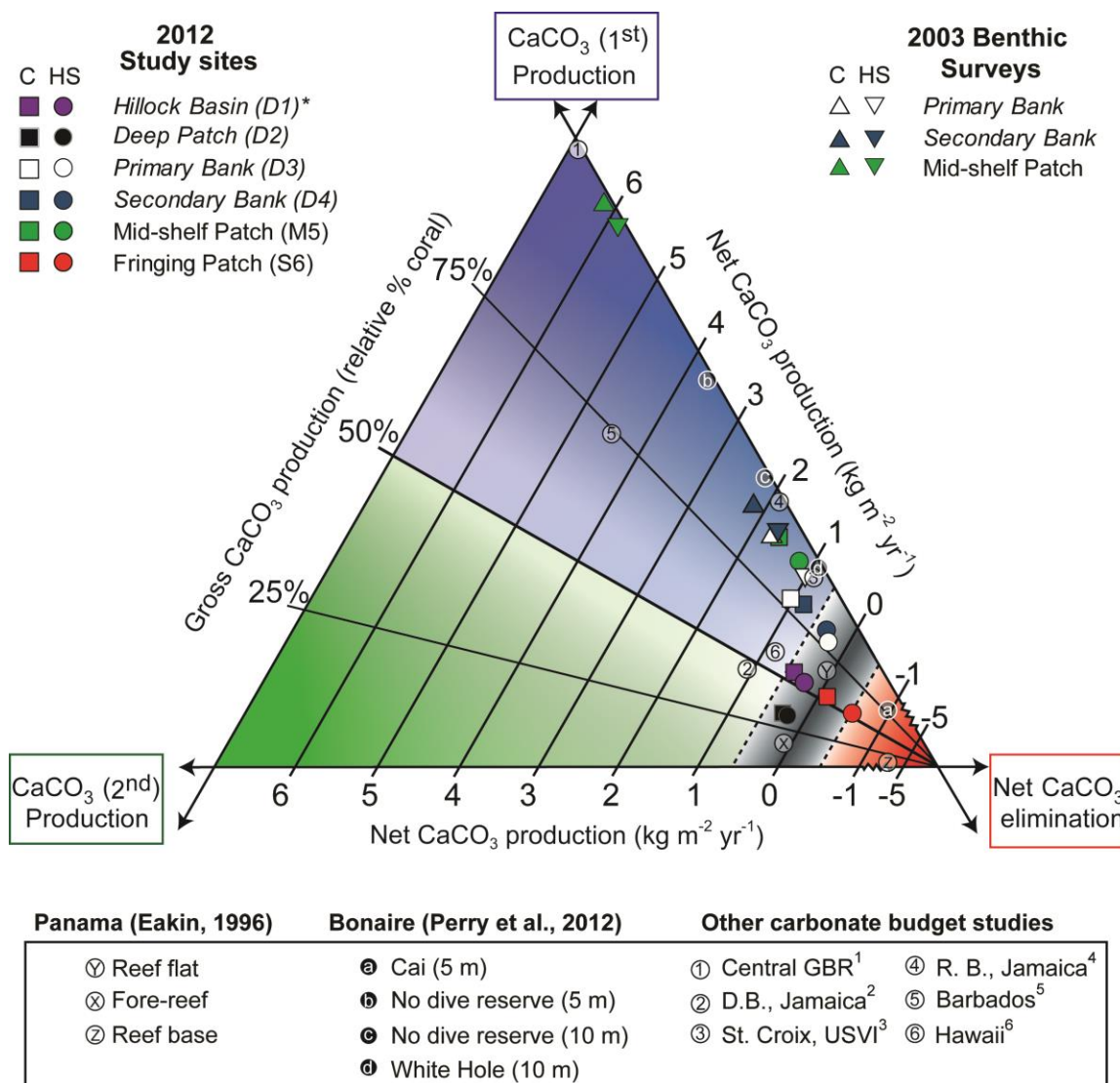
Figure 5.7. Summary of carbonate budget assessments. Temporal comparison between hard substrate (HS) and complete (C) carbonate budgets calculated from 2012 benthic surveys (*benthic survey conducted in 2007, Smith et al., 2007) and from available 2003 benthic survey results, when using the same rugosity measurements and calculated rates obtained over the duration of this dissertation (2010-2013). Italic labels under keys for benthic survey year associated data indicate mesophotic sites. Study results are also shown in relation to carbonate budgets calculated at other locations using multiple techniques, on differing spatial scales (see text for more explanation). Net carbonate production scale discontinuity breaks (zig-zag line) for negative values to display more data. See Fig. 5.2 for diagram interpretation details and the dominant carbonate production state color code). [1]Paluma Shoals, inshore land-attached reef (Browne et a., 2013), [2]Discovery Bay, 0-60 m (Land, 1979), [3]Cane Bay, Fringing reef, 2-60 m (Hubbard et al., 2090), [4]Rio Bueno, turbid site (Mallela and Perry, 2007), [5]Bellairs Reef, <10 m fringing reef (Scoffin et al., 1980), [5]Kailua Bay, 25 m fringing reef (Harney and Fletcher, 2003).
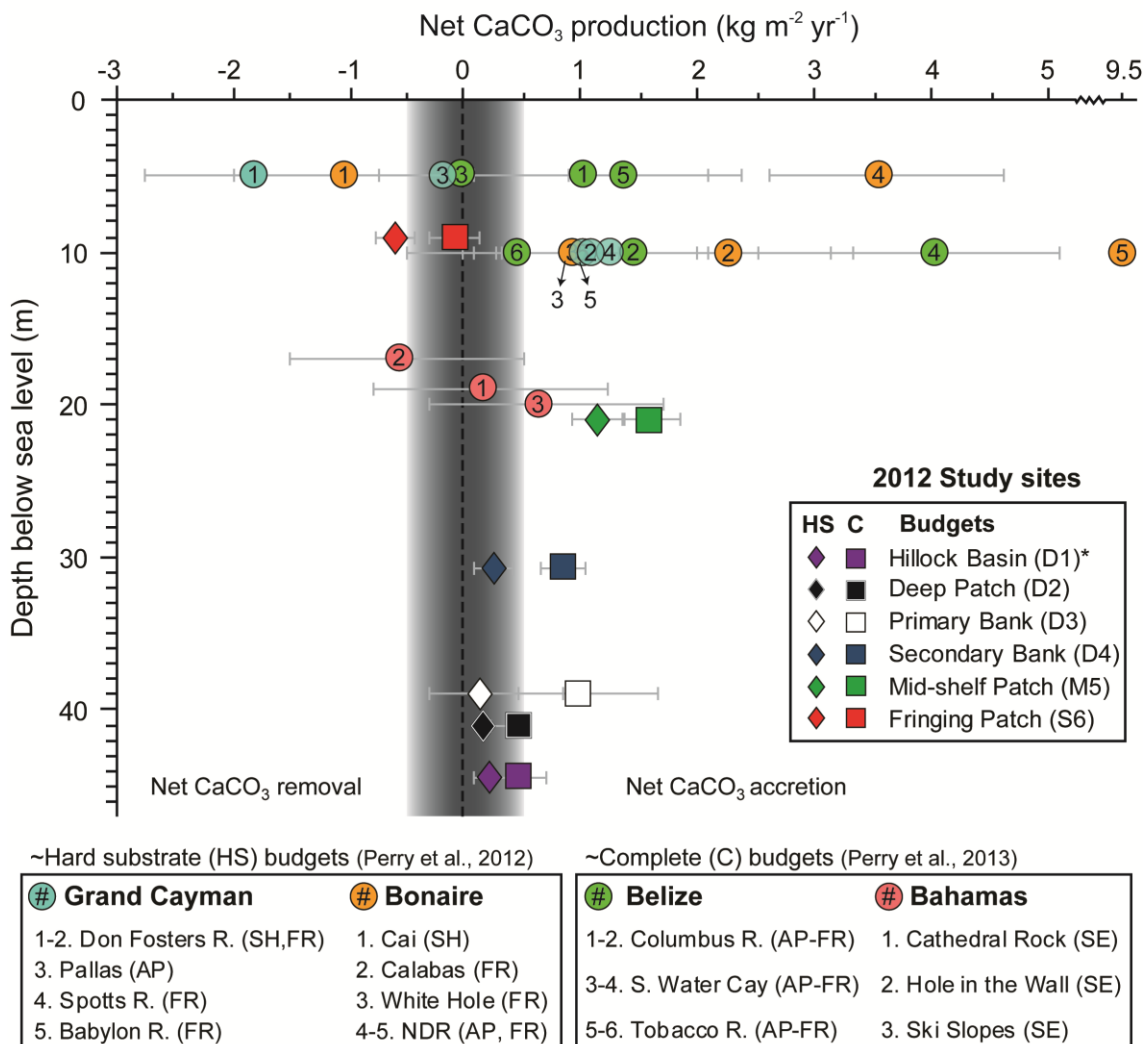
Figure 5.8. Caribbean net carbonate production versus depth. Potential relationship between net carbonate production rates and depth for northern USVI coral reef study sites and comparable, recently conducted Caribbean census-based hard substrate (HS) and complete (C) carbonate budgets in four countries at 19 different reefs between 5-20 m deep). Results from the 19 reefs are plotted as the reef average of 3-5 individual census measurements from different transects within the same reef site. Shaded region represents budgets in potential "stasis" equilibrium. Horizontal scale interval was broken (zig-zag line) to display the rates of all reefs on the same graph. SH = shallow hardground, FR = fore-reef, AP = *Acropora palmata* zone, SE = shelf edge. NDR indicates sites designated as no dive reserves. Error bars equal ± 1 standard. *Results based on benthic surveys conducted in 2007 (Smith et al., 2007).

Table 5.6. Corrected 2003 reef accretion results. Rates of reef accretion based on estimated complete carbonate budget net production rates calculated with benthic survey data from 2003. The top group displays results when applying mean rugosity ($\bar{R}$) measurements from 2012 (see 2003 data in Fig. 5.7) and the bottom group displays results when applying a corrective factor explained in the text (or corrective factor and an additional 15% for bracketed Primary Bank values). Values are presented with $\pm$ 1 standard error.

Geomorphic habitats	Rugosity	Approx. reef accretion rate (mm/yr)	Time until present sea-level (yr)	Calculated 6 ka vertical accumulation (m)
Primary Bank	2.62	1.19 ± 0.43	32908	7.11 ± 2.61
Secondary Bank	1.55	1.51 ± 0.19	20352	9.05 ± 1.15
Mid-shelf Patch	1.18	4.27 ± 1.65	4914	25.64 ± 9.93
Primary Bank	2.87 (3.33)	1.30 ± 0.44 (1.51 ± 0.45)	30006 (25888)	7.80 ± 2.65 (9.04 ± 2.72)
Secondary Bank	2.89	2.81 ± 0.25	10921	16.87 ± 1.52
Mid-shelf Patch	2.32	12.16 ± 4.69	2504	50.32 ± 19.40

Works Cited

Abbey, E., Webster, J.M., Braga, J.C., Jacobsen, G.E., Thorogood, G., Thomas, A.L., Camoin, G., Reimer, P.J., Potts, D.C., 2013. Deglacial mesophotic reef demise on the Great Barrier Reef. Palaeogeogr., Palaeoclimatol., Palaeoecol. 392, 473-494.

Acker, K.L., Risk, M.J., 1985. Substrate destruction and sediment production by the boring sponge Cliona caribbaea on Grand Cayman Island. Journal of Sedimentary Petrology. 55(5), 705-711.

Adams, A.E., Mackenzie, W.S., Guilford, C., 1984. Atlas of sedimentary rocks under the microscope. Longman Scientific and Technical, Essex, England.

Adey, W.H., Burke, R.B., 1977. Holocene bioherms of Lesser Antilles - geologic control of development. American Association of Petroleum Geologists Studies in Geology, 67-81.

Adey, W.H., Burke, R., 1976. Holocene bioherms (algal ridges and bank-barrier reefs) of the eastern Caribbean. Geological Society of America Bulletin, 87(1), 95-109.

Alamaru, A., Loya, Y., Brokovich, E., Yam, R., Shemesh, A., 2009. Carbon and nitrogen utilization in two species of Red Sea corals along a depth gradient: Insights from stable isotope analysis of total organic material and lipids. Geochim.Cosmochim.Acta. 73(18), 5333-5342.

Alvarez-Filip, L., Côté, I.M., Gill, J.A., Watkinson, A.R., Dulvy, N.K., 2011a. Region-wide temporal and spatial variation in Caribbean reef architecture: Is coral cover the whole story? Global Change Biol. 17(7), 2470-2477.

Alvarez-Filip, L., Dulvy, N.K., Côté, I.M., Watkinson, A.R., Gill, J.A., 2011b. Coral identity underpins architectural complexity on Caribbean reefs. Ecol.Appl. 21(6), 2223-2231.

Alvarez-Filip, L., Gill, J.A., Dulvy, N.K., Perry, A.L., Watkinson, A.R., Côté, I.M., 2011c. Drivers of region-wide declines in architectural complexity on Caribbean reefs. Coral Reefs. 30(4), 1051-1060.

Alvarez-Filip, L., Dulvy, N.K., Gill, J.A., Côté, I.M., Watkinson, A.R., 2009. Flattening of Caribbean coral reefs: Region-wide declines in architectural complexity. Proceedings of the Royal Society B: Biological Sciences. 276(1669), 3019-3025.

Anthony, K., Fabricius, K.E., 2000. Shifting roles of heterotrophy and autotrophy in coral energetics under varying turbidity. J.Exp.Mar.Biol.Ecol. 252(2), 221-253.

Anthony, K.R., Hoegh-Guldberg, O., 2003. Variation in coral photosynthesis, respiration and growth characteristics in contrasting light microhabitats: An analogue to plants in forest gaps and understoreys? Funct.Ecol. 17(2), 246-259.

Armstrong, R.A., 2007. Deep zooxanthellate coral reefs of the Puerto Rico: US Virgin Islands insular platform. Coral Reefs. 26, 945.

Armstrong, R.A., Singh, H., Torres, J., Nemeth, R.S., Can, A., Roman, C., Eustice, R., Riggs, L., Garcia-Moliner, G., 2006. Characterizing the deep insular shelf coral reef habitat of the Hind Bank marine conservation district (US Virgin Islands) using the Seabed autonomous underwater vehicle. Cont.Shelf Res. 26(2), 194-205.

Aurell, M., Bádenas, B., 2004. Facies and depositional sequence evolution controlled by high-frequency sea-level changes in a shallow-water carbonate ramp (late Kimmeridgian, NE Spain). Geol.Mag. 141(6), 717-733.

Bagnold, R.A., 1966. An approach to the sediment transport problem from general physics. USGS Professional Paper. 422-I, 37.

Bak, R., Nieuwland, G., Meesters, E., 2005. Coral reef crisis in deep and shallow reefs: 30 years of constancy and change in reefs of Curacao and Bonaire. Coral Reefs. 24(3), 475-479.

Bak, R.P.M., Engel, M.S., 1979. Distribution, abundance and survival of juvenile hermatypic corals (Scleractinia) and the importance of life history strategies in the parent coral community. Mar.Biol. 54(4), 341-352.

Baker, A.C., Glynn, P.W., Riegl, B., 2008. Climate change and coral reef bleaching: An ecological assessment of long-term impacts, recovery trends and future outlook. Estuar.Coast.Shelf Sci. 80(4), 435-471.

Baker, A.C., Starger, C.J., McClanahan, T.R., Glynn, P.W., 2004. Corals' adaptive response to climate change. Nature. 430(7001), 741.

Baker, P.A., Weber, J.N., 1975. Coral growth rate: Variation with depth. Earth Planet.Sci.Lett. 27(1), 57-61.

Banks, K.W., Riegl, B.M., Richards, V.P., Walker, B., Helmle, K.P., Jordan, L.K.B., Phipps, J., Shivji, M.S., Spieler, R.E., Dodge, R.E., 2008. The reef tract of continental southeast Florida (Miami-Dade, Broward and Palm Beach Counties, USA). In: Riegl, B.M., Dodge, R.E. (Eds.), Coral Reefs of the USA. Springer Science, Netherlands, pp. 175-220.

Bare, A.Y., Grimshaw, K.L., Rooney, J.J., Sabater, M.G., Fenner, D., Carroll, B., 2010. Mesophotic communities of the insular shelf at Tutuila, American Samoa. Coral Reefs. 29(2), 369-377.

Barnes, D.J., Lough, J.M., 1999. Porites growth characteristics in a changed environment: Misima Island, Papua New Guinea. Coral Reefs. 18(3), 213-218.

Barnes, D.J., Lough, J.M., 1996. Coral skeletons: Storage and recovery of environmental information. Global Change Biol. 2(6), 569-582.

Barnes, D.J., Taylor, R.B., Lough, J.M., 1995. On the inclusion of trace materials into massive coral skeletons. Part II: Distortions in skeletal records of annual climate cycles due to growth processes. J.Exp.Mar.Biol.Ecol. 194(2), 251-275.

Barnes, D.J., Lough, J.M., 1992. Systematic variations in the depth of skeleton occupied by coral tissue in massive colonies of Porites from the Great Barrier Reef. J.Exp.Mar.Biol.Ecol. 159(1), 113-128.

Barnes, D.J., Lough, J.M., 1989. The nature of skeletal density banding in scleractinian corals: Fine banding and seasonal patterns. J.Exp.Mar.Biol.Ecol. 126(2), 119-134.

Barnes, D.J., Devereux, M.J., 1988. Variations in skeletal architecture associated with density banding in the hard coral Porites. J.Exp.Mar.Biol.Ecol. 121(1), 37-54.

Basan, P.B., 1973. Aspects of sedimentation and development of a carbonate bank in the Barracuda Keys, south Florida. Journal of Sedimentary Research. 43(1), 42-53.

Battey, J.F., Porter, J.W., 1988. Photoadaptation as a whole organism response in *Montastrea annularis.* In: Choat, J.H., Barnes, D., Borowitzka, M.A., Coll, J.C., Davies, P.J., Flood, P., Hatcher, B.G., Hopley, D., Hutchings, P.A., Kingsey, D., Orme, G.R., Pichon, M., Sale, P.F., Sammarco, P., Wallace, C., Wilkinson, C., Wolanski, E., Bellwood, O. (Eds.), Proceedings from the 6th International Coral Reef Symposium. 6th International Coral Reef Symposium Executive Committee, pp. 79-87.

Bianchelli, S., Pusceddu, A., Canese, S., Greco, S., Danovaro, R., 2013. High meiofaunal and nematodes diversity around mesophotic coral oases in the Mediterranean Sea. PLoS ONE. 8(6), e66553.

Birkeland, C., 1997. Geographic differences in ecological processes on coral reefs. In: Birkeland, C. (Ed.), Life and Death of Coral Reefs. Chapman and Hall, New York, pp. 273-287.

Blanchon, P., Jones, B., Kalbfleisch, W., 1997. Anatomy of a fringing reef around Grand Cayman; storm rubble, not coral framework. Journal of Sedimentary Research. 67(1), 1-16.

Blott, S.J., Pye, K., 2001. Gradistat: A grain size distribution and statistics package for the analysis of unconsolidated sediments. Earth Surface Processes and Landforms. 26, 1237-1248.

Bohnsack, J.A., Harper, D.E., 1988. Length-weight relationships of selected marine fish from the southeastern United States and the Caribbean NOAA Technical Memorandum NOAA Technical Memorandum NMFS-SEFC-215, 1-18.

Boland, R.C., Gleason, K.A., Kosaki, R.K., McFall, G.B., Papastamatiou, Y.P., Pyle, R.L., Toonen, R.J., Wagner, D., 2011. New records of commercially valuable black corals (Cnidaria: antipatharia) from the Northwestern Hawaiian Islands at mesophotic Depths. Pac.Sci. 65(2), 249-255.

Bongaerts, P., Muir, P., Englebert, N., Bridge, T.C.L., Hoegh-Guldberg, O., 2013. Cyclone damage at mesophotic depths on Myrmidon Reef (GBR). Coral Reefs, 1-1.

Bongaerts, P., Riginos, C., Hay, K.B., van Oppen, M. J . H., Hoegh-Guldberg, O., Dove, S., 2011. Adaptive divergence in a scleractinian coral: Physiological adaptation of Seriatopora hystrix to shallow and deep reef habitats. BMC Evolutionary Biology. 11(1), 303.

Bongaerts, P., Ridgway, T., Sampayo, E.M., Hoegh-Guldberg, O., 2010. Assessing the 'deep reef refugia' hypothesis: Focus on Caribbean reefs. Coral Reefs. 29(2), 309-327.

Bosellini, F.R., 1998. Diversity, composition and structure of Late Eocene shelf-edge coral associations (Nago Limestone, Northern Italy). Facies. 39(1), 203-225.

Bosellini, F.R., Russo, A., 1992. Stratigraphy and facies of an oligocene fringing reef (Castro Limestone, Salento Peninsula, Southern Italy). Facies. 26(1), 145-165.

Boss, S.K., Liddell, W.D., 1987a. Patterns of sediment composition of Jamaican fringing reef facies. Sedimentology. 34(1), 77-87.

Boss, S.K., Liddell, W.D., 1987b. Back-reef and fore-reef analogs in the Pleistocene of north Jamaica: Implications for facies recognition and sediment flux in fossil reefs. Palaios. 2(3), 219-228.

Bosscher, H., Meesters, E.H., 1993. Depth related changes in the growth rate of *Montastrea annularis.* In: Richmond, R.H. (Ed.), Proceedings from the 7th International Coral Reef Symposium, Guam, pp. 507-512.

Bosscher, H., 1992. Growth potential of coral reefs and carbonate platforms. (Ph.D Dissertation). Proefschrift Vrije Universiteit Amsterdam, Utrecht, Netherlands.

Bosscher, H., Schlager, W., 1992. Computer simulation of reef growth. Sedimentology. 39(3), 503-512.

Bozec, Y., Alvarez-Filip, L., Mumby, P.J., 2014. The dynamics of architectural complexity on coral reefs under climate change. Global Change Biol., 10.1111/gcb.12698.

Braithwaite, C.J.R., 1973. Settling behaviour related to sieve analysis of skeletal sands. Sedimentology. 20(2), 251-262.

Brandano, M., Frezza, V., Tomassetti, L., Pedley, M., Matteucci, R., 2009. Facies analysis and palaeoenvironmental interpretation of the Late Oligocene Attard Member (Lower Coralline Limestone Formation), Malta. Sedimentology. 56(4), 1138-1158.

Brander, L.M., Van Beukering, P., Cesar, H.S.J., 2007. The recreational value of coral reefs: A meta-analysis. Ecol.Econ. 63(1), 209-218.

Breedy, O., Guzman, H.M., 2013. A new species of the genus Eugorgia (Cnidaria: Octocorallia: Gorgoniidae) from Mesophotic reefs in the eastern Pacific - Bulletin of Marine Science, 89(3), 735-743.

Bridge, T., Beaman, R., Done, T., Webster, J., 2012a. Predicting the location and spatial extent of submerged coral reef habitat in the Great Barrier Reef World Heritage Area, Australia. PLoS ONE. 7(10), 1-11.

Bridge, T., Fabricius, K., Bongaerts, P., Wallace, C., Muir, P., Done, T., Webster, J., 2012b. Diversity of Scleractinia and Octocorallia in the mesophotic zone of the Great Barrier Reef, Australia. Coral Reefs. 31(1), 179-189.

Bridge, T.C.L., Done, T.J., Friedman, A., Beaman, R.J., Williams, S.B., Pizarro, O., Webster, J.W., 2011. Variability in mesophotic coral reef communities along the Great Barrier Reef, Australia. Marine Ecology Progress Series. 428, 63-75.

Brock, R.E., 1979. An experimental study on the effect of grazing by parrotfishes and role of refuges in benthic community structure. Marine Biology. 51(4), 381-388.

Brokovich, E., Ayalon, I., Einbinder, S., Segev, N., Shaked, Y., Genin, A., Kark, S., Kiflawi, M., 2010. Grazing pressure on coral reefs decreases across a wide depth gradient in the Gulf of Aqaba, Red Sea. Marine Ecology Progress Series. 399, 69-80.

Brokovich, E., Einbinder, S., Shashar, N., Kiflawi, M., Kark, S., 2008. Descending to the twilight-zone: Changes in coral reef fish assemblages along a depth gradient down to 65 m. Marine Ecology Progress Series. 371, 253-262.

Bromley, R.G., 1978. Bioerosion of Bermuda Reefs. Paleogeogr.Paleoclimatol.Paleoecol. 23(3-4), 169-197.

Brown, B., Le Tissier, M., Howard, L.S., Charuchinda, M., Jackson, J.A., 1986. Asynchronous deposition of dense skeletal bands in *Porites lutea*. Mar.Biol. 93(1), 83-89.

Browne, N.K., Smithers, S.G., Perry, C.T., 2013. Carbonate and terrigenous sediment budgets for two inshore turbid reefs on the central Great Barrier Reef. Mar.Geol. 346, 101-123.

Bruggemann, J.H., van Kessel, A.M., van Rooij, J.M., Breeman, A.M., 1996. Bioerosion and sediment ingestion by the Caribbean parrotfish *Scarus vetula* and *Sparisoma viride*: Implications of fish size, feeding mode and habitat use. Marine Ecology Progress Series. 134(1-3), 59-71.

Bruno, J.F., Bertness, M.D., 2001. Habitat modification and facilitation in benthic marine communities. In: Bertness, M.D., Gaines, S.D., Hay, M.E. (Eds.), Marine community ecology. Sinaur, Sunderland, MA., pp. 201-218.

Bucher, D.J., Harriott, V.J., Roberts, L.G., 1998. Skeletal micro-density, porosity and bulk density of acroporid corals. J.Exp.Mar.Biol.Ecol. 228(1), 117-136.

Budd, A.F., Fukami, H., Smith, N.D., Knowlton, N., 2012. Taxonomic classification of the reef coral family Mussidae (Cnidaria: Anthozoa: Scleractinia). Zool.J.Linn.Soc. 166(3), 465-529.

Budd, A.F., 2000. Diversity and extinction in the Cenozoic history of Caribbean reefs. Coral Reefs. 19, 25-35.

Buddemeier, R.W., 1974. Environmental controls over annual and lunar monthly cycles in hermatypic coral calcification. In: Cameron, A.M., Cambell, B.M., Cribb, A.B., Endean, R., Jell, J.S., Jones, O.A., Mather, P., Talbot, F.H. (Eds.), Proceedings of the 2nd International Coral Reef Symposium. 2, pp. 259-268.

Bunkley-Williams, L., Morelock, J., Williams, E.H., 1991. Lingering effects of the 1987 mass bleaching of Puerto Rican coral reefs in mid to late 1988. J.Aquat.Anim.Health. 3(4), 242-247.

Campion-Alsumard, T., Romano, J.-., Peyrot-Clausade, M., Campion, J., Paul, R., 1993. Influence of some coral reef communities on the calcium carbonate budget of Tiahura reef (Moorea, French Polynesia). Mar.Biol. 115(4), 685-693.

Cantin, N.E., Cohen, A.L., Karnauskas, K.B., Tarrant, A.M., McCorkle, D.C., 2010. Ocean warming slows coral growth in the central Red Sea. Science. 329(5989), 322-325.

Cardoso, S.C., Soares, M.C., Oxenford, H.A., Cote, I.M., 2009. Interspecific differences in foraging behaviour and functional role of Caribbean parrotfish. Marine biodiversity records. 2, 1-6.

Carriquiry, J.D., Risk, M.J., Schwarcz, H.P., 1994. Stable isotope geochemistry of corals from Costa Rica as proxy indicator of the EL Niño/Southern Oscillation (ENSO). Geochim.Cosmochim.Acta. 58(1), 335-351.

Castillo, K.D., Ries, J.B., Weiss, J.M., 2011. Declining coral skeletal extension for forereef colonies of *Siderastrea siderea* on the Mesoamerican Barrier Reef System, southern Belize. PLoS ONE. 6(2), e14615. doi:10.1371/journal.pone.0014615.

Cerrano, C., Danovaro, R., Gambi, C., Pusceddu, A., Riva, A., Schiaparelli, S., 2010. Gold coral (*Savalia savaglia*) and gorgonian forests enhance benthic biodiversity and ecosystem functioning in the mesophotic zone. Biodivers.Conserv. 19(1), 153-167.

Chalker, B.E., Barnes, D.J., 1990. Gamma densitometry for the measurement of skeletal density. Coral Reefs. 9(1), 11-23.

Chan, Y., Pochon, X., Fisher, M.A., Wagner, D., Concepcion, G.T., Kahng, S.E., Toonen, R., Gates, R., 2009. Generalist dinoflagellate endosymbionts and host genotype diversity detected from mesophotic (67-100 m depths) coral *Leptoseris*. BMC Ecology. 9(1), 21.

Chave, K.E., Smith, S.V., Roy, K.J., 1972. Carbonate production by coral reefs. Mar.Geol. 12(2), 123-140.

Chazottes, V., Chevillotte, V., Dufresne, A., 2004. Caractérisation de la production particulaire par l'oursin Echinometra mathaei sur les récifs Indo-Pacifiques : Influence des peuplements coralliens et implications sur la dynamique sédimentaire. Geobios. 37(1), 13-22.

Chazottes, V., Le Campion-Alsumard, T., Peyrot-Clausade, M., 1995. Bioerosion rates on coral reefs: Interactions between macroborers, microborers and grazers (Moorea, French Polynesia). Palaeogeogr., Palaeoclimatol., Palaeoecol. 113, 189-198.

Cheng, N., Chiew, Y., 1999. Analysis of initiation of sediment suspension from bed-load. J.Hydraul.Eng. 125(8), 855-861.

Cherubin, L.M., Nemeth, R.S., Idrisi, N., 2011. Flow and transport characteristics at an *Epinephelus guttatus* (red hind grouper) spawning aggregation site in St. Thomas (U.S. Virgin Islands). Ecol.Model. 222(17), 3132-3148.

Chevillon, C., 1991. Sedimentology of the Great Northern Lagoon of New Caledonia: Description of depositional environments using principal component analysis. Proceedings of the Congress of the International Society for Reef Studies. Moumea, New Caledonia, pp. 165-172.

Chollett, I., Mumby, P.J., 2013. Reefs of last resort: Locating and assessing thermal refugia in the wider Caribbean. Biol.Conserv. 167, 179-186.

Connell, J.H., 1978. Diversity in tropical rain forests and coral reefs. Science. 199(4335), 1302-1310.

Cooper, G.R.J., Cowan, D.R., 2008. Comparing time series using wavelet-based semblance analysis. Comput.Geosci. 34(2), 95-102.

Craig, H., 1957. Isotopic standards for carbon and oxygen and correction factors for mass-spectrometric analysis of carbon dioxide. Geochim.Cosmochim.Acta. 12(1), 133-149.

Crook, E.D., Cohen, A.L., Rebolledo-Vieyra, M., Hernandez, L., Paytan, A., 2013. Reduced calcification and lack of acclimatization by coral colonies growing in areas of persistent natural acidification. Proc.Natl.Acad.Sci.U.S.A. 110(27), 11044-11049.

Dalzell, P., Adams, T.J.H., Polunin, N.V.C., 1996. Coastal fisheries in the Pacific islands. In: Oceanography and Marine Biology: Annual Review, pp. 395-531.

Darwin, C.R., 1842.The Structure and Distribution of Coral reefs. Smith, Elder and Co., London.

Dávalos-Dehullu, E., Hernández-Arana, H., Carricart-Ganivet, J.P., 2008. On the causes of density banding in skeletons of corals of the genus Montastraea. J.Exp.Mar.Biol.Ecol. 365(2), 142-147.

Davies, P.S., 1989. Short-term growth measurements of corals using an accurate buoyant weighing technique. Mar.Biol. 101(3), 389-395.

Della Porta, G., Kenter, J.A.M., Bahamonde, J.R., Immenhauser, A., Villa, E., 2003. Microbial boundstone dominated carbonate slope (Upper Carboniferous, N Spain): Microfacies, lithofacies distribution and stratal geometry. Facies. 49(1), 175-207.

Dill, M.A., Seyrafian, A., Vaziri-Moghaddam, H., 2012. Palaeoecology of the Oligocene-Miocene Asmari Formation in the Dill Anticline (Zagros Basin, Iran). Neues Jahrbuch für Geologie und Paläontologie.Abhandlungen. 263(2), 167-184.

Dodge, R.E., Szmant, A.M., Garcia, R., Swart, P.K., Forester, A., Leder, J.J., 1993. Skeletal structural basis of density banding in the reef coral *Montastrea annularis.* In: Richmond, R.H. (Ed.), Proceedings of the 7th International Coral Reef Symposium. University of Guam Press, UOG Station, Guam1, pp. 186-195.

Dodge, R.E., Brass, G.W., 1984. Skeletal extension, density, and calcification of the reef coral, *Montastrea Annularis*: St. Croix, U.S. Virgin Islands. Bulletin of Marine Science. 34(2), 288-307.

Dodge, R.E., Thomson, J., 1974. The natural radiochemical and growth records in contemporary hermatypic corals from the Atlantic and Caribbean. Earth Planet.Sci.Lett. 23(3), 313-322.

Donnelly, T.W., 1989. Geologic history of the Caribbean and Central American. In: Bally, A.W., Palmer, A.R. (Eds.), The Geology of North America - An overview. Geological Society of America, Boulder, Colorado, pp. 299-321.

Donnelly, T.W., 1964. Evolution of Eastern Greater Antillean Island Arc. AAPG Bull. 48(5), 680-696.

Donner, S.D., Knutson, T.R., Oppenheimer, M., 2007. Model-based assessment of the role of human-induced climate change in the 2005 Caribbean coral bleaching event. Proceedings of the National Academy of Sciences. 104(13), 5483-5488.

Druffel, E.M., 1981. Radiocarbon in annual coral rings from the eastern Tropical Pacific Ocean. Geophys.Res.Lett. 8(1), 59-62.

Dryden, C., Cortes, J., Newman, S., Sanchez, C., Williams, S., Polunin, N., 2012. Future of reefs in a changing environment: An ecosystem approach to managing Caribbean coral reefs in the face of climate change. Preliminary report on the relationship between architectural complexity and reef biodiversity. In: Force Project (Ed.), 7th Framework Programme, pp. 10.

Duane, D.B., 1964. Significance of skewness in recent sediments, western Pamlico Sound, North Carolina. Journal of Sedimentary Research. 34(4), 864-874.

Dullo, W., 2005. Coral growth and reef growth: A brief review. Facies. 51(1-4), 33-48.

Dunham, R.J., 1962. Classification of carbonate rocks according to depositional texture Memoir - American Association of Petroleum Geologists, 108-121.

Dustan, P., Doherty, O., Pardede, S., 2013. Digital reef rugosity estimates coral reef habitat complexity. PLoS ONE. 8(2), e57386.

Dustan, P., Halas, J.C., 1987. Changes in the reef-coral community of Carysfort reef, Key Largo, Florida: 1974 to 1982. Coral Reefs. 6(2), 91-106.

Dustan, P., 1982. Depth-dependent photoadaptation by zooxanthellae of the reef coral *Montastrea annularis*. Marine Biology. 68, 253-264.

Dustan, P., 1975. Growth and form in the reef-building coral *Montastrea annularis*. Mar.Biol. 33(2), 101-107.

Eakin, C.M., 2001. A tale of two enso events: Carbonate budgets and the influence of two warming disturbances and intervening variability, Uva Island, Panama. Bull.Mar.Sci. 69(1), 171-186.

Eakin, C.M., 1996. Where have all the carbonates gone? A model comparison of calcium carbonate budgets before and after the 1982 -1983 El Niño Uva Island in the eastern Pacific. Coral Reefs. 15(2), 109-119.

Eberhard, G., Lomando , A.J., 1999. Recent sedimentary facies of isolated carbonate platforms, Belize-Yucatan System, Central America. Journal of Sedimentary Research. 69(3), 747-763.

Eckman, J.E., Duggins, D.O., Sewell, A.T., 1989. Ecology of under story kelp environments. I. Effects of kelps on flow and particle transport near the bottom. J.Exp.Mar.Biol.Ecol. 129(2), 173-187.

Edinger, E.N., Limmon, G.V., Jompa, J., Widjatmoko, W., Heikoop, J.M., Risk, M.J., 2000. Normal coral growth rates on dying reefs: Are coral growth rates good indicators of reef health? Marine Pollution Bulletin. 40, 404-425.

Edinger, E.N., Risk, M.J., 1994. Oligocene-Miocene extinction and geographic restriction of Caribbean corals: Roles of turbidity, temperature, and nutrients. Palaios. 9, 576-598.

Einbinder, S., Brokovich, E., Tchernov, D., 2009. Changes in morphology and diet of the coral *Stylophora pistillata* along a depth gradient. Marine Ecology Progress Series. 381, 167-174.

Eldredge, L.G., Evenhuts, N.L., 2003. Hawaii's Biodiversity: A detailed assessment of the numbers of species in the Hawaiian islands. Bishop Mus. Occas. Pap. 76, 28.

Emiliani, C., Hudson, J.H., Shinn, E.A., George, R.Y., 1978. Oxygen and carbon isotopic growth record in a reef coral from the Florida Keys and a deep-sea coral from Blake Plateau. Science. 202(4368), 627-629.

Englebert, N., Bongaerts, P., Muir, P., Hay, K.B., Hoegh-Guldberg, O., 2014. Deepest zooxanthellate corals of the Great Barrier Reef and Coral Sea. Marine Biodiversity, 1-2.

Eyre, B.D., Andersson, A.J., Cyronak, T., 2014. Benthic coral reef calcium carbonate dissolution in an acidifying ocean. Nature Climate Change, DOI: 10.1038/NCLIMATE2380.

Fabricius, K.E., Langdon, C., U thicke, S., Humphrey, C., Noonan, S., De'ath, G., Okazaki, R., Muehllehner, N., Glas, M.S., Lough, J.M., 2011. Losers and winners in coral reefs acclimatized to elevated carbon dioxide concentrations. Nature Clim.Change. 1(3), 165-169.

Fairbanks, R.G., Dodge, R.E., 1979. Annual periodicity of the $^{18}O/^{16}O$ and $^{13}C/^{12}C$ ratios in the coral Montastrea annularis. Geochim.Cosmochim.Acta. 43(7), 1009-1020.

Fautin, D.G., Buddemeier, R.W., 2004. Adaptive bleaching: A general phenomenon. Hydrobiologia. 178, 459-467.

Fiechter, J., Steffen, K.L., Mooers, C.N.K., Haus, B.K., 2006. Hydrodynamics and sediment transport in a southeast Florida tidal inlet. Estuar.Coast.Shelf Sci. 70(1–2), 297-306.

Flood, P.G., Scoffin, T.P., 1978. Reefal sediments of the Northern Great Barrier Reef. Philos. Trans. R. Soc. Lond. A. 291(1378), 55-68.

Flügel, E., Flügel-Kahler, E., 1992. Phanerozoic reef evolution: Basic questions and data base. Facies. 26(1), 167-277.

Folk, R.L., 1974a. Petrology of Sedimentary Rocks. The Walter Geology Library, Austin, Texas.

Folk, R.L., 1974b. The natural history of crystalline calcium carbonate: Effect of magnesium content and salinity. Journal of Sedimentary Research. 44(1), 40-53.

Folk, R.L., Robles, R., 1964. Carbonate sands of Isla Perez, Alacran Reef Complex, Yucatan. The Journal of Geology. 72(3), 225-291.

Folk, R.L., Ward, W.C., 1957. Brazos river bar: A study in the significance of grain size parameters. Journal of Sedimentary Research. 27(1), 3-26.

Folk, R.L., 1954. The distinction between grain size and mineral composition in sedimentary-rock nomenclature. J.Geol. 62(4), 344-359.

Ford, M.R., Kench, P.S., 2012. The durability of bioclastic sediments and implications for coral reef deposit formation. Sedimentology. 59(3), 830-842.

Frade, P.R., Bongaerts, P., Winkelhagen , A.J.S., Tonk, L., Bak, R.P.M., 2008a. In situ photobiology of corals over large depth ranges: A multivariate analysis on the roles of environment, host, and algal symbiont. Limnol.Oceanogr. 53(6), 2711-2723.

Frade, P.R., De Jongh, F., Vermeulen, F., Van Bleijswijk, J., Bak, R.P.M., 2008b. Variation in symbiont distribution between closely related coral species over large depth ranges. Mol.Ecol. 17, 691-703.

Fricke, H., Meischner, D., 1985. Depth limits of Bermudan scleractinian corals: A submersible survey. Mar.Biol. 88(2), 175-187.

Fricke, H.W., Schuhmacher, H., 1983. The depth limits of Red Sea stony corals: An ecophysiological problem (a deep diving survey by submersible). Mar.Ecol. 4(2), 163-194.

Fricke, H.W., Vareschi, E., Schlichter, D., 1987. Photoecology of the coral *Leptoseris fragilis* in the Red Sea twilight zone (an experimental study by submersible). Oecologia. 73, 371-381.

Friedman, G.M., Sanders, J.E., 1978. Principles of sedimentology. Wiley, New York.

Friedman, G.M., Amiel, A.J., Schneidermann, N., 1974. Submarine cementation in reefs; example from the Red Sea. Journal of Sedimentary Research. 44(3), 816-825.

Friedman, G.M., 1967. Dynamic processes and statistical parameters compared for size frequency distribution of beach and river sands. Journal of Sedimentary Research. 37(2), 327-354.

Fütterer, D.K., 1974. Significance of the boring sponge Cliona for the origin of fine grained material of carbonate sediments. Journal of Sedimentary Research. 44(1), 79-84.

Gabrié, C., Montaggioni, L., 1982. Sediments from fringing reefs of Réunion Island, Indian Ocean. Sediment.Geol. 31(3–4), 281-301.

Garcia-Sais, J.R., Appeldoorn, R., Battista, T., Bauer, L., Bruckner, A., Bruckner, A., Caldow, C., Carrubba, L., Corredor, J., Diaz, E., Lilyestrom, C., Garcia-Moliner, G., Hernandez-Delgado, E., Menza, C., Morell, J., Pait, A., Sabater, J., Weil, E., Williams, E., Williams, S., 2008. The state of coral reef ecosystems of the commonwealth of Puerto Rico. In: Waddell, J., Clarke, A. (Eds.), The state of coral reef ecosystems of the United States and Pacific Freely Associated States: 2008 NOAA Technical Memorandum NOS NCCOS 78. NOAA/NCCOS Center for Coastal Monitoring and Assessment's Biogeography Team, Silver Spring, MD, pp. 77-116.

Gardner, T.A., Côté, I.M., Gill, J.A., Grant, A., Watkinson, A.R., 2003. Long-term region-wide declines in Caribbean corals. Science. 301, 958-960.

Garrett, P., Smith, D.L., Wilson, A.O., Patriquin, D., 1971. Physiography, ecology, and sediments of two Bermuda patch reefs. J.Geol. 79(6), 647-668.

Geister, J., 1977. The influence of wave exposure on the ecological zonation of Caribbean coral reefs. Proceeding of the 3rd International Coral Reef Symposium, 23-29.

Gherardi, D.F.M., Bosence, D.W.J., 2005. Late Holocene reef growth and relative sea-level changes in Atol das Rocas, equatorial South Atlantic. Coral Reefs, 24(2), 264-272.

Gibbs, R.J., Matthews, M.D., Link, D.A., 1971. The relationship between sphere size and settling velocity. Journal of Sedimentary Research. 41(1), 7-18.

Ginsburg, R., 1956. Environmental relationships of grain size and constituent particles in some South Florida carbonate sediments. AAPG Bull. 40(10), 2384-2427.

Ginsburg, R.N., Harrison, A., Weinstein, D.K., Smith, T.B., 2012. Potential Extent of Mesophotic Coral Ecosystems Across Tropical North America. AGU Fall Meeting (unpublished poster).

Ginsburg, R.N., Reed, J., 2008. Mesophotic Coral Reefs (30-100m), A frontier of reef exploration. Abstracts from the 11th International Coral Reef Symposium, 384.

Ginsburg, R.N., Harris, P.M., Eberli, G.P., Swart, P.K., 1991. The growth potential of a bypass margin, Great Bahama Bank. Journal of Sedimentary Research. 61(6), 976-987.

Ginsburg, R.N., 1983. Geological and biological roles of cavities in coral reefs. In: Barnes, D.J. (Ed.), Perspectives on coral reefs. Australian Institute of Marine Science, Townsville, pp. 148-153.

Ginsburg, R.N., 1974. Introduction to comparative sedimentology of carbonates. The American Association of Petroleum Geologists Bulletin. 58(5), 781-786.

Ginsburg, R.N., Schroeder, J.H., 1973. Growth and submarine fossilization of algal cup reefs, Bermuda*. Sedimentology. 20(4), 575-614.

Ginsburg, R.N., Marszalek, D.S., Schneidermann, N., 1971. Ultrastructure of carbonate cements in a Holocene algal reef of Bermuda. Journal of Sedimentary Research. 41(2), 472-482.

Gischler, E., Swart, P.K., Lomando, A.J., 2009. Stable isotopes of carbon and oxygen in modern sediments of carbonate platforms, barrier reefs, atolls and ramps: Patterns and implications. In: Swart, P.K., Eberli, G.P., McKenzie, J.A., Jarvis, I., Stevens, T. (Eds.), Perspectives in Carbonate Geology: A Tribute to the Career of Robert Nathan Ginsburg . John Wiley & Sons, Ltd, Chichester, West Sussex, UK, pp. 61-74.

Gischler, E., 2008. Accretion patterns in Holocene tropical coral reefs: Do massive coral reefs in deeper water with slowly growing corals accrete faster than shallower branched coral reefs with rapidly growing corals? Int.J.Earth Sci. 97(4), 851-859.

Gischler, E., Hudson, J.H., 1998. Holocene development of three isolated carbonate platforms, Belize, Central America. Mar.Geol. 144(4), 333-347.

Glynn, P.W., 1997. Bioerosion and coral-reef growth: A dynamic balance. In: Birkeland, C. (Ed.), Life and death of coral reefs. Chapman & Hall, New York, Albany etc., pp. 68-95.

Glynn, P.W., 1996. Coral reef bleaching: Facts, hypotheses and implications. Global Change Biology. 2(6), 495-509.

Glynn, P.W., 1988. El Nino-Southern Oscillation 1982-1983: Nearshore population, community, and ecosystem responses. Annu.Rev.Ecol.Syst. 19(1), 309-346.

Goreau, T.F., Land, L.S., 1974. Fore-reef morphology and depositional processes, north Jamaica. In: Laporte, L.F. (Ed.), Reefs in time and space. Society of Economic Paleontologists and Mineralogists, Tulsa, OK, pp. 77-89.

Goreau, T.F., Goreau, N.I., 1973. The ecology of Jamaican coral reefs II: Geomorphology, zonation and sedimentary phases. Bulletin of Marine Science. 23, 399-464.

Goreau, T.F., Hartman, W.D., 1963. Control of coral reefs by boring sponges. In: Sognnaes, R.F. (Ed.), Mechanisms of Hard Tissue Destruction. AAAS Publishing, pp. 25-54.

Goreau, T.F., 1959. The ecology of Jamaican coral reefs I. Species composition and zonation. Ecology. 40(1), 67-90.

Goreau, T.J., 1992. Bleaching and reef community change in Jamaica: 1951-1991. Am.Zool. 32(6), 683-695.

Gori, A., Viladrich, N., Gili, J.M., Kotta, M., Cucio, C., Magni, L., Bramanti, L., Rossi, S., 2012. Reproductive cycle and trophic ecology in deep versus shallow populations of the Mediterranean gorgonian Eunicella singularis (Cap de Creus, northwestern Mediterranean Sea). Coral Reefs. 31(3), 823-837.

Graham, N.A.J., Nash, K.L., 2013. The importance of structural complexity in coral reef ecosystems. Coral Reefs. 32(2), 315-326.

Grammer, G.M., Crescini, C.M., McNeill, D.F., Taylor, L.H., 1999. Quantifying rates of syndepositional marine cementation in deeper platform environments - New insight into a fundamental process. Journal of Sedimentary Research. 69(1), 202-207.

Grammer, G.M., Ginsburg, R.N., 1992. Highstand versus lowstand deposition on carbonate platform margins: Insights from Quatenary foreslopes in the Bahamas. Marine Geology. 103, 125-136.

Grammer, M.G., Ginsburg, R.N., Swart, P.K., McNeill, D.F., Jull, A.J.T., Prezbindowski, D.R., 1993. Rapid growth rates of syndepositional marine aragonite cements in steep marginal slope deposits, Bahamas and Belize. J.Sediment.Petrol. 63(5), 983-989.

Gratwicke, B., Speight, M.R., 2005. Effects of habitat complexity on Caribbean marine fish assemblages. Mar.Ecol.Prog.Ser. 292, 301-310.

Gray, S.C., Gobbi, K.L., Narwold, P.V., 2008. Comparison of sedimentation in bays and reefs below developd versus underveloped watersheds on St. John, U.S. Virgin Islands. Proceedings of the 11th International Coral Reef Symposium, Ft. Lauderdale, Florida. 1, pp. 351-356.

Greenstein, B.J., Pandolfi, J.M., 2003. Taphonomic alteration of reef corals; effects of reef environment and coral growth form: II, The Florida Keys Palaios, 18(6;), 495-509.

Greenstein, B.J., Curran, H.A., Pandolfi, J.M., 1998. Shifting ecological baselines and the demise of *Acropora cervicornis* in the western North Atlantic and Caribbean Province: A Pleistocene perspective. Coral Reefs. 17(3), 249-261.

Grigg, R., 2006. Depth limit for reef building corals in the Au'au Channel, S.E. Hawaii. Coral Reefs. 25(1), 77-84.

Grottoli, A.G., Rodrigues, L.J., Palardy, J.E., 2006. Heterotrophic plasticity and resilience in bleached corals. Nature. 440(7088), 1186-9.

Grottoli, A.G., Wellington, G.M., 1999. Variability of stable isotopes and maximum linear extension in reef-coral skeletons at Kaneohe Bay, Hawaii. Mar.Biol. 135(3), 437-449.

Guzman, H.M., 1991. Restoration of coral reefs in Pacific Costa Rica. Conserv.Biol. 5(2), 189-195.

Gygi, R.A., 1975. *Sparisoma viride* (Bonnaterre), the spotlight parrot a major sediment producer on coral of Bermuda. Eclogae Geologicae Helvetiae. 68(2), 327-359.

Gygi, R.A., 1969. An estimate of the erosional effect of *Sparisoma viride* (Bonnaterre), the green parrotfish, on some Bermuda reefs. In: Ginsburg, R.N., Garrett, P. (Eds.), Reports of Research: 1968 Seminar on Organism-Sediment Interrelationships, Bermuda Biological Station for Research, pp. 137-143.

Hammer, Ø., Harper, D.A.T., Ryan, P.D., 2001. PAST: Paleontological statistics software package for education and data analsysis. Palaeontologia Electronica. 4(1), 9.

Harmelin-Vivien, M.L., Laboute, P., 1986. Catastrophic impact of hurricanes on atoll outer reef slopes in the Tuamotu (French Polynesia). Coral Reefs. 5(2), 55-62.

Harney, J.N., Fletcher, C.H., 2003. A budget of carbonate framework and sediment production, Kailua Bay, Oahu, Hawaii. Journal of Sedimentary Research. 73(6), 856-868.

Harris, D.L., Vila-Concejo, A., Webster, J.M., 2014. Geomorphology and sediment transport on a submerged back-reef sand apron: One Tree Reef, Great Barrier Reef. Geomorphology. 222, 132-142.

Harris, P.T., Bridge, T.C.L., Beaman, R.J., Webster, J.M., Nichol, S.L., Brooke, B.P., 2012. Submerged banks in the Great Barrier Reef, Australia, greatly increase available coral reef habitat. ICES Journal of Marine Science: Journal du Conseil. 70, 284-293.

Hart, D.E., Kench, P.S., 2007. Carbonate production of an emergent reef platform, Warraber Island, Torres Strait, Australia. Coral Reefs. 26(1), 53-68.

Harvey, N., Hopley, D., 1982. The relationship between modern reef morphology and pre-Holocene substrate in the Great Barrier Reef Province. In: Gomez, E.D., Birkeland, C. (Eds.), Proceedings from the 4th International Coral Reef Symposium. 1, pp. 549-554.

Hassan, M., 1998. Modification of carbonate substrata by bioerosion and bioaccretion on coral reefs of the Red Sea. (Ph.D Dissertation), Christian-Albrechts-Universität zu Kiel, Shaker Verlag, Aachen.

Heck, K.L., Jr., Wetstone, G.S., 1977. Habitat complexity and invertebrate species richness and abundance in tropical seagrass meadows. J.Biogeogr. 4(2), 135-142.

Heckel, P.H., 1974. Carbonate buildups in the geologic record: A review. Special Publication - Society of Economic Paleontologists and Mineralogists. 18, 90-154.

Hein, F.J., Risk, M.J., 1975. Bioerosion of coral heads: Inner patch reefs, Florida reef tract. Bulletin of Marine Science. 25(1), 133-138.

Helmle, K.P., Dodge, R.E., 2011. Sclerochronology. In. Hopley, D. (Ed.), Encyclopedia of Modern Coral Reefs: Structure, Form and Process, Springer Netherlands, 958-966.

Helmle, K.P., Dodge, R.E., Swart, P.K., Gledhill, D.W., Eakin, C.M., 2011. Growth rates of Florida corals from 1937 to 1996 and their response to climate change. Nature Communications. 2, 215.

Helmle, K.P., Kohler, K.E., Dodge, R.E., 2002. Relative optical densitometry and the coral x-radiograph densitometry system: CoralXDS Presented Poster (omitted from abstract book, but included in program). International Society of Reef Studies 2002 European MeetingCambridge, England.

Herzlieb, S., Kadison, E., Blondeau, J., Nemeth, R.S., 2005. Comparative assessment of coral reef systems located along the insular platform of St. Thomas, US Virgin Islands and the relative effects of natural and human impacts. Proceedings of the 10th International Coral Reef Symposium. 4, pp. 1144-1151.

Hicks, G.R.F., 1980. Structure of phytal harpacticoid copepod assemblages and the influence of habitat complexity and turbidity. J.Exp.Mar.Biol.Ecol. 44(2), 157-192.

Highsmith, R.C., Lueotow, R.L., Schonberg, C.L., 1983. Growth and bioerosion of three massive corals on the Belize barrier reef. Marine Ecology-Progress Series. 13(2-3), 261-271.

Highsmith, R.C., 1981. Coral bioerosion: Damage relative to skeletal density. The American Naturalist. 117(2), 193-198.

Highsmith, R.C., 1979. Coral growth rates and environmental control of density banding. J.Exp.Mar.Biol.Ecol. 37(2), 105-125.

Hodgson, E.S., Smith, C.L., 1990. Coral reef communities as prime resources for analysis of evolution and physiology of behavior. American Zoologist. 30(3), 559-594.

Hoegh-Guldberg, O., Mumby, P.J., Hooten, A.J., Steneck, R.S., Greenfield, P., Gomez, E., Harvell, C.D., Sale, P.F., Edwards, A.J., Caldiera, K., Knowlton, N., Eakin, C.M., Iglesias-Prieto, R., Muthiga, N., Bradbury, R.H., Dui, A., Hatziolos, M.E., 2007. Coral reefs under rapid climate change and ocean acidification. Science. 318, 1737-1742.

Hoffmeister, J.E., Ladd, H.S., 1944. The antecedent-platform theory. J.Geol. 52(6), 388-402.

Holmes, C.W., Kindinger, J.L., 1985. Late Pleistocene—Holocene geology of the central Virgin Island Platform. Mar.Geol. 64(1–2), 41-64.

Holmes, G., Ortiz, J., Schönberg, C.H.L., 2009. Bioerosion rates of the sponge *Cliona orientalis* Thiele, 1900: Spatial variation over short distances. Facies. 55(2), 203-211.

Holmes, K.E., Edinger, E.N., Hariyadi, Limmon, G.V., Risk, M.J., 2000. Bioerosion of live massive corals and branching coral rubble on Indonesian coral reefs. Marine Pollution Bulletin. 40(7), 606-617.

Holmes, K.E., 1997. Eutrophication and its effect on bioeroding sponge communities. In: Lessios, H.A., MacIntyre, I.G. (Eds.), Proceedings of the 8th International Coral Reef Symposium. Smithsonian Tropical Research InstituteBalboa, Panama. 2, pp. 1411-1416.

Holstein, D.M., 2013. Vertical connectivity in mesophotic coral ecosystems. (Ph.D Dissertation). University of Miami, ProQuest Dissertations and Theses.

Hoskin, C.M., Reed, J.K., Mook, D.H., 1986. Production and off-bank transport of carbonate sediment, Black Rock, southwest Little Bahama Bank. Mar.Geol. 73(1), 125-144.

Hoskin, C.M., Geier, J.C., Reed, J.K., 1983. Sediment produced from abrasion of the branching stony coral Oculina varicosa. Journal of Sedimentary Research. 53(3), 779-786.

Hoskin, C.M., 1966. Coral pinnacle sedimentation, Alacran Reef lagoon, Mexico. Journal of Sedimentary Research. 36(4), 1058-1074.

Hubbard, D.K., 2009. Depth and species-related patterns of Holocene reef accretion in the Caribbean and western Atlantic: A critical assessment of existing models. In: Swart, P.K., Eberli, G.P., McKenzie, J.A. (Eds.), Perspectives in Carbonate Geology: A Tribute

to the Career of Robert Nathan Ginsburg, International Association of Sedimentologists Special Publication. Blackwell, Oxford, pp. 1-18.

Hubbard, D.K., Burke, R.B., Gill, I.P., Ramirez, W.R., Sherman, C., 2008. Coral-reef Geology: Puerto Rico and the US Virgin Islands. In: Riegl, B.M., Dodge, R.E. (Eds.), Coral Reefs of the USA. Springer Netherlands, pp. 263-302.

Hubbard, D.K., Zankl, H., Van Heerden, I., Gill, I.P., 2005. Holocene reef development along the northeastern St. Croix Shelf, Buck Island, U.S. Virgin Islands Journal of Sedimentary Research, 75(1), 97-113.

Hubbard, D.K., 1992. Hurricane-induced sediment transport in open-shelf tropical systems; an example from St. Croix, U.S. Virgin Islands. Journal of Sedimentary Research. 62(6), 946-960.

Hubbard, D.K., Miller, A.I., Scaturo, D., 1990. Production and cycling of calcium carbonate in a shelf-edge reef system (St. Croix, U.S. Virgin Islands) : Applications to the nature of reef systems in the fossil record. Journal of Sedimentary Petrology, 60(3:), 335-360.

Hubbard, D.K., 1989. The shelf-edge reefs of Davis and Cane Bays, Northwestern St. Croix, U.S.V.I. In: Hubbard, D.K. (Ed.), Terrestrial and marine geology of St. Croix, U. S. Virgin Islands. Special Publication No. 8. West Indies Laboratory, St. Croiz, U.S. Virgin Islands, pp. 167-180.

Hubbard, D.K., 1987. A general review of sedimentation as it relates to environmental stress in the Virgin Islands Biosphere Reserve and the Eastern Caribbean in general, Biosphere Reserve Research Report(20), 44.

Hubbard, D.K., Scaturo, D., 1985. Growth rates of seven species of scleractinean corals from Cane Bay and Salt River, St. Croix, USVI. Bulletin of Marine Science. 36(2), 325-338.

Hubbard, D.K., Sadd, J.L., Miller, A.I., Gill, I.P., Dill, R.F., 1981. The production, transportation, and deposition of carbonate sediments on the insular shelf of St. Croix, U.S. Virgin Islands FDU/WIL Tech Rpt MG-1, St. Croix, USVI, 145.

Hudson, J.H., 1982. Response of *Montastrea annularis* to environmental change in the Florida Keys. In: Gomez, E.D., Birkeland, C.E., Buddemeier, R.W., Johannes, R.E., Marsh, J.A., Tsuda, R.T. (Eds.), Proceedings from the 4th International Coral Reef Symposium. 3, pp. 233-240.

Hudson, J.H., 1977. Long-term bioerosion rates on a Florida reef: A new method. Proceedings of the 3rd International Coral Reef Symposium. Miami, Florida, pp. 491-498.

Hudson, J.H., Shinn, E.A., Halley, R.B., Lidz, B., 1976. Sclerochronology: A tool for interpreting past environments. Geology. 4(6), 361-364.

Hughes, T.P., Baird, A.H., Bellwood, D.R., Card, M., Connolly, S.R., Folke, C., Grosberg, R., Hoegh-Guldberg, O., Jackson, J.B.C., Kleypas, J., Lough, J.M., Marshall, P., Nyström, N., Palumbi, S.R., Pandolfi, J.M., Rosen, B., Roughgarden, J., 2003. Climate change, human impacts, and the resilience of coral reefs. Science. 301(5635), 929-933.

Hughes, T.P., 1994. Catastrophes, phase-shifts, and large-scale degradation of a caribbean coral reef. Science. 265(5178), 1547-1551.

Huston, M., 1985. Variation in coral growth rates with depth at Discovery Bay, Jamaica. Coral Reefs. 4(1), 19-25.

Hutchings, P., 2008. Role of polychaetes in bioerosion of coral substrates. In: Wisshak, M., Tapanila, L. (Eds.), Curent Developments in Bioerosion. Springer-Verlag, Berlin, Heidelberg, pp. 249-264.

Hutchings, P.A., Kiene, W.E., Cunningham, R.B., Donnelly, C., 1992. Spatial and temporal patterns of non-colonial boring organisms (polychaetes, sipunculans and bivalve molluscs) in Porites at Lizard Island, Great Barrier Reef. Coral Reefs. 11(1), 23-31.

Hutchings, P.A., 1986. Biological destruction of coral reefs. Coral Reefs. 4, 239-252.

Insalaco, E., Hallam, A., Rosen, B., 1997. Oxfordian (Upper Jurassic) coral reefs in Western Europe: Reef types and conceptual depositional model. Sedimentology. 44(4), 707-734.

Insalaco, E., 1996. Upper Jurassic microsolenid biostromes of northern and central Europe: Facies and depositional environment. Palaeogeogr., Palaeoclimatol., Palaeoecol. 121(3–4), 169-194.

Jackson, J.B.C., 1997. Reefs since Columbus. Coral Reefs. 16(1), S23-S32.

James, N.P., Ginsburg, R.N., 1979. The seaward margin of Belize barrier and atoll reefs: Morphology, sedimentology, organism distribution and late Quaternary history. Blackwell Scientific Publications, Osney Mead, Oxford.

James, N.P., Ginsburg, R.N., Marszalek, D.S., Choquette, P.W., 1976. Facies and fabric specificity of early subsea cements in shallow Belize (British Honduras) reefs. Journal of Sedimentary Research. 46(3), 523-544.

Jell, J.S., Maxwell, W.H.G., McKellar, R.G., 1965. The significance of the larger Foraminifera in the Heron island reef sediments. Journal of Paleontology. 39(2), 273-279.

Jindrich, V., 1969. Recent carbonate sedimentation by tidal channels in the lower Florida Keys. Journal of Sedimentary Research. 39(2), 531-553.

Jolly, W.T., Lidiak, E.G., Dickin, A.P., 2006. Cretaceous to Mid-Eocene pelagic sediment budget in Puerto Rico and the Virgin Islands (northeast Antilles Island arc). Geologica acta. 4(1-2), 35-62.

Jordan, C.F., 1973. Carbonate facies and sedimentation of patch reefs off Bermuda. AAPG Bulletin. 57(1), 42-54.

Kadison, E., Nemeth, R.S., Herzlieb, S., Blondeau, J., 2006. Temporal and spatial dynamics of *Lutjanus cyanopterus* (Pisces: Lutjanidae) and *L. jocu* spawning aggregations in the United States Virgin Islands. Revista de Biología Tropical. 54 (suppl. 3), 69-78.

Kahng, S.E., Copus, J.M., Wagner, D., 2014. Recent advances in the ecology of mesophotic coral ecosystems (MCEs). Current Opinion in Environmental Sustainability. 7(0), 72-81.

Kahng, S.E., Garcia-sais, J.R., Spalding, H.L., Brokovich, E., Wagner, D., Weil, E., Hinderstein, L., Toonen, R.J., 2010. Community ecology of mesophotic coral reef ecosystems. Coral Reefs. 29(2), 255-275.

Kahng, S.E., Kelley, C., 2007. Vertical zonation of megabenthic taxa on a deep photosynthetic reef (50–140 m) in the Au'au Channel, Hawaii. Coral Reefs. 26(3), 679-687.

Kane, C., Kosaki, R.K., Wagner, D., 2014. High levels of mesophotic reef fish endemism in the Northwestern Hawaiian Islands. Bull.Mar.Sci. 90(2), 693-703.

Kench, P.S., 1998. A currents of removal approach for interpreting carbonate sedimentary processes. Mar.Geol. 145(3–4), 197-223.

Kench, P.S., McLean, R.F., 1997. A comparison of settling and sieve techniques for the analysis of bioclastic sediments. Sediment.Geol. 109(1), 111-119.

Kench, P.S., McLean, R.F., 1996. Hydraulic characteristics of bioclastic deposits: New possibilities for environmental interpretation using settling velocity fractions. Sedimentology. 43(3), 561-570.

Kennedy, E. ., Perry, C. ., Halloran, P. ., Iglesias-Prieto, R., Schönberg, C. .L., Wisshak, M., Form, A. ., Carricart-Ganivet, J. ., Fine, M., Eakin, C. ., Mumby, P. ., 2013. Avoiding coral reef functional collapse requires local and global action. Current Biology. 23(10), 912-918.

Kiene, W.E., Hutchings, P.A., 1994. Bioerosion experiments at Lizard Island, Great Barrier Reef. Coral Reefs. 13, 91-98.

Kiene, W.E., Hutchings, P.A., 1993. Long-term bioerosion of experimental coral substrates from Lizard Island, Great Barrier ReefIn: Richmond, R.H. (Ed.), Proceedings from the 7th International Coral Reef Symposium. University of Guam Press, UOG Station, Guam1, pp. 397-403.

Kiene, W.E., 1988a. Biological destruction on the Great Barrier Reef. (Ph.D Dissertation). 361.

Kiene, W.E., 1988b. A model of bioerosion on the Great Barrier Reef.In: Choat, J.H., Barnes, D., Borowitzka, M.A., Coll, J.C., Davies, P.J., Flood, P., Hatcher, B.G., Hopley, D., Hutchings, P.A., Kinsey, D.W., Orme, G.R., Pichon, M., Sale, P.F., Sammarco, P.W., Wallace, C., Wilkinson, C., Wolanski, E., Bellwood, O. (Eds.), Proceedings from the 6th International Coral Reef Symposium. Plenary Addressess and Status review, Townsville, Australia. 3, pp. 449-454.

Kinsey, D.W., 1985. Metabolism, calcification and carbon production: 1 systems level studiesIn: Gabrié, C., Salvat, B. (Eds.), Proceedings of the 5th International Coral Reef CongressTahiti.4, pp. 505-526.

Klaus, J.S., Murray, S.T., Swart, P.K., McNeill, D.F., 2013. Resource partitioning and paleoecology of Neogene free-living corals as determined from skeletal stable isotope composition. Bull.Mar.Sci. 89(4), 937-954.

Klaus, J.S., Lutz, B.P., McNeill, D.F., Budd, A.F., Johnson, K.G., Ishman, S.E., 2011. Rise and fall of Pliocene free-living corals in the Caribbean. Geology. 39(4), 375-378.

Klaus, J.S., Budd, A.F., 2003. Comparison of Caribbean coral reef communities before and after Plio-Pleistocene faunal turnover: Analyses of two Dominican Republic reef sequences. Palaios. 18, 3-21.

Klein, R., Pätzold, J., Wefer, G., Loya, Y., 1993. Depth-related timing of density band formation in *Porites* spp. corals from the Red Sea inferred from X-ray chronology and stable isotope composition. Marine Ecology Progress Series. 97(1), 99-104.

Klein, R., Pätzold, J., Wefer, G., Loya, Y., 1992. Seasonal variations in the stable isotopic composition and the skeletal density pattern of the coral *Porites lobata* (Gulf of Eilat, Red Sea). Mar.Biol. 112(2), 259-263.

Kleypas, J.A., Buddemeier, R.W., Gattuso, J., 2001. The future of coral reefs in an age of global change. Int.J.Earth Sci. 90(2), 426-437.

Knowlton, N., Jackson, J.B.C., 2008. Shifting baselines, local impacts, and global change on coral reefs. PLoS Biology. 6(2), 215-220.

Knutson, D.W., Buddemeier, R.W., Smith, S.V., 1972. Coral chronometers: Seasonal growth bands in reef corals. Science. 177(4045), 270-272.

Kobluk, D.R., Kozelj, M., 1985. Recognition of a relationship between depth and macroboring distribution in growth framework reef cavities, Bonaire, Netherland Antilles. Bulletin of Canadian Petroleum Geology. 33(4), 462-470.

Koch, E.W., Barbier, E.B., Silliman, B.R., Reed, D.J., Perillo, G.M.E., Hacker, S.D., Granek, E.F., Primavera, J.H., Muthiga, N., Polasky, S., Halpern, B.S., Kennedy, C.J., Kappel, C.V., Wolanski, E., 2009. Non-Linearity in ecosystem services: Temporal and spatial variability in coastal protection. Front Ecol. Environ. 7(1), 29-37.

Kohler, K.E., Gill, S.M., 2006. Coral Point Count with Excel extensions (CPCe): A Visual Basic program for the determination of coral and substrate coverage using random point count methodology. Computers and Geosciences. 32(9), 1259-1269.

Komar, P.D., 1981. The applicability of the Gibbs equation for grain settling velocities to conditions other than quartz grains in water. Journal of Sedimentary Research. 51(4), 1125-1132.

Kostylev, V.E., Erlandsson, J., Ming, M.Y., Williams, G.A., 2005. The relative importance of habitat complexity and surface area in assessing biodiversity: Fractal application on rocky shores. Ecological Complexity. 2(3), 272-286.

Kühlmann, D.H., 1983. Composition and ecology of deep-water coral associations. Helgoländer Meeresuntersuchungen. 36(2), 183-204.

Kwiatkowski, L., Cox, P.M., Economou, T., Halloran, P.R., Mumby, P.J., Booth, B.B.B., Carilli, J., G., H.M., 2013. Caribbean coral growth influenced by anthropogenic aerosol emissions. Nature Geosci. 6(5), 362-366.

Land, L., Goreau, T.F., 1970. Submarine lithification of Jamaican reefs. Journal of sedimentary research. 40(1), 457-462.

Land, L.S., 1979. The fate of reef-derived sediment on the north Jamaican island slope. Mar.Geol. 29(1–4), 55-71.

Lang, J.C. (Ed.), 2003. Status of coral reefs in the western Atlantic: Results of initial surveys, Atlantic and Gulf Rapid Reef Assessment (AGRRA) program. Atoll Research Bulletin, The Smithsonian Institution, Washington, D. C.

Lang, J.C., Wicklund, R.I., Dill, R.F., 1988. Depth- and habitat-related bleaching of zooxanthellate reef organisms near Lee Stocking Island, Exuma Cays, Bahamas.In: Choat, J.H., Barnes, D., Borowitzka, M.A., Coll, J.C., Davies, P.J., Flood, P., Hatcher, B.G., Hopley, D., Hutchings, P.A., Kinsey, D., Orme, G.R., Pichon, M., Sale, P.F., Sammarco, P., Wallace, C.C., Wilkinson, C., Wolanski, E., Bellwood, O. (Eds.),

Proceedings from the 6th International Coral Reef Symposium. 6th International Coral Reef Symposium Executive Committee, Townsville, Australia.Townsville, Australia., pp. 269-274.

Langdon, C., Atkinson, M.J., 2005. Effect of elevated pCO_2 on photosynthesis and calcification of corals and interactions with seasonal change in temperature/irradiance and nutrient enrichment. Journal of Geophysical Research: Oceans. 110(C9), C09S07.

Lapointe, B.E., Barile, P.J., Littler, M.M., Littler, D.S., 2005a. Macroalgal blooms on southeast Florida coral reefs: II. Cross-shelf discrimination of nitrogen sources indicates widespread assimilation of sewage nitrogen. Harmful Algae. 4(6), 1106-1122.

Lapointe, B.E., Barile, P.J., Littler, M.M., Littler, D.S., Bedford, B.J., Gasque, C., 2005b. Macroalgal blooms on southeast Florida coral reefs: I. Nutrient stoichiometry of the invasive green alga *Codium isthmocladum* in the wider Caribbean indicates nutrient enrichment. Harmful Algae. 4(6), 1092-1105.

Lapointe, B.E., 1997. Nutrient thresholds for bottom-up control of macroalgal blooms on coral reefs in Jamaica and southeast Florida. Limnology and Oceanography. 42, 1119-1131.

Le Campion-Alsumard, T., Golubic, S., Hutchings, P., 1995. Microbial endoliths in skeletons of live and dead corals: *Porites lobata* (Moorea, French Polynesia). Mar.Ecol.Prog.Ser. 117, 149-157.

Le Tissier, M.A., Clayton, B., Brown, B.E., Davis, P.S., 1994. Skeletal correlates of coral density banding and an evaluation of radiography as used in sclerochronology. Marine Ecology Progress Series. 110(1), 29-44.

Leder, J.J., Szmant, A.M., Swart, P.K., 1991. The effect of prolonged "bleaching" on skeletal banding and stable isotopic composition in *Montastrea annularis*. Coral Reefs. 10(1), 19-27.

Leichter, J.J., Genovese, S.J., 2006. Intermittent upwelling and subsidized growth of the scleractinian coral Madracis mirabilis on the deep fore-reef slope of Discovery Bay, Jamaica. Mar.Ecol.Prog.Ser. 316, 95-103.

Lenihan, H.S., Adjeroud, M., Kotchen, M.J., Hench, J.L., Nakamura, T., 2008. Reef structure regulates small-scale spatial variation in coral bleaching. Mar. Ecol. Prog. Ser. 370, 127-141.

Lesser, M., Slattery, M., 2011. Phase shift to algal dominated communities at mesophotic depths associated with lionfish (*Pterois volitans*) invasion on a Bahamian coral reef. Biol.Invasions. 13(8), 1855-1868.

Lesser, M.P., Slattery, M., Stat, M., Ojimi, M., Gates, R.D., Grottoli, A., 2010. Photoacclimatization by the coral *Montastraea cavernosa* in the mesophotic zone: Light, food, and genetics. Ecology. 91(4), 990-1003.

Lesser, M.P., Slattery, M., Leichter, J.J., 2009. Ecology of mesophotic coral reefs. Journal of Experimental Marine Biology and Ecology. 375(1-2), 1-8.

Lesser, M.P., 2000. Depth-dependent photoacclimatization to solar ultraviolet radiation in the Caribbean coral Montastraea faveolata. Marine Ecology Progress Series. 192, 137-151.

Lewis, J., 2002. Evidence from aerial photography of structural loss of coral reefs at Barbados, West Indies. Coral Reefs. 21(1), 49-56.

Liddell, W.D., Avery, W.E., 2000. Temporal change in hard substrate communities 10-250 m, the Bahamas.In: Moosa, M.K., Soemodihardjo, S., Soegiarto, A., Romimohtarto, K., Nontji, A., Soekarno, S. (Eds.), Proceedings from the 9th International Coral Reef Symposium. International Society for Reef Studies, BaliBali2, pp. 1053-1058.

Lidz, B.H., Hallock, P., 2000. Sedimentary petrology of a declining reef ecosystem, Florida Reef Tract (U. S. A.). Journal of Coastal Research. 16(3), 675.

Lidz, B.H., Robbin, D.M., Shinn, E.A., 1985. Holocene carbonate sedimentary petrology and facies accumulation, Looe Key National Marine Sanctuary, Florida. Bulletin of Marine Science. 36(3), 672-700.

Lighty, R.G., 1985. Preservation of internal reef porosity and diagenetic sealing of submerged early Holocene barrier reef, southeast Florida shelf. In: Schneidermann, N., Harris, P.M. (Eds.), Carbonate Cements, pp. 123-151.

Locker, S., Armstrong, R., Battista, T., Rooney, J., Sherman, C., Zawada, D., 2010. Geomorphology of mesophotic coral ecosystems: Current perspectives on morphology, distribution, and mapping strategies. Coral Reefs. 29(2), 329-345.

Lokier, S.W., Wilson, M.E.J., Burton, L.M., 2009. Marine biota response to clastic sediment influx: A quantitative approach. Palaeogeogr., Palaeoclimatol., Palaeoecol. 281(1–2), 25-42.

Lombardi, M., Godfrey, J., 2011. In-water strategies for scientific diver based examinations of the vertical mesophotic coral ecosystem (vMCE) from 50 to 150 metersIn: Pollock, N.W. (Ed.), Diving for Science, Dauphin Island, Alabama, pp. 13-21.

Longman, M.W., 1981. A process approach to recognizing facies of reef complexes. In: Toomey, D.F. (Ed.), European fossil reef models. Society for Economic Paleontologists and Mineralogists (SEPM), Tulsa, Ok, pp. 9-40.

Lough, J.M., Cooper, T.F., 2011. New insights from coral growth band studies in an era of rapid environmental change. Earth-Sci.Rev. 108(3–4), 170-184.

Lough, J.M., Barnes, D.J., 1989. Possible relationships between environmental variables and skeletal density in a coral colony from the central Great Barrier Reef. J.Exp.Mar.Biol.Ecol. 134(3), 221-241.

Luck, D.G., Forsman, Z.H., Toonen, R.J., Leicht, S.J., Kahng, S.E., 2013. Polyphyly and hidden species among Hawai'i's dominant mesophotic coral genera, Leptoseris and Pavona (Scleractinia: Agariciidae). PeerJ. 1, e132.

Luckhurst, B.E., Luckhurst, K., 1978. Analysis of the influence of substrate variables on coral reef fish communities. Mar.Biol. 49(4), 317-323.

MacArthur, R.H., MacArthur, J.W., 1961. On bird species diversity. Ecology. 42(3), 594-598.

Macdonald, I.A., Perry, C.T., 2003. Biological degradation of coral framework in a turbid lagoon environment, Discoverery Bay, north Jamaica. Coral Reef. 22, 523-535.

Macintyre, I.G., Rützler, K., Norris, J.N., Smith, K.P., Cairns, S.D., Bucher, K.E., Steneck, R.S., 1991. An early Holocene reef in the western Atlantic: Submersible investigations of a deep relict reef off the west coast of Barbados, W.I. Coral Reefs. 10(3), 167-174.

Macintyre, I.G., 1988. Modern coral reefs of western Atlantic: New geological perspective. AAPG Bull., 72(11), 1360-1369.

Macintyre, I.G., Marshall, J.F., 1988. Submarine lithification in coral reefs: Some facts and misconceptions. Proceedings from the 6th International Coral Reef Symposium. 1, pp. 263-272.

Macintyre, I.G., Glynn, P.W., 1976a. Evolution of modern Caribbean fringing reef, Galeta Point, Panama AAPG Bulletin, 60(7), 1054-1072.

Macintyre, I.G., Glynn, P.W., 1976b. Evolution of modern Caribbean fringing reef, Galeta Point, Panama. American Association of Petroleum Geologists Bulletin. 60(7), 1054-1072.

MacIntyre, I.G., Smith, S.V., 1974. X-radiographic studies of skeletal development in coral coloniesIn: Cameron, A.M., Cambell, B.M., Cribb, A.B., Endean, R., Jell, J.S., Jones, O.A., Mather, P., Talbot, F.H. (Eds.), Proceedings of the 2nd International Coral Reef Symposium. 2, pp. 277-287.

Macintyre, I.G., Smith, S.V., Zieman, J.C.J., 1974. Carbon flux through a coral-reef ecosystem: A Conceptual Model. J.Geol. 82(2), 161-171.

Madin, J.S., Dell, A.I., Madin, E.M.P., Nash, M.C., 2013. Spatial variation in mechanical properties of coral reef substrate and implications for coral colony integrity. Coral Reefs. 32(1), 173-179.

Maiklem, W.R., 1970. Carbonate sediments in the Capricorn Reef complex, Great Barrier Reef, Australia. Journal of Sedimentary Research. 40(1), 55-80.

Maiklem, W.R., 1968. Some hydraulic properties of bioclastic carbonate grains. Sedimentology. 10(2), 101-109.

Mallela, J., Perry, C., 2007. Calcium carbonate budgets for two coral reefs affected by different terrestrial runoff regimes, Rio Bueno, Jamaica. Coral Reefs. 26(1), 129-145.

Manzello, D.P., Kleypas, J.A., Budd, D.A., Eakin, C.M., Glynn, P.W., Langdon, C., 2008. Poorly cemented coral reefs of the eastern tropical Pacific: Possible insights into reef development in a high-CO_2 world. Proceedings of the Nation Academy of Sciences of the United States of America. 105(30), 10450-10455.

Manzello, D.P., Brandt, M., Smith, T.B., Lirman, D., Hendee, J.C., Nemeth, R.S., 2007. Hurricanes benefit bleached corals. Proceedings of the National Academy of Sciences. 104(29), 12035-12039.

Maragos, J.E., Crosby, M.P., McManus, J.W., 1996. Coral reefs and biodiversity: A critical and threatened relationship. Oceanography. 9(1), 83-99.

Marshall, J.F., 1986. Regional distribution of submarine cements within an epicontinental reef system: Central Great Barrier Reef, Australia. In: Schroeder, J.H., Purser, B.H. (Eds.), Reef Diagenesis. Springer, Berlin, pp. 8-26.

Marshall, J.F., 1983a. Marine lithification in coral reefs. In: Barnes, D.J. (Ed.), Perspectives on coral reefs. Australian Institute of Marine Science, Townsville, pp. 231-239.

Marshall, J.F., 1983b. Marine lithification in coral reefs. In: Barnes, D.J. (Ed.), Perspectives on Coral Reefs. Published for the Australian Institute of Marine Science by B. Clouston, Townsville, Australia, pp. 231-239.

Mass, T., Einbinder, S., Brokovich, E., Shashar, N., Vago, R., Erez, J., Dubinsky, Z., 2007. Photoacclimation of *Stylophora pistillata* to light extremes: Metabolism and calcification. Marine ecology Progress series (Halstenbek). 334, 93-102.

Mateu-Vicens, G., Pomar, L., Ferràndez-Cañadell, C., 2012. Nummulitic banks in the upper Lutetian 'Buil level', Ainsa Basin, South Central Pyrenean Zone: The impact of internal waves. Sedimentology. 59(2), 527-552.

Matsuda, S., Iryu, Y., 2011. Rhodoliths from deep fore-reef to shelf areas around Okinawa-jima, Ryukyu Islands, Japan. Mar.Geol. 282(3), 215-230.

Maxwell, W.G.H., Jell, J.S., McKellar, R.G., 1964. Differentiation of carbonate sediments in the Heron Island reef. Journal of Sedimentary Research. 34(2), 294-308.

May, J.P., 1981. Chi (x); a proposed standard parameter for settling tube analysis of sediments. Journal of Sedimentary Research. 51(2), 607-610.

McCave, I.N., Swift, S.A., 1976. A physical model for the rate of deposition of fine-grained sediments in the deep sea. Geological Society of America Bulletin. 87(4), 541-546.

McClain, C.R., Barry, J.P., 2010. Habitat heterogeneity, disturbance, and productivity work in concert to regulate biodiversity in deep submarine canyons. Ecology. 91(4), 964-976.

McConnaughey, T., 1989. ^{13}C and ^{18}O isotopic disequilibrium in biological carbonates: I. Patterns. Geochim.Cosmochim.Acta. 53(1), 151-162.

Menza, C., Kendall, M., Rogers, C., Miller, J., 2007. A deep reef in deep trouble. Continental Shelf Research. 27(17), 2224-2230.

Mesolella, K.J., 1967. Zonation of uplifted Pleistocene coral reefs on Barbados, West Indies. Science. 156, 638-640.

Mihaljević, M., Renema, W., Welsh, K., Pandolfi, J.M., 2014. Eocene-Miocene sheallow-water carbonate platforms and incrased habitat diversity in Sarawak, Malaysia. Palaios. 29, 378-391.

Miller, J., Waara, R., Muller, E., Rogers, C., 2006. Coral bleaching and disease combine to cause extensive mortality on reefs in US Virgin Islands. Coral Reefs. 25(3), 418-418.

Millero, F.J., Huang, F., 2009. The density of seawater as a function of salinity (5 to 70 g kg−1) and temperature (273.15 to 363.15 K). Ocean science. 5(2), 91-100.

Millero, F.J., Chen, C., Bradshaw, A., Schleicher, K., 1980. A new high pressure equation of state for seawater. Deep Sea Research Part A.Oceanographic Research Papers. 27(3–4), 255-264.

Mitchell, J.T., Land, L.S., Miser, D.E., 1987. Modern marine dolomite cement in a north Jamaican fringing reef. Geology. 15(6), 557-560.

Moberg, F., Folke, C., 1999. Ecological goods and services of coral reef ecosystems. Ecol.Econ. 29(2), 215-233.

Montaggioni, L.F., Behairy, A.K.A., El-Sayed, M.K., Yusuf, N., 1986. The modern reef complex, Jeddah area, Red Sea: A facies model for carbonate sedimentation on embryonic passive margins. Coral Reefs. 5(3), 127-150.

Moore, C.H., Shedd, W.W., 1977. Effective rates of sponge bioerosion as a function of carbonate production. In: Taylor, D.L. (Ed.), Proceedings of Third International Coral Reef Symposium. Rosenstiel School of Marine and Atmospheric ScienceMiami, Florida. 2, pp. 499-505.

Moore, C.H., Graham, E.A., Land, L.S., 1976. Sediment transport and dispersal across the deep fore-reef and island slope (-55 m to -305 m), Discovery Bay, Jamaica. Journal of Sedimentary Research. 46(1), 174-187.

Moore, W.S., Krishnaswami, S., 1974. Correlation of x-radiography revealed banding in corals with radiometric growth rates. In: Cameron, A.M., Cambell, B.M., Cribb, A.B., Endean, R., Jell, J.S., Jones, O.A., Mather, P., Talbot, F.H. (Eds.), Proceedings of the 2nd International Coral Reef Symposium. 2, pp. 269-276.

Morsilli, M., Bosellini, F.R., Pomar, L., Hallock, P., Aurell, M., Papazzoni, C.A., 2012. Mesophotic coral buildups in a prodelta setting (Late Eocene, southern Pyrenees, Spain): A mixed carbonate-siliciclastic system. Sedimentology. 59(3), 766-794.

Moura, R.L., Secchin, N.A., Amado-Filho, G.M., Francini-Filho, R.B., Freitas, M.O., Minte-Vera, C.V., Teixeira, J.B., Thompson, F.L., Dutra, G.F., Sumida, P.Y.G., Guth, A.Z., Lopes, R.M., Bastos, A.C., 2013. Spatial patterns of benthic megahabitats and conservation planning in the Abrolhos Bank. Cont.Shelf Res. 70, 109-117.

Mumby, P.J., 2009. Herbivory versus corallivory: Are parrotfish good or bad for Caribbean coral reefs?. Coral Reefs. 28(3), 683-690.

Mumby, P.J., 2006. The impact of exploiting grazers (*Scaridae*) on the dynamics of Caribbean coral reefs. Ecol.Appl. 16(2), 747-769.

Munnecke, A., Westphal, H., Kölbl-Ebert, M., 2008. Diagenesis of plattenkalk: Examples from the Solnhofen area (Upper Jurassic, southern Germany). Sedimentology. 55(6), 1931-1946.

Murray, S.P., Hsu, S.A., Roberts, H.H., Owens, E.H., Crout, R.L., 1982. Physical processes and sedimentation on a broad, shallow bank. Estuar.Coast.Shelf Sci. 14(2), 135-157.

Muscatine, L., Porter, J.W., Kaplan, I.R., 1989. Resource partitioning by reef corals as determined from stable isotope composition. Mar.Biol. 100(2), 185-193.

Nemeth, R.S., Smith, T.B., Blondeau, J., Kadison, E., Calnan, J.M., Gass, J., 2008. Characterization of deep water reef communities within the marine conservation district, St. Thomas, U.S. Virgin Islands Final report submitted to the Caribbean Fisheries Management Council (CFMC/NOAA), 90.

Nemeth, R.S., 2005. Population characteristics of a recovering US Virgin Islands. Marine Ecology Progress Series. 56, 81-97.

Novak, M.J., Liddell, W.D., Torruco, D., 1993. Sedimentology and community structure of reefs of the Yucatan Peninsula, Mexico. In: Richmond, R.H. (Ed.), Proceedings of the 7th International Coral Reef Symposium. University of Guam Press UOG Station, Guam. 1, pp. 265-272.

Novak, V., Santodomingo, N., Rösler, A., Di Martino, E., Braga, J.C., Taylor, P.D., Johnson, K.G., Renema, W., 2013. Environmental reconstruction of a late Burdigalian (Miocene) patch reef in deltaic deposits (East Kalimantan, Indonesia). Palaeogeogr., Palaeoclimatol., Palaeoecol. 374, 110-122.

Ogden, J.C., Lobel, P.S., 1978. The role of herbivorous fishes and urchins in coral reef communities. Environmental Biology of Fishes. 3, 49-63.

Ohara, T., Fujii, T., Kawamura, I., Mizuyama, M., Montenegro, J., Shikiba, H., White, K.N., Reimer, J.D., 2013. First record of a mesophotic *Pachyseris foliosa* reef from Japan. Marine Biodiversity. 43(2), 71-72.

Ohlhorst, S.L., Liddell, R.J., 1988. The effect of substrata microtopography on reef community structure 60-120m. In: Choat, J.H., Barnes, D., Borowitzka, M.A., Coll, J.C., Davies, P.J., Flood, P., Hatcher, B.G., Hopley, D., Hutchings, P.A., Kinsey, D.W., Orme, G.R., Pichon, M., Sale, P.F., Sammarco, P.W., Wallace, C., Wilkinson, C., Wolanski, E., Bellwood, O. (Eds.), Proceedings from the 6th International Coral Reef SymposiumTownsville, Australia. 3, pp. 319-324.

Orme, G.R., Flood, P.G., Sargent, G.E.G., 1978. Sedimentation trends in the lee of outer (ribbon) reefs, northern region of the Great Barrier Reef Province. Philos. Trans. R. Soc. Lond. A. 291(1378), 85-99.

Orme, G.R., Flood, P.G., Ewart, A., 1974. An investigation of the sediments and physiography of Lady Muscgrave Reef - A preliminary account. In: Cameron, A.M., Cambell, B.M., Cribb, A.B., Endean, R., Jell, J.S., Jones, O.A., Mather, P., Talbot, F.H. (Eds.), Proceedings of the 2nd International Coral Reef Symposium Brisbane, Australia. 2, pp. 371-386.

Orpin, A.R., Ridd, P.V., Stewart, L.K., 1999. Assessment of the relative importance of major sediment transport mechanisms in the central Great Barrier Reef lagoon. Aust.J.Earth Sci. 46(6), 883-896.

Pandolfi, J.M., Llewellyn, G., Jackson, J.B.C., 1999. Pleistocene reef environments, constituent grains, and coral community structure: Curaçao, Netherlands Antilles. Coral Reefs. 18(2), 107-122.

Pandolfi, J.M., Greenstein, B.J., 1997. Preservation of community structure in death assemblages of deep water Caribbean reef corals. Limnology and Oceanography. 42, 1505-1516.

Pandolfi, J.M., Jackson, J.B.C., Baron, N., Bradbury, R.H., Guzman, H.M., Hughes, T.P., Kappel, C.V., Micheli, F., Ogden, J.C., Possingham, H.P., Sala, E., 2005. Are U.S. coral reefs on the slippery slope to slime? Science. 307(5716), 1725-1726.

Pang, R.K., 1973. The ecology of some Jamaican excavating sponges. Bulletin of Marine Science. 23(2), 227-243.

Pari, N., Peyrot-Clausade, M., Hutchings, P.A., 2002. Bioerosion of experimental substrates on high islands and atoll lagoons (French Polynesia) during 5 years of exposure. Journal of Experimental Marine Biology & Ecology. 276(1), 109.

Parrish, F.A., Littnan, C.L., 2007. Changing perspectives in Hawaiian monk seal research using animal-borne imaging. Mar.Technol.Soc.J. 41(4), 30-34.

Passega, R., 1957. Texture as characteristic of clastic deposition. AAPG Bulletin. 41(9), 152-1984.

Perry, C., 1996. The rapid response of reef sediments to changes in community composition; implications for time averaging and sediment accumulation. Journal of sedimentary research. 66(3), 459-467.

Perry, C.T., Murphy, G.N., Kench, P.S., Edinger, E.N., Smithers, S.G., Steneck, R.S., Mumby, P.J., 2014. Changing dynamics of Caribbean reef carbonate budgets: Emergence of reef bioeroders as critical controls on present and future reef growth potential. Proceedings of the Royal Society B: Biological Sciences. 281(1796).

Perry, C.T., Murphy, G.N., Kench, P.S., Smithers, S.G., Edinger, E.N., Steneck, R.S., Mumby, P.J., 2013. Caribbean-wide decline in carbonate production threatens coral reef growth. Nat Commun. 4, 1402.

Perry, C.T., Edinger, E., Kench, P., Murphy, G., Smithers, S., Steneck, R., Mumby, P., 2012. Estimating rates of biologically driven coral reef framework production and erosion: A new census-based carbonate budget methodology and applications to the reefs of Bonaire. Coral Reefs. 31(3), 853-868.

Perry, C.T., Hepburn, L.J., 2008. Syn-depositional alteration of coral reef framework through bioerosion, encrustation and cementation: Taphonomic signatures of reef accretion and reef depositional events. Earth Science Reviews. 86(1-4), 106-144.

Perry, C.T., Smithers, S.G., Palmer, S.E., Larcombe, P., Johnson, K.G., 2008a. 1200 year paleoecological record of coral community development from the terrigenous inner shelf of the Great Barrier Reef. Geology. 36(9), 691-694.

Perry, C.T., Spencer, T., Kench, P.S., 2008b. Carbonate budgets and reef production states: A geomorphic perspective on the ecological phase-shift concept. Coral Reefs. 27(4), 853-866.

Perry, C.T., 2000. Factors controlling sediment preservation on a North Jamaican fringing reef: A process-based approach to microfacies analysis. Journal of Sedimentary Research. 70(3), 633-648.

Perry, C.T., 1999. Reef framework preservation in four contrasting modern reef environments, Discovery Bay, Jamaica. J.Coast.Res. 15(3), 796-812.

Perry, C.T., 1998. Macroborers within coral framework at Discovery Bay, north Jamaica: Species distribution and abundance, and effects on coral preservation. Coral Reefs. 17(3), 277-287.

Peyrot-Clausade, M., Le Campion-Alsumard, T., Hutchings, P., Le Campion, J., Payri, C., Fontaine, M., 1995. Initial bioerosion and bioaccretion on experimental substrates in high islands and atoll lagoons (French Polynesia). Oceanologican Acta. 18(5), 531-541.

Peyrot-Clausade, M., Bruno, J.F., 1990. Distribution patterns of macroboring organisms on Tulear reef flats (SW Madagascar). Marine Ecology Progress Series. 61(1-2), 133-144.

Phillips, N.W., Gettleson, D.A., Spring, K.D., 1990. Benthic biological studies of the southwest Florida Shelf. Am.Zool. 30(1), 65-75.

Pilkey, O.H., Morton, R.W., Luternauer, J., 1967. The carbonate fraction of beach and dune sands. Sedimentology. 8(4), 311-327.

Pindell, J.L., Barrett, S.F., 1990. Geological evolution of the Caribbean region; a plate tectonic perspective. In: Dengo, G., Case, J.E. (Eds.), The Geology of North America. Geological Society of America: Boulder, CO, United States, United States, pp. 405-432.

Plaisance, L., Caley, M.J., Brainard, R.E., Knowlton, N., 2011. The Diversity of Coral Reefs: What Are We Missing? PLoS ONE. 6(10), e25026.

Playford, P.E., 1980. Devonian "Great Barrier Reef" of Canning Basin, Western Australia. AAPG Bulletin. 64, 814-840.

Pomar, L., Hallock, P., 2008. Carbonate factories: A conundrum in sedimentary geology. Earth-Sci.Rev. 87(3–4), 134-169.

Pomar, L., 2001. Ecological control of sedimentary accommodation: Evolution from a carbonate ramp to rimmed shelf, Upper Miocene, Balearic Islands. Palaeogeogr., Palaeoclimatol., Palaeoecol. 175(1), 249-272.

Pomponi, S.A., 1979. Ultrastructure and cytochemistry of the etching area of boring sponges. In: Levi, C., Boury-Esnault, N. (Eds.), Biologie et Spongiaires. Colloques Internationaux du Centre Nationale de la Recherche Scientifique, pp. 317-323.

Poole, D.M., 1957. Size analysis of sand by a sedimentation technique. Journal of Sedimentary Research. 27(4), 460-468.

Porter, J.W., 1976. Autotrophy, heterotrophy, and resource partitioning in Caribbean reef-building corals. American Naturalist. 110, 731-742.

Potts, D.C., Jacobs, J.R., 2000. Evolution of reef-building scleractinian corals in turbid environments: A paleo-ecological hypothesis. In: Moosa, M.K., Soemodihardjo, S., Soegiarto, A., Romimohtarto, K., Nontji, A., Soekarn, A., Suharsono, A. (Eds.), Proceedings from the 9th International Coral Reef SymposiumBali, Indonesia. 1, pp. 249-254.

Powell, E.N., Davies, D.J., 1990. When is an "old" shell really old?. J.Geol. 98(6), 823-844.

Prager, E.J., Southard, J.B., Vivoni-Gallart, E.R., 1996. Experiments on the entrainment threshold of well-sorted and poorly sorted carbonate sands. Sedimentology. 43(1), 33-40.

Proni, J., Huang, H., Dammann, W., 1994. Initial dilution of southeast Florida ocean outfalls. J.Hydraul.Eng. 120(12), 1409-1425.

Puglise, K.A., Hinderstein, L.M., Marr, J.C.A., Dowgiallo, M.J., Martinez, F.A., 2009. Mesophotic Coral Ecosystems Research Strategy: International Workshop to Prioritize Research and Management Needs for Mesophotic Coral Ecosystems, Jupiter, Florida, 12-15 July 2008. Silver Spring, MD: NOAA National Centers for Coastal Ocean Science, Center for Sponsored Coastal Ocean Research, and Office of Ocean Exploration and Research, NOAA Undersea Research Program. NOAA Technical Memorandum NOS NCCOS 98 and OAR OER, 24.

Purdy, E., 1974. Karst-determined facies patterns in British Honduras: Holocene carbonate sedimentation model. AAPG Bull. 58(5), 825-855.

Purdy, E.G., Gischler, E., Lomando, A.J., 2003. The Belize margin revisited. 2. Origin of Holocene antecedent topography. Int.J.Earth Sci. 92(4), 552-572.

Purdy, E.G., 1963. Recent calcium carbonate facies of the Great Bahama Bank. 1. Petrography and reaction groups. J.Geol. 71(3), 334-355.

Purkis, S.J., Rowlands, G.P., Kerr, J.M., 2014. Unravelling the influence of water depth and wave energy on the facies diversity of shelf carbonates. Sedimentology, doi: 10.1111/sed.12110.

Pusey, W.C., 1975. Holocene carbonate sedimentation on Nothern Belize Shelf: Part 1. In: Wantland, K.L., Pusey, W.C. (Eds.), Belize shelf - carbonate sediments, clastic sediments, and ecology. AAPG Studies in Geology, Tulsa, Oklahoma, pp. 131-165.

Pyle, R.L., Earle, J.L., Green, B.D., 2008. Five new species of the damselfish genus *Chromis* (Perciformes: Labroidei: Pomacentridae) from deep coral reefs in the tropical western Pacific. Zootaxa. 1671, 3-31.

Pyle, R.L., 2000. Assessing undiscovered fish biodiversity on deep coral reefs using advanced self-contained diving technology. Mar.Technol.Soc.J. 34(4), 82-91.

Pyle, R.L., 1998. Use of advanced mixed-gas diving technology to explore the coral reef "twilight zone." In: Tanacredi, J.T., Loret, J., Earlse, S.A. (Eds.), Ocean Pulse: A Critical Diagnosis. Plenum Publishing Corporation, New York, NY, pp. 71-88.

R Core Team, 2014. R: A language and environment for statistical computing.

Randall, J.E., 1974. The effect of fishes on coral reefs.In: Cameron, A.M., Cambell, B.M., Cribb, A.B., Endean, R., Jell, J.S., Jones, O.A., Mather, P., Talbot, F.H. (Eds.), Proceedings of the 2nd International Coral Reef Symposium. The Great Barrier Reef Committee, Brisbane, Australia.Brisbane, Australia. 21, pp. 159-166.

Randazzo, A.F., Baisley, K.J., 1995. Controls on carbonate facies distribution in a high-energy lagoon, San Salvador Island, Bahamas. Geological Society of America Special Paper. 300, 157-175.

Rankey, E.C., Reeder, S.L., Garza-Peréz, R.G., 2011. Controls on links between geomorphical and surface sedimentology variability: Aitutaki and Maupiti Atolls, South Pacific Ocean. Journal of Sedimentary Research. 81, 885-900.

Rankin, D.W., 2002. Geology of St. John, U.S. Virgin Islands. U.S. Dept. of Interior, U.S. Geological Survey, Denver, CO.

Rasser, M., Riegl, B., 2002. Holocene coral reef rubble and its binding agents. Coral Reefs. 21(1), 57-72.

Reaka-Kudla, M., Feingold, J.S., Glynn, P.W., 1996. Experimental studies of rapid bioerosion of coral reefs in the Galápagos Islands. Coral Reefs. 15(2), 101-107.

Reed, J.K., Pomponi, S.A., 1997. Biodiversity and distribution of deep and shallow water sponges in the BahamasIn: Lessios, H.A., MacIntyre, I.G. (Eds.), Proceedings of the 8th International Coral Reef Symposium, Smithsonian Tropical Research Institute, Panama. 2, pp. 1387-1392.

Reed, J.K., 1985. Deepest distribution of Atlantic hermatypic corals discovered in the Bahamas. Proceedings of the 5th International Coral Reef Congress. Smithsonian Tropical Research Institute, Panama, Tahiti. 6, pp. 249-254.

Renema, W., Bellwood, D.R., Braga, J.C., Bromfield, K., Hall, R., Johnson, K.G., Lunt, P., Meyer, C.P., McMonagle, L.B., Morley, R.J., O'Dea, A., Todd, J.A., Wesselingh, F.P., Wilson, M.E.J., Pandolfi, J.M., 2008. Hopping hotspots: Global shifts in marine biodiversity. Science. 321(5889), 654-657.

Rice, M.E., Macdonald, I.A., 1982. Distribution of spiuncula in the coral reef community, Carrie Bow Cay, Belize. In: Rützler, K., Macdonald, I.A. (Eds.), The Atlantic barrier reef ecosystem at Carrie Bow Cay, Belize 1: Structure and communities. Smithsonian Contributions to Marine Sciences, Washington D. C., pp. 311-320.

Riding, R., 2002. Structure and composition of organic reefs and carbonate mud mounds: Concepts and categories. Earth Science Reviews. 58(1-2), 163-231.

Riegl, B., Piller, W.E., 2003. Possible refugia for reefs in times of environmental stress International Journal of Earth Sciences, 92(4), 520-531.

Riegl, B.M., Purkis, S.J., 2009. Markov models for linking environments and facies in space and time (recent Arabian gulf, Miocene Paratethys). In: Swart, P.K., Eberli, G.P., McKenzie, J.A., Jarvis, I., Stevens, T. (Eds.), Perspectives in Carbonate Geology: A Tribute to the Career of Robert Nathan Ginsburg . John Wiley & Sons, Ltd, Chichester, West Sussex, UK, pp. 337-360.

Risk, M.J., Sammarco, P.W., Edinger, E.N., 1995. Bioerosion in *Acropora* across the continental shelf of the Great Barrier Reef Coral Reefs, 14(2), 79-86.

Risk, M.J., 1972. Fish diversity on a coral reef in the Virgin Islands. Atoll Research Bulletin. 49, 317-323.

Rivero-Calle, S., Armstrong, R.A., Soto-Santiago, F.J., 2008. Biological and physical characteristics of a mesophotic coral reef: Black Jack reef, Vieques, Puerto Rico. Proceedings of the 11th International Coral Reef Symposium. 1, pp. 574-578.

Roberts, C.M., Ormond, R.F.G., 1987. Habitat complexity and coral reef fish diversity and abundance on Red Sea fringing reefs. Mar.Ecol.Prog.Ser. 41(1), 1-8.

Roberts, H.H., 1989. Physical processes as agents of sediment transport in carbonate systems: Examples from St. Croix, USVI. 12th Caribbean Geological Conference Special Publication. West Indies LibraryTeague Bay, St. Croix. 8, pp. 95-104.

Roberts, H.H., Murray, S.P., Suhayda, J.N., 1977. Physical processes on a fore-reef shelf environment. In: Taylor, D.L. (Ed.), Proceedings of the 3rd International Coral Reef Symposium. Miami, Florida. 2, pp. 507-516.

Robinson, E., 1969. Geological field guide to Neogene sections in Jamaica, West Indies: Prepared for the 19th annual convention of the Gulf Coast Association of Geological Societies and the Society of Economic. SEPM, New Orleans, La.

Roduit, N., 2008. JMicroVision: Image analysis toolbox for measuring and quantifying components of high-definition images((accessed 11/12/2013)).

Roehl, P.O., Choquette, P.W., 1986. Carbonate Petroleum Reservoirs. Springer-Verlag, New York.

Rogers, A., Blanchard, J. ., Mumby, P. ., 2014. Vulnerability of coral reef fisheries to a loss of structural complexity. Current Biology. 24(9), 1000-1005.

Rong, H., Jiao, Y., Wu, L., Wang, R., Gu, Y., Wang, X., 2013. Architecture and evolution of calciclastic marginal slope fans of the Ordovician carbonate platform in the Yijianfang outcrop of the Bachu area, west Tarim Basin. AAPG Bull. 97(10), 1657-1681.

Rooney, J., Donham, E., Montgomery, A., Spalding, H.L., Parrish, F.A., Boland, R.C., Fenner, D., Gove, J., Vetter, O., 2010. Mesophotic coral ecosystems in the Hawaiian Archipelago. Coral Reefs. 29(361), 367.

Rosen, B.R., Aillud, G.S., Bosellini, F.R., Clack, N.J., Insalaco, E., Valldeperas, F.X., Wilson, M.E.J., 2000. Platy coral assemblages: 200 million years of functional stability in response to the limiting effects of light and turbidity. In: Moosa, M.K., Soemodihardjo, S., Soegiarto, A., Romimohtarto, K., Nontji, A., Soekarno, Suharsono (Eds.), Proceedings from the 9th International Coral Reef SymposiumBali. 1, pp. 255-264.

Rosenfeld, M., Yam, R., Shemesh, A., Loya, Y., 2003. Implication of water depth on stable isotope composition and skeletal density banding patterns in a *Porites lutea* colony: Results from a long-term translocation experiment. Coral Reefs. 22, 337-345.

Rosenzweig, M.L., Winakur, J., 1969. Population ecology of desert rodent communities: Habitats and environmental complexity. Ecology. 50(4), 558-572.

Rothenberger, P., Blondeau, J., Cox, C., Curtis, S., Fisher, W.S., Garrison, V., Hillis-Starr, Z., Jeffrey, C.F.G., Kadison, E., Lundgren, I., Miller, W.J., Muller, E., Nemeth, R., Paterson, S., Rogers, C., Smith, T.B., Spitzack, A., Taylor, M., Toller, W., Wright, J.,

Wusinich-Mendez, D., Waddell, J.E., 2008. The state of coral reef ecosystems of the U.S. Virgin Islands. In: Waddell, J.E., Clarke, A.M. (Eds.), The State of Coral Reef Ecosystems of the United States and Pacific Freely Associated States. NOAA Technical Memorandum NOS NCCOS 73, Silver Spring, MD, pp. 29-73.

Runnalls, L.A., Coleman, M.L., 2003. Record of natural and anthropogenic changes in reef environments (Barbados West Indies) using laser ablation ICP-MS and sclerochronology on coral cores. Coral Reefs. 22(4), 416-426.

Rützler, K., 1975. The role of burrowing sponges in bioerosion. Oecologia. 19(3), 203-216.

Rützler, K.K., Rieger, G., 1973. Sponge burrowing: Fine structure of *Cliona lampa* penetrating calcareous substrata. Mar.Biol. 21(2), 144-162.

Rützler, K., 1974. The burrowing sponges of Bermuda. Smithson.Contrib.Zool.(165), 1-32.

Ryan, D.A., Opdyke, B.N., Jell, J.S., 2001. Holocene sediments of Wistari Reef: Towards a global quantification of coral reef related neritic sedimentation in the Holocene. Palaeogeogr., Palaeoclimatol., Palaeoecol. 175(1–4), 173-184.

Sammarco, P.W., 1996. Comments on coral reef regeneration, bioerosion, biogeography, and chemical ecology: Future directions. J.Exp.Mar.Biol.Ecol. 200(1–2), 135-168.

Sammarco, P.W., Risk, M.J., 1990. Large scale patterns in internal bioerosion of *Porites*: Cross continental shelf trends on the Great Barrier Reef. Marine Ecology-Progress Series. 59(1-2), 145-156.

Sammarco, P.W., Risk, M.J., Rose, C., 1987. Effects of grazing and damselfish territoriality on internal bioerosion of dead corals: Indirect effects. J.Exp.Mar.Biol.Ecol. 112(2), 185-199.

Sammarco, P.W., 1982. Echinoid grazing as a structuring force in coral communities: Whole reef manipulations. Journal of Experimental Marine Biology and Ecology. 61, 31-55.

Sammarco, P.W., 1980. *Diadema* and its relationship to coral spat mortality: Grazing, competition, and biological disturbance. Journal of Experimental Marine Biology and Ecology. 45, 245-272.

Sarg, J.F., 1988. Carbonate sequence stratigraphy. In: Wilgus, C.K., Posamentier, H.W., Hastings, B.S., Wagoner, J.V., Ross, C.A., Kendall, G.G.S.C. (Eds.), Sea-level changes: an integrated approach. Society of Economic Paleontolgists and Mineralogists, Tulsa, pp. 155-182.

SAS Institute Inc., . JMP 2012, 10.0.

Schlager, W., 1981. The paradox of drowned reefs and carbonate platforms. Geological Society of America Bulletin. 92, 197-211.

Scholle, P.A., 1978. A color illustrated guide to carbonate rock constituents, textures, cements, and porosities. American Association of Petroleum Geologists, Tulsa, Oklahoma.

Schönberg, C., Wilkinson, C., 2001. Induced colonization of corals by a clionid bioeroding sponge. Coral Reefs. 20(1), 69-76.

Schonberg, C.H.L., 2002. Substrate effects on the bioeroding demosponge Cliona orientalis. 1. Bioerosion Rates. Marine Ecology. 23(4), 313.

Scoffin, T.P., 1992. Taphonomy of coral reefs: A review. Coral Reefs. 11(2), 57-77.

Scoffin, T.P., Tudhope, A.W., 1985. Sedimentary environments of the central region of the Great Barrier Reef of Australia. Coral Reefs. 4(2), 81-93.

Scoffin, T.P., Stearn, C.W., Boucher, D., Frydl, P., Hawkins, C.M., Hunter, I.G., MacGeachy, J.K., 1980. Calcium carbonate budget of a fringing reef on the west coast of Barbados; Part II, Erosion, sediments and internal structure. Bulletin of Marine Science. 3(2), 475-508.

Scott, P.J.B., 1988. Distribution, habitat and morphology of the Caribbean coral- and rock-boring bivalve, *Lithophaga bisulcata* (d'Orbigny) (Mytilidae: Lithophaginae). J.Molluscan Stud. 54(1), 83-95.

Scott, P.J.B., Risk, M.J., 1988. The effect of *Lithophaga* (Bivalvia: Mytilidae) boreholes on the strength of the coral *Porites lobata*. Coral Reefs. 7(3), 145-151.

Scott, P.J.B., Risk, M.J., Carriquiry, J.D., 1988. El Niño, bioerosion and the survival of east Pacific reefs. In: Choat, J.H., Barnes, D., Borowitzka, M.A., Coll, J.C., Davies, P.J., Flood, P., Hatcher, B.G., Hopley, D., Hutchings, P.A., Kinsey, D., Orme, G.R., Pichon, M., Sale, P.F., Sammarco, P.W., Wallace, C., Wilkinson, C., Wolanski, E., Bellwood, O. (Eds.), Proceedings of the 6th International Coral Reef Symposium. Contributed Papers, Townsville, AustraliaTownsville, Australia. 2, pp. 517-520.

Searle, D.E., 1983. Late Quaternary regional controls on the development of the Great Barrier Reef - Geophysical evidence. BMR Journal of Australian Geology & Geophysics. 8(3), 267-276.

Serrano, X., Baums, I.B., O'Reilly, K., Smith, T.B., Jones, R.J., Shearer, T.L., Nunes, F.L.D., Baker, A.C., 2014. Geographic differences in vertical connectivity in the

Caribbean coral Montastraea cavernosa despite high levels of horizontal connectivity at shallow depths. Mol.Ecol. 23(17), 4226-4240.

Sheppard, C.R.C., Spalding, M., Bradshaw, C., Wilson, S., 2002. Erosion vs. recovery of coral reefs after 1998 El Niño: Chagos reefs, Indian Ocean. Ambio. 31(1), 40-48.

Sherman, C., Nemeth, M., Ruíz, H., Bejarano, I., Appeldoorn, R., Pagán, F., Schärer, M., Weil, E., 2010. Geomorphology and benthic cover of mesophotic coral ecosystems of the upper insular slope of southwest Puerto Rico. Coral Reefs. 29(2), 347-360.

Shinn, E., 1963. Spur and groove formation on the Florida Reef Tract. Journal of Sedimentary Research. 33(2), 291-303.

Shinn, E.A., Hudson, H.J., Halley, R.B., Lidz, B., Robbin, D.l.M., Macintyre, I.G., 1982. Geology and sediment accumulation rates at Carrie Bow Cay, Belize Smithsonian Contributions to the Marine Sciences, 12, 63-75.

Siegel, S., Castellan, N., Jr., 1988. Nonparametric statistics for the behavioural sciences. McGraw-Hill Int., New York.

Sinniger, F., Morita, M., Harii, S., 2013. "Locally extinct" coral species *Seriatopora hystrix* found at upper mesophotic depths in Okinawa. Coral Reefs. 32(1), 153-153.

Slattery, M., Lesser, M.P., 2012. Mesophotic coral reefs: A global model of community structure and function. Proceedings of the 12th International Coral Reef Symposium, pp. 9C.

Slattery, M., Lesser, M.P., Brazeau, D., Stokes, M.D., Leichter, J.J., 2011. Connectivity and stability of mesophotic coral reefs. J.Exp.Mar.Biol.Ecol. 408(1-2), 32-41.

Smith, D.A., Cheung, K.F., 2002. Empirical relationships for grain size parameters of calcareous sand on Oahu, Hawaii. J.Coast.Res. 18(1), 82-93.

Smith, L.W., Barshis, D., Birkeland, C., 2007. Phenotypic plasticity for skeletal growth, density and calcification of Porites lobata in response to habitat type. Coral Reefs. 26(3), 559-567.

Smith, S.V., Kinsey, D.W., 1978. Calcification and organic carbon metabolism as indicated by carbon dioxide.

Smith, T.B., Kadison, E., Henderson, L., Gyory, J., Brandt, M.E., Calnan, J.M., Kammann, M., Wright, V., Nemeth, R.S., Rothenberger, J.P., 2012. The United States Virgin Islands territorial coral reef monitoring program. 2011 Annual Report. University of the Virgin Islands, United States Virgin Islands.

Smith, T.B., Kadison, E., Calnan, J.M., Brandt, M.E., Taylor, M., Blondeau, J., Tyner, E., Nemeth, R.S., 2011a. Coral Reef Monitoring in St. Croix and St. Thomas, United States Virgin Islands. 2008-2010 Final Report., 53.

Smith, T.B., Kadison, E., Henderson, L., Brandt, M.E., Gyory, J., Kammann, M., Write, V., Nemeth, R.S., 2011b. The United States Virgin Islands Territorial Coral Reef Monitoring Program. Year 11 Annual Report. Version 1.

Smith, T.B., Blondeau, J., Nemeth, R.S., Pittman, S.J., Calnan, J.M., Kadison, E., Gass, J., 2010. Benthic structure and cryptic mortality in a Caribbean mesophotic coral reef bank system, the Hind Bank Marine Conservation District, U.S. Virgin Islands. Coral Reefs. 29(2), 289-308.

Smith, T.B., Nemeth, R.S., Blondeau, J., Calnan, J.M., Kadison, E., Herzlieb, S., 2008. Assessing coral reef health across onshore to offshore stress gradients in the US Virgin Islands. Marine Pollution Bulletin. 56, 1983-1991.

Smith, T.B., Blondeau, J., Taylor, M., Nemeth, R.S., Calnan, J.M., Tyner, E., 2007. Continuation and Expansion of the Territorial Biological Monitoring Program. Final Report. Submitted to the USVI Department of Environmental Protection, 69.

Soulsby, R., 1997. Dynamics of Marine Sands. Thomas Telford Publications, London.

Spiske, M., Jaffe, B.E., 2009. Sedimentology and hydrodynamic implications of a coarse-grained hurricane sequence in a carbonate reef setting. Geology. 37(9), 839-842.

Stambler, N., Dubinsky, Z., 2005. Corals as light collectors: An integrating sphere approach. Coral Reefs. 24(1), 1-9.

Stanley, G.D., Fautin, D.G., 2001. Palenotology and evolution: The origins of modern corals. Science. 291(5510), 1913-1914.

Stanley, G.D., Jr., Swart, P.K., 1995. Evolution of the coral-zooxanthenllae symbiosis during the Triassic: A geochemical approach. Paleobiology. 21(2), 179-199.

Stearn, C.W., Scoffin, T.P., 1977. Carbonate budget of a fringing reef, Barbados. Proceedings of the 3rd International Coral Reef Symposium. Rosenstiel School of Marine and Atmospheric Science, University of Miami : Miami, FL, United States, United States. 23, pp. 471-476.

Stearn, C.W., Scoffin, T.P., Martindale, W., 1977. Calcium carbonate budget of a fringing reef on the west coast of Barbados: Part 1-Zonation and productivity. Bulletin of Marine Science. 27(3), 479-510.

Steneck, R.S., 1994. Is herbivore loss more damaging to reefs than hurricanes? Case studies from two Caribbean reef systems (1978-1988). In: Ginsburg, R.N. (Ed.), Rosenstiel School of Marine and atmospheric Science, University of Miami, pp. 220-226.

Stoddart, D.R., 1969. Ecology and morphology of recent coral reefs. Biological Reviews. 44, 433-498.

Storlazzi, C.D., Ogston, A.S., Bothner, M.H., Field, M.E., Presto, M.K., 2004. Wave- and tidally-driven flow and sediment flux across a fringing coral reef: Southern Molokai, Hawaii. Cont.Shelf Res. 24(12), 1397-1419.

Storlazzi, C.D., Logan, J.B., Field, M.E., 2003. Quantitative morphology of a fringing reef tract from high-resolution laser bathymetry: Southern Molokai, Hawaii. Geological Society of America Bulletin. 115(11), 1344-1355.

Swart, P.K., Melim, L.A., 2000. The Origin of dolomites in Tertiary sediments from the margin of Great Bahama Bank. Journal of Sedimentary Research. 70(3), 738-748.

Swart, P.K., Burns, S.J., Leder, J.J., 1991. Fractionation of the stable isotopes of oxygen and carbon in carbon dioxide during the reaction of calcite with phosphoric acid as a function of temperature and technique. Chemical Geology. 86(2), 89-96.

Swart, P.K., 1983. Carbon and oxygen isotope fractionation in scleractinian corals: A review. Earth-Sci.Rev. 19(1), 51-80.

Swinchatt, J.P., 1965. Significance of constituent composition, texture, and skeletal breakdown in some recent carbonate sediments. Journal of Sedimentary Petrology. 35(1), 71-90.

Thompson, R.C., Wilson, B.J., Tobin, M.L., Hill, A.S., Hawkins, S.J., 1996. Biologically generated habitat provision and diversity of rocky shore organisms at a hierarchy of spatial scales. J.Exp.Mar.Biol.Ecol. 202(1), 73-84.

Titlyanov, E.A., Titlyanova, T.V., 2002. Reef-building corals-symbiotic autotrophic organisms: 2. Pathways and mechanisms of adaptation to light. Russ.J.Mar.Biol. 28(1), S16-S31.

Titschack, J., Nelson, C.S., Beck, T., Freiwald, A., Radtke, U., 2008. Sedimentary evolution of a Late Pleistocene temperate red algal reef (Coralligène) on Rhodes, Greece: Correlation with global sea-level fluctuations. Sedimentology. 55(6), 1747-1776.

Torrence, C., Compo, G.P., 1998. A practical guide to wavelet analysis. Bull.Amer.Meteor.Soc. 79(1), 61-78.

Tribollet, A., Golubic, S., 2011. Reef bioerosion: Agents and processes. In: Dubinsky, Z., Stambler, N. (Eds.), Coral reefs: An ecosystem in transition. Springer Netherlands, pp. 435-449.

Tribollet, A., Decherf, G., Hutchings, P., Peyrot-Clausade, M., 2002. Large-scale spatial variability in bioerosion of experimental coral substrates on the Great Barrier Reef (Australia): Importance of microborers. Coral Reefs. 21(4), 424-432.

Tucker, M.E., Wright, V.P., 1990. Carbonate Sedimentology. Blackwell Scientific Publishing, Oxford, United Kingdom.

Tunnicliffe, V., 1981. Breakage and Propagation of the Stony Coral Acropora cervicornis. Proc.Natl.Acad.Sci.U.S.A. 78(4), 2427-2431.

van Gestel, J., Mann, P., Dolan, J.F., Grindlay, N.R., 1998. Structure and tectonics of the upper Cenozoic Puerto Rico-Virgin Islands carbonate platform as determined from seismic reflection studies. Journal of Geophysical Research: Solid Earth. 103(B12), 30505-30530.

Vandermeulen, J.H., Watabe, N., 1973. Studies on reef corals. I. Skeleton formation by newly settled planula larva of Pocillopora damicornis. Mar.Biol. 23(1), 47-57.

Vecsei, A., 2001. Fore-reef carbonate production: Development of a regional census-based method and first estimates. Palaeogeogr., Palaeoclimatol., Palaeoecol. 175(1–4), 185-200.

Veron, J.E.N., 1995. Corals in space and time: Biogeography and evolution of the *Scleractinians*. Cornell University Press, Ithaca, NY.

Vogel, K., Gektidis, M., Golubic, S., Kiene, W.E., Radtke, G., 2000. Experimental studies on microbial bioerosion at Lee Stocking Island, Bahamas, and One Tree Island, Great Barrier Reef, Australia; implications for paleoecological reconstructions. Lethaia. 33(3), 190-204.

Wanless, H.R., Burton, E.A., Dravis, J., 1981. Hydrodynamics of carbonate fecal pellets. Journal of Sedimentary Petrology. 51(1), 27-36.

Weber, J., 1974. $^{13}C/^{12}C$ ratios as natural isotopic tracers elucidating calcification processes in reef-building and non-reef-building corals. In: Cameron, A.M., Cambell, B.M., Cribb, A.B., Endean, R., Jell, J.S., Jones, O.A., Mather, P., Talbot, F.H. (Eds.), Proceedings of the 2nd International Coral Reef SymposiumBrisbane, Australia. 2, pp. 289-300.

Weber, J.N., Deines, P., Weber, P.H., Baker, P.A., 1976. Depth related changes in the 13C12C ratio of skeletal carbonate deposited by the Caribbean reef-frame building coral

Montastrea annularis: Further implications of a model for stable isotope fractionation by scleractinian corals. Geochim.Cosmochim.Acta. 40(1), 31-39.

Weinstein, D.K., Klaus, J.S., Smith, T.B., 2014. Mesophotic bioerosion: Variability and structural impact on U.S. Virgin Island deep reefs. Geomorphology. 222, 14-24.

Wellington, G.M., Glynn, P.W., 1983. Environmental influences on skeletal banding in eastern Pacific (Panama) corals. Coral Reefs. 1(4), 215-222.

Whelan, K., Miller, J., Sanchez, O., Patterson, M., 2007. Impact of the 2005 coral bleaching event on *Porites porites* and *Colpophyllia natans* at Tektite Reef, US Virgin Islands. Coral Reefs. 26(3), 689-693.

White, K.N., Ohara, T., Fujii, T., Kawamura, I., Mizuyama, M., Montenegro, J., Shikiba, H., Naruse, T., McClelland, T., Denis, V., Reimer, J.D., 2003. Typhoon damage on a shallow mesophotic reef in Okinawa, Japan. PeerJ 1. 1, e151.

Wilkinson, C., Souter, D., 2008. The status of Caribbean coral reefs after bleaching and hurricanes in 2005, Coral Reef Monitoring Network.

Wilson, J., L., 1975. Carbonate facies in geologic history. Springer-Verlag, New York, New York.

Wilson, M.E.J., 2005. Development of equatorial delta-front patch reefs during the Neogene, Borneo. Journal of Sedimentary Research. 75(1), 114-133.

Wórum, F.P., Carricart-Ganivet, J.P., Benson, L., Golicher, D., 2007. Simulation and observations of annual density banding in skeletons of *Montastraea* (Cnidaria: Scleractinia) growing under thermal stress associated with ocean warming. Limnol. Oceanogr. 52(2), 2317-2323.

Yamazato, K., 1972. Bathymetric distribution of corals in the Ryukyu Islands. In: Mukundan, C., Pillai, C.S.G. (Eds.), Proceedings of the Symposium on Corals and Coral Reefs. Marine Biological Association of India, India, Cochin, pp. 121-133.

Yates, K.K., Halley, R.B., 2003. Measuring coral reef community metabolism using new benthic chamber technology. Coral Reefs. 22(3), 247-255.

APPENDIX A

Abbreviation List

	Full Name	Page*
ADCP	acoustic doppler current profiler	46
CV$_{max}$	Average spring-neap tidal cycle current velocity maximum	60
CV$_{mean}$	Average spring-neap tidal cycle current velocity mean	60
ANOVA	analysis of variance	49
BD	slice bulk density	143
BW$_{wax}$	buoyant weight of wax-coated slice	143
CO$_2$	carbon dioxide	44
CCA	crustose coralline algae	5
DW$_{clean}$	dry weight of slice (no wax)	142
DW$_{wax}$	dry weight of wax-coated slice	143
ECS	exposed consolidated substrate	180
EPS	extracellular polymeric substances	86
HMC	high-magnesium calcite	48
HSD	honestly significant difference	49
IMS	intercostal mortality syndrome	114
LMC	Low-magnesium calcite	48
MCDFB	Marine Conservation Deep Flat Basin	23
MCE	marine coral ecosystems	2
NMDS	non-metric multidimensional scaling	50
OACX	*Orbicella spp.* (formally *Montastraea annularis* coral species complex	34
PM	potential mobility	53
RHMCD	Red Hine Marine Conservation District	19
RSMAS	Rosenstiel School of Marine and Atmospheric Science	138
SEM	scanning electron microscope	47
STDA	standardized anomaly	163
TCRMP	United States Virgin Islands Territorial Coral Reef Monitoring Program	24
USGS	United States Geological Survey	26
USVI	United States Virgin Islands	4
V$_{enclosed}$	enclosed volume in the slice	143
w$_s$	settling velocity	51
XRD	X-ray diffraction	48
ΔLE	linear extensions rate	146
ΔC	calcification rates	143

* first time the abbreviation is used in the text.

Study sites

Code	Geomorphology	Sample names
D1	Hillock Basin	S166
D2	Deep Patch	MCDP
D3	Primary Bank	Gram (Grammanik Bank)
D4	Secondary Bank	Coll (College Shoal)
M5	Mid-shelf Patch	Sea (Seahorse Cottage)
S6	Fringing Patch (shallow)	BP (Black Point)

APPENDIX B

Extended bioerosion literature review

Bioerosion geological history and preservation

Bioeroding organisms have been associated with reef deposits throughout the organic history of Earth. The earliest occurrence of microboring endoliths was documented in Mesoproterozoic stromatolites (Zhang and Golubic, 1987), followed by the identification of microborers in Neoproterozoic deposits (Knoll et al., 1986) and deposits throughout the Paleozoic (Campbell, 1980). Though sparse, macroboring worms first appeared in the Lower Cambrian, as evidenced by traces found in archaeocyathid reefs (James et al., 1977). The first major increase in macroborer diversity and macroboring rates occurred in the Late Ordovician and is termed the Ordovician Bioerosion Revolution (Wilson and Taylor, 2006).

A second major macroboring diversification occurred in the Devonian, with many borings similar to those found in modern reefs (Wilson, 2007). Boring bivalves and sponges, first appearing in the lower Paleozoic, were not abundant bioeroders until the Mesozoic, potentially because the higher density of rugose coral compared to scleractinian coral prevented major Paleozoic erosion (Vogel, 1993). Macroborer diversity peaked in Jurassic, a pinnacle greater than any other time period in geological history (Wilson and Taylor, 2006). Bivalves and worms dominated these peak periods of macroboring diversity but became subdominant to sponges from the Early Miocene until Recent (Perry and Bertling, 2000).

The first substrate grazing organisms, primarily gastropods and echinoids, appeared in the Triassic but were not major substrate modifiers until the Jurassic or

Cretaceous periods (Vogel, 1993). Scaridae (parrotfish), the most efficient reef

excavators in the Recent, first appeared in the Miocene (Bellwood and Choat, 1990). The

relatively late appearance of parrotfish in the geological record indicates that early

Cenozoic reef bioerosion was substantially different than in modern times, and implies

reef shaping processes have not always been the same (Vogel, 1993). The long history of

reef bioerosion and the importance of bioeroders in reworking reef material implies a

need to comprehend how bioerosion affects the development of different reef habitats,

the overall structure of an autonomous reef ecosystem, and the amount of reef material

that can potentially be preserved as structure-forming framework (Kiene, 1988; Kiene

and Hutchings, 1993; Perry, 1999).

Bioeroder classification and methodology

Bioerosion is defined as any form of biological penetration into a hard substrate

(Neumann, 1966; Bromley, 1978). Bioeroding groups, classified by method of erosion,

include: (1) macroborers (> 100 μm diameter traces); (2) microborers/etchers (< 100 μm

diameter trace); and (3) grazers (Golubic et al., 1975; Warme, 1975; Hutchings, 1986).

The macroboring group can be divided between meiofauna (0.1-1 mm), and macrofauna,

(>1mm; (Tribollet and Golubic, 2011). Golubic et al. (1981) classified lithobionts, rock-

inhabiting microorganisms, as: (1) endoliths (living within skeletons); (2) chasmoliths

(residing in holes and cracks); or (3) epiliths (occupying exposed surfaces.

Macroboring macrofauna primarily consist of boring sponges, polychaete

annelids, sipunculid worms, pholadid and mytilid bivalves, and such other less pervasive

organisms as foraminifera, crustaceans (barnacles, crabs, shrimp, etc.), decapods,

brachiopods, bryozoan, and gastropods (Warme, 1975; Hutchings, 1986; Glynn, 1997;

Perry and Hepburn, 2008). Clionid sponges are considered the most important

macroborers, often comprising 75- 90% of the total macroboring community within a

substrate (Goreau and Hartman, 1963; Perry, 1998). Meiofauna are comprised of small

foraminifera and polychaetes, as well as the larvae of macrofauna (Tribollet and Golubic,

2011). Microborings are produced by cyanobacteria, rhodophytes and chlorophytes, and

heterotrophic fungi and bacteria (Golubic et al., 1975).

Grazers remove surface carbonate while grazing algae. They mainly consist of

fish (primarily parrotfish, surgeonfish,and some triggerfish, filefish, and puffers),

echinoids, gastropods, and chiton, with fish and echinoids being the most dominant

(Warme, 1975; Hutchings, 1986; Glynn, 1997). Many of these organisms obtain their

primary sustenance from algae and sometimes live coral (Randall, 1974), mechanically

eroding the carbonate substrate that their nutrients resides. Parrotfish use strong beaklike

jaws and a pharyngeal mill to remove, grind, and breakdown substrate, often imprinting a

characteristic double groove on the eroded substrate (Randall, 1974; Ogden, 1977).

Echinoids use their hard Aristotle's lantern to rasp algae and carbonate (Glynn, 1997).

Both groups digest the organic material; the carbonate remainder passes through the gut

as sand and mud (Ogden, 1977).

Although many organisms have been found to bore into carbonate substrates, the

reason for boring is not fully understood, with the exception of fungi, which bore to

obtain nourishment through organic skeletal matrices (Warme, 1975). Early hypotheses

that organisms bore into carbonate to escape predation were quickly refuted (at least for

microborers) when fossil evidence identified microborings in Mesoproterozoic deposits,

long before the occurrence of grazing predators (Zhang and Golubic, 1987). A recent

review suggested possible reasons for carbonate boring. These include UV radiation protection, nutrient procurement, resource competition, and prevention of mineralization entombment (Cockell and Herrera, 2008). The appearance of "black rot" and the deterioration of boring sponge tissue exposed to sunlight (compared to more healthy tissue shaded from sunlight) in laboratory studies confirmed that boring into substrate serves such multiple functions as protection from harmful sunlight and shielding from disease and parasites (Schönberg and Wisshak, 2012).

Methods for boring are more understood, although determination of actual chemical reactions employed by many of these organisms is still elusive. Microborings are created by phototrophic and organotrophic microorganisms that penetrate by dissolving dead substrate or substrate with living tissue, enter through lateral fissures, or enter at the base of the structure (Tribollet and Golubic, 2011). Acidulation was originally thought to be the primary microboring mechanism, but this idea was highly contested given that oxygenic photosynthesis causes carbonate precipitation and not dissolution (Garcia-Pichel, 2006). Garcia-Pichel (2006) suggested alternative methods involving either spatial or temporal separation of respiration and photosynthesis, or calcium ion extrusion. Further testing found that cyanobacteria can take up Ca^{2+} at the front of excavation, enabling enough decrease in the local extracellular calcium carbonate ion activity product for spontaneous dissolution and subsequent exportation of Ca^{2+} along the cyanobacterial trichomes for excretion at the distal borehole opening (Garcia-Pichel et al., 2010).

Macroboring organisms use mechanical techniques, chemical techniques, or a combination of these to erode carbonate (Glynn, 1997). Clionid sponges, often

considered the most destructive and common coral boring organisms, primarily erode substrate mechanically (Acker and Risk, 1985). However, the process involves extension of pseudopodial from amoebocytes that detach substrate by partially dissolving contacts through carbonic anhydrase regulation of secreted acid (Pomponi, 1979). This produces characteristic carbonate chips which are expelled, along with the amoebocyte cell, out of the papillae (Glynn, 1997). Some bivalves, like the family *Pholadidae,* are mechanical borers, while others, such as *Lithophagid* bivalves, use mantle glands to secrete an acid that dissolves and soften carbonate before the bivalve rotates its shell to penetrate deeper into the substrate (Purchon, 1968; Ansell and Nair, 1969; Warme and Marshall , 1969; Kleeman, 1990; Glynn, 1997). Polychaetes and sipunculids are diverse groups that employ several different mechanical or physico-chemical techniques (Glynn, 1997).

Sessile epilithic organisms, called calcareous epibionts (or secondary carbonate producers), make up another group commonly described tangentially with bioeroders. These organisms primarily consist of crustose coralline algae (CCA), sipunculid, mollusks, bryozoans, and foraminifera. Multiple factors regulate the growth and distribution of these calcified epibiont communities, including light availability, habitat type (exposed or cryptic), stability of substrate, wave strength, and sedimentation (Choi and Ginsburg, 1983; Martindale, 1992; Fabricius and De'ath, 2001). Collectively, secondary carbonate producers promote cementation (Scoffin, 1992), which helps reefs withstand strong wave energy, retain loose framework components, bind and stabilize reef framework (Rasser and Riegl, 2002), and ultimately improve potential framework preservation (Perry and Hepburn, 2008). Although not as abundant in shallow back-reef or deep fore-reef sites, secondary encrustation in shallow fore-reef and terrace sites in

Jamaica was found to be the dominant early diagenetic process for reef preservation by binding coral rubble to produce *in situ* coral rubble accumulations. Additionally, encrusting organisms can promote the larval recruitment of other framework-builders (Morse et al., 1988; Fabricius and De'ath, 2001) and may function as indicators of past palaeocecological conditions (Martindale, 1992).

The activity of calcareous epibionts is often related to bioerosional processes. Some epibionts serve as nutrients for grazing organisms (Randall, 1974). Other interactions include the ability of some secondary accreting organisms like CCA to form a protective cover around underlying substrate, blocking endolithic surface access holes (Bromley, 1978; Peyrot-Clausade and Bruno, 1990). Therefore, the increase of encrusting organisms decreases macroboring infiltration and potentially improves the preservation of reef framework. Relatedly, if low grazing intensity allows sessile epilithic colonization to proceed unperturbed, secondary carbonate producers potentially can make significant contributions to a reef's overall carbonate budget, helping to strengthen the reef and add mass to the overall reef complex (Gherardi and Bosence, 2005; Perry and Hepburn, 2008).

Living and dead coral substrate

Coral skeleton, comprising a large proportion of carbonate produced by modern coral reefs, is the most common modern carbonate reef substrate excavated by endolithic boring organisms (Golubic et al., 1981). The carbonate skeleton of coral can be eroded both while the coral polyp communities continue to grow and after the coral community has perished. Some fish can obtain sustenance by feeding on live coral polyps, but these actions are thought to have a nominal impact on coral colony growth (Randall, 1974).

Parrotfish, one of the most abundant fish groups on Caribbean coral reefs (see Mumby, 2009), can graze on living coral colonies and subsequently remove underlining carbonate skeleton. This behavior is relatively minor though, as parrotfish primarily opt to feed on algae growing on top or within dead coral skeleton framework and coral rubble (Bruggemann et al., 1996). Besides fish, other grazing organisms such as echinoderms, zoanthids, bryozoans, and foraminifers have been observed to damage coral skeleton both in the presence and absence of a living coral surface (Glynn, 1997).

Macroborers primarily infiltrate coral substrate though skeleton cracks or dead, exposed sections of carbonate substrate once they settle as planktonic larvae (Hutchings, 1986). Additionally, sponges sometimes colonize through tissue extension (Schönberg, 2003), and some polychaetes colonize as juveniles (Hutchings and Murray, 1982). Few of these organisms are able to bore through living coral tissue. Exceptions include the sponge *Cliona orientalis* (Schönberg and Wilkinson, 2001) and the bivalve *Lithophaga bisulcata* (Scott, 1988). However, macroborings are still found within the skeleton of living coral colonies collected for analysis (see Fig. 3.2a and Fig. 4.3 for examples). Coral colonies are essentially thin veneers of living tissue covering previously produced, older skeleton. Therefore, macroboring organisms are able to erode the majority of a coral colony if they can find a surface void of live tissue cover (usually on the underside of platy coral or at the base of massive coral) to penetrate. Macroborings have even been found to topple and overturn coral colonies by weakening the base supporting them (Glynn, 1997).

Similar to their larger counterparts, microboring organisms can colonize and dissolve the carbonate skeleton of dead substrate as well as substrate covered with living

coral polyps. Microboring organisms with the ability to bore through living coral tissue and keep up with surrounding coral calcification include cyanobacteria (such as *Ostreobium quekettii* and *Plectonema terebrans)* and fungi (see review paper by Tribollet and Golubic, 2011). With varying light requirements, microborer penetration depths are species dependent. At a maximum, microborers can penetrate up to 1 cm below the surface (*O. quekettii* and *P. terebrans* have been shown to penetrate to these depths, Chazottes et al. 1995). *O. quekettii*, responsible for the formation of green bands within the coral skeleton (Fig. 4.3, red arrows), can potentially dissolve up to 25% of the carbonate (Le Campion-Alsumard et al., 1995).

Bioeroder interactions

Bioerosion does not directly preserve original reef framework, but instead acts to modify the skeleton and facilitate lithification through cement precipitation. This becomes apparent when recognizing that many ancient reef deposits are primarily composed of cemented coral rubble and sediment, not the unburied *in situ* coral framework seen when swimming over a modern reef (Hubbard et al., 1990; Blanchon et al., 1997). As a result, Davies and Hopley (1983) suggested that analysis of reef systems should concern sedimentary facies and not coral framework   Although preserved *in situ* framework is rare, it is thought to occur when there is rapid burial and early marine cementation (Hoffmeister and Multer, 1968; Perkins, 1977; Walker and Diehl, 1985; Greenstein and Pandolfi, 2003).

The first and potentially most significant process governing reef preservation is the cumulative effect of bioerosional and secondary accretion. Bioeroding organisms do not exist as independent entities when considering their overall impact on the reef.

Instead, they have various complex relationships and interacting processes that ultimately help shape the carbonate system they are a part of and dictate the system taphonomy (Sammarco, 1996). Bioeroder interactions are perhaps most evident with grazers, which have the ability to affect overall bioerosion rates, endolithic community population dynamics, and community structure (Sammarco, 1996). Phototrophic microborers can only penetrate several millimeters from the outer surface. However, they share a cooperative relationship with grazers by loosening up substrate to allow for easier grazing. This increases light penetration deeper into the substrate, allowing microboring activity to continue and penetrate deeper (Tribollet and Golubic, 2011).

Grazing is also thought to have important interactions with macroboring processes. Changes in grazing intensity can alter the endolithic sponge community by shifting growth rates and larval recruitment of endoliths, and by changing the amount of exposed substrate available for erosion, colonization, or both (Sammarco et al., 1987; Sammarco and Risk, 1990; Kiene and Hutchings, 1994; Risk et al., 1995). However, it is generally thought that interactions between macroboring community groups affects overall bioerosion rates less than succession sequences (Highsmith et al., 1983; Scoffin and Bradshaw, 2000), which are thought to change with the age of the host substrate (Hutchings et al., 1992; Kiene and Hutchings, 1994).

Bioeroder interactions can have drastic effects on reef preservation, especially if a bioeroding group becomes overly dominate. Nearly 40% of the upper Jurassic patch reef volume on top of the Portland Limestone Formation was removed by boring endoliths, leading researchers to suggest that macroboring alone has the potential to considerably reduce the overall volume of reef framework (Fürsich et al., 1994). The borings created

can also help with overall reef preservation by providing cementation sites to help lithify and strengthen the deposit. If macroboring were extremely intense, maybe as a result of increased nutrient input (Rose and Risk, 1985), it could become difficult or impossible to distinguish coral from adjacent matrix in ancient reef deposits, even if the coral were to make up a large quantity of the deposit.

Elevated grazing erosion has the potential to completely destroy the topographic relief of a reef (Reaka-Kudla et al., 1996). This could hypothetically remove most traces of the original reef habitat, suggesting the potential that many ancient reefs were not preserved in the fossil record. However, reef grazing deficiencies can result in a shift from coral dominated reefs to reefs dominated by macroalgae communities that lack the ability to create diverse, three-dimensional habitats. Under these situations, coral directly competes with macroalgae for reef space (McCook et al., 2001). Coral growth rates have been shown to decrease when in direct contact with macroalgae (Tanner, 1995). Moreover, coral larvae recruits are unable to settle on macroalgae (Steneck, 1988) and can be smothered by sediment trapped by algae (Birkeland, 1977). When macroalgae outcompete coral for reef space, ecological phase shifts are possible, and can highly jeopardize the ultimate preservation of the reef if the shifts continue unabated (McClanahan and Muthiga, 1998; Knowlton and Jackson, 2008).

Rates of bioerosion

Bioerosion rates are influenced by the magnitude and interaction of many environmental properties. This implies that bioerosion rates are mostly controlled by those factors and processes that can change the reef community as a whole (Sammarco, 1996). These properties include: light availability; depth and geography; habitat type;

sedimentation; eutrophication; substrate type; and biological succession. Studies conducted near Lee Stocking Island, Bahamas, and One Tree Island, Great Barrier Reef, suggest that factors such as light attenuation, substrate type, and geographical position greatly control the distribution and abundance of microborers (Vogel et al., 2000). In contrast, Vogel et al. (2000) found that reef nutrient fertilization (specifically additions in phosphate and ammonium) had no impact on micro-bioerosion rates. Bioerosion rates have also been found to vary between shallow-water reef environments with different geomorphology in the Great Barrier Reef (Hutchings et al., 1992; Kiene and Hutchings, 1994). The cause for this observed spatial variability was believed to result from both environmental factors and ecological succession patterns.

Sedimentation can also facilitate bioerosion variability as a result of the impact of sediment on water clarity and sunlight penetration, coral growth, and primary producer photosynthesis (Pang, 1973; Carballo et al., 1994; Scoffin et al., 1997; McKenna and Ritter, 1999). Macdonald and Perry (2003) found that sponges dominated the macroboring communities in clear-water areas while bivalves and some worms dominated the bioeroding communities in areas with high sedimentation. However, high levels of bivalve abundance was found to offset sponge bioerosion reduction such that overall macroboring infestation levels were comparable between north Jamaican clear and turbid water reefs (Macdonald and Perry, 2003). On the Great Barrier Reef, macroboring density increases were shown to correspond to increasing levels of turbidity and chlorophyll *a,* a proxy for water column primary productivity (Le Grand and Fabricius, 2011). Similarly, chlorophyll *a* concentrations were found to positively correlate with macro-bioerosion rates on the coast of Kenya. Macroborer community

composition in these Kenyan reefs was also shown to vary depending on grazer dominance type. Worms or sponges were more abundant when reef grazing was dominated by sea urchins or fish, respectively (Carreiro-Silva and McClanahan, 2012). The study also compared macroboring rate differences in water velocity, and temperature but found no correlation (personal communications with Carreiro-Silva, 2012). In contrast to results from Vogel et al. (2000), studies have found that seawater eutrophication can increase the levels of bioerosion (Smith et al., 1981; Hallock, 1988; Holmes et al., 2000; Pari et al., 2002; Carreiro-Silva et al., 2005).

Variability in substrate properties such as composition, density, and porosity have also been shown to affect bioerosion rates (Vogel et al., 2000; Schonberg, 2002). Endolithic borers (when dominated by sponges) erode more material and inflict more damage to denser substrates (Highsmith, 1981; Highsmith et al., 1983; Vogel et al., 2000; Schonberg, 2002). Schonberg (2002) found that the bioeroding sponge *Cliona orientalis* would use pre-existing pores when available, resulting in the removal of less material than in denser substrates. Additionally, preferential degradation has been known to occur with different coral species or morphologies, providing evidence that some coral species are more susceptible to macroboring (Pang, 1973; Hubbard et al., 1986; Perry, 1998).

Studies have determined that the amount of available dead substrate is directly related to bioerosion succession (Highsmith et al., 1983; Scoffin and Bradshaw, 2000). Therefore, the identification of succession sequences is another important factor to consider when studying bioerosion rates. In Moorea Island, French Polynesia, microborers were extremely important in the beginning stages of infaunal boring, accounting for more than 50% of the total bioerosion recorded in the first two months

(Chazottes et al., 1995). After two months, Chazottes et al. (1995) found that macroboring increased considerably, and by six months, grazers became the dominate bioeroders, accounting for 89% of the overall bioerosion. Similar results were found on the Great Barrier Reef (Kiene, 1988; Kiene and Hutchings, 1993).

Macroboring communities have been shown to change with the increasing age of the host substrate, beginning with small, short-lived worms, followed by longer-lived larger worms, sipunculans, mollusks, and sponges (Hutchings et al., 1992; Kiene and Hutchings, 1994). Choi (1984) found a three-year succession pattern in northern Florida reef tract coral rubble, beginning with encrusting foraminifers, boring bivalves, and serpulid worms, followed by most bryozoan species and sponges along with solitary bryozoans and non-boring bivalves. A different pattern, which began with polychaete borers, was found at Lizard Island, Great Barrier Reef (Davies and Hutchings, 1983). In areas subject to high levels of grazing, substrates, on average, are likely to be younger in age than in areas with less grazing. Therefore, these younger substrates would likely have a lower abundance of more mature macroboring communities, such as those dominated by sponges, compared to substrates that experience lower levels of grazing bioerosion (Hutchings et al., 1992; Kiene and Hutchings, 1994).

Impact of coral reef degradation drivers on bioerosion

   -Pollution

The direct effect each particular form of land-based pollution has on bioerosion has not been fully addressed. Evidence suggests that in general, bioerosional processes can be highly altered by pollution and sedimentation. Various studies have suggested, and some have confirmed, that eutrophication stimulates increased erosion rates by some

bioeroding organisms, especially when compared to the strong negative impact pollution has on coral reef growth (Smith et al., 1981; Hallock, 1988; Edinger et al., 2000; Holmes et al., 2000). Smith et al. (1981) found that sewage input eventually favors the growth of carbonate eroding organisms. Some studies have discovered that eutrophication (in addition to low herbivory) increases microboring bioerosion (Chazottes et al., 1995; Chazottes et al., 2002; Carreiro-Silva et al., 2005). Other studies found no change in microboring bioerosion rates when exposed to nutrient enrichment (Koop et al., 2001). Elevated sewage and nutrient input stimulates algal turf production, which may increase grazing and result in higher bioerosion rates overall (Peyrot-Clausade et al., 1995).

Physiological reasons why terrestrial pollution alters bioerosional processes are not fully understood. Excavating bioeroders like sponges are filter feeders (Holmes, 1997). Therefore, one possible explanation for pollution-driven increases in bioerosion rates and biomass is that bioeroders, especially their larva, obtain sustenance from suspended organic matter and nutrients (Highsmith, 1980; Smith et al., 1981; Hallock and Schlager, 1986). Healthy reefs are assumed to have, and have been recorded as having, nearly balanced rates of carbonate production and erosion, with accretion maintained by calcification slightly outpacing bioerosion (Hein and Risk, 1975; Highsmith, 1980; Scoffin et al., 1980; Davies and Hutchings, 1983; Glynn, 1997; Baker et al., 2008). For this reason, the most common explanation given for why nutrient enrichment increases bioerosion is more related to the coral. Because eutrophication can significantly slow coral calcification, even relatively small enrichments in nutrients can swing the general state of a reef from net production to net erosion (Highsmith, 1980; Hallock and Schlager, 1986; Hallock, 1988). However, high rates of bioerosion have also been

recorded in pristine coral reef environments, triggering some doubt to the claim that anthropogenic effects bring about increased rates of bioerosion (Pari et al., 2002). Instead, Pari et al., (2002) suggested that the amount of dead substrate available for bioeroder colonization and grazing is the critical factor regulating bioerosional-induced reef degradation, and claimed that in general, increased sedimentation rates and reduced water quality promote higher boring rates and bioerosional grazer populations.

Beyond their role as primary sediment producers (Acker and Risk, 1985), bioeroders have also been shown to be affected by sedimentation, depending on the bioeroder group and sediment type. Macdonald and Perry (2003) proposed that sedimentation-induced stress and the potential damage it causes to coral tissue may even encourage bioerosion. High sedimentation, lacking fertilizer and nutrient contamination, is thought to impede (and sometimes prevent) the settlement of endolithic and epilithic alga (Hutchings et al., 2005). Feedback form this situation induces protection of coral substrates from grazing but possibly increases levels of macroborer recruitment (Hutchings et al., 2005). Similarly, turbid water from terrestrial runoff was believed to restrict bioeroding organisms from colonizing, which in turn reduced the amount of grazing (Tribollet et al., 2002). However, Pari et al. (2002) showed earlier, if sedimentation is high in nutrients, macroboring, microboring, and grazing rates all increase. Sedimentation is also thought to influence bioerosion in a similar way to eutrophication; the reduction in water clarity by sedimentation can impede coral growth, and primary producer photosynthesis, causing bioerosional rates to increase relative to primary carbonate production (Pang, 1973; Carballo et al., 1994; Scoffin et al., 1997; McKenna and Ritter, 1999; Wilson et al., 2008).

- Overfishing

The effect overfishing has on bioerosional processes is often indirect, generally impacting ecological invertebrate relationships and interactions critical to the overall reef net carbonate balance that favors high reef biodiversity. As discussed earlier, it has been suggested that intense, rapid grazing limits the establishment of mature macroboring communities (Kiene and Hutchings, 1994). Therefore, an overfishing-induced reduction in grazing would likely increase the amount of macroboring activity found within the reef. However, this might not happen if other grazing organisms prosper because of the overfishing. For example, live coral cover was significantly lower on Kenyan reefs suffering from overfishing compared to unexploited reefs (McClanahan and Muthiga, 1988). McCanahan and Muthiga (1988) suggested that this resulted from higher recorded levels of bioeroding sea urchin biomass brought on by overfishing-induced competitive exclusion. Similarly in the Caribbean, overfishing was also attributed to increased biomass of the sea urchin *Diadema* (Sammarco, 1980; Carpenter, 1984). Although this effect appeared to lower fleshy macroalgae on Caribbean reefs, the increase of *Diadema* was thought to depress coral recruitment, elevate levels of coral mortality (Sammarco, 1980), and facilitate slight reductions in topographic complexity (Glynn, 1997).

Lower-levels of tropic organisms, such as sea urchins, increase a reef's susceptibility to diseases when population biomass density increases to a critical threshold (Hochachka and Dhondt, 2000). Therefore, it has been speculated that overfishing was a main driver for the 1983 Caribbean massive die-off of *Diadema* and related ecological phase shifts (Jackson et al., 2001). Particularly in Jamaican reefs, macroalgae was found to proliferate and induce coral to algae phase changes (Hughes,

1994). In the Great Barrier Reef, some coral reefs suffered significant degradation as a result of widespread outbreaks of *Acanthaster*, a crown-of-thorns starfish that feeds on coral. The primary cause of this outbreak was believed to be overfishing, reducing the predation of the starfish and allowing its biomass to increase beyond normal balanced levels (Bradbury and Seymour, 1997).

- Climate change and ocean acidification

Review papers that discuss the adverse effects of climate change almost never address how bioerosion processes are independently affected. Instead, these studies defer to the effect bioerosion has in relation to more frequent occurrences of coral reef bleaching and the related availability of additional dead substrate (Glynn, 1993; Glynn, 1996; Hoegh-Guldberg, 1999; Hoegh-Guldberg et al., 2007). Various studies have documented the debilitating effects of rapid bioerosion following major bleaching events (Glynn, 1988; Reaka-Kudla et al., 1996; Eakin, 2001, and see extensive list by Baker et al., 2008). However, few studies have actually tested the direct effects temperature increases will have on bioerosional processes and rates. Although coral physiology is often drastically harmed by bleaching events, Glynn (1996) suggested that the same environmental protrusions do not appear to directly harm corallivores, carbonate grazers, or bioeroding organisms, allowing for greater decreases in topographic complexity.

One basic approach to examine the effect of temperature on bioerosion is based on classic kinetic molecular theory. Arrhenius' equation explains how the rate of chemical reactions is greatly affected by temperature. However, it is unlikely that this principle guarantees that climate change increases chemical bioerosion. There are many other variables to consider such as the extent of temperature increase, the initial speed of

the chemical reaction, and if the chemical reaction is continuously occurring or buffered by additional biological mediation. Although clionid sponge growth rates have been found to correlate positively with water temperature (Rützle, 2002; Carver et al., 2010), direct sampling found that higher temperatures had little effect on sponge growth or boring rates (Wisshak et al., 2011; Carreiro-Silva and McClanahan, 2012; Duckworth and Peterson, 2013). Bioerosion research in Bermuda cited potential increases in sponge bioerosion associated with lower temperatures, although data was inconclusive (Rützler, 1975). Increased temperatures may increase grazing bioerosion, given the previously described increase in macroalgae competition after coral bleaching events. Regardless, more definitive research is needed before the effect of temperature on bioerosional mechanisms is fully known.

Compared to temperature, more research has been conducted to predict the potential effect of ocean acidification on bioerosion. A laboratory experiment found that carbonate dissolution rates by microboring euendoliths were almost 50% higher in treatments with elevated pCO_2 compared to ambient levels (Tribollet et al., 2009). Low carbonate saturation rates in eastern tropical Pacific reefs have been suggested to be associated with higher recorded bioerosion rates (Manzello et al., 2008). In another study across the Pacific basin, live *Porites* macroboring rates were found to increase significantly with decreased levels of carbonate saturation state (related to ocean acidification), particularly under high-nutrient conditions (DeCarlo et al., 2014). The boring rates of sponges also increased when pCO_2 was elevated in laboratory studies (Wisshak et al., 2012). Wisshak et al. (2012) suggested that these increases in sponge bioerosion rates resulted from an amplified efficiency (lower metabolic cost) of

bioerosional processes that already need to lower pH at boring interfaces to enable chemical etching. When examining greater reef carbonate fluctuations on a small spatial scale in Kāneʻohe Bay, Hawaiʻi (~10 m), erosion rates were found to increase as pH levels decreased. Additionally, pH levels were found to better predict experimental substrate balance between accretion and erosion than by any other tested environmental driver (Silbiger et al., 2014).

Acidification will likely have unknown effects on the actual encrusting and eroding organisms as well, potentially weakening existing skeletons and the skeletal formations of many important bioeroding benthic calcifies (such as polychaete, sponges, mollusks and echinoderms) but to different degrees of debilitation (Przeslawski et al., 2008). Grazing communities have also been predicted to shift as a result of ocean acidification, with the outcome of carbonate grazing unknown (Atkinson and Cuet, 2008). Another unknown factor is how coral might adapt to changing ocean pH levels. For example, one potential adaptive response to ocean acidification impediment of calcification is to reduce skeletal density while maintaining energy levels needed for normal physical extension and growth rates (Hoegh-Guldberg et al., 2007). Like all attempts to adapt, there are potential side effects. Some grazers like parrotfish prefer lower-density coral substrates when feeding (Bruggemann et al., 1996), and boring sponges erode more carbonate and inflict more damage when excavating denser substrates (Highsmith, 1981; Highsmith et al., 1983; Rose and Risk, 1985; Schonberg, 2002). These substrate/bioerosion reaction properties could therefore make adaptive responses that decrease skeletal density more detrimental by encouraging increased bioerosional activity.

Works Cited (additional material)

Acker, K.L., Risk, M.J., 1985. Substrate destruction and sediment production by the boring sponge Cliona caribbaea on Grand Cayman Island. Journal of Sedimentary Petrology. 55(5), 705-711.

Ansell, A.D., Nair, N.B., 1969. A comparative study of bivalves which bore mainly by mechanical means. Am.Zool. 9(3), 857-868.

Atkinson, M.J., Cuet, P., 2008. Possible effects of ocean acidification on coral reef biogeochemistry: topics for research. Mar.Ecol.Prog.Ser. 373, 249-256.

Baker, A.C., Glynn, P.W., Riegl, B., 2008. Climate change and coral reef bleaching: An ecological assessment of long-term impacts, recovery trends and future outlook. Estuar.Coast.Shelf Sci. 80(4), 435-471.

Bellwood, D.R., Choat, J.H., 1990. A functional analysis of grazing in parrotfishes (family Scaridae): The ecological implications. Environ.Biol.Fishes. 28(1-4), 189-214.

Birkeland, C., 1977. The importance of rate of biomass accumulation in early successional stages of benthic communities in the survival of coral recruits. Proceedings of the 3rd International Coral Reef Symposium. 1, 15-21.

Blanchon, P., Jones, B., Kalbfleisch, W., 1997. Anatomy of a fringing reef around Grand Cayman: Storm rubble, not coral framework. Journal of Sedimentary Research. 67(1), 1-16.

Bradbury, R., Seymour, R., 1997. Waiting for COTSIn: Lessios, H.A., MacIntyre, I.G. (Eds.), Proceedings from the 8th International Coral Reef Symposium. Smithsonian Tropical Research Institute, PanamaPanama2, pp. 1357-1362.

Bromley, R.G., 1978. Bioerosion of Bermuda Reefs. Paleogeogr.Paleoclimatol.Paleoecol. 23(3-4), 169-197.

Bruggemann, J.H., van Kessel, A.M., van Rooij, J.M., Breeman, A.M., 1996. Bioerosion and sediment ingestion by the Caribbean parrotfish *Scarus vetula* and *Sparisoma viride*: Implications of fish size, feeding mode and habitat use. Marine Ecology Progress Series. 134(1-3), 59-71.

Campbell, S.E., 1980. Palaeoconchocelis starmachii, a carbonate boring microfossil from the Upper Silurian of Poland (425 million years old): Implications for the evolution of the Bangiaceae (Rhodophyta). Phycologia. 19, 25-36.

Carballo, J.L., Sanchez-Moyano, J.E., Garcia-Gomez, J.C., 1994. Taxonomic and ecological remarks on boring sponges (Clionidae) from the Straits of Gibraltar (southern

Spain): Tentative bioindicators? Zoological Journal of the Linnean Society. 112(4), 407-424.

Carpenter, R.C., 1984. Predator and population density control of homing behavior in the Caribbean echinoid *Diadema antillarum*. Mar.Biol. 82(1), 101-108.

Carreiro-Silva, M., McClanahan, T.R., 2012. Macrobioerosion of dead branching *Porites*, 4 and 6 yr after coral mass mortality. Mar.Ecol.Prog.Ser. 458, 103-122.

Carreiro-Silva, M., McClanahan, T.R., Kiene, W.E., 2005. The role of inorganic nutrients and herbivory in controlling microbioerosion of carbonate substratum. Coral Reefs. 24(2), 214-221.

Carver, C.E., Mallet, A.L., Theriault, I., 2010. Infection of cultured eastern oysters Crassostrea virginica by the boring sponge *Cliona celata*, with emphasis on sponge life history and mitigation strategies. J.Shellfish Res. 29, 905-915.

Chazottes, V., Le Campion-Alsumard, T., Peyrot-Clausade, M., Cuet, P., 2002. The effects of eutrophication-related alterations to coral reef communities on agents and rates of bioerosion (Reunion Island, Indian Ocean). Coral Reefs. 21(4), 375-390.

Chazottes, V., Le Campion-Alsumard, T., Peyrot-Clausade, M., 1995. Bioerosion rates on coral reefs: Interactions between macroborers, microborers and grazers (Moorea, French Polynesia). Palaeogeogr., Palaeoclimatol., Palaeoecol. 113, 189-198.

Choi, D.R., 1984. Ecological succession of reef cavity-dwellers (Coelobites) in coral rubble. Bulletin of Marine Science. 35, 72-80.

Choi, D.R., Ginsburg, R.N., 1983. Distribution of coelobites (cavity-dwellers) in coral rubble across the Florida Reef Tract. Coral Reef. 2(3), 165-172.

Cockell, C.S., Herrera, A., 2008. Why are some microorganisms boring? Trends Microbiol. 16(3), 101-106.

Davies, P.J., Hopley, D., 1983. Growth facies and growth rates of Holocene reefs in the Great Barrier Reef. BMR Journal of Australian Geology and Geophysics, 8(3; 3), 237-251.

Davies, P.J., Hutchings, P.A., 1983. Initial colonization, erosion and accretion on coral substrate: experimental results. Lizard Island Great Barrier Reef. Coral Reefs. 2, 27-35.

DeCarlo, T.M., Cohen, A.L., Barkley, H.C., Cobban, Q., Young, C., Shamberger, K.E., Brainard, R.E., Golbuu, Y., 2014. Coral macrobioerosion is accelerated by ocean acidification and nutrients. Geology, doi:10.1130/G36147.1.

Duckworth, A.R., Peterson, B.J., 2013. Effects of seawater temperature and pH on the boring rates of the sponge *Cliona celata* in scallop shells. Mar.Biol. 160(1), 27-35.

Eakin, C.M., 2001. A tale of two ENSO events: Carbonate budgets and the influence of two warming disturbances and intervening variability, Uva Island, Panama. Bull.Mar.Sci. 69(1), 171-186.

Edinger, E.N., Limmon, G.V., Jompa, J., Widjatmoko, W., Heikoop, J.M., Risk, M.J., 2000. Normal coral growth rates on dying reefs: Are coral growth rates good indicators of reef health?. Marine Pollution Bulletin. 40, 404-425.

Fabricius, K., De'ath, G., 2001. Environmental factors associated with the spatial distribution of crustose coralline algae on the Great Barrier Reef. Coral Reefs. 19(4), 303-309.

Fürsich, F.T., Palmer, T.J., Goodyear, K.L., 1994. Growth and disintegration of bivalve-dominated patch reefs in the Upper Jurassic of southern England. Palaeontology. 37, 131-171.

Garcia-Pichel, F., Ramírez-Reinat, E., Gao, Q., 2010. Microbial excavation of solid carbonates powered by P-type ATPase-mediated transcellular Ca^{2+} transport. Proceedings of the National Academy of Sciences. 107(50), 21749-21754.

Garcia-Pichel, F., 2006. Plausible mechanisms for the boring on carbonates by microbial phototrophs. Sediment.Geol. 185(3–4), 205-213.

Gherardi, D.F.M., Bosence, D.W.J., 2005. Late Holocene reef growth and relative sea-level changes in Atol das Rocas, equatorial South Atlantic. Coral Reefs, 24(2), 264-272.

Glynn, P.W., 1997. Bioerosion and coral-reef growth: A dynamic balance. In: Birkeland, C. (Ed.), Life and death of coral reefs. Chapman & Hall, New York, Albany etc., pp. 68-95.

Glynn, P.W., 1996. Coral reef bleaching: Facts, hypotheses and implications. Global Change Biology. 2(6), 495-509.

Glynn, P.W., 1993. Coral reef bleaching: Ecological perspectives. Coral Reefs. 12(1), 1-17.

Glynn, P.W., 1988. El Nino-Southern Oscillation 1982-1983: Nearshore population, community, and ecosystem responses. Annu.Rev.Ecol.Syst. 19(1), 309-346.

Golubic, S., Friedmann, I., Schneider, J., 1981. The lithobiontic ecological niche, with special reference to microorganisms. Journal of Sedimentary Research. 51(2), 475-478.

Golubic, S.S., Perkins, R.D., Lukas, K.J., 1975. Boring microorganisms and microborings in carbonate substrates. In: Frey, R.W. (Ed.), Study of Trace Fossils. Springer, Berlin and Heidelberg, pp. 229; 229-259; 259.

Goreau, T.F., Hartman, W.D., 1963. Control of coral reefs by boring sponges. In: Sognnaes, R.F. (Ed.), Mechanisms of Hard Tissue Destruction. AAAS Publishing, pp. 25-54.

Greenstein, B.J., Pandolfi, J.M., 2003. Taphonomic alteration of reef corals: Effects of reef environment and coral growth form: II, The Florida Keys Palaios, 18(6), 495-509.

Hallock, P., 1988. The role of nutrient availability in bioerosion: Consequences to carbonate buildups. Palaeogeography, Palaeoclimatology, Palaeoecology. 63(1-3), 275-291.

Hallock, P., Schlager, W., 1986. Nutrient excess and the demise of coral reefs and carbonate platforms. Palaios. 1, 389-398.

Hein, F.J., Risk, M.J., 1975. Bioerosion of coral heads: Inner patch reefs, Florida reef tract. Bulletin of Marine Science. 25(1), 133-138.

Highsmith, R.C., Lueotow, R.L., Schonberg, C.L., 1983. Growth and bioerosion of three massive corals on the Belize barrier reef. Marine Ecology-Progress Series. 13(2-3), 261-271.

Highsmith, R.C., 1981. Coral bioerosion: Damage relative to skeletal density. The American Naturalist. 117(2), 193-198.

Highsmith, R.C., 1980. Geographic patterns of coral bioerosion: A productivity hypothesis. Journal of Experimental Marine Biology and Ecology. 46(2), 177-196.

Hochachka, W.M., Dhondt, A.A., 2000. Density-dependent decline of host abundance resulting from a new infectious disease. Proceedings of the National Academy of Sciences. 97(10), 5303-5306.

Hoegh-Guldberg, O., Mumby, P.J., Hooten, A.J., Steneck, R.S., Greenfield, P., Gomez, E., Harvell, C.D., Sale, P.F., Edwards, A.J., Caldiera, K., Knowlton, N., Eakin, C.M., Iglesias-Prieto, R., Muthiga, N., Bradbury, R.H., Dui, A., Hatziolos, M.E., 2007. Coral reefs under rapid climate change and ocean acidification. Science. 318, 1737-1742.

Hoegh-Guldberg, O., 1999. Climate change, coral bleaching and the future of the world's coral reefs. Mar.Freshwater Res. 50(8), 839-866.

Hoffmeister, J.E., Multer, H.G., 1968. Geology and origin of the Florida Keys. Geological Society of America Bulletin. 79(11), 1487-1502.

Holmes, K.E., Edinger, E.N., Hariyadi, Limmon, G.V., Risk, M.J., 2000. Bioerosion of live massive corals and branching coral rubble on Indonesian coral reefs. Marine Pollution Bulletin. 40(7), 606-617.

Holmes, K.E., 1997. Eutrophication and its effect on bioeroding sponge communities. In: Lessios, H.A., MacIntyre, I.G. (Eds.), Proceedings of the 8th International Coral Reef Symposium. Smithsonian Tropical Research Institute Balboa, Panama. 2, pp. 1411-1416.

Hubbard, D.K., Miller, A.I., Scaturo, D., 1990. Production and cycling of calcium carbonate in a shelf-edge reef system (St. Croix, U.S. Virgin Islands): Applications to the nature of reef systems in the fossil record. Journal of Sedimentary Petrology, 60(3), 335-360.

Hubbard, D.K., Burke, R.B., Gill, I.P., 1986. Styles of reef accretion along a steep, shelf-edge reef, St. Croix, U.S. Virgin Islands. Journal of Sedimentary Petrology, 56(6), 848-861.

Hughes, T.P., 1994. Catastrophes, phase-shifts, and large-scale degradation of a caribbean coral reef. Science. 265(5178), 1547-1551.

Hutchings, P., Peyrot-Clausade, M., Osnorno, A., 2005. Influence of land runoff on rates and agents of bioerosion of coral substrates. Mar.Pollut.Bull. 51(1–4), 438-447.

Hutchings, P., Murray, A., 1982. Patterns of recruitment of polychaetes to coral substrates at Lizard Island, Great Barrier-Reef - an experimental approach. Australian Journal of Marine and Freshwater Research. 33(6), 1029-1037.

Hutchings, P.A., Kiene, W.E., Cunningham, R.B., Donnelly, C., 1992. Spatial and temporal patterns of non-colonial boring organisms (polychaetes, sipunculans and bivalve molluscs) in *Porites* at Lizard Island, Great Barrier Reef. Coral Reefs. 11(1), 23-31.

Hutchings, P.A., 1986. Biological destruction of coral reefs. Coral Reefs. 4, 239-252.

Jackson, J.B.C., Kirby, M.X., Berger, W.H., Bjorndal, K.A., Botsford, L.W., Bourque, B.J., Bradbury, R.H., Cooke, R., Erlandson, J., Estes, J.A., Hughes, T.P., Kidwell, S., Lange, C.B., Lenihan, H.S., Pandolfi, J.M., Peterson, C.H., Steneck, R.S., Tegner, M.J., Warner, R.R., 2001. Historical overfishing and the recent collapse of coastal ecosystems. Science. 293(5530), 629-637.

James, N.P., Kobluk, D.R., Pemberton, S.G., 1977. The oldest macroborers: Lower Cambrian of Labrador. Science. 197(4307), 980-983.

Kiene, W.E., Hutchings, P.A., 1994. Bioerosion experiments at Lizard Island, Great Barrier Reef. Coral Reefs. 13, 91-98.

Kiene, W.E., Hutchings, P.A., 1993. Long-term bioerosion of experimental coral substrates from Lizard Island, Great Barrier ReefIn: Richmond, R.H. (Ed.), Proceedings from the 7th International Coral Reef Symposium. University of Guam Press, UOG Station, Guam1, pp. 397-403.

Kiene, W.E., 1988. Biological destruction on the Great Barrier Reef, (Ph.D Dissertation). 361.

Kleeman, K., 1990. Boring and growth in chemically boring bivalves from the Caribbean, Eastern Pacific and Australia's Great Barrier Reef. Senckenbergiana marit. 21, 101-154.

Knoll, A.H., Golubic, S., Green, J., Swett, K., 1986. Organically preserved microbial endoliths from the late Proterozoic of East Greenland. Nature, 321, 856-857.

Knowlton, N., Jackson, J.B.C., 2008. Shifting baselines, local impacts, and global change on coral reefs. PLoS Biology. 6(2), 215-220.

Koop, K., Booth, D., Broadbent, A., Brodie, J., Bucher, D., Capone, D., Coll, J., Dennison, W., Erdmann, M., Harrison, P., Hoegh-Guldberg, O., Hutchings, P., Jones, G.B., Larkum, A.W.D., O'Neil, J., Steven, A., Tentori, E., Ward, S., Williamson, J., Yellowlees, D., 2001. ENCORE: The effect of nutrient enrichment on coral reefs. Synthesis of results and conclusions. Mar.Pollut.Bull. 42(2), 91-120.

Le Campion-Alsumard, T., Golubic, S., Hutchings, P., 1995. Microbial endoliths in skeletons of live and dead corals: *Porites lobata* (Moorea, French Polynesia). Mar.Ecol.Prog.Ser. 117, 149-157.

Le Grand, H.M., Fabricius, K.E., 2011. Relationship of internal macrobioeroder densities in living massive *Porites* to turbidity and chlorophyll on the Australian Great Barrier Reef. Coral Reefs. 30(1), 97-107.

Macdonald, I.A., Perry, C.T., 2003. Biological degradation of coral framework in a turbid lagoon environment, Discoverery Bay, north Jamaica. Coral Reef. 22, 523-535.

Manzello, D.P., Kleypas, J.A., Budd, D.A., Eakin, C.M., Glynn, P.W., Langdon, C., 2008. Poorly cemented coral reefs of the eastern tropical Pacific: Possible insights into reef development in a high-CO2 world. Proceedings of the Nation Academy of Sciences of the United States of America. 105(30), 10450-10455.

Martindale, W., 1992. Calcified epibionts as palaeoecological tools: Examples from the Recent and Pleistocene reefs of Barbados. Coral Reefs. 11(3), 167-177.

McClanahan, T.R., Muthiga, N.A., 1998. An ecological shift in a remote coral atoll of Belize over 25 years. Environ.Conserv. 25(2), 122-130.

McClanahan, T.R., Muthiga, N.A., 1988. Changes in Kenyan coral reef community structure and function due to exploitation. Hydrobiologia. 166(3), 269-276.

McCook, L.J., Jompa, J., Diaz-Pulido, G., 2001. Competition between corals and algae on coral reefs: A review of evidence and mechanisms. Coral Reefs. 19(4), 400-417.

McKenna, S.A., Ritter, J., 1999. *Cliona lampa* and disturbance on the coral reefs of Castle Harbour, Bermuda. Memoirs of the Queensland Museum. 44, 360.

Morse, D.E., Hooker, N., Morse, A.N.C., Jensen, R.A., 1988. Control of larval metamorphosis and recruitment in sympatric agariciid corals. J.Exp.Mar.Biol.Ecol. 116(3), 193-217.

Mumby, P.J., 2009. Herbivory versus corallivory: Are parrotfish good or bad for Caribbean coral reefs? Coral Reefs. 28(3), 683-690.

Neumann, A.C., 1966. Observations on coastal erosion in Bermuda and measurements of the boring rate of the sponge, *Cliona lampa* . Limnology and Oceanography. 11(1), 92-108.

Ogden, J.C., 1977. Carbonate-sediments production by parrot fish and sea urchins on Caribbean reefs. American Association of Petroleum Geologists Studies in Geology, 281-288.

Pang, R.K., 1973. The ecology of some Jamaican excavating sponges. Bulletin of Marine Science. 23(2), 227-243.

Pari, N., Peyrot-Clausade, M., Hutchings, P.A., 2002. Bioerosion of experimental substrates on high islands and atoll lagoons (French Polynesia) during 5 years of exposure. Journal of Experimental Marine Biology & Ecology. 276(1), 109.

Perkins, R.D., 1977. Depositional framework of Pleistocene rocks in South Florida. In: Enos, P., Perkins, R.D. (Eds.), Quaternary sedimentation in South Florida. Geological Society of America Mem., pp. 131-198.

Perry, C.T., Hepburn, L.J., 2008. Syn-depositional alteration of coral reef framework through bioerosion, encrustation and cementation: Taphonomic signatures of reef accretion and reef depositional events. Earth Science Reviews. 86(1-4), 106-144.

Perry, C.T., Bertling, M., 2000. Spatial and temporal patterns of macroboring within Mesozoic and Cenozoic coral reef systems. Geological Society, London, Special Publications. 178(1), 33-50.

Perry, C.T., 1999. Reef framework preservation in four contrasting modern reef environments, Discovery Bay, Jamaica. J.Coast.Res. 15(3), 796-812.

Perry, C.T., 1998. Macroborers within coral framework at Discovery Bay, north Jamaica: Species distribution and abundance, and effects on coral preservation. Coral Reefs. 17(3), 277-287.

Peyrot-Clausade, M., Le Campion-Alsumard, T., Hutchings, P., Le Campion, J., Payri, C., Fontaine, M., 1995. Initial bioerosion and bioaccretion on experimental substrates in high islands and atoll lagoons (French Polynesia). Oceanologican Acta. 18(5), 531-541.

Peyrot-Clausade, M., Bruno, J.F., 1990. Distribution patterns of macroboring organisms on Tulear reef flats (SW Madagascar). Marine Ecology Progress Series. 61(1-2), 133-144.

Pomponi, S.A., 1979. Ultrastructure and cytochemistry of the etching area of boring sponges. In: Levi, C., Boury-Esnault, N. (Eds.), Biologie et Spongiaires. Colloques Internationaux du Centre Nationale de la Recherche Scientifique, pp. 317-323.

Przeslawski, R., Ahyong, S., Byrne, M., Wörheide, G., Hutchings, P., 2008. Beyond corals and fish: The effects of climate change on noncoral benthic invertebrates of tropical reefs. Global Change Biol. 14(12), 2773-2795.

Purchon, R.D., 1968. The biology of the Mollusca. Pergamon Press, Oxford, New York, 560.

Randall, J.E., 1974. The effect of fishes on coral reefs. In: Cameron, A.M., Cambell, B.M., Cribb, A.B., Endean, R., Jell, J.S., Jones, O.A., Mather, P., Talbot, F.H. (Eds.), Proceedings of the 2nd International Coral Reef Symposium. The Great Barrier Reef Committee, Brisbane, Australia.Brisbane, Australia. 21, pp. 159-166.

Rasser, M., Riegl, B., 2002. Holocene coral reef rubble and its binding agents. Coral Reefs. 21(1), 57-72.

Reaka-Kudla, M., Feingold, J.S., Glynn, P.W., 1996. Experimental studies of rapid bioerosion of coral reefs in the Galápagos Islands. Coral Reefs. 15(2), 101-107.

Risk, M.J., Sammarco, P.W., Edinger, E.N., 1995. Bioerosion in *Acropora* across the continental shelf of the Great Barrier Reef. Coral Reefs, 14(2), 79-86.

Rose, C.S., Risk, M.J., 1985. Increase in *Cliona delitrix* infestation of *Montastrea cavernosa* deads on an organically polluted portion of the Grand Cayman fringing reef. Marine Ecology. 6(4), 345-363.

Rützle, K., 2002. Impact of crustose clionid sponges on Caribbean reef corals. Acta Geologica Hispanica. 37(1), 61-72.

Rützler, K., 1975. The role of burrowing sponges in bioerosion. Oecologia. 19(3), 203-216.

Sammarco, P.W., 1996. Comments on coral reef regeneration, bioerosion, biogeography, and chemical ecology: future directions. J.Exp.Mar.Biol.Ecol. 200(1–2), 135-168.

Sammarco, P.W., Risk, M.J., 1990. Large scale patterns in internal bioerosion of *Porites*: cross continental shelf trends on the Great Barrier Reef. Marine Ecology-Progress Series. 59(1-2), 145-156.

Sammarco, P.W., Risk, M.J., Rose, C., 1987. Effects of grazing and damselfish territoriality on internal bioerosion of dead corals: Indirect effects. J.Exp.Mar.Biol.Ecol. 112(2), 185-199.

Sammarco, P.W., 1980. *Diadema* and its relationship to coral spat mortality: Grazing, competition, and biological disturbance. J.Exp.Mar.Biol.Ecol. 45(2), 245-272.

Schönberg, C., 2003. Substrate effects on the bioeroding demosponge *Cliona orientalis*. 2. Substrate Colonisation and Tissue Growth. Mar.Ecol. 24(1), 59-74.

Schönberg, C., Wilkinson, C., 2001. Induced colonization of corals by a clionid bioeroding sponge. Coral Reefs. 20(1), 69-76.

Schonberg, C.H.L., 2002. Substrate effects on the bioeroding demosponge *Cliona orientalis*. 1. Bioerosion Rates. Marine Ecology. 23(4), 313.

Schönberg, C.H.L., Wisshak, M., 2012. The perks of being endolithic. Aquatic biology. 17(1), 1-5.

Scoffin, T.P., Bradshaw, C., 2000. The taphonomic significance of endoliths in dead-versus live-coral skeletons. Palaios. 15(3), 248-254.

Scoffin, T.P., Brown, B.E., Dunne, R.P., Le Tissier, M. D. A., 1997. The controls on growth form of intertidal massive corals, Phuket, South Thailand. Palaios. 12(3), 237-248.

Scoffin, T.P., 1992. Taphonomy of coral reefs: A review. Coral Reefs. 11(2), 57-77.

Scoffin, T.P., Stearn, C.W., Boucher, D., Frydl, P., Hawkins, C.M., Hunter, I.G., MacGeachy, J.K., 1980. Calcium carbonate budget of a fringing reef on the west coast of Barbados: Part II, Erosion, sediments and internal structure. Bulletin of Marine Science. 3(2), 475-508.

Scott, P.J.B., 1988. Distribution, habitat and morphology of the Caribbean coral- and rock-boring bivalve, *Lithophaga bisulcata* (d'Orbigny) (Mytilidae: Lithophaginae). J.Molluscan Stud. 54(1), 83-95.

Silbiger, N.J., Guadayol, Ò., Thomas, F.I.M., Donahue, M.J., 2014. Reefs shift from net accretion to net erosion along a natural environmental gradient. Mar. Ecol. Prog. Ser. 515, 33-44.

Smith, S.V., Kimmerer, W.J., Laws, E.A., Brock, R.E., Walsh, T.W., 1981. Kaneohe Bay sewage dispersion experiment. Perspectives on ecosystem responses to nutritional perturbation. Pacific Science. 35, 279-385.

Steneck, R.S., 1988. Herbivory on coral reefs: A synthesis. In: Choat, J.H., Barnes, D., Borowitzka, M.A., Coll, J.C., Davies, P.J., Flood, P., Hatcher, B.G., Hopley, D., Hutchings, P.A., Kingsey, D., Orme, G.R., Pichon, M., Sale, P.F., Sammarco, P., Wallace, C., Wilkinson, C., Wolanski, E., Bellwood, O. (Eds.), Proceedings from the 6th International Coral Reef Symposium. 6th International Coral Reef Symposium Executive Committee1, pp. 37-49.

Tanner, J.E., 1995. Competition between scleractinian corals and macroalgae: An experimental investigation of coral growth, survival and reproduction. J.Exp.Mar.Biol.Ecol. 190(2), 151-168.

Tribollet, A., Golubic, S., 2011. Reef bioerosion: Agents and processes. In: Dubinsky, Z., Stambler, N. (Eds.), Coral reefs: An ecosystem in transition. Springer Netherlands, pp. 435-449.

Tribollet, A., Godinot, C., Atkinson, M., Langdon, C., 2009. Effects of elevated pCO_2 on dissolution of coral carbonates by microbial euendoliths. Global Biogeochemical Cycles, 23(3), GB3008.

Tribollet, A., Decherf, G., Hutchings, P., Peyrot-Clausade, M., 2002. Large-scale spatial variability in bioerosion of experimental coral substrates on the Great Barrier Reef (Australia): Importance of microborers. Coral Reefs. 21(4), 424-432.

Vogel, K., Gektidis, M., Golubic, S., Kiene, W.E., Radtke, G., 2000. Experimental studies on microbial bioerosion at Lee Stocking Island, Bahamas, and One Tree Island, Great Barrier Reef, Australia: Implications for paleoecological reconstructions. Lethaia. 33(3), 190-204.

Vogel, K., 1993. Bioeroders in fossil reefs. Facies. 28(1), 109-113.

Walker, K.R., Diehl, W.W., 1985. The role of marine cementation in the preservation of lower Paleozoic assemblages. Philos.Trans.R.Soc.Lond.Ser.B-Biol.Sci. 311(1148), 143-153.

Warme, J.E., 1975. Borings as trace fossils, and the processes of marine bioerosion. In: Frey, R.W. (Ed.), The study of trace fossils. Springer-Verlag, New York, N.Y., United States, pp. 181-227.

Warme, J.E., Marshall , N.F., 1969. Marine borers in calcareous terrigenous rocks of the Pacific Coast. Am.Zool. 9(3), 765-774.

Wilson, M.A., 2007. Macroborings and the evolution of marine bioerosion. In: Miller, W.I. (Ed.), Trace fossils: Concepts, problems, prospects. Elsevier, Amsterdam-Oxford-New York, pp. 356-367.

Wilson, M.A., Taylor, P.D., 2006. Patterns and processes in the Ordovician Bioerosion Revolution. Ichnos. 13(3), 109-112.

Wilson, S.K., Fisher, R., Pratchett, M.S., Graham, N.A.J., Dulvy, N.K., Turner, R.A., Cakacaka, A., Polunin, N.V.C., Rushton, S.P., 2008. Exploitation and habitat degradation as agents of change within coral reef fish communities. Global Change Biol. 14(12), 2796-2809.

Wisshak, M., Schönberg, C.H.L., Form, A., Freiwald, A., Dupont, S., 2012. Ocean acidification accelerates reef bioerosion. PLoS ONE. 7(9), 1-8.

Wisshak, M., Schönberg, C., Form, A., Friwald, A., 2011. Global change and bioerosion - preliminary results. In: Carreiro-Silva, M., Ávila, S.P. (Eds.), Programme and Abstrates: 7th International Bioerosion Workshop, Faial, Azores, Faial, AzoresFaial, Azores, pp. 33.

Zhang, Y., Golubic, S., 1987. Endolithic microfossils (cyanophyta) from early Proterozoic stromatolites, Hebei, China. Acta Micropaleontologica Sinica. 4, 1-12.

APPENDIX C

Reflection on initial research question

The initial question that drove this study has evolved since the beginning of research. The recognition of diverse mesophotic habitats in the U.S. Virgin Islands (USVI) led to a question: whether variability in major sedimentary reef processes and the interplay of these processes are primarily responsible for the development and maintenance of the structurally diversity observed. This question, however, produced a hypothesis which could not be tested. While the sedimentary processes examined in this study are implicated as controls on reef architectural integrity and geomorphology, documenting variability in these processes at the different mesophotic habitats can only be said to correlate with structural differences, and cannot directly identify the drivers of geomorphic heterogeneousness. Additional research beyond the scope and resources currently available would be required to fully address the initial research-driving question. Therefore, a related more feasible research question was developed.

APPENDIX D

Research permits

GOVERNMENT OF THE VIRGIN ISLANDS OF THE UNITED STATES
========
DEPARTMENT OF PLANNING AND NATURAL RESOURCES
DIVISION OF FISH AND WILDLIFE
6291 ESTATE NAZARETH
ST. THOMAS, VIRGIN ISLANDS 00802
PHONE: (340) 775-6762, FAX: (340) 775-3972
SCIENTIFIC COLLECTION/ EXPORT
STT-036-10

Permittee: David Weinstein and Dr. Tyler Smith

Phone Number: (301)-775-8250; (340)-693-1394

Mailing Address: Rosenstiel School of Marine and Atmospheric Science
University of Miami
Marine Geology and Geophysics
4600 Rickenbacker Causeway
Miami, FL 33149

Alternate Address: University of the Virgin Islands
#2 John Brewers Bay
St. Thomas, Virgin islands 00802

Rational: The complex geomorphic structure of coral reefs provides critical ecosystem services crucial for sustained environmental health. With reefs threatened by numerous hazards, it is essential to understand the different biological and physical processes controlling reef development. Bioerosion is a fundamental process assisting in the regulation of the overall functionality of all coral reef habitats. Affecting the development and eventual preservation of a reef, bioerosion is a key process in defining the reef carbonate budget (Scoffin et al. 1980, Risk et al. 1995), subsequently implicating bioerosion as a primary process influencing reef development, accretion, destruction, and preservation. Given the importance of bioeroders in reworking reef material, it is essential to study the bioerosional process to understand the carbonate budget of a reef and how much of the reef will be preserved as structure-forming framework.

Common Name	Number	Description
Coral Rubble	50-70	dead samples of coral ruble (rock)
Dead Coral framework	30	Dead coral broken from in situ framework
Previously planted coral substrates	~80	

305

Location of activity: South St. Thomas to include Hind Bank Marine Conservation District

Methods to be used in activity: The study will be conducted at Hind Bank Marine Conservation District, in the United States Virgin Islands. The chosen location provides good access to different MCE zones and collaboration with team members from the University of the Virgin Islands. Four previous identified MCE zones will be sampled (high bank, patch/low bank, flat basin, Hillocks basin) using a linear transect method. At each zone, three to five 20 meter transects will be deployed to best represent the area studied. Each transect will consist of 4 sampling stations (one at each end and two in the middle). Three to five samples of coral rubble will be collected off the reef surface at each station. Fragments of dead coral framework will also be broken off and collected to assist with our study. All sites will be photographed for future reference. Additionally, pre-cut coral disks attached to PVC will be placed above the coral canopy at each transect site for future bioerosion rate studies. These substrates were created at an earlier date by cutting previously drilled samples of *Montastraea faveolata* into 10 inch diameter 2 inch thick disks. Prior to deployment, the disks will be numbered, weighed, and attached to the PVC with screws placed in holes drilled through the center of the disks.

Collected samples photographed, and divided into two equivalent subgroups. The first subgroup will be used to determine the amount and type of borings present. Samples will be cut in half along the growth axis and scanned onto a computer. The images will be analyzed using a point count method. The number and spatial coverage of borings will be calculated and categorized by which organism made the boring. The second subgroup will be used for biological analysis, specifically determining the number of major groups of bioeroders present. The samples will be placed in a 7% formaldehyde solution. Next, the samples will be cut into smaller pieces and prepared for light microscopy analysis by dissolving the substrate in Pereny's solution (4 vol. 10% nitric acid, 3 vol. 0.5% chromic acid, 3 vol. 90% ethanol). The remaining organic material can then be examined. The coral disks will be collected at six to twelve month intervals for a three year period. A similar analysis to the method for the rubble will be used for the disks.

Details of holding/retention facilities (include dimensions and construction material of cage)*: The purpose of this study does not require the collection of living specimens. The coral rubble and collected substrate blocks will be put in bleach to clean them up. They will then be packaged in zip-lock bags or plastic containers to be shipped to the University of Miami.

Shipping details (method, destination, name/address of consignor): All samples will be transported to the University of Miami by David Weinstein or other authorized representatives. The method will either be postal or transport with the research team on aircraft.

Reason for activity: Our *long-range goal* is to form a complete understanding of the significance of bioerosion in developing, maintaining and destroying mesophotic reefs, while contributing overall to the exploration of MCEs. The *objective of this research*, which is the next step in pursuit of that goal, is to determine how bioerosion abundance, intensity, and net bioerosion versus net accretion levels varies between different MCE facies and habitats, and also with their shallow water counterparts.

1. **Determine the abundance of all bioeroders and the bioerosion rates in each habitat.**
   The working hypothesis for this aim, based on literature reviews presented under p*reliminary studies,* is that boring sponges are the dominate macroborers and bioerosion rates and abundance distributions are homogeneous throughout all MCE habitats. To test this hypothesis, we will identify and quantify bore holes found in collected mesophotic coral rubble samples, and follow a similar method with pre-measured coral substrate disks placed at each habitat which will be collected at different time intervals to obtain a rate.

2. **Calculate ratio of net accretion to net bioerosion in each habitat.**
   The working hypothesis for this aim is that the ratio will be the same for all habitats as long as they are composed of the same framework building coral species. The approach used to test this hypothesis will be to combine known growth rate data and previous compositional surveys in mesophotic reefs with recorded bioerosion rates from this study.

Conditions and Restrictions:
1. Permit must be present at all times when collecting.
2. Collection may not include techniques that would injure or destroy non-target species, coral or benthic features.
3. The permit holder is responsible for any damage to surrounding organisms.
4. Be careful of introducing diseases when collecting and placing coral substrates.
5. Samples may not be collected within 200 meters of dive moorings.
6. Samples collected may be exported for laboratory analysis.
7. The permittee is responsible for any and all Federal or International permits required for the collection and transportation of these samples.
8. A copy of this permit must be provided to the shipper and/or presented to authorities upon departure from the Territory.
9. This permit is only valid for territorial waters of St. Thomas, Virgin Islands.
10. No collecting from Coki Point to Cabrita Point or from the North and West sides of Buck, Islands, St. Thomas.
11. This permit does not allow collection within;
    a) St. John National Park
    b) Virgin Islands Coral Reef National Monument
    c) The small pond at Frank Bay Marine Reserve
    d) Cas Cay/Mangrove Lagoon Marine Reserve
    e) St. James Marine Reserve
    f) Compass Point Marine Reserve

STT036-10 Scientific Research/Export Weinstein & Smith 4

12. Copies of reports, a final report, paper, thesis and publications stemming from this collection will be mailed to:
Division of Fish and Wildlife
6291 Estate Nazareth
St. Thomas, VI 00802

13. **Permit Expires August 31, 2013**.

_____ 4/27/10
Robert S. Mathes   Date
Commissioner, DPNR

_____ 6/24/2010
Beulah Dalmida-Smith   Date
Director, Div. Fish and Wildlife

David Weinstein   6/17/2010
_____
David Weinstein   Date
Tyler Smith
Applicant